CHRONIC STRESS INDUCES CELLULAR SENESCENCE: IMPLICATIONS FOR AGING AND NEURODEGENERATIVE DISORDERS

A DISSERTATION SUBMITTED TO THE FACULTY OF

THE UNIVERSITY OF MINNESOTA BY

Carey Elizabeth Lyons

IN PARTIAL FULFILLMENT OF THE REQUIREMENTS

FOR THE DEGREE OF DOCTOR OF PHILOSOPHY

Advised by Alessandro Bartolomucci, PhD

June 2022

ACKNOWLEDGEMENTS

First and foremost, I would like to thank my advisor, Alessandro Bartolomucci, whose support, mentorship, and unending enthusiasm have shaped me into the scientist I am today. I am so grateful to have found a mentor who will always make time for me, and will support me even as he pushes me to be better. I also owe a huge debt of gratitude to my thesis committee, Drs Jonathan Gewirtz, Sylvain Lesne, Laura Niedernhofer and Deb Ferrington (committee member emeritus) for their guidance on my projects and for bearing with me on the wild and arguably overambitious journey of my PhD.

Thank you to my labmates. Maria Razzoli has taught me nearly everything I know about working with mice, and has helped hone my gallows humor to its 5mm lancet-sharp point. I don't know how I could have accomplished these projects without her scientific contributions and moral support. I've been incredibly lucky to have Rachel Mansk, first as an undergraduate researcher and later as a lab technician, helping me with my project from the very beginning. Pedro Rodriguez and Jean-Pierre Pallais have been the lab siblings I never knew I needed – thank you to them for yanking me out of my own head many times. Thank you also to Seth McGonigle, Maddie Berg and Nivi Sabarinathan for both your practical help, and for making our lab a pleasant place to be.

I'd like to thank my parents as well – Karen and Greg Lyons who have always encouraged me to pursue what will make me happy. Even if that meant (almost) 6 more years of school thousands of miles from home. I also could not have endured the aforementioned (not quite!) 6 years of school without the support of my graduate school cohort – Jenn Brown, Maria Linn-Evans, Natalie Lopresti, Megan Monko, Tim Monko, Carlee Toddes and Roman Tyshynsky. Thank you for being the best support system I could have asked for, and for making sure I occasionally left the house as I wrote this dissertation. Thank you also to my friends far away: the gremlins themselves – Sarah-Jane Kerwin, Emma Lehmann and Erica Morelli, and my feelings friend Emily Polstein. Thank you to my former coaches Danny Richards and Ray Appenheimer for being my first mentors, and for enabling me to use running as a coping mechanism throughout my PhD.

I would like to thank the University of Minnesota Graduate Program in Neuroscience, and the numerous funding sources that have supported my training. In particular the NIH/NIA T32 AG029796 “Functional Proteomics of Aging” training grant which both supported me, and played an invaluable role in my education on aging biology. The projects in my dissertation were supported by numerous grants, including the MN Partnership for Biotechnology and Molecular Genomic #18.4 to A.B., NIH/NIDDK R01DK117504-03S1 to A.B. This work was also supported in parts by grants from NIH/National Institute on Aging (R01AG046170, RF1AG057440, R01AG057907, U01AG052411, R01AG062355, U01AG058635, RF1AG054014, RO1AG068030 and R56AG058655), NIH/National Institute of Allergy and Infectious Diseases (U01AI111598), NIH/National Institute of Dental and Craniofacial Research (R03DE026814), NIH/NIDDK (R01DK118243) to BZ.

p16-3MR mice were supplied by Judith Campisi and Unity Biotechnology. PS19 mice and p16-creERT2 mice were supplied by Darren Baker and Jan van Deursen at the Mayo Clinic.

I have also received vital support from several core services at the UMN and elsewhere. The UMN Histology & Research Laboratory, Imaging Core, and Genomics Core were crucial in executing the spatial transcriptomics experiments. Behavioral testing was performed with the support and guidance of the Mouse Behavior Core. Plasma corticosterone radioimmunoassays were performed by the Behavioral and Cognitive Core of the University of Cincinnati Mouse Metabolic Phenotyping Center (NIH grant U2C DK-59630; RRID:SCR_015367).

Chapter 5 includes data collected through the Banner Sun Health Research Institute Brain and Body Donation Program of Sun City, Arizona, led by Dr. Thomas G. Beach. Gene expression data came from the Mount Sinai/JJ Peters VA Medical Center NIH Brain and Tissue Repository. I would like to thank the physicians, scientists and most of all donors who contributed to these data resources.

ABSTRACT

Chronic stress can shorten lifespan and is a risk factor for a diverse range of aging-related diseases. Despite the consistency of this relationship, it remains unclear how stress might affect aging biology. An association between stress exposure and induction of a fundamental aging process such as cellular senescence has been proposed, but experimental evidence is lacking. A complicating factor in human and rodent stress research is the variability of stressors and stress responses themselves. This dissertation presents several studies interrogating the biological processes by which chronic stress may affect aging and disease risk, and probing the relevance of stressor type to these effects. The thesis starts with a review of existing literature supporting the hypothesis that chronic psychological stress can induce cellular senescence. Chapter 2 provides the first experimental evidence causally linking chronic stress with an increase in senescent cells. Moreover, it suggests that a social stress model (chronic subordination stress; CSS), and a nonsocial psychological stress model (restraint stress) despite both most prominently affecting the brain, may be biased towards different senescence pathways (p16 or p21 respectively) and brain regions (hippocampus and cortex). Spatial transcriptomic profiling of the brains of CSS-exposed mice implicates the DNA Damage Response and elevated Ras/Raf signaling as mediators of CSS-induced senescence. CSS-induced SNCs also appears to alter the local microenvironment via pathways including interleukin signaling, and changes to the extracellular matrix. They are also associated with elevated glutamatergic neurotransmission. However, a lifelong pharmacogenetic strategy to eliminate senescent cells was detrimental to healthspan and lifespan and further exacerbates CSS-induced deficits in those measures. With the CNS emerging as a key target of stress-induced SNC, Chapter 3 reviews the association between stress and Alzheimer's disease, with an emphasis on rodent models. Chapter 4 demonstrates differential effects of CSS and restraint stress on a mouse model of tau pathology (PS19) – one of the hallmarks of Alzheimer's disease (AD). Although our study found only minor detrimental effects of either model, CSS appears to affect some cognitive function via a tau-independent mechanism. Lastly, Chapter 5 presents an unbiased analysis of the proteomic changes shared by mice exposed to lifelong CSS and AD patients. This work replicates the lack-of-effect of CSS on tau pathology, while demonstrating that most of the

overlapping proteins were functionally associated with enhanced NMDA receptor mediated glutamatergic signaling, an excitotoxicity mechanism known to affect neurodegeneration. These findings support the association between stress and AD progression and provide valuable insight into potential early biomarkers and protein mediators of this relationship. The results of these studies provide novel insight into the mechanisms by which stress may affect aging and risk for neurodegenerative disease.

TABLE OF CONTENTS

LIST OF TABLES

LIST OF FIGURES

Chapter 2

Chapter 3

Chapter 4

Chapter 5

Appendix

LIST OF ABBREVIATIONS

8-OHdG - 8-hydroxy-2'-deoxyguanosine

8-oxodG - 8-oxo-7, 8-dihydro-2'-deoxyguanosine

Aβ - Amyloid β

ACE – angiotensin converting enzyme

ACTH - Adrenocorticotropic hormone

AD – Alzheimer's disease

AOI – Area of Interest

APOE – Apolipoprotein E

APP – amyloid precursor protein

ARRB1 – arrestin b-1

BACE – β site APP cleavage enzyme

BDNF – brain-derived neurotrophic factor

CPS – chronic psychosocial stress

CRH - Corticotropin releasing hormone

CRHR1 – Corticotropin releasing hormone receptor 1

CS – conditioned stimulus

CSS – chronic subordination stress

CUMS – chronic unpredictable mild stress

DDR – DNA Damage Response

DEP – Differentially Expressed Protein

DSBs - Double strand breaks

FE – Fold Enrichment

GC – Glucocorticoid

GCV - Ganciclovir

GR - Glucocorticoid receptor

GSEA – Gene Set Enrichment Analysis

H2O2 - hydrogen peroxide

HSP70 - Heat shock protein 70

HPA – hypothalamic pituitary adrenal axis

hTau – human Tau

IsoP – isoprostanes

MAP2 – microtubule assembling protein 2

MAPK - mitogen-activated protein kinase

MAPT - Microtubule associated protein tau

MCI – Mild Cognitive Impairment

MDA - malondialdehyde

MDM2 - murine double mutant 2

mPFC- medial prefrontal cortex

mTau – mouse Tau

N.A. - numerical aperture

NFT - Neurofibrillary tangle

NO – nitric oxide

NOX2 - NADPH oxidase

OH- hydroxyl radical

p16 – p16INK4a

PBMC – peripheral blood mononuclear cell

PFC- prefrontal cortex

MAPTP301SPS19 – PS19

PSD-95 – postsynaptic density protein 95

PSEN – presenilin

Restricted Maximum Likelihood (REML)

RIA – Radioimmunoassay

RNS reactive nitrogen species

ROS – Reactive Oxygen Species

SA β-gal – senescence-associated b-galactosidase

SAM - Sympathetic-adrenal medullary

scWAT – subcutaneous white adipose tissue

SES – socioeconomic status

SNC – senescent cell

SOD – superoxide dismutase

TBARS thiobarbituric acid-reactive substance

TNF-α - Tumor necrosis factor alpha

US – Unconditioned Stimulus

UV - ultraviolet

VEGF – Vascular endothelial growth factor

CHAPTER 1

INTRODUCTION: DOES CHRONIC STRESS PROMOTE CELLULAR SENESCENCE?

1.1 Introduction

Chronic stress is linked to a multitude of health risks. In particular, it is associated with elevated risk for chronic, aging related diseases, which severely degrade quality of life and are the primary causes of death in older adults. Stress increases risk for cardiovascular disease, Alzheimer's disease, vascular dementia, Parkinson's disease, diabetes and osteoarthritis (Johnston, 2000; Mejfa *et al.*, 2003; Gu *et al.*, 2012; Hemmerle *et al.*, 2012; Mo *et al.*, 2014; Gerritsen *et al.*, 2017; Harris *et al.*, 2017; Bonanni *et al.*, 2018; Yuede *et al.*, 2018; Kivimäki *et al.*, 2018; Yao *et al.*, 2019).

Annual surveys conducted by the American Psychological Association find that the average reported stress level among adults has steadily increased over the past 5 years (American Pyschological Association, 2021). The ongoing COVID-19 pandemic has disproportionately elevated stress among certain populations. Hispanic, Black, and Asian adults report higher pandemic-related stress levels than White adults. People with annual household incomes below $50K were also more likely to score below 3.00 on the Brief Resilience score. These findings are especially alarming given that living with low socioeconomic status already confers an immense burden of stress and is highly associated with all-cause mortality risk (Signorello *et al.*, 2014).

With overwhelming evidence for the detrimental health effects of stress, and signs indicating that stress burden will continue to rise for millions of people, it is critical to understand the biological mechanisms at play.

1.2 The stress response

Over the years, the stress research field has needed to revise its nomenclature to define and restrict the circumstances that can be described as stress. In the stress biology field, the term "stress" describes the perception of an uncontrollable threat that requires adaptations outside of an individual's regulatory range (Koolhaas *et al.*, 2011). All organisms must be capable of managing and adapting to perturbations to homeostasis; a certain degree of physical, emotional, and social challenge is a constant feature of life. However, sometimes the slings and arrows of outrageous fortune impose physiological demands that are outside and individual's adaptive capacity. These challenges are defined as stressors.

The neuroendocrine stress response is described by its two major components: the sympathetic-adrenal medullary (SAM) system and the hypothalamic pituitary adrenal (HPA) axis (for review, see Charmandari et al., 2005 and Ulrich-Lai and Herman, 2009). In response to a stressor, the SAM system, colloquially referred to as the "fight or flight response", (Cannon, 1915) is rapidly activated; preganglionic neurons in the sympathetic nervous system activate chromaffin cells in the adrenal medulla, resulting the release of epinephrine (and to a lesser extent, norepinephrine) into general circulation. Circulating epinephrine (also termed adrenaline) and norepinephrine, released from sympathetic nerve terminals, exert their effects in a wide range of tissues via adrenergic receptors. Notably, they cause increased heart rate, respiratory rate, glycolysis, glycogenolysis and lipolysis.

The HPA axis originates with neurons in the paraventricular nucleus of the hypothalamus, which in response to perceived threat, release corticotropin releasing hormone (CRH) into a collection of blood vessels termed the hypophysial portal system. Through this specialized vasculature, CRH reaches the anterior pituitary gland, causing it to release adrenocorticotropic hormone (ACTH) into general circulation. ACTH stimulates cells in the adrenal cortex to produce glucocorticoids (GCs) which act on a number of targets. GCs also exert negative feedback on the hypothalamus and pituitary gland, halting release of CRH and ACTH respectively. This feedback loop halts continued HPA activity; however, in cases of sustained stress or aging, GC hypersecretion can persist (Sapolsky *et al.*, 1986; Spiga *et al.*, 2014). This negative feedback system becomes impaired with age

due in large part to downregulation of glucocorticoid receptors (GR) in the hippocampus (Sapolsky *et al.*, 1986). HPA axis hyperactivity is associated with numerous adverse conditions, including major depression (Pariante & Lightman, 2008), immune suppression (Oppong & Cato, 2015) and memory impairment (Tatomir *et al.*, 2014).

In addition to the canonical "stress axes" described above, several additional neural and neuroendocrine system have been shown to regulate the acute stress response (see Sapolsky *et al.*, 2000; Ulrich-Lai & Herman, 2009 for review) including a newly identified role for osteocalcin (Berger *et al.*, 2019).

1.3 Stress and social determinants of health and aging

Life experiences endemic to low socioeconomic status (SES) confer an immense burden of stress. The factors involved can include financial insecurity, uncertainty about future stability, and feelings of exclusion or marginalization due to occupational or economic status (Marmot *et al.*, 1991; Adler *et al.*, 1994; Stringhini *et al.*, 2017; Marmot, 2020). While a number of factors contribute to the myriad negative health outcomes associated with low SES — poorer access to healthcare being one critical factor — material deprivation does not entirely explain this phenomenon. Rather, it is widely hypothesized that chronic stress and its physiological consequences underlie the shorter lifespan and numerous poor disease outcomes associated with low SES. Lower SES is associated with higher basal levels of catecholamines and cortisol, as well as reported levels of stress (Cohen *et al.*, 2006). Supporting psychosocial stress as a principal intermediary of SES and health is a study showing that low SES individuals who still experience a high sense of control have health metrics comparable with individuals in higher income groups (Lachman & Weaver, 1998).

Low SES is associated with elevated mortality risk from nearly all causes (Marmot *et al.*, 1991; Elo, 2009). Disadvantage early in life has a particularly severe effect on both lifespan, and the number of years lived without functional impairment, sometimes termed "healthspan" (Karas Montez *et al.*, 2014). Exposure to an increasing number of adverse childhood experiences elevates risk for chronic diseases in adulthood, including ischemic heart disease, cancer, and chronic lung disease (Felitti *et al.*, 1998).

One observational cohort study followed >3,000 participants aged 6–18 years at baseline for over 30 years via eight repeated biomedical examinations (Kivimäki *et al.*, 2018). The findings suggested that experiencing lower SES and its associated stressors accelerates age-related metabolic changes. At baseline, groups with high vs low SES stress did not differ in any metabolic traits, but by early adulthood the low SES group had notably increased blood lipid levels, decreased insulin sensitivity, and increased compensatory insulin secretion that was still insufficient to normalize circulating glucose concentrations. By middle age, low SES individuals were more likely to be obese, hypertensive, and have a fatty liver and diabetes compared with those who consistently lived in high SES neighbourhoods (Kivimäki *et al.*, 2018).

Another study found that SES from each life course period (childhood, early adulthood, and late adulthood) additively combines to predict the number of years an individual can expect to live with or without dementia (Cha *et al.*, 2021). Childhood adversities alone have a profound effect on the likelihood of developing dementia. The risk of developing dementia for individuals experiencing three disadvantages and two disadvantages were found to be 87% ($p < .001$), and 56% ($p < .001$) higher, respectively, than for those with no socioeconomic disadvantages during childhood. Low SES status during all three life periods shortened life expectancy for both men and women by 8.66 years (for men) and 6.89 years (for women). 18% of those years for men, or 17% for women were predicted to be lived with dementia, compared with 3% for men or 4% for women who experienced high SES throughout all life stages (Cha *et al.*, 2021).

Though the relationship between low SES and poorer health/lifespan has long been documented, the biological mechanisms underlying this effect have remained difficult to study. Some important recent advancements have been made — The Environmental Risk Longitudinal Twin Study found that children raised in more socioeconomically disadvantaged neighbourhoods develop epigenetic DNA methylation patterns distinct from their more advantaged peers (Reuben *et al.*, 2020). However, more precise studies on the physiological underpinnings of the health risks conferred by low social status require the use of animal models.

Social gradients in health can be observed in species of social mammals other than humans. In baboons, social rank as well as the strength/stability of an individual's social bonds predict survival (Silk *et al.*, 2010; Archie *et al.*, 2014). Subordinate status within a group of mice has been studied as a model for low socioeconomic status in humans (e.g., low occupational position, living in socioeconomically disadvantaged neighbourhoods) (Snyder-Mackler *et al.*, 2020).

Social stressors, such as chronic subordination stress (CSS), are particularly potent activators of stress response compared with other types, such as physical (cold water stress, foot shock) or psychological (restraint stress, forced swim) (Koolhaas *et al.*, 1997; Bartolomucci, 2007). This parallels human research, which finds that stressors with a social aspect are particularly potent. Tasks involving a social-evaluative threat (in which task performance could be negatively judged by others) elicit strong ACTH and cortisol release as well as long times to recovery (Kirschbaum *et al.*, 1993).

The striking similarity in findings across species suggests that social mammals including laboratory mice can be highly relevant models to study the contribution of social stress to aging and healthspan. A recent study demonstrated that in mice, subordinate social status shortens lifespan, accelerated onset of age-related pathologies, and leads to an increase in several markers of cellular senescence (Razzoli *et al.*, 2018).

1.4 Cellular senescence

Cellular senescence is the fundamental aging process in which cells cease division and undergo a number of other distinctive phenotypic changes (Hayflick & Moorhead, 1961; McHugh & Gil, 2018). Throughout a cell's lifespan, it is subjected to internal and external challenges leading to gradual accrual of damage. Simultaneously, as cells divide, they incrementally lose telomeric DNA at the ends of chromosomes. If telomeres become too short, this destabilizes the entire chromosomal structure. Both of these forms of injury make a cell susceptible to developing deleterious DNA mutations.

Senescence programming prevents damaged cells from passing on damaged DNA to the next generation. This makes it a potent tumor suppressive mechanism as it stops cells with potentially oncogenic gene mutations from replicating. This is highly beneficial in ensuring that an individual survives long enough to reproduce; however, it appears to be

less advantageous to an aging organism. Senescent cells become resistant to many apoptotic signals, contributing to their tendency to accumulate with age (Campisi & d'Adda di Fagagna, 2007). As these cells remain metabolically active and take on a number of phenotypic changes, their accrual can result in severe penalties to tissue function. They have been demonstrated to accumulate in tissues over the lifespan in multiple species, making the deleterious effects of senescent cells more pronounced in older age (Dimri *et al.*, 1995).

Apart from telomere erosion, multiple forms of cellular damage can induce senescence. Non-telomeric DNA damage, mitochondrial dysfunction, oxidative stress, chromatin disruption, and oncogene signaling are all capable of activating senescence programming (Campisi & d'Adda di Fagagna, 2007). These cellular stresses can result from internal or external sources. Regardless of the initial stimulus, signaling converges on one of two pathways to halt progression through the cell cycle.

There are two main tumor-suppressive pathways responsible for cell cycle arrest, and senescence induction. These are controlled by $p16^{INK4a}$ (p16)/ pRB (retinoblastoma protein), and p53 respectively. While both are capable of halting replication, the two pathways are not entirely equivalent. In addition to being activated by different stimuli, the p53 pathway, via the effector p21, induces escapable cell cycle arrest, while p16/pRB induction results in permanent cell cycle arrest (Campisi & d'Adda di Fagagna, 2007).

p21 activation is the downstream result of the DNA damage response (DDR). Shortened telomeres or other forms of DNA injury prompt a DDR, which activates the master gene regulator, p53. Depending on the nature and severity of the DNA damage, p53 activation can result in either cell death via apoptosis, or cellular senescence (Chen & Ames, 1994; Chen *et al.*, 2000; Debacq-Chainiaux *et al.*, 2005; Probin *et al.*, 2006). The interplay between these dueling cell fates remains unclear. In conditions favoring senescence, p53 activates transcription of the cyclin-dependent kinase inhibitor p21 (Zhang *et al.*, 1999). p21 prevents progression through the cell cycle by blocking the cyclin-dependent kinases responsible for moving the cell from G1 to S phase. If the damage is repaired and DDR signaling ceases, p21-induced arrest also ceases and the now healthy cell is able to re-enter the cell cycle.

If the DNA damage is not repaired, sustained arrest eventually causes induction of p16, which results in permanent exit from the cell cycle (Dulić *et al.*, 2000). p16 can also be activated independently in response to oncogenic Ras or BRAF signaling, but the processes by which p16 is activated remain incompletely understood (Lin *et al.*, 1998a; Di Micco *et al.*, 2006; Campisi & d'Adda di Fagagna, 2007). Bias towards p16 vs p21 activation varies between cell types and species (Campisi & d'Adda di Fagagna, 2007).

In addition to exit from the cell cycle, senescent cells are also characterized by:

- Resistance to apoptosis (Seluanov *et al.*, 2001)
- Increased lysosomal volume and β-galactosidase production (senescence-associated b-galactosidase; SA β-Gal) (Lee *et al.*, 2006)
- Chromatin remodeling (Adams, 2007)
- Enlarged and flattened morphology (Cho *et al.*, 2004)
- Senescence associated secretory phenotype - SASP (Coppé *et al.*, 2010)

SASP composition varies between cell types, but in general includes a host of pro-inflammatory cytokines, chemokines, extracellular matrix molecules and even reactive oxygen species (for full review, see Coppé *et al.*, 2010). These secreted molecules act as paracrine signals; in this way, senescent cells can alter their tissue microenvironment and detrimentally affect the function of neighboring cells. While overexpression of p16 alone is sufficient to induce replicative arrest, DDR signaling is required for the SASP (Rodier *et al.*, 2009; Coppé *et al.*, 2011).

It is believed that secretion of these pro-inflammatory molecules underlies both the beneficial and detrimental effects of senescent cells. Increasing evidence suggests that senescent cells may be major drivers of the functional decline associated with aging. Thus far, senescent cells have been demonstrated to actively impel a number of diseases, including atherosclerosis (Childs *et al.*, 2016), cancer (Campisi & d'Adda di Fagagna, 2007) and Alzheimer's disease (Bussian *et al.*, 2018; Musi *et al.*, 2018; Zhang *et al.*, 2019).

Several lineages of research support associations between chronic stress, and multiple senescence triggers. In aggregate, they present a compelling body of evidence to

support the theory that chronic stress induces cellular senescence. This review will summarize this evidence for the first time.

1.5 Effects of stress on telomeres

Telomeres are repeated TTAGGG DNA sequences that cap the ends of chromosomes. During DNA replication, incomplete terminal synthesis of the lagging strand results in a loss of some telomeric DNA. Over repeated cell divisions, this results in progressively shortening of the telomeres. In addition to preventing loss of genomic DNA during cell division, telomeres also play a crucial role in maintaining chromosomal stability. The guanosine-rich telomere DNA forms secondary structures and interacts closely with a set of telomere binding proteins collectively termed the shelterin complex (De Lange, 2005). These structures protect the single-stranded DNA overhang from being recognized as a double-strand break and triggering a DDR (Henderson & Blackburn, 1989; De Lange, 2009). Human telomeres can range up to 15 kilobases in length and cells lose 50-200 kb during each S phase (Harley *et al.*, 1990). Thus, many cell divisions are possible before chromosomal stability is compromised.

Short telomeres destabilize the chromosomal structure, making the DNA susceptible to end-to-end fusion, mutation and carcinogenesis (McClintock, 1942). Before telomeres are completely lost, they reach a critical length, termed the Hayflick limit, which triggers the DDR and activation of the tumor suppressor p53 resulting in either apoptosis, or exit from the cell cycle (Saretzki *et al.*, 1999). In a given cell, the different chromosomes may have a range of telomere lengths; however the stability and viability of the cell is defined by the shortest telomere present (Hemann *et al.*, 2001)

The progressive shortening of telomeres is counterbalanced by the activity of telomerase (Greider & Blackburn, 1985). Telomerase is a cellular ribonucleoprotein reverse transcriptase enzyme that adds TTAGGG repeats to shortened telomeres, extending telomere length, and protecting the chromosome. Numerous environmental factors can affect telomere length maintenance.

While many studies had identified a link between chronic stress and earlier onset of disease, the first study to directly link stress with biological aging came in 2004 (Epel *et al.*, 2004). In this study, researchers sought to study the relationship between maternal

caregiving stress and telomere length. Participants were premenopausal mothers to either a healthy child or a chronically ill child. Telomere length and telomerase activity was measured in peripheral blood mononuclear cells (PBMCs) isolated from blood samples. Within the group of mothers with chronically ill children, there was a negative correlation between duration of caregiving and telomere length, independent of age. However, the researchers found that rather than the health status of the child, the degree of perceived stress reported by the women was a better predictor of telomere length and telomerase activity. Although the average age of the two groups was similar, telomeres in the higher stress group were shorter by an average of 550-bp. Based on estimates of telomere shortening during adulthood, this change in telomere length corresponds to a 9–17-years difference in age. The high stress group also had lower telomerase activity and levels of higher oxidative stress. This negative correlation between stress level and telomere length has been replicated in subsequent studies (Damjanovic *et al.*, 2007; Parks *et al.*, 2009). It has also been shown that urinary catecholamine content is associated with shorter telomeres (Parks *et al.*, 2009).

Low SES has been associated with lower telomere length in some (Cherkas *et al.*, 2006) but not all studies (Adams *et al.*, 2007). These differing findings may be influenced by the observation that in older adults, stress-associated differences in telomere length are more difficult to parse. In older age, other factors such as disease burden and disease survivorship account for greater variability, obscuring most impacts of stress (Schaakxs *et al.*, 2016). Despite this, the negative effect of adverse childhood events can still be discerned in the telomere length of older adults (Schaakxs *et al.*, 2016).

Unlike the relatively straightforward negative association between stress and telomere length, there seems to be a more dynamic relationship between psychological stress and telomerase activity. One study found that high stress caregivers to a family member with dementia have lower baseline telomerase activity; however when exposed to an acute stressor they display an increase in telomerase activity equivalent to that of age-matched low stress controls (Epel *et al.*, 2010). The increases in telomerase activity were associated with the magnitude of cortisol response to the stressor. However, another study found that caregivers to a dementia patient had higher basal telomerase activity, despite shorter telomeres (Damjanovic *et al.*, 2007).

Follow-up studies have looked for possible interventions for stress-induced telomere erosion. It was found that regular physical exercise can buffer the effect of stress-induced telomere shortening in post-menopausal women (Puterman *et al.*, 2010).

1.6 Stress-induced production of ROS and oxidative damage

Of the numerous triggers for cellular senescence, reactive oxygen species (ROS) are particularly interesting as they have been independently proposed as a primary driver of aging. The free radical theory of aging, first proposed in the 1950s, posits that aging is the result of accumulated damage created by ROS (Harman, 2009). Though it has now been shown that oxidative damage does not drive aging alone, it is certainly one of the mechanisms driving the aging process. ROS, and the damage that they wreak are a major cause of cellular senescence. ROS and oxidative damage increase with age, and increased production of ROS shortens lifespan (Stadtman, 1992; Kirkwood & Kowald, 2012).

ROS are byproducts of normal cellular metabolism and are present at low levels during homeostasis (Boonstra & Post, 2004). ROS serve as signaling molecules and are present in optimally functioning cells (Atanackovic *et al.*, 2003). However, ROS can also cause damage to DNA and organelles. These molecules — including hydrogen peroxide (H_2O_2), hydroxyl radical (OH-), and nitric oxide (NO) — have fundamentally unstable chemical structures, making them "reactive". Protein oxidation and nitrosylation by ROS and reactive nitrogen species (RNS) can impair enzymatic activity leading to cellular dysfunction (for review, see Stadtman & Levine, 2000).

ROS are also capable of a number of modifications to DNA bases. The most frequent form of oxidative damage to DNA is 8-hydroxylation of guanine (Poulsen *et al.*, 2014) This modification can be misread as thymine during transcription, making it a highly dangerous modification. High urinary levels of 8-hydroxy-2'-deoxyguanosine (8-OHdG) increase risk for developing several common cancers (Loft *et al.*, 2013).

In some cases, ROS-induced damage causes rupture to the DNA sugar-phosphate backbone resulting in single or double strand breaks (DSB). DSBs are the most dangerous form of DNA damage as they are the most difficult to repair. Attempts to repair DSBs can cause loss or translocation of chromosomal segments. In worst case scenarios this can result in tumorigenesis if a tumor suppressor gene is deleted or if an oncogenic gene is

amplified (Khanna & Jackson, 2001). DSBs trigger the DDR signaling cascade, which can result in replicative senescence. Specialized protein kinases sense the DSB, causing local phosphorylation of the histone H2AX (called γ-H2AX in its phosphorylated form) and a signaling cascade culminating in activation of the master regulator p53. p53 induces cell cycle arrest by activating transcription of p21, as described in section 1.4.

The balance of ROS production and neutralization is tightly regulated under normal conditions. Oxidative damage occurs when there is an imbalance between ROS formation and antioxidant defense systems. A series of studies over the last 30 years have demonstrated that psychological stress, both acute and chronic, can result in the formation of ROS.

Both observational and experimental studies in humans demonstrate that acute stress results in a rapid increase in ROS. A number of studies have used university students taking exams as a model to study the effects of acute stress on measures of oxidative damage. One looked at measures of oxidative damage in lymphocytes in the same group of undergraduate students immediately prior to an exam, and on a "non-stress" occasion for comparison (Sivoňová *et al.*, 2004). They found an increase in DNA damage as measured by the comet assay, greater lipid susceptibility to oxidation, and decreased antioxidant levels in plasma on the exam day. Another study found lower levels of thiol, and higher levels of serum protein carbonyl and malondialdehyde (MDA) levels in students when taking an exam (Nakhaee *et al.*, 2013). Semen samples from medical students immediately before final exams contained lower levels of endogenous antioxidants glutathione and free sulphydryl and lower quality sperm than samples taken 3 months after exams (Eskiocak *et al.*, 2005).

Exposure to the Trier Social Stress Test, in which participants perform a public speaking task and then attempt mental arithmetic, elevates saliva levels of miRNAs miR-20b, -21, and -26b (Wiegand *et al.*, 2018). miR-21 is classified as an oncogene as it directly inhibits superoxide dismutase (SOD), resulting in impaired ROS degradation, and promoting tumorigenesis.

Antioxidant defense systems also appear to be activated by acute stress. In another study on undergraduate students, exam stress increased saliva levels of the antioxidant

catalase and sialic acid, and decreased levels of oxidized proteins. (Tsuber *et al.*, 2014). The increase in catalase was greater in female participants than in male, indicative of greater intrinsic antioxidant defense. This could represent a compensatory mechanism to combat elevated ROS.

However, chronic as well as acute stress is associated with greater ROS, suggesting that compensatory mechanisms to combat acute stress-induced ROS are insufficient in the long term. Adolescents who experience multiple severe adverse events have increased urinary levels of the oxidative stress markers F2-isoprostanes (IsoPs) (Horn *et al.*, 2019). Socioeconomic disadvantage is associated with elevated plasma serum IL-6, and thiobarbituric acid-reactive substance (TBARS) (Mansur *et al.*, 2016). A recent meta-analysis showed that markers for DNA damage — 8-OHdG and 8-oxo-7,8-dihydro-2'-deoxyguanosine (8-oxodG) — are significantly higher in lymphocyte and urine samples from patients with bipolar disorder or schizophrenia (Goh *et al.*, 2021). Hypertensive patients with high trait anxiety have higher plasma levels of norepinephrine, which correlates with increased ROS in mononuclear immune cells (Yasunari *et al.*, 2006).

Rodent studies have recapitulated the stress-induced ROS phenomenon observed in humans and have shed greater light on the mechanisms underlying this effect. Acute air jet stress in rats increases plasma levels of 8-isoprostane (a marker of lipid peroxidation) (D'Angelo *et al.*, 2010). A single 5-hour exposure to the communication box stress paradigm did not affect rats' liver levels of OH^8dG – a product of hydroxyl radical induced DNA damage (Adachi *et al.*, 1993). However, after a second, third or fourth exposure, stress-exposed rats had significantly higher levels of OH^8dG in liver nuclear DNA. The induced increase returned to levels equivalent to that of controls 1-hour after the stress exposure. Thus, it appears that neutralization of ROS is possible after several repeated stress exposures.

Another experiment further elucidated the time course in which stress-induced ROS recovery ceases to be possible. This experiment employed the same communication box stress paradigm on rats in a chronic study design. The rats were exposed for 1-hour per day for 1, 3 or 5 weeks. Researchers subsequently found an increase in lipid peroxidation marker MDA content in the masseter muscles after 3 and 5 weeks but not 1 week of stress

(Li, Zhang, *et al.*, 2011). Concurrently, following 3 or 5 weeks of stress, they found a decrease in the activity of antioxidant enzymes SOD, glutathione peroxidase, and catalase in the masseter muscles. In rats exposed for 5 weeks there was also an elevation in the cellular stress-sensitive protein HSP70. Together, these studies demonstrate that psychological stress is capable of inducing an imbalance favoring greater ROS and resulting in oxidative damage, despite upregulation of the protective HSP70.

These findings can also be extended to other rodent psychological stress models. Both acute (90 minute) and chronic (15 min/day for 15 days) water immersion stress increased cytochrome c reduction, lipid peroxidation and DNA fragmentation in rat intestinal and gastric mucosa (Bagchi *et al.*, 1999).

Psychological stress is capable of increasing ROS in numerous tissue types, though it seems to have a particularly profound effect on the brain. 14 days of restraint stress resulted in higher levels of ROS in the hippocampus and cerebral cortex, and higher levels of nitric oxide in the hippocampus and cerebellum in mice (Son *et al.*, 2016). It also induced greater levels of lipid peroxidation marker MDA in all three brain regions and protein peroxidation marker protein carbonyl in the hippocampus and cortex. In contrast it reduced levels of the antioxidant enzymes SOD and glutathione reductase-transferase.

In rats, elevated levels of 8-OHdG in the brain can be detected prior to the advent of other stress induced pathologies. 2 weeks of social isolation is sufficient to increase mRNA expression in the nucleus accumbens and hypothalamus of NADPH oxidase (NOX2), an enzyme that catalyzes formation of superoxide anion O_2^- (Schiavone *et al.*, 2012; Colaianna *et al.*, 2013). This is associated with an increase in 8-OHdG in both regions, and an increase in nitrotyrosine – a marker of reactive RNS— in the hypothalamus. After 4 weeks, elevations of NOX2 and 8-OHdG in the prefrontal cortex can be detected as well. After 7 weeks, these markers are also elevated in the adrenal glands (Colaianna *et al.*, 2013). The majority of 8-OHdG and nitrotyrosine positive cells in the hypothalamus were neurons. In the prefrontal cortex, the NOX2 subunit $p47^{phox}$ was increased specifically in pyramidal neurons, not in GABAergic neurons, astrocytes, or microglia (Schiavone *et al.*, 2012). Alterations in behavior, increase in glutamate levels and loss of parvalbumin were detectable after 4 weeks of social isolation (Schiavone *et al.*, 2012).

In the accelerated senescence SAMP-10 mouse model, confrontational housing — a model for psychosocial stress — increased levels of the DNA damage marker 8-oxo-dG can be found in the cerebral cortex (Unno *et al.*, 2011). This was also associated with accelerated cognitive decline and shorter lifespan. Out of place

It appears possible that in some circumstances, a positive feedback loop between the stress response and ROS production could exist. Overexpression of genes glyoxalase 1 and glutathione reductase 1 in the cingulate cortex increase anxiety-like behavior, while local inhabitation of glyoxalase 1 expression by RNA interference decreases the anxiety-like behavior (Hovatta *et al.*, 2005). However, these results were found to be highly dependent on mouse strain.

The physiological mechanisms underlying stress-induced ROS overproduction have been further illuminated using cell cultures. Acute exposure to cortisol or norepinephrine was sufficient to increase levels of electrochemically measured ROS and RNS in breast cancer cells, while addition of their respective receptor antagonists mitigated this effect (Flaherty *et al.*, 2017). Exposure to the hormones also resulted in an increase in γ-H2AX foci, indicative of DNA damage. Presence of a nitric oxide synthase inhibitor also attenuated the effect of cortisol on DNA damage, indicating that this is the mechanism by which cortisol causes DNA damage. Mice injected with breast cancer cells and subjected to 1 hour restraint stress 3 days per week for 4 weeks had higher iNOS expression in tumors than singly housed control mice (Flaherty *et al.*, 2017).

This substantial body of work provides convincing evidence that stress causes an increase in ROS production, and that this results in oxidative damage to DNA in numerous organs. Additionally, the consistency between human and rodent physiology in this regard suggests that even more insight can be gained through research on rodent stress models. Stress-induced ROS overproduction directly results in DNA damage — one of the primary triggers for cellular senescence. This alone presents compelling evidence for stress-induced cellular senescence as a potential phenomenon.

1.7 Stress and DNA damage repair

In addition to causing DNA damage via increased ROS and RNS production, some studies indicate that stress may impair the repair of damaged DNA. Short term (<30

minute) in vitro exposure of murine 3T3 cells to cortisol or norepinephrine not only increases DNA damage on its own, but also interferes DNA repair in cells exposed to UV radiation (Flint *et al.*, 2007). Epinephrine exposure produced a similar degree of DNA damage but did not impair DNA repair. All three stress hormones induced upregulation of DNA damage sensors Chk1 and Chk2, and the proto-oncogene CDC25A, which is involved in cell cycle delay following DNA damage (Flint *et al.*, 2007).

24-hour exposure to epinephrine or norepinephrine increases DNA damage, as assessed by comet assay, in the murine 3T3 cell line (Flint *et al.*, 2013). This effect is blocked by pre-treatment with the β-adrenergic receptor antagonist propranolol. This damage is functionally relevant, as cells treated with either catecholamine undergo greater malignant transformation in-vitro and become tumors more rapidly in-vivo when implanted in mice (Flint *et al.*, 2013).

This finding can be extended to other cell types and species. In human breast cancer cells, DNA repair following exposure to H_2O_2 was impaired in the presence of cortisol (Flaherty *et al.*, 2017). This is backed up by studies using cells sampled from a clinical population. Lymphocytes sampled from participants who scored highly for distress on the Minnesota Multiphasic Personality Inventory exhibited poorer DNA repair 5 hours after X-irradiation (Kiecolt-Glaser *et al.*, 1985).

Mice treated with the synthetic epinephrine analogue isoproterenol accumulated DNA damage in the thymus, as quantified by γ-H2AX (Hara *et al.*, 2011). Interestingly, isoproterenol treatment also decreased levels of the DNA damage responder, and senescence regulator p53. These findings were replicated in vitro in several cell lines and was further demonstrated to be mediated specifically by b2-adrenergic receptor (β2-AR) signaling. β2-AR activation, via a phosphoinositide 3-kinase/AKT cascade, resulted in phosphorylation of murine double mutant 2 (MDM2). MDM2, with aid from the adaptor arrestin β-1 (ARRB1), causes export of p53 from the nucleus to the cytosol, and subsequently ubiquitination and degradation. The authors suggest that stress-induced sympathetic nervous system activity, promotes DNA damage both directly, and indirectly via suppression of p53-mediated DNA repair. This may consequently result in worse DNA

damage, and a lower likelihood of successful repair ultimately leading to permanent senescence.

Overall, multiple stress hormones appear to induce DNA damage via increased ROS production, as well as impair DNA repair. Taken together, the resulting DNA damage would make cellular senescence much more likely.

1.8 Stress, inflammation and SASP

A systemic rise in inflammatory mediators is a common feature of aging. This phenomenon, termed "inflammaging" is associated with elevated risk for cardiovascular disease as well as a number of other chronic aging-related diseases (Ferrucci & Fabbri, 2018). The root causes of inflammaging remain poorly understood, though immune dysregulation is a critical factor (Ferrucci *et al.*, 2010; Fulop *et al.*, 2018).

A large body of research indicates that psychological stress promotes inflammation both in the brain, and in the periphery (Frank *et al.*, 2006; Rohleder, 2014; Calcia *et al.*, 2016). This finding has been replicated in both humans and laboratory rodents. Caregiver stress, low SES, work-related stress and childhood adversity are all associated with elevations in inflammatory markers (Rohleder, 2014). Chronic unpredictable mild stress increases circulating plasma levels of IL-6, IL-1β, TNF-α and IL-10 in rats (López-López *et al.*, 2016). Changes in circulating cytokine levels are apparent after 20 days of stress and continued up until the conclusion of the experiment at 60 days. This preceded elevations in markers of oxidative damage to proteins and lipids in the liver.

During an extended period of chronic stress, there are fluctuations in multiple cytokines. This was demonstrated in a study that subjected female mice to 6-hours of daily restraint stress for 28 days, monitoring serum cytokine levels throughout, and during 2 weeks of recovery (Voorhees *et al.*, 2013). Circulating plasma levels of IL-6 were overall increased throughout the 4 weeks of restraint stress but returned to levels indistinguishable from controls during by day 7 of recovery. Serum IL-10 was lower overall during the both the restraint and recovery phases. In the brain — specifically the cortex and hippocampus — IL-10 was reduced throughout the period of restraint and recovery as well.

Neuroinflammation in particular is a well-known consequence of chronic stress and increased inflammation is a common phenotype of normal brain aging across species (Frank *et al.*, 2006). A number of stressors promote microglial activation, as measured by Iba1 activity (Calcia *et al.*, 2016). In particular, a very strong effect has been found in area CA1 of the hippocampus. (Kojo *et al.*, 2010; Bian *et al.*, 2012). This increase in microglial activation has been demonstrated to lead to the secretion of cytokines and chemokines, which facilitate development of anxiety-like behavior (Tynan *et al.*, 2010; Wohleb *et al.*, 2011, 2012, 2013). Stress exposure also promotes production of proinflammatory monocytes in the bone marrow, which are released into general circulation and can migrate and localize in the brain in addition to other organs (Wohleb *et al.*, 2011; Powell *et al.*, 2013; Heidt *et al.*, 2014).

The relationship between senescence and inflammation is interesting and multifaceted. On the one hand, an imbalance of inflammatory signaling can result in ROS and DNA damage, and thus promoting senescence. Additionally, senescent cells, via the SASP, have been proposed as a primary contributor to inflammaging (Olivieri *et al.*, 2018). This bidirectional interplay may be an important feature of aging.

1.9 Conclusions

Chronic stress poses a significant public health threat. It is associated with elevated risk for chronic aging related diseases, which are the primary causes of disability and death in older adults. Psychosocial stress is a particularly potent form of stress and is a key contributor to the numerous adverse health outcomes associated with low SES.

Chronic stress has long been theorized to accelerate the aging process. In this Review, we gave an overview of the scientific literature that implicates a link between psychological stress and cellular senescence. Stress has been demonstrated to promote a number of senescence triggers, including telomere erosion, oxidative damage, and DNA damage. Moreover, stress is associated with systemic inflammation, which can both promote senescence-inducing cellular damage, and also be a consequence of senescent cell accumulation. Cellular senescence should be considered as a consequence of chronic stress and a potential mediator of stress-induced vulnerability to aging-associated dysfunction.

CHAPTER 2

CHRONIC STRESS INDUCES SENESCENT CELL ACCUMULATION IN MICE

Others' Contributions: Maria Razzoli, Rachel Mansk, Giada Caviola, Madeleine Berg, Nivedita Sabarinathan and Jean-Pierre Pallais assisted with in vivo experiments. Matthew Yousefzadah conducted the qPCRs on the peripheral blood mononuclear cells from 20 and 26 month old mice. Seth McGonigle conducted qPCRs on the kidney, liver and lung.

2.1 Summary

Chronic stress can shorten lifespan and is a risk factor for a diverse range of aging-related diseases. This phenomenon was described over a century ago in humans and has been recapitulated in both wild and laboratory populations of social mammals. Despite the consistency of this relationship, it remains unclear how stress might affect aging biology. An association between stress exposure and induction of a fundamental aging process such as cellular senescence has been proposed, but experimental evidence is lacking. Here we establish that a social stress model — chronic subordination stress (CSS) — induces a progressive and time-dependent increase in *p16*-positive senescent cells even in young mice. 4 weeks of CSS is sufficient to increase the number of cells expressing senescence markers *p16, p21,* and/or senescence-associated β-galactosidase in peripheral blood mononuclear cells, the hippocampus, neural cortex, and subcutaneous white adipose tissue. Conversely, restraint stress, a widely used model of non-social psychological stress, induces expression of *p21* only in the brain, and in a *p16*-independent manner. Confirming the brain as a primary target of CSS-induced senescent cells (SNCs), we interrogated their cell type identity using two independent mouse models and a variety of molecular

approaches. We determined that the majority of *p16*/*p21* expressing SNCs caused by CSS were neurons and astrocytes, with other cell types representing only a small fraction. Spatial transcriptomic profiling of the brains of CSS-exposed mice implicates the DNA Damage Response and elevated Ras/Raf signaling as mechanisms of CSS-induced senescence in the brain. Moreover, CSS-induced SNCs alter their local microenvironment, via pathways including interleukin signaling, and changes to the extracellular matrix. Clearing SNCs with a pharmacogenomic approach prevented CSS-induced accumulation of *p16*/*p21* positive SNCs, while leaving stress-induced physiological changes unabated. Lastly, lifelong pharmacogenetic removal of SNCs is detrimental to healthspan and lifespan, and further exacerbates CSS-induced deficits in these measures. These findings establish that different forms of stress can elevate expression of senescence markers but involve different senescence induction pathways. Moreover, they add to previous literature documenting a role for senescent cells for health maintenance in aging. By demonstrating that stress, particularly social stress, promotes cellular senescence, this study suggests a possible mechanistic link between stress and aging.

2.2 Introduction

Stress is associated with numerous aging-related diseases including Alzheimer's Disease, vascular dementia, Huntington's Disease, Parkinson's Disease, type 2 diabetes, and atherosclerosis (Yudkin *et al.*, 2000; Gu *et al.*, 2012; Hemmerle *et al.*, 2012; Mo *et al.*, 2014; Gerritsen *et al.*, 2017; Harris *et al.*, 2017; Yuede *et al.*, 2018; Yao *et al.*, 2019). However, there are no individual, or unifying mechanistic explanations for these associations. One unifying factor for this diverse group of diseases is that they are primarily diseases of aging. Although it has long been believed that stress can accelerate biological aging, the nature of this phenomenon has not been characterized.

A complicating factor in human and rodent stress research is the variability of stressors and stress responses themselves. Different rodent stress models activate the HPA and SAM systems to varying degrees (Ulrich-Lai & Herman, 2009; Koolhaas *et al.*, 2011). "True" stress is proposed to only be present in conditions characterized by unpredictability, uncontrollability, and real or perceived life threat (Koolhaas *et al.*, 2011).Using this definition, social stressors such as chronic subordination stress (CSS) are particularly

potent activators of stress response compared with other types, such as physical (cold water stress, foot shock) or psychological (restraint stress, forced swim) (Koolhaas *et al.*, 1997; Bartolomucci, 2007). A model like restraint stress elicits a less dramatic HPA response than social stress models and can eventually result in habituation (Girotti *et al.*, 2006; Koolhaas *et al.*, 2011). The range of stress types and intensities likely contributes to our lack of understanding of the relationship between stress and biological aging.

Given the diversity of aging-related diseases precipitated by stress, the possibility should be considered that stress affects a fundamental aging process that contributes to the etiology of each of these pathologies. Correlational evidence points to an association between chronic stress and cellular senescence. In one study, women who reported higher stress levels had shorter telomeres and lower telomerase activity in circulating immune cells than those with low reported levels of stress (Epel *et al.*, 2004). Shortened telomeres are the classical trigger for cellular senescence (Hayflick & Moorhead, 1961). High stress is also associated with greater oxidative stress – an independent senescence promoter (Aschbacher *et al.*, 2013). Low socioeconomic status (SES) and life stress have been associated with lower telomere length in some studies (Cherkas *et al.*, 2006) as well as greater oxidative damage (Mansur *et al.*, 2016; Horn *et al.*, 2019). Lower SES has also been associated with increased expression of the senescence marker $p16^{INK4a}$ (*p16*) (Rentscher *et al.*, 2019). Finally, a recent study established that this phenomenon may be evolutionary conserved in rodents; the study demonstrated that subordinate mice exposed to lifelong psychosocial stress had shortened lifespan and increased expression of senescence markers p16 and p53 in several organs (Razzoli *et al.*, 2018).

Cell cycle arrest, the central feature of senescent cells (SNCs) can be initiated by two different cyclin-dependent kinase inhibitors, but they are not identical either in the sequence of events that leads to their activation, or in the permanence of the senescence they induce (Campisi & d'Adda di Fagagna, 2007). p21 becomes activated by a signaling cascade beginning with the DNA damage response (DDR). p21-induced senescence is escapable, acting as a temporary recess from the cell cycle until DNA damage can be repaired. If p21-induced arrest is sustained however, eventually p16 becomes expressed as well, resulting in permanent cell-cycle arrest. p16 can also be directly induced by other factors, including oncogenic signals (Lin *et al.*, 1998b; Di Micco *et al.*, 2006). In addition

to growth arrest, SNCs take on a number of other distinctive characteristics including secretion of a set of molecules termed the Senescence Associated Secretory Phenotype, or SASP. The SASP develops over the course of weeks and is primarily driven by the DDR (Rodier *et al.*, 2009). Its composition varies depending on cell type, but it primarily consists of inflammatory, growth promoting and remodeling factors, such as cytokines, matrix metalloproteinases, and monocyte chemoattractant proteins (Coppé *et al.*, 2010). The SASP is the primary mechanism by which SNCs can alter their microenvironment and can exert both beneficial and detrimental effects depending on the context. SNCs are resistant to apoptosis and must be cleared by immune cells, which the SASP can help to attract (Kang *et al.*, 2011; Childs *et al.*, 2014).

Transient accumulation of SNCs can exert a number of beneficial effects, including wound healing, and aiding in embryonic development; they also appear to play a crucial role in maintaining liver integrity during aging (Demaria *et al.*, 2014; Grosse *et al.*, 2020). However, perpetually lingering SNCs and their accompanying SASP can contribute to chronic inflammation, a hallmark of aging and major factor in aging-related diseases. SNCs have been shown to actively drive aging-related diseases in transgenic mouse models of atherosclerosis, osteoarthritis and Alzheimer's disease, (Baker *et al.*, 2016; Jeon *et al.*, 2017, 2018; Bussian *et al.*, 2018; Musi *et al.*, 2018; Zhang *et al.*, 2019). Their role in so many diseases makes SNCs an alluring target for intervention (Kirkland *et al.*, 2017; Niedernhofer & Robbins, 2018; Kim & Kim, 2019; van Deursen, 2019; Robbins *et al.*, 2021). However, such treatments would need to be highly targeted so as not to interfere with the beneficial roles played by senescent cells (Grosse *et al.*, 2020). As of now, key characteristics remain uncertain, including disagreement on the cell type identity of the SNCs in these disease contexts, and a poor understanding of the environmental drivers that prompt maladaptive accumulation of SNCs. Such questions will need to be answered in order for senolytic treatments to be developed and appropriately administered.

The set of diseases shown to be actively driven by SNCs is remarkably similar to the set promoted by chronic stress in animals and humans. This, together with the evidence that stress induces senescence initiators such as oxidative damage and telomere erosion, supports the theory that chronic stress can accelerate accumulation of SNCs. However, this phenomenon has never been comprehensively examined nor its consequence were

evaluated. Here, we demonstrate that: 1) Chronic Subordination Stress (CSS), but not Chronic Restraint Stress, causes gradual accumulation of senescent immune cells; 2) both CSS and restraint stress upregulate senescence markers in the brain, with CSS-induced senescence being p16-dependent, and restraint stress p16-independent; 3) the majority of CSS-induced SNCs in the brains of young mice are neurons and astrocytes; 4) CSS-induced senescence is associated with increased DDR and Ras/Raf signaling; and finally 5) short term clearance of CSS-induced SNCs has no short-term physiological effect, but long term clearance exacerbates lifelong CSS-induced shortening of lifespan.

2.3 Results

Chronic subordination stress but not chronic restraint stress gradually upregulates *p16* expression in PBMCs

Previous work established a link between chronic stress and elevations in some markers of cellular senescence (Razzoli *et al.*, 2018; Rentscher *et al.*, 2022). However, the time course, tissue specificity and cell-type specificity of this effect have not previously been investigated. To determine whether social and/or non-social psychological stress would induce accumulation of SNCs, we exposed mice to one of two established models of chronic stress — chronic subordination stress (CSS) or chronic restraint stress (Fig 1A).

We assessed the temporal dynamic of stress-induced accumulation of SNCs by longitudinally measuring *p16* expression in peripheral blood mononuclear cells (PBMCs). CSS-exposed mice developed the expected hyperphagia and body weight gain characteristic of the model (**Figure 1B, 1C**). We found that CSS caused a time course-dependent elevation in *p16* transcript in PBMCs first apparent after 4 weeks (**Figure 1D**). Following the 4 weeks of daily defeats, the CSS mice remained cohoused in sensory contact with their aggressor, sustaining the perceived threat/stressor (Razzoli *et al.*, 2018) (**Figure 1A**) and we continued to sample PBMCs over time. The increase in *p16* expression was sustained and continued to rise at a higher rate than that of singly housed control mice (significant group effect p=0.0353; **Fig 1D**). Conversely, though restraint stress induced the expected decrease in body weight (significant main group effect p=0.0053**; Figure 1F**), restraint stress did not affect PBMC *p16* expression at any time point analyzed (**Figure 1G**).

Based on this result demonstrating that CSS elevates *p16* expression in young mice (up to 7 months of age at the latest time point assessed), we repeated the same sampling protocol in an independent cohort of mice that had underwent the same CSS + aging paradigm (Razzoli *et al.*, 2018) and were 20 months old at the first analysis time point. At 20 months of age, CSS-exposed mice had a seven-fold elevation in PBMC *p16* expression compared with age-matched, singly housed controls ($p<0.0001$; **Figure 1H**). This disparity in *p16* expression continued to expand over time; by 26 months of age, CSS mice had 12-times higher expression of *p16* in PBMCs ($p<0.0001$; **Figure 1I**). In the window between 20 and 26 months, there is a significant increase in *p16* expression in the surviving CSS mice, but not the control group ($p<0.0001$; **Figure 1J**).

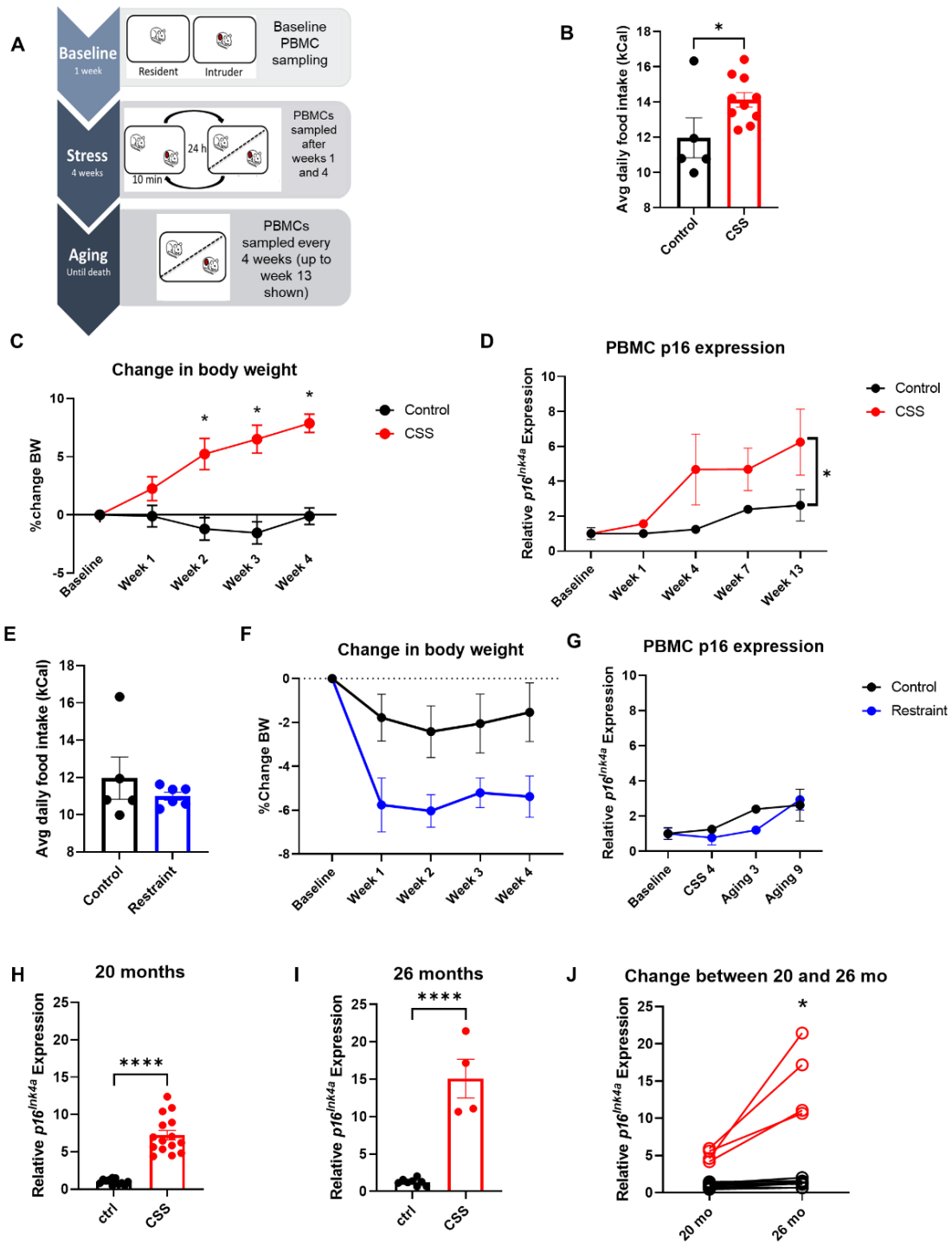

Figure 1 Chronic subordination stress but not chronic restraint stress gradually upregulates *p16* expression in PBMCs A) Experimental timeline **B)** Average daily food intake**.** CSS-exposed mice consumed significantly more calories daily than control mice (p=0.0455). Unpaired t test. **C)** Change in body weight over course of baseline and stress phase. CSS-exposed mice gain significantly more body weight. 2-way repeated measures ANOVA (Group: p = 0.0017, Time

p=0.0011, Group x Time: p<0.0001. with Tukey post hoc. **D)** Relative *p16* mRNA transcript abundance over time. CSS-exposed mice have a significant increase in *p16* expression over the course of the stress experiment. Mixed effects analyses (REML). Group: p=0.0353, Time: p=0.0934, Group x Time: p=0.8469 Tukey posthoc. Main effect of group p=0.0353. **E)** Average daily food intake. No significant difference between groups. Unpaired t test. **F)** Change in body weight over course of baseline and stress phase. Restraint-exposed mice lose significantly more weight than control mice 2-way repeated measures ANOVA Group: p<0.0001, Time: p=0.0054, Group x Time: p<0.0001. Tukey post hoc. **G)** No significant difference in PBMC *p16* expression between control and restraint-exposed mice. Mixed effects analysis (REML) Group: p=0.4465, Time: p=0.0269, Group x Time: p=0.3204. Tukey post hoc. **H)** Relative *p16* transcript abundance in PBMCs at 20 months of age. CSS-exposed mice have significantly higher *p16* expression relative to singly-housed controls (p<0.0001). Unpaired t test. **I)** Relative *p16* transcript abundance in PBMCs at 26 months of age. CSS-exposed mice have significantly higher *p16* expression relative to singly-housed controls (p<0.0001). **J)** PBMC *p16* expression in mice surviving to 26 months of age. CSS-exposed mice have a significant increase in *p16* expression in this time frame (p<0.0001) while control mice do not. 2-way repeated measures ANOVA Group: p<0.0001, Time: p=0.0002, Group x Time: p=0.0003. Sidak's multiple comparisons test. * indicates p<0.05, ** indicates p<0.01 *** indicates p<0.001, **** indicates p<0.0001. Histogram bars and X/Y data points represent group mean. Error bars represent standard error.

CSS induces senescence in the brain via a p16-dependent mechanism

Having established that 4 weeks of CSS was sufficient to increase senescence markers in PBMCs of young mice, we next sought to ascertain whether this occurred in other organ systems.

Senescence-associated β-galactosidase staining (SA β-gal) is an established biomarker for cellular senescence, and its activity correlates with increased expression of other senescence markers, such as *p16*, in multiple organs (Dimri *et al.*, 1995). Though a robust marker of senescence in some tissues, reports indicate that SA β-gal is not a good marker for cellular senescence in the brain (Piechota *et al.*, 2016).

Mice subjected to 4 weeks of CSS had significantly more SA β-gal positive cells in the subcutaneous white adipose tissue (scWAT) than controls (p=0.001; **Figure 2B, 2C**).

White adipose tissue is known to be particularly senescence sensitive (Schafer *et al.*, 2016), and previous work from our lab and others indicated that CSS can alter adipose tissue function (Sanghez *et al.*, 2016). In contrast, there was no significant change in SA β-gal staining in the liver (**Figure 2D**), kidneys or lung (not shown). The brain was not analyzed based on previous published work (Piechota *et al.*, 2016).

We next expanded our assessment to a broader panel of tissues and sought to determine whether changes in senescence markers were dependent on p16 expression. We took advantage of the selective p16+ cell detection and elimination mechanism inherent to the p16-3MR mouse line (Demaria *et al.*, 2014) in order to determine whether removal of p16+ cells would also ameliorate expression of other senescence and SASP markers. In the p16-3MR model, the $p16^{INK4a}$ promoter drives expression of a viral thymidine kinase, which unlike mammalian thymidine kinase, has a high affinity for the antiviral drug ganciclovir (GCV). When phosphorylated by the thymidine kinase, GCV is converted into a DNA chain terminator, causing cell death. Thus, by administering GCV we are able to selectively remove p16+ senescent cells. Control, CSS and restraint-exposed mice were dosed with two rounds of GCV injections, or an equal volume of vehicle (see **Figure 2A** for experimental design).

We used RT-qPCR to measure the abundance of key senescence and SASP-related genes in a panel of tissues — brain (cerebellum, cortex, hippocampus), kidney, liver, lung, scWAT. We chose the hippocampus, cortex, and cerebellum as regions of interest as they are anatomically and functionally distinct brain regions. 4-weeks of CSS induced an increase in senescence and SASP markers in some but not all tissues examined. The organ we found to be most sensitive to SNC accumulation was the brain. The hippocampus and cortex (Fig 2E, G), but not cerebellum of CSS mice had elevated levels of *p16* and its proxy *mRFP* ($p<0.05$). The hippocampus of CSS-exposed mice also had significantly higher expression of *p21* and *IL-1β* ($p<0.05$; **Figure 2E**). The scWAT also exhibited strong trends towards elevated levels of multiple senescence markers, though not to the point of statistical significance (**Appendix Supplementary Figure 1**). Conversely, expression of SNC markers remained unaffected in the cerebellum, kidneys, liver, and lung (**Appendix Supplementary Figure 1**).

Importantly, treatment with GCV successfully ameliorated the CSS-induced elevation of SNC markers. In the hippocampus, this effect was not limited to *mRFP* and *p16* but extended to *p21* and *IL-1β* (**Figure 2E**). As expected, considering the young age of the experimental subjects, GCV treatment in control animals had minimal and insignificant impact on gene expression.

mRFP expression across all organs increased linearly with *p16* (Pearson's $r=0.7147$; $p<0.0001$; **Figure 2I**) indicating successful function of the p16-3MR mechanism. *p21* expression in the hippocampus of CSS mice correlates linearly with *p16* (Pearson's $r=0.7708$; $p<0.0001$; **Figure 2J**), but does not in restraint mice (**Figure 2K**).

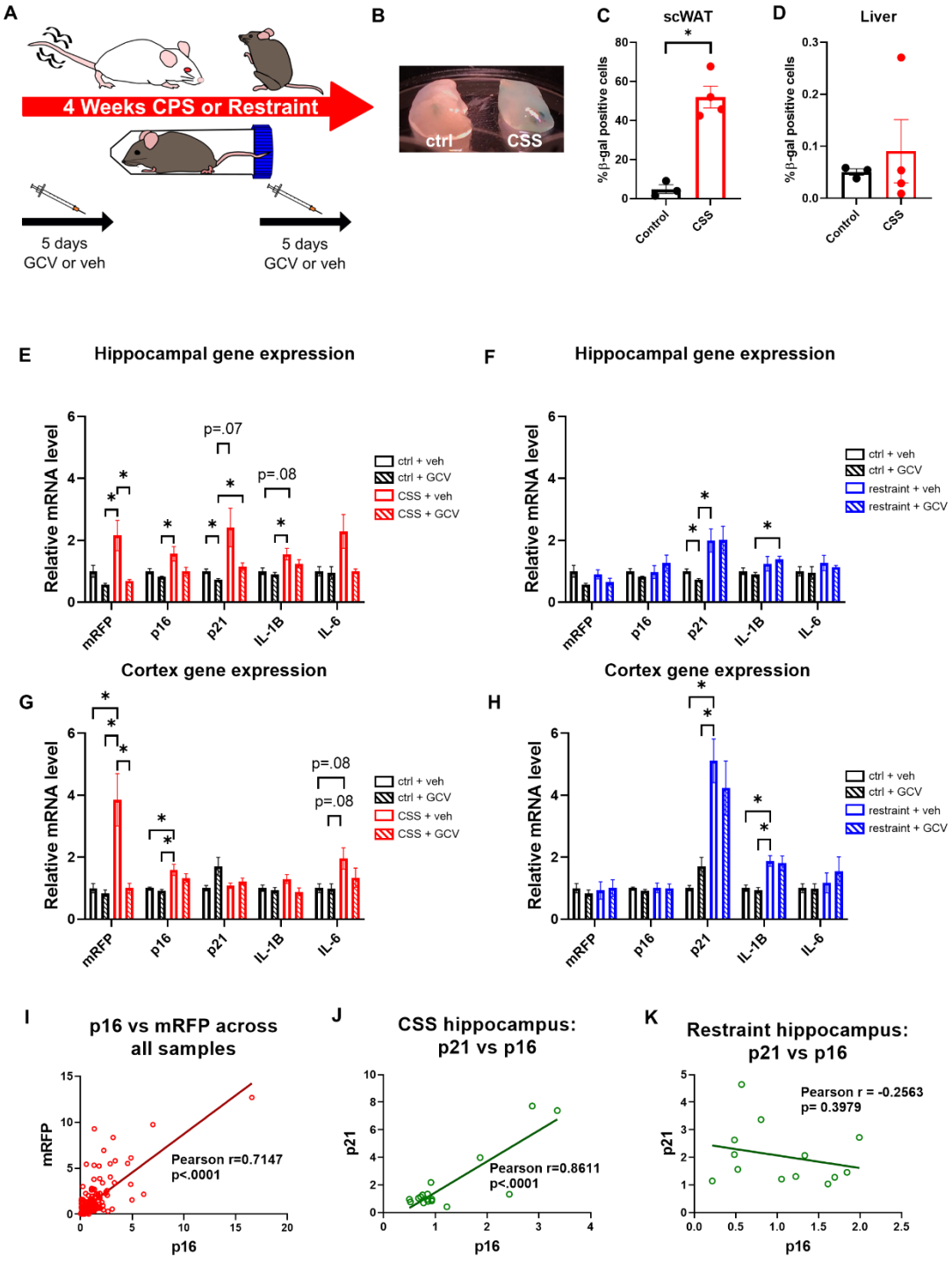

Figure 2 CSS induces senescence in the brain via a *p16*-dependent mechanism; restraint stress increases *p21* and *IL-1β* in the brain A) Illustration of experimental design. **B)** Representative gross image of subcutaneous white adipose tissue (scWAT) of a control and CSS mouse following senescence-associated β-galactosidase staining. **C)** CSS mice have significantly more SA β-gal positive cells in the scWAT than control mice (p=0.001). Unpaired t test. **D)** No significant

difference between control and CSS mice in SA β-gal staining in the liver. Unpaired t test. **E)** Expression of senescence and SASP genes in the hippocampus of control and CSS-exposed mice in the presence or absence of ganciclovir (GCV). Mixed effects analysis (REML) Group: p=0.0233, Gene: p=0.4742, Group x Gene p=0.1204. Tukey post hoc. **F)** Expression of senescence and SASP genes in the hippocampus of control and restraint-exposed mice in the presence or absence of ganciclovir (GCV). 2-way repeated measures ANOVA. Group: p=0.0107, Gene: p=0.0135, Group x Gene p=0.1564. Tukey posthoc. **G)** Expression of senescence and SASP genes in the cortex of control and CSS-exposed mice in the presence or absence of ganciclovir (GCV). Mixed effects analysis (REML). Group: p=0.0055, Gene: p=0.1402, Group x Gene: p<0.0001. Tukey posthoc. Significant main effect of group p=0.0055. **H)** Expression of senescence and SASP genes in the cortex of control and restraint-exposed mice in the presence or absence of ganciclovir (GCV). 2-way repeated measures ANOVA Group p<0.0001, Gene: p<0.0001, Group x Gene: p<0.0001. Tukey posthoc. Significant main effect of group (p<0.0001). **I)** There is significant correlation between *p16* and *mRFP* expression across all samples and tissues analyzed. Pearson's correlation coefficient r=0.7944, p<0.0001. **J)** There is significant correlation between *p16* and *p21* expression in the hippocampus of CSS-exposed mice. Pearson's correlation coefficient r=0.7147, p<0.0001). * indicates p<0.05, ** indicates p<0.01 *** indicates p<0.001, **** indicates p<0.0001. Histogram bars and X/Y data points represent group mean. Error bars represent standard error.

Restraint stress induces an elevation in *p21* and *IL-1β* in the brain

Employing the same timescale and GCV treatment regime, we assessed whether chronic restraint stress would affect senescence/SASP-related gene expression in the brain. In contrast to the effects observed in CSS-exposed mice, we found that mice subjected to 4 weeks of restraint stress manifested highly elevated levels of *p21* and *IL-1β* in the cortex and hippocampus (p<0.05), but not *p16* or its proxy in the p16-3MR line, *mRFP* **(Figures 2F, 2H**). Furthermore, while the CSS induced changes in gene expression were sensitive to GCV treatment, the increase in *p21* and *IL-1β* in restraint-exposed mice were not, suggesting that their elevation is p16 independent. We did not observe changes in senescence or SASP-related gene expression in the scWAT or any other organ of restraint-exposed mice (**Appendix Supplementary Figure 1**).

Neurons and astrocytes are susceptible to CSS-induced senescence

Having established that CSS increases SNC abundance in select brain regions, we next sought to characterize the cell type identity of the putative SNCs. Previous studies have reported conflicting findings regarding identity of SNCs in the brain with separate studies proclaiming neurons, microglia, astrocytes and oligodendrocyte precursors to be

the primary SNC type found in the brains of mouse disease models (Bussian *et al.*, 2018; Musi *et al.*, 2018; Zhang *et al.*, 2019; Ogrodnik *et al.*, 2021). We first used RNAscope fluorescent in situ hybridization to interrogate the identity of stress induced SNCs in the brain. Though it is not a high-throughput method, it gives an accurate representation of the cell-types breakdown of *p16*/*p21*+ cells in the brain. We co-labeled 4 sets of brain sections with probes for *Cdkn2a* (*p16*), *Cdkn1a* (*p21*) and a cell type marker for either *Aldh1l1* (astrocytes), *Rbfox3* (NeuN; neurons), *Cspg4* (NG2; oligodendrocyte precursors), or *Tmem119* (microglia). After visual inspection of the whole brains, we identified subregions that were particularly abundant in either *p16* or *p21*. These were the hippocampus, the somatosensory cortex, and the orbitofrontal cortex. Notably, presence of *p16/p21* in other stress-sensitive regions such as amygdala and midbrain regions was minimal (data not shown). 24 fields of view were recorded from the subiculum, CA1, CA3, dentate gyrus, somatosensory cortex, and orbitofrontal cortex from each brain, netting a total of 96 fields of view per mouse. The images were thresholded by an observer blinded to experimental condition, and a custom pipeline in CellProfiler was used to colocalize markers appearing on the same nuclei (Erben *et al.*, 2017).

We found that across all brain regions, *p16* puncta most frequently colocalized with a neuronal marker NeuN; 45% of *p16* expressing cells expressed NeuN (**Figure 3C**). Just slightly less abundant were *p16*+ astrocytes (34% **Figure 3C**). A much smaller fraction colocalized with Tmem119 (microglia; 14%) and NG2 Cspg4 (oligodendrocyte precursors; 7%), Though this method was not suitable for full quantification of senescent cells in the brain, it was notably consistent with qPCR results, showing that vehicle-treated CSS mice displayed elevated levels of *p16* positive cells and that GCV treatment abolished this effect, normalizing cell counts back to control levels.

p21 proved to be expressed at higher levels than *p16*, even in control mice. *p21* preferentially colocalized with *NeuN*-expressing cells with 71% of *p21*+ cells also expressing *NeuN* (**Figures 3G, 3H, 3I, 3J**). Again, *Aldh1l1*+ astrocytes were the next most frequent *p21*+ cell type (19%) with a small population of *Tmem119*+ microglia (8%) and *NG2*+ oligodendrocyte precursors (2%).

The cell type composition of *p16/p21* double positive cells was quite similar to that of *p16*-only positive cells. 47% of the *p16/p21* double positive cells were *NeuN* positive, 28% expressed *Aldh1l1*, 17% expressed *Tmem119* and 8% expressed *NG2* **(Figure 3K**). There was some regional variability in double positive cell type breakdown. Neurons represented a greater fraction in the cortex (58%) (**Figure 3M**) while astrocytes and microglia were more prominent in the hippocampus (31% and 20% respectively) (**Figure 3L**).

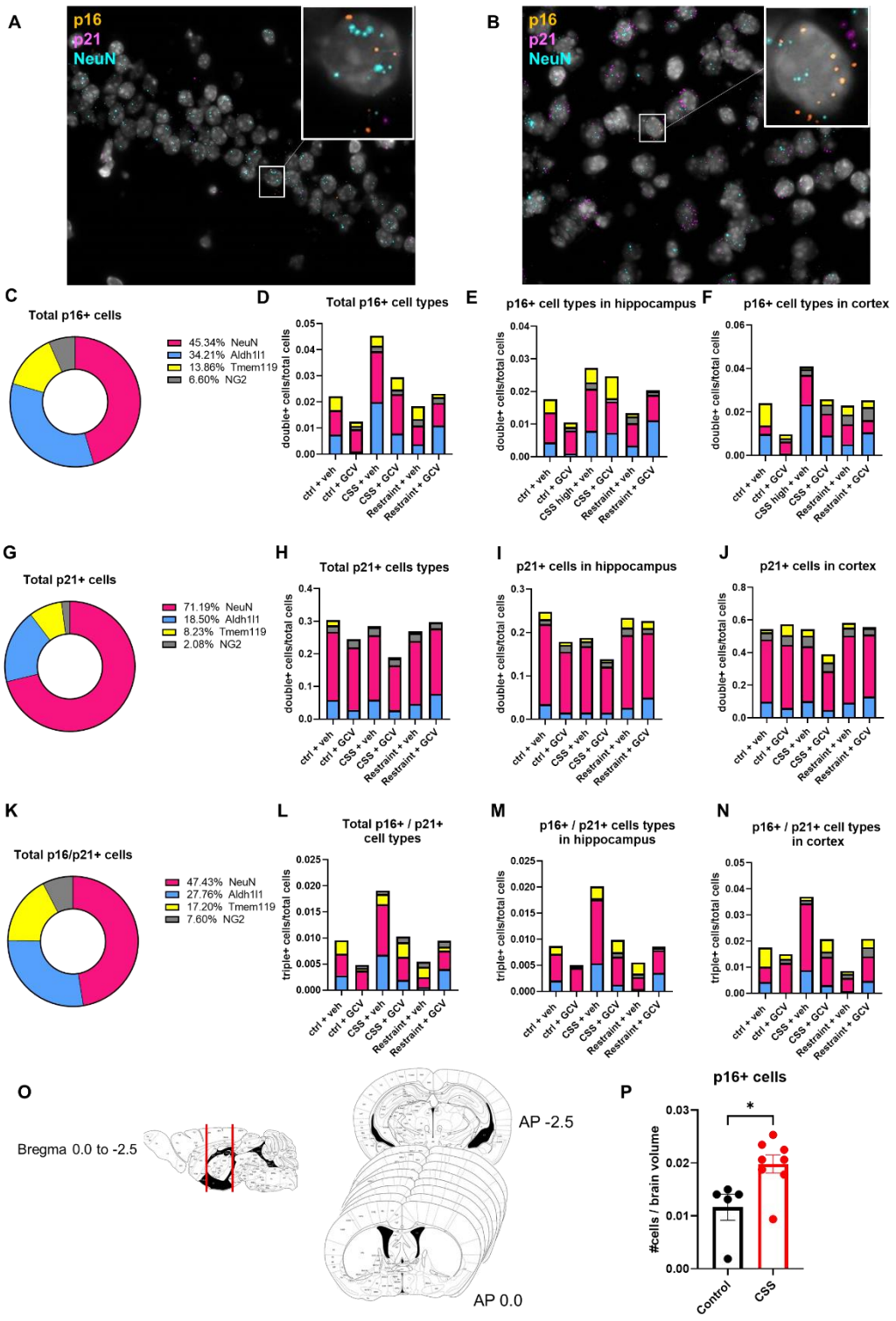

Figure 3. Neurons and astrocytes are susceptible to CSS-induced senescence A), B) Representative images of fluorescent in situ hybridization labeling of *p16*, *p21* and *NeuN* in CSS + veh brains. **C)** Percentage breakdown of *p16*+ cell types across all images. **D)** Number of *p16*+

cells of each cell type/total number of cells in those images across all brain regions. **E)** Number of *p16*+ cells of each cell type/total number of cells in those images in the hippocampus. **F)** Number of *p16*+ cells of each cell type/total number of cells in those images in the cortex. **G)** Percentage breakdown of *p21*+ cell types across all images. **H)** Number of *p21*+ cells of each cell type/total number of cells in those images across all brain regions. **I)** Number of *p21*+ cells of each cell type/total number of cells in those images in the hippocampus. **J)** Number of *p21*+ cells of each cell type/total number of cells in those images in the cortex. **K)** Percentage breakdown of *p16*+/*p21*+ cell types across all images. **L)** Number of *p16*+/*p21*+ cells of each cell type/total number of cells in those images across all images. **M)** Number of *p21*+ cells of each cell type/total number of cells in those images in the hippocampus. **N)** Number of *p21*+ cells of each cell type/total number of cells in those images in the cortex. **O)** Illustration of methods used to quantify number of p16+/tdTomato+ cells in the brains of p16CreERT2 x Ai14 mice. **P)** CSS-exposed mice have significantly more tdTomato+ cells in the brain than control mice ($p=0.0169$). Unpaired t test. * indicates $p<0.05$, ** indicates $p<0.01$ *** indicates $p<0.001$, **** indicates $p<0.0001$. Histogram bars represent group mean. Error bars represent standard error.

Next, to independently confirm the identity of stress-induced SNCs, and considering that p16 is a more specific marker for SNCs than p21 (Childs et al., 2017), we used a novel p16 reporter mouse line generated by crossing a p16CreERT2 line with the Ai14 line (p16CreERT2 x Ai14) (Van Deursen et al., unpublished). The p16-CreERT2 line was created by knocking CreERT2 into the endogenous p16 locus. CreERT2 encodes a Cre recombinase-mutant estrogen receptor fusion protein that is exclusively activatable by the estrogen receptor modulator tamoxifen. Ai14 mice have a tdTomato reporter gene controlled by the ubiquitous CAG promoter that becomes active after the removal of a "floxed" STOP cassette by Cre-mediated recombination. Thus, in the presence of tamoxifen, p16-expressing cells are strongly fluorescent and can be identified using fluorescence microscopy.

The p16CreERT2 x Ai14 mice were subjected to 4 weeks of CSS or were singly housed as controls. Restraint was not included as a manipulation in this experiment as our previous results indicated that it had no effect on p16 expression. All mice were acclimatized to a tamoxifen-supplemented diet for 2 weeks before beginning the CSS phase and were maintained on this diet until the end of the experiment. Previous independent studies confirmed the specificity of this model and that in absence of tamoxifen there is minimal expression of tdTomato (not shown).

To identify and quantify the abundance of tdTomato-expressing cells in the brain, we took fluorescent images of 9 whole coronal brain sections from approximately Bregma -0.94 to -0.22 from each mouse (**Figure 3O**). Visual inspection confirmed the hippocampus and the somatosensory cortex to be the brain regions where occurrence of tdTomato+ cells is most prominent. Expression in other brain areas was negligible. A blinded observer counted the number of tdTomato+ cells. We observed a significant increase in tdTomato+ cells in the brains of CSS exposed mice (p=0.0169; **Figure 3P**). Notably, nearly all tdTomato+ cells had a distinct neuron-like morphology (soma, axon) and were located in cortical/hippocampal cell layers primarily made up by neurons.

Transcriptomic profiling of CSS-induced SNCs and their microenvironment

To determine 1) the pathways that mediate CSS-induced senescence in the brain and 2) what changes the presence of CSS-induced SNCs might have on the local microenvironment, we used the spatial transcriptomics platform, the Nanostring GeoMx Digital Spatial Profiler. We used a high-sensitivity in situ hybridization assay to label *p16*+ senescent cells in the brains of CSS-exposed mice, then defined areas of interest (AOIs) within brain subregions with high and low *p16* abundance (*p16* high; *p16* low) (**Figure 4A**) ensuring matched AOIs for each brain subregion in each sample. We achieved clear distinction between *p16* high and *p16* low AOIs **(Figure 4B**).

We then conducted individual t-tests with BH correction to compare gene expression between the *p16* high and *p16* low areas and determine what changes are associated with CSS-induced SNCs. There were widespread changes in gene expression between *p16* high and *p16* low AOIs. To determine the functional relevance of these changes, we used a Gene Set Enrichment Analysis (GSEA). We found significant enrichment in numerous pathways related to cellular senescence. In particular, there were multiple pathways involved in DNA damage recognition, response, and subsequent signaling by p53 (**Figure 5C**). These included “Global Genome Nucleotide Excision Repair (GG-NER)”, “DNA Damage Recognition in GG-NER”, and “Nucleotide Excision Repair”.

Other enriched pathways directly involving p53 (also called TP53) included “p53-Dependent G1/S DNA damage checkpoint”, “p53-Dependent G1 DNA Damage

Response", Transcriptional Regulation by TP53", "Regulation of TP53 Activity Through Methylation", "TP53 Regulates Metabolic Genes", and "TP53 Regulates Transcription of DNA Repair Genes" (**Figure 5C**).

Additionally, there was significant enrichment in genes involved in Ras/Raf signaling, whose over activity is known to independently activate both p53 and p16. Specific pathways included "Regulation of RAS by GAPs", "MAPK Signaling Cascades", "MAPK4 Signaling", RAS/MAP Kinase Cascade", MAPK1/MAPK3 Signaling", "RAF Activation", and "RAS processing" (**Figure 5D**).

In addition to changes in senesce-related signaling, there was also significant enrichment of pathways involved in cellular response to extracellular stimuli. These pathways included pro-inflammatory cytokine functions like "Interleukin-1 signaling", and "Interleukin-17 signaling", responses to growth factors such as "Signaling by VEGF" and responses to cellular stressors such as "Cellular responses to stress", cellular response to hypoxia", "Cellular response to heat stress", and "Regulation of HSF mediated heat shock response" (**Figure 5E**). There were also changes to pathways involved in extracellular matrix organization, and cellular interactions with it like "L1CAM interactions", "Extracellular matrix organization" and "Degradation of the extracellular matrix" (**Figure 5E**). In the hippocampus, there was selective enrichment in functions related to chemical synaptic transmission — in particular there was an enhancement in glutamate release — "Glutamate neurotransmitter release" and AMPA-mediated signaling — "Trafficking of GluR2-containing AMPA receptors" (**Figure 5F**).

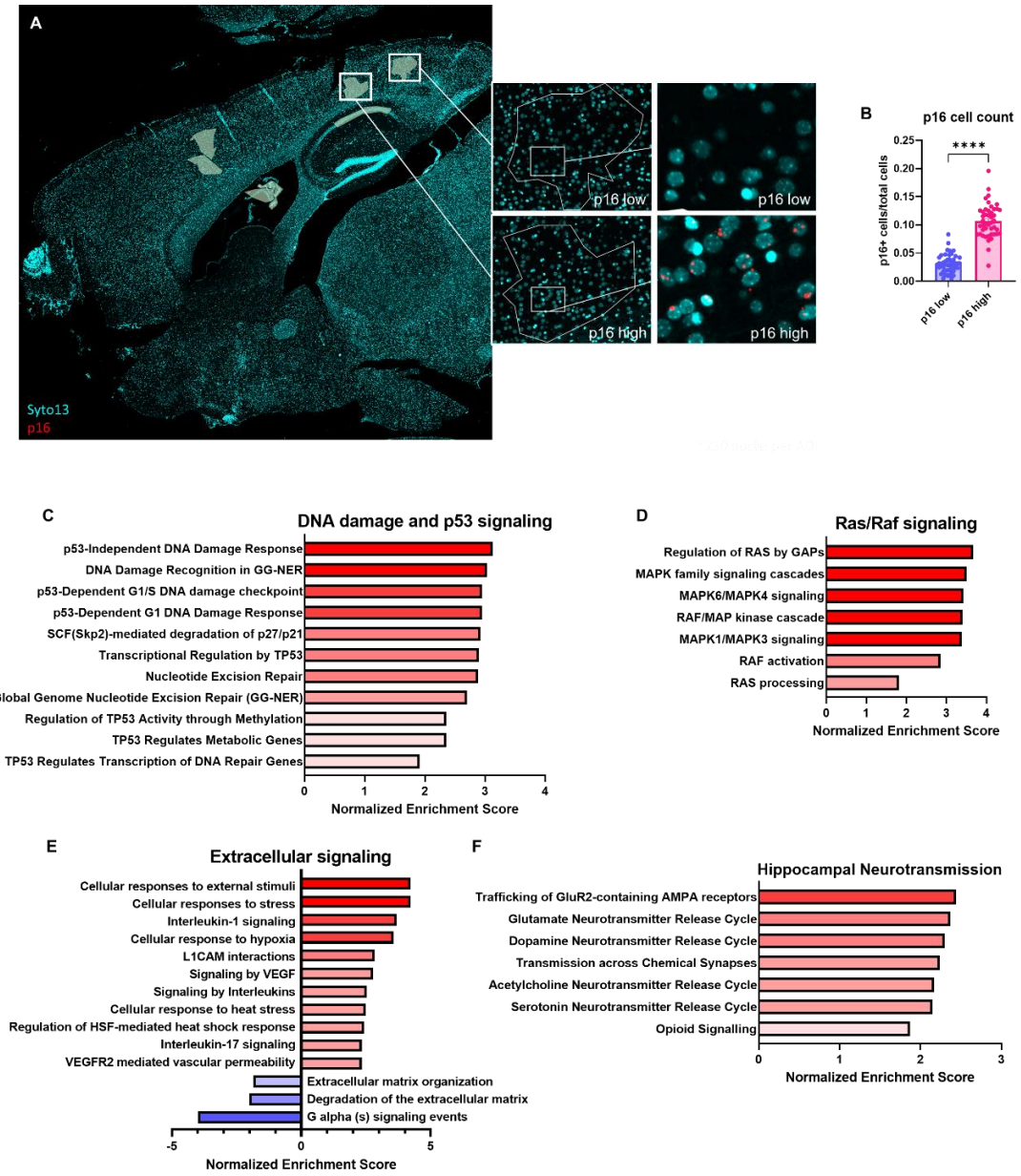

Figure 4 Transcriptomic profiling of CSS-induced SNCs and their microenvironment A) Representative image of *p16* transcript labeling and AOI selection for spatial transcriptomic profiling. **B)** Successful separation between *p16* low and *p16* high AOI ($p<0.0001$). Unpaired t test. Histogram bars represent group mean. Error bars represent standard error. **C)** DNA damage and p53-signaling related pathways identified by Gene Set Enrichment Analysis (GSEA) identified as significantly enriched in *p16* high AOIs compared with *p16* low AOIs in CSS-exposed mice. **D)** Ras/Raf signaling pathways identified by Gene Set Enrichment Analysis (GSEA) identified as significantly enriched in *p16* high AOIs compared with *p16* low AOIs in CSS-exposed mice. **E)** Cell interactions with the extracellular environment-related pathways identified by Gene Set Enrichment Analysis (GSEA) identified as significantly enriched in *p16* high AOIs compared with *p16* low AOIs in CSS-exposed mice. **F)** Synaptic transmission-related pathways identified by Gene

Set Enrichment Analysis (GSEA) identified as significantly enriched/reduced in *p16* high AOIs compared with *p16* low AOIs in the hippocampus of CSS-exposed mice. * indicates p<0.05, ** indicates p<0.01 *** indicates p<0.001, **** indicates p<0.0001.

Short term clearance of p16+ SNCs does not affect stress-induced physiological changes while lifelong clearance is detrimental to healthspan and lifespan

Having established that CSS induces accumulation of SNCs in multiple organs and that clearance of p16 expressing cells with GCV normalizes this effect in p16-3MR mice, we next sought to test the effect on SNC clearance on healthspan and lifespan.

Consistent with previous characterizations of the model, CSS-exposed p16-3MR mice manifested higher basal corticosterone, hyperphagia and a significant increase in body weight, while restraint-exposed mice displayed slightly lower food intake and reduced body weight (Bartolomucci *et al.*, 2009a; Sanghez *et al.*, 2013; Voorhees *et al.*, 2013; Razzoli *et al.*, 2015, 2018) (**Figure 5A—5F**). GCV-treatment did not affect any of these measures. As in males, female mice exposed to restraint stress exhibited a reduction in body weight in response to restraint stress (**Appendix Supplementary Figure 2**).

Repeating the lifelong CSS paradigm established by our lab previously (Razzoli *et al.*, 2018; Lyons *et al.*, 2021), we also treated subgroups of control and CSS mice with GCV (5 days of injections, with 14 days between injection cycles). As a general measurement of healthspan, we assessed physical frailty using an established 31-item mouse frailty index (Whitehead *et al.*, 2014). As expected, frailty score increased with age in control mice (**Figure 5G**). CSS accelerated the age-dependent increase in frailty, resulting in a significantly higher frailty score compared with controls by 22 months of age (**Figure 5H**).

GCV treatment was detrimental to frailty in both control and CSS-exposed mice. This effect was apparent by 10 months of age, when GCV-treated mice of both groups scored had higher frailty scores compared with their vehicle-treated counterparts (**Figure 6H**). At later time points, differences in frailty between the two CSS-exposed groups were not detectable. However, GCV-treated controls remained frailer than untreated controls up to 22 months of age. At 26 months, there were no GCV-treated CSS mice remaining, and too few GCV-treated controls for a reliable group assessment.

Survival analysis by Kaplan-Meier curves and log-rank test (Mantel-Cox with Bonferroni correction) found significant main effects of both CSS (Log rank test=2.80, p=0.0052) and GCV (Log rank test=2.75, p=0.006) on survival. GCV-treated CSS mice the lowest survival rate of any of the groups (**Figure 5H**). GCV-treated CSS mice also had a shorter median, and maximal lifespan than every other group (**Figure 5I**).

GCV significantly reduced but did not completely ameliorate the CSS-induced elevation in *p16* expression in PBMCs (**Figure 5J**), while it had no effect on PBMC *p16* expression in controls (**Figure 5J**).

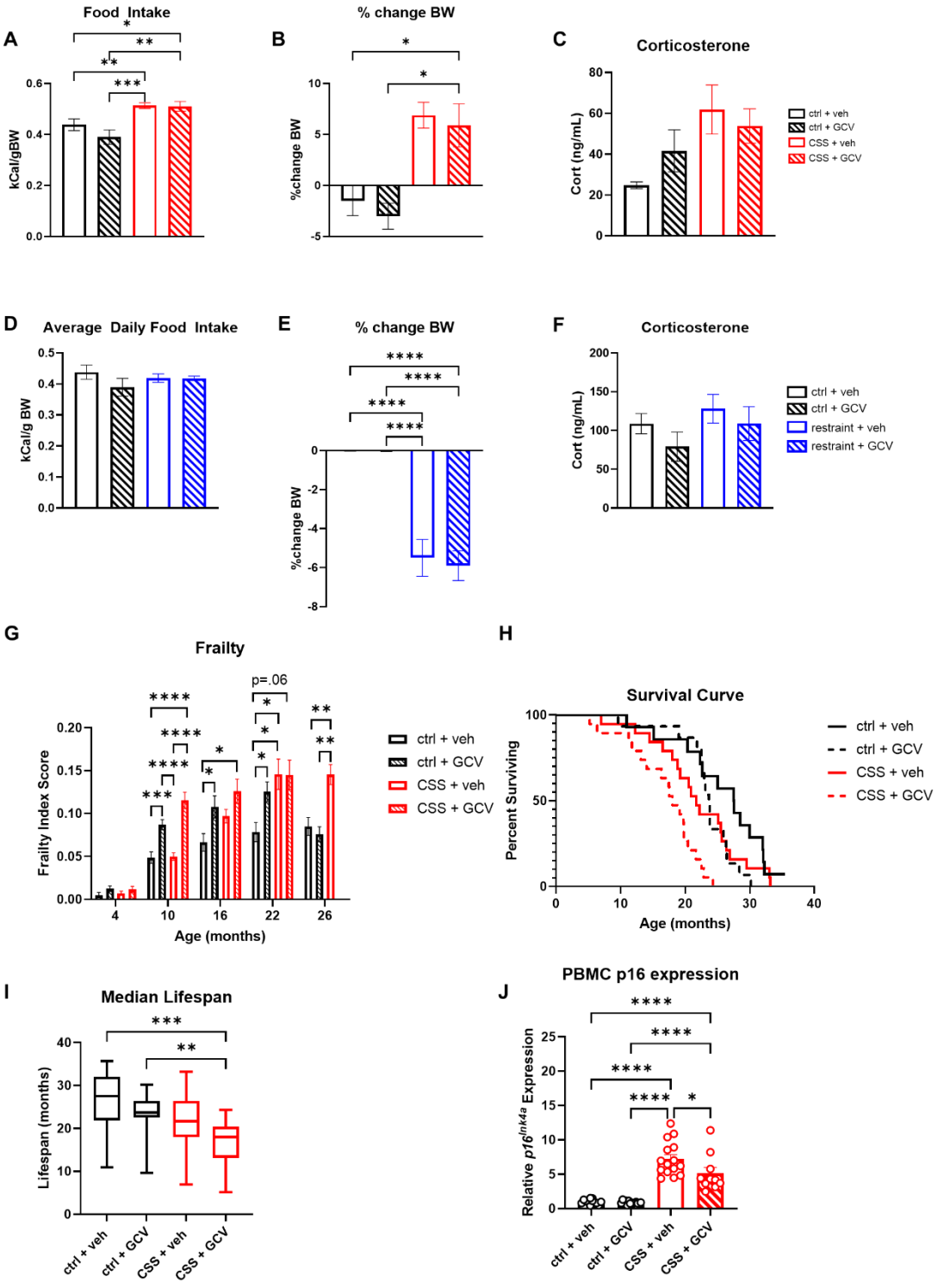

Figure 5 Short term clearance of p16+ SNCs does not affect stress-induced physiological changes while lifelong clearance is detrimental to healthspan and lifespan A) CSS-exposed mice treated with either vehicle or GCV consume significantly more calories per gram body weight.

2-way ANOVA. CSS: p<0.0001, GCV: p=0.2067. CSS x GCV: p=0.2601. Tukey post hoc. **B)** CSS-exposed mice gain significantly more body weight than control mice, regardless of vehicle/GCV treatment 2-way ANOVA. CSS: p<0.0001, GCV: p=0.4926, CSS x Group: p=0.8853. Tukey post hoc. **C)** Basal plasma corticosterone levels. 2-way ANOVA. CSS: p=0.1392, GCV: p=0.7898, CSS x GCV: p=0.4496. Tukey post hoc. **D)** Restraint stress does not affect daily calories/gram body weight. 2-way ANOVA. Restraint: p=0.8310, GCV: p=0.2380. Restraint x GCV: 0.2557. Tukey post hoc. **E)** Restraint-exposed mice lose significantly more body weight than control mice, regardless of vehicle/GCV treatment. 2-way ANOVA. Restraint: p<0.0001, GCV: p=0.7810. Restraint x GCV: 0.7902 **F)** Basal corticosterone levels. **G)** Frailty index score at 4, 10, 16, 22, and 26-months of age in mice that were singly housed or subjected to lifelong CSS in the presence/absence of GCV treatment. Mixed-effects analysis (REML). Group: p<0.0001, Age: p=0.0002, Group x Age: p<0.0001. Tukey post hoc. **H)** Kaplan-Meier survival curve for mice that were singly housed or subjected to lifelong CSS in the presence/absence of GCV treatment. **I)** Box and whisker plots show median lifespan (horizontal line), 2nd and 3rd quartiles (box) and min/max (vertical bars) lifespan for each group. CSS + GCV treated mice have significantly shorter median lifespan than ctrl + veh and ctrl + GCV groups. Kruskal-Wallis test p=0.0004. Dunn's multiple comparisons test. **J)** PBMC *p16* expression in mice either singly housed or subjected to lifelong CSS in the presence/absence of GCV at 20-months of age. Both CSS groups have significantly greater *p16* expression. GCV treatment partially, but not fully, attenuates the effect of CSS on *p16* expression. 2-way ANOVA. CSS: p<0.0001, GCV p=0.0384, CSS x GCV: p=0.0596. Tukey post hoc. * indicates p<0.05, ** indicates p<0.01 *** indicates p<0.001, **** indicates p<0.0001. Unless otherwise specified, Histogram bars represent group mean and error bars represent standard error.

2.4 Discussion

Chronic stress, low SES and emotional trauma have long been believed to accelerate the aging process (Steptoe & Zaninotto, 2020). However, despite the prevalence of this belief, there has been very little study on what biological phenomena might underlie this effect. Here, we used two mouse models of chronic stress to demonstrate for the first time that stress results in accumulation of SNCs in several disparate organ systems and identify the cell types affected in the brain.

CSS is an ethologically relevant model of stress in mice as it recapitulates the formation of dominance hierarchies and the negative consequence of chronic subordination — an important aspect of mouse social behavior. Conversely, restraint stress is one of the most widely used rodent stress models and imposes both psychological and physical challenges to the mouse. These models were selected because they are commonly used in biomedical research, they both increase HPA axis activity, anxiety-like and depression-like

behavior (Bartolomucci *et al.*, 2010; Dadomo *et al.*, 2011; Voorhees *et al.*, 2013; Jiang & Eiden, 2016). However, they differ in several key aspects, including: 1) restraint often results in habituation of the neuroendocrine stress response while CSS does not (Girotti *et al.*, 2006); 2) they have an opposite effects on energy balance, positive in the case of CSS, and negative for chronic restraint stress (Bartolomucci *et al.*, 2009b; Jeong *et al.*, 2013; Sanghez *et al.*, 2013; Razzoli *et al.*, 2015, 2018) 3) CSS has been shown to induce progressive aging-associated diseases such as early stage atherosclerosis, hypertension and decrease life expectancy, while to the best of our knowledge, no previous study has investigated these changes in mice exposed to chronic restraint stress.

CSS but not chronic restraint stress gradually upregulates *p16* expression in PBMCs

Using RT-qPCR, we longitudinally monitored expression of the cell cycle inhibitor *p16* in PBMCs of mice exposed to CSS. Expression of *p16* in peripheral immune cells correlates strongly with age in humans (Liu *et al.*, 2009). We also found a significant main effect of time on *p16* expression, as expected for an aging biomarker. We found that 4 weeks of CSS increased *p16* expression in circulating PBMCs. This rise was sustained, and the difference between CSS-exposed and singly housed control mice continued to widen over time. These findings parallel previous clinical research showing an association between high stress levels, shorter telomeres (Epel *et al.*, 2004), and higher *p16* expression in PBMCs (Rentscher *et al.*, 2019). In contrast, there was no effect of restraint stress on PBMC *p16* expression.

CSS upregulates expression of senescence and SASP markers in a p16 dependent manner, while restraint does so in a p16-independent manner

Having established 4 weeks as a time frame sufficient for CSS to induce an increase in *p16* in PBMCs, we next sought to determine whether this effect extended to other organs. A panel of tissues (cerebellum, cortex, hippocampus, kidney, liver, lung, scWAT) was collected following 4 weeks of CSS, restraint, or single housing and the abundance of senescent cells was assessed using SA β-galactosidase staining and RT-qPCR for senescence-related genes.

4 weeks of CSS was sufficient to increase levels of SA β-galactosidase in the scWAT, but not the liver, kidney, or lung. SA β-gal is one of the best-established markers

for cellular senescence. Senescent cells have expanded lysosomal volume, resulting in far greater lysosomal galactosidase activity, which is detectable at pH 6.0 (Lee *et al.*, 2006). We found an increased proportion of SA β-gal positive cells in the scWAT of CSS exposed mice compared with controls. Though it is a robust marker of senescence in some tissues such as scWAT, reports indicate that SA β-gal is not a good marker for cellular senescence in all tissues, particularly the brain (Piechota *et al.*, 2016).

While no single marker for cellular senescence exists, p16 is expressed by most senescent cells (Ohtani *et al.*, 2004), and increases in both mice and humans with aging (Krishnamurthy *et al.*, 2004; Ressler *et al.*, 2006). Several mouse lines have now been engineered and validated using p16 to target senescent cells, including the p16-3MR (Demaria *et al.*, 2014), INK-ATTAC (Baker *et al.*, 2011), p16LUC (Burd *et al.*, 2013; Pereira *et al.*, 2017) and two independent p16CreERT2 x Ai14 (Omori *et al.*, 2020; van Deursen, unpublished).

To further interrogate the stress-induced senescence phenomenon, we used RT-qPCR to measure the expression of several senescence and SASP related genes. Because many components of the SASP can be secreted in other contexts, we used the p16-3MR mouse line, a line that allowed us to selectively remove p16+ senescent cells in vivo. Downstream of the p16 promoter, these mice express a viral thymidine kinase, which converts its substrate GCV into a DNA chain terminator, triggering cell death. Thus, we were able to establish whether the presence of senescence and SASP factors was contingent upon the presence of p16.

As a second confirmation of *p16* expression, we also measured expression of *mRFP*, which in the p16-3MR line is also controlled by the p16 promoter. We also measured expression of the cyclin-dependent kinase inhibitor *p21*, which can induce a senescent state independent from p16. We found that *mRFP* gene expression increased linearly with that of *p16*, indicating that the p16-3MR functionality was intact.

In CSS-exposed mice, senescence-related gene expression was altered to the greatest extent in the brain (hippocampus and cortex, but not cerebellum), only slightly in the scWAT, and not at all in any other organs assessed. The hippocampus of CSS-exposed mice had greater expression of *mRFP*, *p16*, *p21* and *IL-1β*. In the cortex CSS exposed

mice manifested elevated *mRFP* and *p16* levels. Both the hippocampus and cortex of CSS exposed mice strongly trended towards elevated *IL-6* as well, falling just short of statistical significance in each case due to the variability in the CSS group. This variability is unsurprising when using bulk qPCR to measure gene expression relevant to the relatively rare population of SNCs. Conversely, we did not detect any changes in expression of senescence-related genes in the cerebellum, kidney, liver, or lung. This result is partially at variance with our previous study in which SNC markers were found to be increased in liver of mice exposed to CSS up to 17 months of age (Razzoli *et al.*, 2018), suggesting that a lifelong stress exposure is required to induce expression in some organs while the PBMCs, brain, and scWAT are sensitive to even short-term stress.

Treatment with GCV ameliorated the CSS-induced increase in all of these genes, establishing that stress mediators activated by CSS cause a p16-dependent accumulation of SNCs expressing both cell cycle inhibitors *p16* and *p21*. It additionally demonstrates that *p16*+ cells in the brain serve as a source of SASP factors like *IL-1β*.

In mice subjected to restraint stress, we observed a significant increase in the cyclin-dependent kinase inhibitor *p21*, but not *p16* in both the neural cortex and hippocampus. Unlike CSS-exposure, restraint stress had a greater effect on gene expression in the cortex than in the hippocampus. Restraint-exposed mice also had elevated expression of *IL-1β* in both brain regions. GCV treatment did not affect expression of either gene, further indicating that these restraint-induced changes in gene expression occur independently from *p16*.

While two stress models, CSS and restraint, both induce increases in senescence markers, they produce different signatures and preferentially affect different tissues. CSS induces both *p16* and *p21* expression, and its greatest effects are in the hippocampus and to a smaller extent the cortex. *p16* and *p21* expression are strongly correlated in CSS-exposed mice. Restraint stress induces *p21* but not *p16* with larger effects in the cortex than hippocampus.

Our gene expression data indicate that CSS induces senescence via simultaneous p16 and p21 signaling, whereas restraint stress induces only p21. These cell cycle inhibitors are induced by different signaling cascades and at different stages of senescence induction.

Both p16 and p21 are classified as cyclin-dependent kinase inhibitors — they bind to cyclin dependent kinases, blocking their signaling and thus preventing the cell from progressing through the cell cycle.

These pathways and their effectors can act either independently or in tandem. However, their effects are not entirely equivalent (Albanese *et al.*, 1995). Damage to nuclear DNA results in activation of the DDR, which among other effects, activates the master regulator p53. p53 in turn induces expression of p21, which blocks the signaling of cyclin dependent kinases, preventing progression through the cell cycle. p21 is crucial for the initial entry into cell cycle arrest, while sustained p21-mediated arrest eventually causes induction of p16, resulting in permanent exit from the cell cycle (Dulić *et al.*, 2000). p16 can also be activated independently of p53/p21 in response to excessive pro-oncogenic Ras or BRAF signaling (Lin *et al.*, 1998b; Di Micco *et al.*, 2006; Campisi & d'Adda di Fagagna, 2007). The prominence of p16 and p21 in cellular senescence varies between cell types and species (Campisi & d'Adda di Fagagna, 2007).

However, although p16 alone induces replicative arrest, DDR signaling is required to produce a SASP (Rodier *et al.*, 2009; Coppé *et al.*, 2011). The *p16*-dependent detection of pro-inflammatory *IL-1β* and *IL-6* in the tissues of CSS-exposed mice suggests a persistent DDR in *p16*+ cells. Chronic stress is known to promote oxidative damage; chronic stress causes an increase in reactive oxygen species and DNA damage (Herbet *et al.*, 2017). Given that chronic stress is known to promote neuroinflammation and ROS, and that these factors contribute to DNA damage, our data suggest that this could be the mechanism by which stress causes cellular senescence. Persistence of the DDR and p21 signaling ultimately leads to the induction of p16 in CSS-exposed mice, whereas restraint-stress induced DDR signaling does not remain sustained long enough to induce p16.

Neurons and astrocytes are susceptible to CSS-induced senescence

Despite their potential as therapeutic targets in diseases and general age-related decline, a major challenge for the field has been determining the cell type identities of SNCs. Previous studies have largely studied senescence within homogenous cell cultures or evaluated senescence in vivo at an organ-wide level of spatial resolution. While these methods have made immense contributions to our understanding of senescence as a

phenomenon, a higher level of spatial resolution is necessary to understand senescent cells and their interactions via SASP with surrounding tissue. To determine the cell-type identity of stress-induced senescent cells in the brain, we used the fluorescent in-situ hybridization technique RNAscope. We co-labeled brain sections with the senescence markers *p16* and *p21*, along with one of four cell type markers for neurons, astrocytes, microglia, and oligodendrocyte precursor cells, each of which have been identified in previous studies (Bussian *et al.*, 2018; Musi *et al.*, 2018; Zhang *et al.*, 2019). As in our qPCR data, CSS mice treated with vehicle had more *p16* and *p21* positive cells than other groups. The majority of *p16*/*p21*+ cells were positive for the neuron marker NeuN. Astrocytes were the next most prominent *p16*/*p21*+ cell type in the brain. CSS did not greatly change the overall composition of SNCs; thus we conclude that CSS-induced senescence thus appears to primarily occur in neurons and astrocytes.

For a more thorough quantification and independent validation of *p16* expressing SNC accumulation in the brain, we employed a p16CreERT2 x Ai14 cross to generate p16 fluorescent reporter mice. In accordance with our qPCR and RNAscope data, we found that 4 weeks of CSS induced an increase in tdTomato+ cells in the brain. They were most prominently observable in the hippocampus and somatosensory cortex. Fibers were apparent in white matter tracts, in particular the fimbria and striatum. The fimbria contains fibers projecting to/from the hippocampus while the striatum is crossed by bilateral projections connecting the cortical and subcortical regions. We can thus be reasonably confident that these fibers originated from similar cell populations to the cell bodies we observed in the hippocampus and cortex.

Adult neurons are postmitotic, but under some conditions — including neurodegenerative disease, traumatic brain injury, and stroke — DNA damage and repair causes upregulation of cell cycle proteins and thus pressure to re-enter the cell cycle (Fielder *et al.*, 2017; Welch & Tsai, 2022). DNA damage, particularly double strand breaks, also activates the cellular DDR, one of the major senescence triggers (Campisi & d'Adda di Fagagna, 2007). The DDR activates the master regulator p53, which can lead to either apoptosis or senescence (Rodier *et al.*, 2009).

Multiple neuron subtypes can attain a senescence-like phenotype, exhibiting features including chromatin remodeling, γH2AX foci, and expression of p21 and IL-6 (Jurk *et al.*, 2012). p16 has also been implicated in neuronal senescence. One study showed that pyramidal neurons from elderly human patients (77 years old) have increased expression of p16 (Kang *et al.*, 2015). p16 expression is also negatively correlated with neurogenesis in aging mice (Molofsky *et al.*, 2006). Neurofibrillary containing neurons that were laser-capture microdissected from the cortex of patients with Alzheimer's disease have upregulated levels of transcripts associated with cell survival and downregulated gene expression for functions related to apoptosis and cell death — consistent with the apoptosis resistant senescent phenotype (Musi *et al.*, 2018).

The circumstances that dictate which outcome occurs are unclear. In neurons, DDR-induced p53 activation is thought to be one of the primary routes to neuronal apoptosis in neurodegenerative diseases (Folch *et al.*, 2011). However compelling evidence suggests that under some conditions, p53 activates p21 resulting in a senescent state in neurons, as it does in other cell types (Sturmlechner *et al.*, 2021; Welch & Tsai, 2022).

Presence of CSS-induced SNCs is associated with elevated DNA damage response, Ras/Raf, Interleukin signaling, changes to the extracellular matrix, and upregulated hippocampal neurotransmitter release

To interrogate the pathways involved in CSS-induced senescence, we employed spatial transcriptomic technology to compare areas with high and low *p16* expression (identified with RNAscope). Despite *p16*+ cells making up only about 11% of the population of *p16* high regions, we were able to detect many changes in gene expression between *p16* high and low areas (*p16* low regions contained <3.5% *p16*+ cells). To identify the functions of these genes, we used a GSEA to identify significantly enriched pathways.

p16 high areas were characterized by an elevation in numerous senescence-related pathways. In particular, two main senescence-induction functions were apparent: DDR and RAS/RAF signaling. Pathways involved in DNA damage recognition, response and repair were enriched in *p16* high regions. These included "Global Genome Nucleotide Excision Repair (GG-NER)", "DNA Damage Recognition in GG-NER", and "Nucleotide Excision

Repair". This, combined with an enrichment in functions related to p53 and p21 signaling suggest that DNA damage is a primary driver of CSS-induced senescence in the brain. p53 (also called TP53) signaling is greatly elevated in brain regions high in SNCs. Enriched pathways included "p53-Dependent G1/S DNA damage checkpoint", "p53-Dependent G1 DNA Damage Response", Transcriptional Regulation by TP53", "Regulation of TP53 Activity Through Methylation", "TP53 Regulates Metabolic Genes", and "TP53 Regulates Transcription of DNA Repair Genes". These results strongly suggest that DNA damage, and subsequent p53/p21 signaling is a major mediator of CSS-induced senescence in the brain.

However, this was not the only senescence-induction pathway implicated. Ras/Raf signaling is known to activate both p16 and p53, though the precise mechanisms remain unclear. *p16* high regions of CSS-exposed mouse brains were enriched with genes involved in pathways such as "Regulation of RAS by GAPs", "MAPK Signaling Cascades", "MAPK4 Signaling", RAS/MAP Kinase Cascade", MAPK1/MAPK3 Signaling", "RAF Activation", and "RAS processing".

Substantial evidence indicates that stress, particularly social stress, results in DNA damage. Socioeconomic disadvantage and adverse childhood experiences are associated with elevations in oxidative damage markers (Horn et al., 2019). In both humans and mice, it has been demonstrated that acute stress causes an increase in reactive oxygen species (ROS), resulting in damage to DNA and other cell structures (Adachi *et al.*, 1993; Bagchi *et al.*, 1999; Sivoňová *et al.*, 2004; Eskiocak *et al.*, 2005; Nakhaee *et al.*, 2013; Wiegand *et al.*, 2018). Acute induction of ROS can be neutralized relatively quickly, but long-term or chronic stress results in uncompensated ROS balance and subsequent DNA damage (Li, Poi, *et al.*, 2011; Horn *et al.*, 2019).

The brain has been found to be particularly vulnerable to stress-induced ROS and DNA damage in rodent studies. Elevations in ROS and markers of DNA damage are detectable after 2-weeks of stress in the brain; earlier than in peripheral organs where increased ROS and DNA damage could be found after 7 weeks of stress (Schiavone *et al.*, 2012; Colaianna *et al.*, 2013; Son *et al.*, 2016). This may be linked with our finding that the brain is the most prominent target for stress induced SNC marker elevation following

4 weeks of stress. CSS-induced DNA damage thus seems a compelling mechanism for senescence induction in the brain.

As in the case of DNA damage, Ras/Raf and mitogen-activated protein kinase (MAPK) activation have also been shown to be upregulated psychological stress (Bierhaus *et al.*, 2003). The Ras/Raf signaling cascade — also called the Ras-Raf-MEK-ERK pathway — is exceedingly complex, with numerous downstream targets. At its core, it is a pathway that couples signals from cell surface receptors to transcription factors (Chang *et al.*, 2003). It can be activated by multiple forms of cellular injury, including oxidative damage to DNA, lipids, and proteins (Rezatabar *et al.*, 2019). Dysregulation of this pathway results in uncontrolled proliferation and is common in most cancers (Chang *et al.*, 2003). Though not fully characterized, Ras/Raf cascade activation of p53 and p16 is known to occur, and represents a feedback mechanism to prevent uncontrolled growth and cancer (Lin *et al.*, 1998a; Zou *et al.*, 2019). This research, in combination with our own findings suggests that CSS may promote senescence via damage-induced elevations in Ras/Raf signaling.

The DDR and Ras/Raf signaling cascade interact substantially via bidirectional interplay between Ras/Raf and p53. The Ras/Raf signaling cascade can be induced by p53 (Lee *et al.*, 2000). Simultaneously, Ras/Raf signaling can result in activation of p53 (Feng *et al.*, 2016). In fact, Ras/Raf activation of p53 has been shown to occur specifically in neurons following brain injury (Feng *et al.*, 2016)

A model in which chronic subordination stress exposure causes DNA damage, and consequently activation of the p53 and Ras/Raf signaling pathways, ultimately leading to senescence mediated by both p21 and p16 fits neatly with previous research. Future experiments will be needed to confirm this model, but our experiments here establish a strong basis for this hypothesis.

In addition to informing on the induction mechanisms involved in CSS-induced SNC accumulation, the transcriptomic data provides valuable insight into the changes that occur to the senescent microenvironment. Areas with high *p16* expression exhibit upregulation of interleukin signaling — specifically IL-1 and IL-17. This aligns with our previous qPCR data indicating an elevation in *IL-1β.* Additionally, there is an enrichment

for genes involved in growth factor signaling (VEGF), and indications of changes to the extracellular matrix. These functions are consistent with known SASP components. Pro-inflammatory signaling and remodeling of the extracellular matrix may alter the function on the cells surrounding SNCs.

A future analysis of this rich dataset will more deeply elucidate the consequences of CSS-induced senescence in the brain. One finding with important functional implications, is that *p16* high regions of the hippocampus were enriched with genes involved in signaling via numerous neurotransmitters. Most prominently, pathways regulating glutamate neurotransmitter release and the trafficking of AMPA receptors were upregulated. Excessive glutamatergic signaling can result in abnormally high calcium influx through NMDA receptors, resulting in cellular damage and activation of cell death pathways (Li & Wang, 2016). This phenomenon, known as excitatory neurotoxicity can lead to gradual loss of synaptic function and neuronal death, and is known to play a role in AD and other neurodegenerative diseases (Choi, 1988; Wang & Reddy, 2017; Kodis *et al.*, 2018) (see also Chapter 4: proteomic analysis demonstrating high glutamatergic tone in mice subjected to lifelong CSS).

Short-term clearance of *p16+* senescent cells does not affect stress-induced physiological changes while lifelong clearance is detrimental to healthspan and lifespan.

Crucially, having established that social stress in a major physiological driver of SNC accumulation, we were interested in whether CSS-induced SNCs have functional consequences to health. In the short term, SNC elimination does not have obvious effects on health or physiology under our experimental conditions in the p16-3MR mouse model. GCV treatment did not affect the metabolic phenotypes that characterize CSS or restraint stress. However, given that SNC accumulation is primarily an age-associated phenomenon, we were interested in whether removal of CSS-induced SNCs would reverse the detrimental effects of CSS in the long term.

To determine whether CSS-induced SNCs were detrimental to healthspan and/or lifespan, we employed our previously published lifelong CSS paradigm, and treated mice with GCV or vehicle injections every 2 weeks (Razzoli *et al.*, 2018; Lyons *et al.*, 2021).

To assess overall healthspan, we utilized the previously established 31-item mouse frailty index (Whitehead et al., 2014). In accordance with the conceit of this assay, there was a significant increase in frailty with age. CSS exacerbated the age-dependent increase in frailty, resulting in a significantly higher frailty score compared with controls by 22 months of age.

Notably however, GCV treatment was detrimental to frailty in both control and CSS-exposed mice. This effect was apparent by 10 months of age, when GCV-treated mice of both groups scored significantly higher on the mouse frailty index compared with vehicle-treated mice of either group. GCV-treated control mice remained frailer than untreated controls up to 22 months of age, the final time point with a sufficient number of living mice in the GCV group for an accurate assessment. These results present two possibilities — that regular, wholesale elimination of SNCs is hazardous to physical health when begun at a young age, or that GCV treatment has adverse toxic effects. Further studies should test this hypothesis by using alternative senotherapeutic approaches.

Consistent with our previous work, lifelong CSS significantly shortened survival. However, we also found that GCV-treatment shortens lifespan. When the effects of CSS and GCV clearance of SNC are combined, the shortening of lifespan was compounded. The GCV treated CSS group had significantly reduced survival rate, shorter median lifespan, and the shortest maximum lifespan of any group by over 5 months.

In summary, we found that GCV-treatment starting at 3 months of age results in health deficits by 10 months of age, and a continued elevation in physical frailty until early death. When this insult is coupled with lifelong stress, the effect on healthspan and lifespan is exacerbated. These findings regarding frailty and lifespan are in agreement with previous literature showing that naturally occurring SNCs play an important role in health maintenance (Grosse *et al.*, 2020), but at odds with other studies showing a beneficial effect of SNC removal on lifespan (Baker *et al.*, 2011, 2016; Xu *et al.*, 2018; Yousefzadeh *et al.*, 2018).

An alternative hypothesis is that GCV exerts negative effects on health and lifespan independently from SNC removal. In vitro and in human patients, GCV has been demonstrated to be toxic to macrophage and erythrocyte progenitors (Sommadossi &

Carlisle, 1987; Perrottet *et al.*, 2009). Neurotoxicity and hepatic toxicity have also been reported in multiple case studies (Perrottet *et al.*, 2009). Alternate senolytic treatments such as dasatinib + quercetin, fisetin and Navitoclax (ABT263) should be pursued.

2.5 Conclusion

Cellular senescence is an evolutionarily advantageous process that suppresses tumorigenesis, increasing the likelihood that an individual will live long enough to reproduce. However, traits that favor health and survival in a young organism do not necessarily benefit it in old age.

We found that 4-week exposure to one of two stress paradigms — CSS or restraint stress — is sufficient to increase expression of senescence markers in male mice. However, the senescence-related gene changes and organs affected were highly dependent on the paradigm. CSS-exposed mice manifested increased *p16* expression in PBMCs, scWAT, cortex and hippocampus, along with elevated *p21*, and SASP factors in the hippocampus. In contrast, restraint exposed mice showed only elevated *p21* in the cortex and hippocampus. These findings suggest that stress, particularly social stress, can promote cellular senescence.

Using two independent methods — multiplexed in situ hybridization, and a p16 reporter mouse line — we determined that the majority of cells in the brain induced to senesce by CSS were neurons and astrocytes. Although neurons are postmitotic cells, evidence suggests that they can take on a senescence-like phenotype under conditions that induce DNA damage. This process is implicated in neurodegenerative disease and suggests an avenue by which chronic stress can increase risk for these conditions.

Areas of the brain with high *p16* expression following CSS exposure are characterized by enrichment in gene sets involved in two well-known senescence induction pathways. DNA damage recognition and response, and Ras/Raf signaling are the likely mechanisms by which CSS induces cellular senescence in the brain. Elevations in these functions have previously been linked with chronic psychological stress, but our results are the first to indicate that they may be associated with SNC accumulation.

Moreover, areas with a high number of *p16+* cells have increased expression of genes involved in proinflammatory cytokine signaling, growth factor signaling, and downregulation of pathways involved in maintenance of the extracellular matrix.

Future efforts should be made to determine whether SNC-removal in the context of lifelong stress is in fact detrimental, or whether our findings were the result of off target drug effects of GCV. This information will be vital to understand the role played by CSS-induced senescence in health and aging.

2.6 Methods

Subjects

p16-3MR mice: line contains a copy of a bacterial artificial chromosome in which the senescence-sensitive p16INK4a promoter drives expression of the widely used 3MR fusion protein (Demaria *et al.*, 2014). The trimodal 3MR fusion protein contains functional domains for Renilla luciferase, monomeric Red Fluorescent Protein, and a truncated herpes simplex virus thymidine kinase.

4-week stress studies: Males: ctrl+veh N=16; ctrl+GCV N=7; CSS+veh N=30; CSS+GCV N=14 restraint+veh N=6; restraint+GCV N=6. Females: ctrl+veh N=5; ctrl+GCV N=5; restraint+veh N=6; restraint+GCV N=5.

Repeated PBMC sampling study: ctrl N=6; CSS N=11; restraint N=6

Lifelong CSS study: ctrl+veh N=14; ctrl+GCV N=15; CSS+veh N=19; CSS+GCV N=19

p16CreERT2 x Ai14 mice: p16-CreERT2 mice were created by knocking CreERT2 into the endogenous p16 locus. CreERT2 encodes a Cre recombinase-mutant estrogen receptor fusion protein that is exclusively activatable by the estrogen-like agonist Tamoxifen. Ai14 mice (Jackson labs, Stock no: 007908) have a tdTomato reporter gene controlled by the ubiquitous CAG promoter that becomes active after the removal of a floxed (Lox-STOP-Lox) STOP cassette by Cre-mediated recombination. Mice were acclimated to Tamoxifen-supplemented diet (Envigo TD.130856). ctrl N=5; CSS N=8.

CD1 mice were purchased from Charles River Laboratories

All mice had ad-libitum access to food (2018 Tecklad or 2014 Tecklad starting at 10 months of age in the lifelong study) and water. Mice were housed on a 14h:10h light:dark cycle for the duration of the experiments. All procedures were conducted with the approval of the University of Minnesota Institutional Animal Care and Use Committee.

Stress paradigms

3-month-old p16-3MR mice were exposed to 4-weeks of chronic subordination stress, restraint stress, or remained singly housed as controls. 3-month-old male p16CreERT2 x Ai14 mice were exposed to 4 weeks of chronic subordination stress or remained singly housed as controls.

Chronic subordination stress (CSS): Male mice were subjected to a 4-week chronic subordination stress paradigm. Mice were paired with mice from the highly aggressive CD1 strain. Daily, between the hours of 9:00am and 11:00am, the paired p16-3MR and CD1 mice were allowed to interact for a maximum of 10 minutes. Following this interaction, a perforated partition was used to separate the mice, allowing continuous sensory contact and preventing any additional physical contact. Mice used for repeated blood sampling (N=11) remained in sensory housing with their aggressor until the final sampling.

Restraint stress: 3-month-old male and female p16-3MR mice were restrained for 3 hours daily 6 days/week in modified 50mL conical tubes (Carroll et al., 2011). Mice used for repeated blood sampling remained in single-housing following the 4 weeks of stress until the final sampling.

Control mice were singly housed and handled daily.

Facial vein blood sampling: Mice were restrained by scruffing the skin of the dorsal neck and a 5-mm lancet (Goldenrod Animal Lancet, Medipoint, Mineola, NY) was used to puncture the facial vein on the right side of the face. Approximately 50-200µL of blood was collected by allowing it to freely drip into an EDTA coated MiniCollect tube (Greiner). There were at least 2 weeks between each blood sampling event. As all mice weighed greater than 25g, this volume ensured that no more than 10% of total blood volume was

collected, in accordance with the NIH Office of Animal Care and Use Guidelines. Blood was stored at room temperature until further processing.

GCV Treatment

Mice received intraperitoneal injections of 25 mg/kg ganciclovir (5mg/mL; Frontier scientific) in sterile PBS with 4% DMSO for two rounds of 5 consecutive days (Demaria *et al.*, 2014). These injections occurred on days 2-6 and 23-27 of the stress procedures for the 4-week protocols, or every 2-weeks in the lifelong CSS experiment. Vehicle treated mice were injected with an equal volume of PBS with 4% DMSO.

Experimental procedures and statistical analysis

Unless otherwise specified, all statistical analyses (described individually below) were performed using Graphpad Prism.

Food intake and body weight measurements

Food intake was measured by weighing the amount of food provided to each mouse at the beginning of the week and weighing the amount remaining at the end of the week. Average daily food intake was analyzed using unpaired t-tests, or 2-way ANOVA with tukey post hoc when appropriate. Body weight was measured at least twice per week (Monday and Friday) and was additionally measured on each day of GCV/vehicle injections to calculate proper dosage volume. Body weight change over time was analyzed using a 2-way Repeated Measures ANOVA and pairwise comparisons performed using Tukey test. Total change in body weight was measured using 2-way ANOVA with Tukey post hoc. Average daily food intake was analyzed using unpaired t-tests.

Frailty Index

Frailty index was calculated as outlined in (Whitehead et al., 2014). Briefly, each mouse was visually inspected for physical deficits by an observer blinded to experimental condition. The experimenter was the same across time points. The sum of deficits was calculated for each individual mouse. Longitudinal data was analyzed using mixed linear model (REML). Pairwise comparisons were performed using Tukey test.

Survival analysis

Survival rate was calculated using Kaplan-Meier curves with Montel-Cox test and Bonferroni correction. Median lifespan was analyzed using Kruskal-Wallis test and Dunn's multiple comparison's test. Average lifespan was analyzed using 2-way ANOVA and Tukey pairwise comparisons.

PBMC isolation from whole blood

Blood samples were centrifuged at 2000rpm for 5 minutes at room temperature. Plasma and buffy coat layer were removed and resuspended in 1mL ACK lysis buffer (Thermo Fisher Scientific). Samples were incubated for 5 minutes to lyse red blood cells. Samples were then centrifuged at 2000rpm for 5 minutes at room temperature. ACK lysis buffer was removed and the cell pellet was washed twice in ice-cold DPBS to remove red blood cells. Cell pellets were resuspended in 850µL lysis buffer from the Mouse RiboPure Blood RNA Isolation kit (Thermo Fisher Scientific) and stored at -80˚ until further use.

Corticosterone Radioimmunoassay

Plasma corticosterone and was measured by radioiummunoassay as described previously (Ulrich-Lai & Engeland, 2000) by the Behavioral and Cognitive Core of the University of Cincinnati Mouse Metabolic Phenotyping Center.

qPCRs

RNA from was extracted using either a Mouse RiboPure Blood RNA Isolation kit (for PBMCs; Thermo Fisher Scientific), an RNAeasy Lipid Tissue Mini Kit (for adipose tissue; Qiagen) or a PureLink RNA Mini Kit (for all other tissues; Thermo Fisher Scientific) according to the manufacturer's protocol. Transcription into cDNA was performed using the iScript cDNA synthesis kit (Bio-Rad) according to the manufacturer's directions. Each cDNA sample was run in duplicate using the iTaq Universal SYBR Green PCR Master Mix (Bio-Rad) to a final volume of 10µl in a CFX Connect thermal cycler and optic monitor (Bio-Rad). Primer sequences can be found in **Appendix Table 1** below. For *p16* assessment in PBMCs, expression was normalized to GAPDH. The expression of senescence/SASP genes in our tissue panel was normalized to the geometric mean of two housekeeping genes – for brain tissue: actin and GAPDH, for all other tissues: actin and transcription factor II. Fold change was calculated using delta-delta Ct method.

For single time point assessments of PBMC *p16* expression, unpaired t-tests, or 2-way ANOVAs with Tukey post hoc were used to test for statistical differences. Longitudinal measurements of PBMC expression were analyzed using a Restricted Maximum Likelihood (REML) linear mixed-effects model, to account for several individual's values missing at various time points due to insufficient blood sample collection. Change in *p16* expression between 20 and 26 months was analyzed using 2-way Repeated Measures ANOVA.

For the senescence/SASP panel, data was analyzed for each tissue by REML mixed effects model and pairwise comparisons performed using Tukey test.

Senescence-associated β-Galactosidase Assay

Staining was performed using a kit according to manufacturer's instructions (Cell Signaling 9860S). Freshly harvested chunks of tissue were washed in ice cold PBS, then lightly fixed in fixative solution for 15 minutes. Tissue was then incubated with X-Gal solution for 16 hours at 37˚C. It was then postfixed with 4% PFA overnight at 4˚C. The tissue was cryopreserved by incubating in a 30% sucrose solution for 3 days. It was then cryosectioned (10µm) and mounted on Superfrost Plus microscope slides. Slides were counterstained with DAPI (1µg/mL) and imaged using a Nikon Eclipse microscope equipped with a 60x oil-immersion objective (N.A. = 1.40). 10 fields of view for each sample. An observer blinded to experimental condition manually counted the total number of cells, and the number of cells containing at least 1 X-gal crystal, and the percentage of X-gal positive cells was calculated for each sample. Unpaired t-tests were performed using Graphpad Prism.

Immunohistochemistry

Tissue was immersion fixed in 4% PFA overnight. It was then cryopreserved by incubating in a 30% sucrose solution for 3 days or until tissue sank to bottom of tube. Tissue was cryosectioned (brain: 40µm, all other tissues: 10µm) and mounted on Superfrost Plus microscope slides (Fisher Scientific). Slides were washed 3 times for 5 minutes each in PBS. Tissue was then permeabilized with 0.3% Triton X-100 in PBS for 15 minutes. Nonspecific binding was blocked by incubating tissue with 5% Normal Donkey Serum (Jackson Immuno) in PBS with 0.1% Triton-X 100 (blocking buffer) for 1 hour at room

temperature. Primary antibodies (see **Appendix table 2**) were diluted in blocking buffer and incubated overnight at 4˚ C. They were subsequently washed 3 times for 5 minutes each in PBS. Tissue was incubated with secondary antibodies diluted in blocking buffer for 1 hour at room temperature. Tissue was washed 3 times for 5 minutes each in PBS and counterstained with DAPI (1µg/mL) for 10 minutes. Slides were briefly rinsed in deionized water and coverslipped using ProLong Diamond antifade mountant (ThermoFisher). For quantification of tdTomato+ cells in the brain, imaging was performed using a Keyence microscope equipped with a 10X objective (N.A. = 0.45). All other imaging was performed using a Nikon Eclipse microscope equipped with a 20X objective (N.A. = 0.75).

Quantification of tdTomato+ cells

For each mouse, 9 coronal brain sections were scanned on a Keyence microscope at 10X magnification (N.A. = 0.45). tdTomato+ cells were manually counted by a researcher blinded to the experimental condition of the samples. The position of the cells was recorded, and their authenticity confirmed by imaging at higher magnification. The number of tdTomato+ cells for each mouse was normalized to the total volume of brain tissue examined in the 9 scans. Statistical differences between control and CSS mice were tested using unpaired t-test.

In situ hybridization

Florescent in situ hybridization was performed using RNAscope reagents on 10µm sagittal sections were cut from fresh frozen mouse brains. Probes used were Cdkn2a (411011), Cdkn1a (408551-C2), Aldh1l1 (405891-C3), Cspg4 (404131-C3), Rbfox3 (313311-C3) Tmem119 (472901-C3). Imaging was performed on a Nikon Eclipse microscope equipped with a 60x oil objective (N.A. = 1.40). Images were collected in the following manner: 3 images from the subiculum, 5 from CA1, 5 from CA3, 3 from the dentate gyrus, 5 from the somatosensory cortex, and 3 from the orbito-frontal cortex. Images were thresholded and converted to binary in ImageJ by a researcher blinded to experimental condition. The number of nuclei containing puncta from each channel, and colocalization of puncta from each channel on the same nuclei was then measured using a custom pipeline in the program CellProfiler. Cell counts were normalized to number of DAPI stained nuclei per field of

view. No statistical analyses were performed as this data is qualitative rather than quantitative in nature.

Spatial Transcriptomics

The 6 brains from CSS-exposed mice used in spatial transcriptomics experiments were dissected and immersion fixed in 4% PFA made with nuclease-free water overnight, then stored in nuclease-free 70% ethanol until embedding in paraffin blocks by the University of Minnesota Histology Core. Blocks were microtome sectioned to a thickness of 5 µm and mounted of Superfrost Plus slides (Fisher Scientific). Sections were placed within the central 36.2 mm x 14.6 mm area of the slides to ensure tissues fit within the gasketed GeoMx slide holder. Mounted tissues were dried in a hood overnight at room temperature. Within 24 hours of sectioning, Cdkn2a transcripts were labeled using the RNAscope 2.5 HD Assay – RED and a Cdkn2a probe (411011), according to the manufacturer's specifications.

Immediately following the RNAscope labeling, the slides proceeded to the GeoMx Whole Mouse Transcriptome Atlas protocol outlined by the manufacturer (Nanostring Technologies), starting at the 5-minute postfixation step in 10% formalin. Prepared tissues were flooded with whole transcriptome RNA probes (Nanostring Technologies, Cat#121401102) attached to oligonucleotide barcodes via photocleavable linkers. Slides were covered with HybriSlip hybridization covers (Grace Bio-Labs, Cat#714022) and hybridized overnight at 37°C in a hybridization oven (Boekel Scientific RapidFISH Slide Hybridizer, Cat#240200). Following hybridization, unbound probes were washed away using a wash solution of equal parts 4XSSC and deionized formamide (ThermoFisher, Cat#AM9342). Nuclei were labeled using SYTO 13 green fluorescent nucleic acid stain (ThermoFisher, Cat# S7575). Tissues were blocked with Buffer W (Nanostring Technologies, Cat#121300313) in a light impermeable humidity chamber (Simport, Cat#M920-2) for 30 minutes at room temperature. Following blocking, morphology markers were incubated at room temperature for 1 hour. Slides were washed in 2XSSC and loaded into GeoMx DSP instrument slide holder.

The GeoMx DSP instrument performs multiplexed wide field fluorescence microscopy and utilizes an ultraviolet (UV) laser to release oligonucleotide barcodes from a specific area

of illumination (AOI). The labeled Cdkn2a transcripts enable precise selection of regions within a tissue based upon fluorescent intensity. The GeoMx instrument has a complement of four fluorescence imaging channels with the following specifications (Channel, Excitation (peak/bandwidth), Emission (peak/bandwidth)): FITC, 480/28 nm, 516/23 nm; Cy3, 538/19 nm, 564/15 nm; Texas Red, 588/19 nm, 623/30 nm; Cy5, 645/19 nm, 683/30 nm. Multiple segments can be chosen for each region of interest (ROI) with a maximum ROI size of 660 µm x 785 µm. This segmentation is performed using the onboard GeoMx software which selects pixels within the image based upon fluorescent intensity thresholds. Only the selected areas are then illuminated by UV light thereby photocleaving the linker molecule and liberating the oligonucleotide barcodes in specific regions within the ROI. Thresholds can be adjusted for each segment and for each fluorescent channel and corresponding fluorescently labeled morphology marker.

AOIs were manually drawn based on visual inspection of Cdkn2a expression, and aimed to have approximately 230 nuclei per AOI. 2 AOIs per brain region were selected from each brain section — one with a high number of Cdkn2a (*p16* high) and one with a low number of Cdkn2a puncta (*p16* low). The brain regions inspected were areas CA1 and CA3 of the hippocampus, the somatosensory cortex, the motor cortex, and the choroid plexus. This yielded a total of 10 matched AOIs per brain sample. Selected AOIs were illuminated by UV laser in the GeoMx instrument and photocleaved barcodes were collected and deposited into a 96-well microplate by the instruments onboard microfluidics system. Collection plates were sealed to prevent contamination and stored at -80°C prior to library preparation.

Indexed AOIs were pooled and purified into two rounds of AMPure XP (Beckman Coulter, Cat#A63880) PCR purification using a 1.2x bead:sample ratio. Samples were then sequenced on an Illumina NextSeq 2000. FASTQ files were filtered and demultiplexed using DND2.0 with the following parameters: quality trim score = 20, adaptor trim match length = 10, adaptor trim max mismatch = 3, barcode max mismatch = 1, stitching max mismatch = 2, dedup-hd = 1. DND is used to convert the raw FASTQ files to Digital Count Conversion (DCC) file format.

Individual DCC files were aggregated and checked for probe-level quality prior to data analysis. For the WTA, each gene is mapped to a single probe.

Analysis was performed using Nanostring's GeoMx DSP Analysis Suite. For each sample, Limit of Quantification (LOQ) was derived. LOQ for a given gene is defined as the geometric mean of pool-specific negative probes times the geometric standard deviation of negative probes raised to a power of 2 (i.e., LOQ2). These LOQ values were used as a basis of filtering genes that are expressed near background. We required that a given gene needed to be above LOQ2 in at least 20% of the AOIs. Any probes that failed Grubb's outlier test in >20% of segments were excluded. Individual probe counts were normalized to the median probe count for each AOI. Differential gene expression between *p16* high and *p16* low AOIs was determined using unpaired t-tests with Benjamini Hochberg correction. Gene Set Enrichment Analysis (GSEA) was performed within the DSP Analysis Suite with minimum coverage of genes in pathway set at 20%, minimum number of genes in each pathway set as 5, minimum pathway size as 15, and maximum as 500, and number of permutations at 1000.

CHAPTER 3

STRESS AND ALZHEIMER'S DISEASE: A SENESCENCE LINK?

Chapter 3 contains work that was previously published in *Neuroscience and Biobehavioral reviews* 2020.

Lyons, C.E., Bartolomucci, A. Stress and Alzheimer's disease: A senescence link? Neuroscience and Biobehavioral Reviews (Vol. 115, pp. 285–298). Elsevier Ltd. https://doi.org/10.1016/j.neubiorev.2020.05.010

3.1 Summary

Chronic stress has been shown to promote numerous aging-related diseases, and to accelerate the aging process itself. Of particular interest is the impact of stress on Alzheimer's disease (AD), the most prevalent form of dementia. The vast majority of AD cases have no known genetic cause, making it vital to identify the environmental factors involved in the onset and progression of the disease. Age is the greatest risk factor for AD, and measures of biological aging such as shorter telomere length, significantly increase likelihood for developing AD. Stress is also considered a crucial contributor to AD, as indicated by a formidable body of research although the mechanisms underlying this association remain unclear. Here we review human and animal literature on the impact of stress on AD and discuss the mechanisms implicated in the interaction. In particular we will focus on the burgeoning body of research demonstrating that senescent cells, which

accumulate with age and actively drive a number of aging-related diseases, may be a key mechanism through which stress drives AD.

3.2 Introduction

Chronic stress is a risk factor for a number of aging-related diseases, including Alzheimer's disease (AD), the most prevalent form of dementia. The vast majority of AD cases have no known genetic cause, indicating an important role for environmental factors. In humans, high stress levels increase risk for developing AD (Moceri *et al.*, 2001; Wilson *et al.*, 2003). High stress levels both accelerate the age of onset for familial early-onset AD, and increase likelihood of progressing to advanced stages of the disease in late-onset AD (Moceri *et al.*, 2001; Peavy *et al.*, 2012). In addition to chronological age, measures of biological aging, such as shorter telomere length, significantly increase likelihood for developing AD (Honig *et al.*, 2012; Zhan *et al.*, 2015). Here, we will survey the current literature on the impact of stress on AD and discuss the mechanisms implicated in the interaction, particularly a role for cellular senescence as mediator.

3.3 The stress response

Since its first descriptions, the phenomenon known as stress has been intimately linked to disease and aging (Selye, 1936, 1950). While its definition has been, and continues to be debated and updated over time (Selye, 1936; McEwen, 1998; Sapolsky *et al.*, 2000; Pacák & Palkovits, 2001; Romero *et al.*, 2009; Koolhaas *et al.*, 2011; Nederhof & Schmidt, 2012; Kagan, 2016), this association has endured. The stress nomenclature has been revised to restrict it to conditions characterized by uncontrollability and unpredictability that exceed the regulatory range and adaptive capacity of an individual (Koolhaas *et al.*, 2011). Challenges to homeostasis and the body's associated physiological responses are a constant feature of living organisms. Stressors are distinguished from these challenges by having physiological demands outside the natural regulatory capacity for an organism. Activation of the acute stress response is a normal part of homeostatic regulation of the body, but under some conditions this response becomes sustained. This persistent activation is associated with a number of maladies, can lead to sudden death in vulnerable individuals, and can significantly shorten individual lifespan (Razzoli et al., 2020, 2018;

Snyder-Mackler N, et al. 2020; Stringhini et al., 2017; Tung et al., 2016; Zipple et al., 2019).

The neuroendocrine stress response is classically defined as having two major components: the sympathetic-adrenal medullary (SAM) system and the hypothalamic pituitary adrenal (HPA) axis (for review, see Charmandari et al., 2005 and Ulrich-Lai and Herman, 2009). In response to a stressor, the SAM system, commonly referred to as the "fight or flight response", (Cannon, 1915) is rapidly activated. Preganglionic neurons in the sympathetic nervous system activate chromaffin cells in the adrenal medulla resulting the release of epinephrine (and to a lesser extent, norepinephrine) into general circulation. These chemicals act on via adrenergic receptors in a wide range of tissue types, resulting in increased heart rate, respiratory rate, glycolysis, glycogenolysis and lipolysis.

In the second component, the HPA axis, activated neurons in the paraventricular nucleus of the hypothalamus release corticotropin releasing hormone (CRH) into the hypophysial portal system. CRH reaches the anterior pituitary gland, causing it to release adrenocorticotropic hormone (ACTH) into general circulation. ACTH stimulates the adrenal cortex to produce glucocorticoids (GCs) which act on a number of targets. GCs also exert negative feedback on the hypothalamus, halting the release of CRH, and on the pituitary, halting the release of ACTH. However, in cases of sustained stress or aging, GC hypersecretion can persist (Sapolsky *et al.*, 1986; Spiga *et al.*, 2014). Additionally, this negative feedback system is impaired with age, largely through the downregulation of glucocorticoid receptors (GR) in the hippocampus (Sapolsky *et al.*, 1986). HPA axis hyperactivity is associated with numerous negative outcomes, including major depression (Pariante & Lightman, 2008), immune suppression (Oppong & Cato, 2015) and memory impairment (Tatomir *et al.*, 2014).

In addition to the canonical "stress axes" described above, several additional neural and neuroendocrine system have been shown to regulate the acute stress response (see Sapolsky *et al.*, 2000; Ulrich-Lai & Herman, 2009 for review) including a newly identified role for osteocalcin (Berger *et al.*, 2019).

3.4 Stress and Alzheimer's disease

In humans, stress has been associated with a number of neurodegenerative diseases, including Alzheimer's Disease (AD) (Yuede *et al.*, 2018), other dementias (Johnston, 2000; Bonanni *et al.*, 2018), and Parkinson's Disease (Hemmerle *et al.*, 2012). AD is the most common form of dementia and results in a debilitating loss of memory and cognitive function. Early on, the disease primarily manifests in the form of impaired memory, reflecting the location of initial neural degeneration in the entorhinal cortex and hippocampus. Subsequently, neural atrophy spreads to other limbic and neocortical regions and symptoms progress to severely alter cognitive and behavioral domains (Braak & Braak, 1991; Braak *et al.*, 2006). The pathophysiological process begins years, and even decades before the onset of clinical symptoms (Morris, 2005). Since its identification by Alois Alzheimer in 1910, AD neuropathology has been characterized by profound neuron loss as well as two hallmarks: neurofibrillary tangles (NFTs) and amyloid β (Aβ) plaques. NFTs appear intracellularly and are comprised of aggregated hyperphosphorylated tau protein (Del C. Alonso *et al.*, 1996). Neurotoxic Aβ plaques occur extracellularly and are composed of clumped Aβ peptide (Selkoe, 2001). While these are considered markers of the disease and their presence in postmortem analysis is required for a definitive AD diagnosis, neuron and synapse loss are believed to underlie the declines in memory and cognition. Indeed, studies have shown that one of the best pathological correlate to early disease progression is synapse loss (Davies *et al.*, 1987; Masliah *et al.*, 2001; Scheff *et al.*, 2007).

With the exception of rare early onset forms, symptoms typically first appear in patients over age 65, making AD primarily a disease of aging. Though the cause(s) of AD remain poorly understood (over 90% of cases have no known genetic cause (Bertram & Tanzi, 2004), it is clear that biological aging plays a role in its etiology. Multiple studies show a correlation between shorter telomere length in circulating immune cells and increased risk for AD (Blasco, 2005; Honig *et al.*, 2012). A more sophisticated analysis established a causal link between shorter telomeres and AD risk, concluding that for each standard deviation above average telomere attrition rate, risk for AD increases by 36% (Zhan *et al.*, 2015). Additionally, it is widely believed that environmental factors such as

air pollution (Killin *et al.*, 2016), nutrition (Morris, 2009) and stress (Yuede *et al.*, 2018) play a role in disease onset and progression, along with biological factors such as aging (Prather *et al.*, 2015). Interactions between such environmental elements with aging processes like telomere length, oxidative stress and cellular senescence may play a critical role in their effect on AD risk.

In humans, there is strong epidemiological evidence linking chronic stress and dementia. For example, in the Religious Orders study, individuals who scored in the 90th percentile for "proneness to psychological distress" were twice as likely to develop AD as those with scores in the 10th percentile. In particular, distress proneness was associated with a decline in episodic memory, though not with other cognitive domains (Wilson *et al.*, 2003). Thus, individuals who experienced a higher degree of perceived stress were at much higher risk for developing AD. A similar result was found in a broader population as well (Crowe *et al.*, 2007). In this study, higher reactivity to stress was associated with a dementia diagnosis 30 years later, even within twins. Furthermore, veterans with posttraumatic stress disorder have a 2-fold higher risk for developing dementia than veterans without the condition (Yaffe *et al.*, 2010).

Several measures of socioeconomic status predict risk for AD. Low socioeconomic status can confer an immense burden of stress involving economic insecurity, uncertainty about future stability, and feelings of exclusion or marginalization due to occupational or economic status (Marmot *et al.*, 1991; Stringhini *et al.*, 2017; Marmot, 2020). It has been observed that low education and occupational attainment increase risk of AD (Stern *et al.*, 1994; Räihä *et al.*, 1998). In particular, low socioeconomic status in childhood increases an individual's risk of AD by 1.8 times. This increase in risk is even greater if the individual also has the apolipoprotein (APOE) E4 allele, a variant associated with late onset AD. People with this gene variant who grew up in a low socioeconomic household were 2.35 times more likely to develop AD than carriers who grew up in higher socioeconomic status households, and 7.44 times more likely than non-carriers who grew up in higher socioeconomic status households (Moceri *et al.*, 2001). Since this effect is greater than additive, it suggests an interaction between genes and environment (Moceri *et al.*, 2001). Some reports suggest that APOE function may influence circulating glucocorticoid levels, as carriers of the APOE E4 allele tend to have higher cortisol concentrations in the

cerebrospinal fluid, irrespective of AD diagnosis (Peskind *et al.*, 2001). This report, along with several others, further observes that stress can accelerate the age of onset in familial AD (Mejfa *et al.*, 2003). High job strain (high demands combined with low control) increases risk for developing AD later in life, but is not affected by APOE genotype (Wang *et al.*, 2012).

Additionally, stress later in life can also precipitate transition to late onset AD. Mild cognitive impairment (MCI) is sometimes classified as preclinical or early stage dementia (Morris *et al.*, 2001). Occurrence of highly stressful events is associated with accelerated cognitive decline in MCI patients resulting in full dementia over a 2-3-year period (Peavy *et al.*, 2012). In these patients, the level of salivary cortisol, one of the classical endocrine markers of chronic stress, was not correlated with disease progression (Peavy *et al.*, 2012). However, AD patients frequently exhibit elevated cortisol levels (salivary, plasma, cerebrospinal fluid) compared with cognitively normal individuals (Vyas *et al.*, 2016) and higher cortisol levels are associated with accelerated progression and increased severity of dementia (Davis *et al.*, 1986; Csernansky *et al.*, 2006). This suggests a differential effect of cortisol depending on the extent of neuropathology and underlines the complexity of the relationship between neuroendocrine pathways implicated in stress and AD.

Though it will not be the focus of this review, it is notable that stress has also been linked to a number of other neurodegenerative disorders, including vascular dementia (Gerritsen *et al.*, 2017) Parkinson's Disease (Hemmerle *et al.*, 2012) and Huntington's Disease (Mo *et al.*, 2014). This indicates that stress can more broadly promote degeneration in multiple neural systems.

3.5 Insights into stress and neurodegenerative pathology from rodent research

Studies in animals mirror the stress-induced association and exacerbation of AD-related pathology observed in humans (Carroll *et al.*, 2011). They furthermore contribute insights into the molecular mechanisms underlying this association. Evidence exists for interactions between stress and neuropathology in animal models that carry human AD-associated mutations, as well as molecular and behavioral changes in wildtype animals. Although age-related cognitive decline is common across species, no animals aside from

humans (and arguably non-human primates (Kalinin *et al.*, 2013; Uchihara *et al.*, 2016; Latimer *et al.*, 2019)) spontaneously develop AD (Gallagher & Nicolle, 1993; Herndon *et al.*, 1997). Though wildtype rodents do not develop AD, studying neural alterations associated with cognitive decline in wildtype rodents can help to identify the preclinical molecular changes that facilitate or appear prior to plaques and tangles. These earlier stages of pathology are key in understanding how and why AD develops and may be the point at which intervention is possible. A key turning point in AD research was the development of transgenic rodent models of AD that carry human copies of genes mutations known to cause familial AD in humans (Games *et al.*, 1995; Hsiao *et al.*, 1996). These AD mouse models have allowed profound insights into the pathophysiology of tau and Aβ inclusions and serve central roles in preclinical testing. Thus, much has been learned from studies in rodents, both wildtype and transgenic, about the interaction between stress and AD-related outcomes.

3.6 Stress effects on neurofibrillary tangles and tau

NFTs, one of the hallmarks of AD, are comprised of aggregates of the microtubule binding protein tau. The incidence of NFTs is correlated with cognitive deficits and neuronal loss in AD (Arriagada *et al.*, 1992). Tau is abundant in neurons, where it binds and stabilizes microtubules in the cytoskeleton, but is less common in other cell types. Tau structure, encoded by the MAPT gene, is largely conserved among mammals, with differences largely confined to the N-terminal domain (Hernández *et al.*, 2019). Mouse tau specifically differs from human tau in its lack of 11 amino acid residues in the N-terminal region. Mouse tau also exists primarily in only 3 isoforms, while in humans it occurs in 6. All of these isoforms are generated by alternative splicing and have a number of potential phosphorylation sites, which when occupied disrupt the protein's capacity for microtubule binding and stabilization (Mandelkow & Mandelkow, 2012). Additionally, hyperphosphorylated tau can self-aggregate to form insoluble paired helical filaments which can then aggregate further to form NFTs (Gustke *et al.*, 1992; Del C. Alonso *et al.*, 1996). Although NFTs appear later in disease progression, and correlate with disease stage, many researchers now believe that soluble, non-aggregated tau can also drive cognitive decline (Kopeikina *et al.*, 2012). Thus, the abundance of phosphorylated tau, both aggregated and not, appears to play an important role in AD pathogenesis.

In wildtype rodents, it is well established that stress can increase phosphorylation of tau (**Table 1**). Over 20 years ago, it was first shown that acute cold water stress exposure increases tau phosphorylation in rat and mouse brain (Korneyev *et al.*, 1995). This result has since been replicated in numerous experiments (Korneyev, 1998; Okawa *et al.*, 2003; Feng *et al.*, 2005) and acute immobilization stress and restraint stress have also been demonstrated to increase tau phosphorylation (Filipcik *et al.*, 2012; Kvetnansky *et al.*, 2016). Acute stress-induced tau phosphorylation extends to many brain areas, including not only subregions of the hippocampus, but also frontal cortex, nucleus basalis of Meynert and the locus coeruleus (Filipcik *et al.*, 2012).

Additionally, several different rodent models of chronic stress have been shown to increase tau phosphorylation. Chronic restraint stress has been reported to increase levels of both soluble hyperphosphorylated tau and insoluble tau (Rissman *et al.*, 2007; Yan *et al.*, 2010). It also decreases levels of the microtubule assembly-promoting protein MAP2 (Yan *et al.*, 2010). This decrease in MAP2 may reflect additional neuronal destabilization. Chronic restraint stress additionally changes the distribution of tau, with more tau in areas of the hippocampus that also exhibit decreased MAP2 expression (Yan *et al.*, 2010). Three weeks of chronic unpredictable mild stress (CUMS) in young adult rats is sufficient to increase tau phosphorylation (Yang *et al.*, 2014). Furthermore, vulnerable rats that develop anhedonia in the sucrose preference test, indicative of a depression-like state, after 6 weeks of CUMS, have increased tau hyperphosphorylation as well as increased levels of $A\beta_{40}$ (Briones *et al.*, 2012). 4 weeks of CUMS in aged rats (15 months), in addition to increasing tau hyperphosphorylation, also upregulates angiotensin converting enzyme (ACE) and downregulates structural proteins, such as MAP2 and synuclein-gamma (AbdAlla *et al.*, 2015).

Stress-induced tau hyperphosphorylation appears to occur very rapidly, with just 4 minutes of cold water exposure sufficient to induce an effect (Korneyev *et al.*, 1995). The reversibility of this effect seems to scale with the chronicity of stressor exposure. With a single stressor exposure, phosphorylated tau levels return to amounts indistinguishable from those of unstressed controls 2 hours after cessation of immobilization stress (Rissman *et al.*, 2007; Filipcik *et al.*, 2012), Reversal of tau hyperphosphorylation remains possible

24-hours post final stressor exposure following 6 (Kvetnansky *et al.*, 2016), but not 14 days (Rissman *et al.*, 2007) of daily stressor exposure. In keeping with this pattern, after 6 weeks of CUMS, increased tau phosphorylation is still detectable 7 days after the final stress exposure (Briones *et al.*, 2012). Thus, it appears that recovery from stress-induced tau hyperphosphorylation is possible but becomes increasingly impaired the longer stress exposure continues.

Although the evidence is compelling that chronic stress can cause changes in the brain and behavior in wildtype rodents associated with neurodegeneration, the limitation remains that these animals have not been shown under any condition to develop AD. However, by employing the use of transgenic humanized mouse models of AD, it is possible to study the interaction between stress and the proteins most closely tied to AD.

Unlike work in transgenic lines that model Aβ pathophysiology, few stress studies have been performed in mouse lines that model the tauopathy component of AD. However, it has been demonstrated that in mice that carry mutant copies of the tau gene that mimic those found in human disease, chronic stress further exacerbates tau-related pathologies. In the PS19 mouse model, which is characterized by hyperphosphorylated tau that forms neurofibrillary tangles, 4 weeks of restraint stress promotes tau hyperphosphorylation, accumulation of insoluble tau, and worsened fear memory (Carroll *et al.*, 2011). Additionally, chronic restraint stress in the Tg2576 mouse line, which models Aβ pathology, also increases phosphorylation of tau (Lee *et al.*, 2009). Another study treated 3xTg-AD mice, which harbor knock-in mutations of presenilin 1, APP and tau, with the synthetic glucocorticoid dexamethasone for 7 days. This treatment increased mislocalization of tau to the somatodendritic region of neurons in the hippocampus, cortex and amygdala, but did not increase levels of phosphorylation (Green *et al.*, 2006). However, this same treatment regimen in rTg4510 mice, which express the same tau and presenilin 1 mutations as the 3xTg-AD model, but not the APP mutation, did not alter levels of tau, suggesting that elevated glucocorticoid signaling may not play a direct role in this tau mislocalization; rather it occurs downstream of an interaction between the glucocorticoids and APP (Green *et al.*, 2006).

Overall, the evidence is compelling that stress can both acutely and chronically alter tau expression and hyperphosphorylation. These changes are highly relevant to AD, as decreasing levels of tau, even without disrupting NFTs can improve cognitive function (Oddo *et al.*, 2006).

Table 1: Rodent studies on impact of stress on AD-related markers tau and Aβ

Stress paradigm	Duration	Animal model	Effect on tau pathology	Effect on Aβ pathology	Reference(s)
Acute cold water	(4-10 min)	Wildtype rat	↑ phosphorylation	---	Korneyev et al., 1995; Korneyev, 1998; Okawa et al., 2003; Feng et al., 2005
Acute multimodal stress	5h	3xTg-AD mouse	No change	↑ Aβ, ↑ACE	Baglietto-Vargas et al., 2015
Restraint Stress	30 min	Wildtype mouse, CRHR2 KO mouse	↑ phosphorylation (soluble and insoluble) up until 90min after acute stress	---	Rissman et al., 2007
	3h	Wildtype rat	---	↑ APP, ↑ Aβ	Ray et al., 2011
	30min/day; 14 days	Wildtype mouse	↑ phosphorylation (soluble and insoluble) changes still present 24h after final stressor	---	Rissman et al., 2007
	1h/day; 14 days	Wildtype rat	↑ phosphorylation (soluble and insoluble); changes distribution	---	Yan et al., 2010
	2h/day; 16 days	Tg2576 mouse	↑ phosphorylation	↑ Aβ, ↑ plaque deposition	Lee et al., 2009
	2h/day; 7 days or 6h/day; 21 days	Wildtype rat	---	↑ APP	Rosa et al., 2005
	(6h/day; 5 days)	5XFAD mouse	---	↑ Aβ, ↑ APP, ↑ BACE1, ↑ plaque deposition in females but not males	Devi et al., 2010
	(6h/day; 6 days/week; 4 weeks)	PS19 mouse	↑ phosphorylation, ↑ insoluble forms, ↑ aggregation	---	Carroll et al., 2011
	(6h/day; 6 days/week; 4 weeks)	Tg2576 mouse	---	↑ ACE	Carroll et al., 2011

Chronic unpredictable mild stress	(3 weeks)	Wildtype rat	↑ phosphorylation	---	Yang et al., 2014
	(6 weeks)	Wildtype rat	↑ phosphorylation	↑ $A\beta_{40,}$ ↑ BACE1	Briones et al., 2012
	(4 weeks)	Wildtype rat	↑ phosphorylation	↑ ACE	AbdAlla et al., 2015; Sotiropoulos et al., 2015
Elevated open platform	10-20 days	Wildtype rat	---	↑ APP	Sayer et al., 2008
Chronic isolation	3 months	Tg2576 mouse	---	↑ Aβ, ↑ plaque deposition, earlier age of onset for plaques	Kang et al., 2007
	5-8 months	Tg2576 mouse	---	↑ Aβ, ↑ plaque deposition	Dong et al., 2004
Chronic mild social stress (random cage composition)	6h/day; 2-3 days / week; 6 weeks	3xTg-AD mouse	No change	↑ Aβ	Rothman et al., 2012
Maternal separation	3h/day; PND 2-21	Wildtype rat	↑ phosphorylation	↑ Aβ,↑ $A\beta_{40,}$ ↑ $A\beta_{42}$, ↑ BACE1	Solas et al., 2010; Martisova et al., 2013
Postnatal reduced bedding material	PND2-9	APP/PS1 mouse	---	↑ Aβ, ↑ plaque deposition	Hoeijimakers et al., 2017
	PND2-P9	APP-V717I x Tau-P301L mouse	No change	↑Aβ	Lesuis et al., 2016
Immobilization Stress	10, 30, 60, 90 or 120 minutes	Wildtype mouse	↑ phosphorylation at 30 min; no change after other durations	–––	FIlipicik et al., 2012
	10, 30, 60, 90 or 120 minutes	CRH KO mouse	No change	–––	FIlipicik et al., 2012
	2h/day; 7 days	Wildtype mouse; CRH KO mouse	↑ phosphorylation	–––	Kvetnansky et al., 2016

3.7 Stress effects on Aβ plaques

The other main marker of AD is the accumulation of Aβ plaques. Much research focus has been put into their ontology, based on the "amyloid hypothesis", which postulates that the buildup of Aβ, particularly the longer, more hydrophobic Aβ42 isoform, is the root cause of AD (Selkoe & Hardy, 2016). The Aβ peptide is derived from the longer amyloid precursor protein (APP) through two cleavage events, the first executed by BACE1 (β site APP cleavage enzyme 1), and the second by a γ secretase complex. APP can alternatively be processed by sequential cleavage by γ secretase and γ secretase, which does not produce Aβ (O'brien & Wong, 2011). Familial early onset forms of AD are caused by mutations in the precursor protein APP, or in the γ -secretase components, presenilin 1 and presenilin 2 (PSEN1, PSEN2), which result in an increased ratio of $A\beta_{42}$ to $A\beta_{40}$ (Scheuner *et al.*, 1996). Given this causal relationship between Aβ -related genetic mutations and AD, the amyloid hypothesis has been compelling and widely accepted. The theory posits that an increase in $A\beta_{42}$ results in oligomerization and the formation of Aβ plaques. The plaques accumulate, impairing synaptic activity and causing reactive inflammation in surrounding cells and setting off a cascade of reactions, including tau tangle formation, synapse loss and neuron death, which together lead to the cognitive deficits that constitute dementia (for review, see Selkoe and Hardy, 2016). However, recent findings have called into question the precise role of plaques in AD. In particular, the failure of clinical trials targeting Aβ plaques (Mullane & Williams, 2013; Egan *et al.*, 2018) and the observation that there is a very weak correlation between the abundance of Aβ plaques and degree of cognitive impairment (Nelson *et al.*, 2012) have put the original amyloid hypothesis into question, underlining the need for further research. Regardless of their precise role in the genesis of AD, it is clear that Aβ cleavage and buildup are core processes in the disease. Additionally, there is a compelling body of research on the effect of stress on Aβ (**Table 1**) which will be discussed below.

Similar to its effect on tau phosphorylation, stress in wildtype rats and mice increases levels of APP mRNA and protein and Aβ (Rosa *et al.*, 2005; Sayer *et al.*, 2008; Solas *et al.*, 2010; Ray *et al.*, 2011). Daily maternal separation during the first 3 weeks of life increases levels of $A\beta_{40}$ and $A\beta_{42}$ in adulthood and increases expression of the BACE1

(Martisova *et al.*, 2013). It also results in decreased hippocampal cell number, lower brain-derived neurotrophic factor (BDNF) levels and diminished synaptophysin and postsynaptic density-95 (PSD-95) (Martisova *et al.*, 2013). 4 weeks of CUMS in aged (15 month old) rats increases levels of ACE and 6 weeks of CUMS in young adult rats increases levels of $A\beta_{40}$ (Briones *et al.*, 2012; AbdAlla *et al.*, 2015).

Chronic stress also aggravates amyloid pathology in numerous transgenic mouse models of AD. In mice that express APP with a mutation known to cause familial early onset AD (Tg2576; Hsiao et al., 1996), several stress procedures intensify pathology. 3 months of social isolation stress not only elevates levels of Aβ but also increases plaque deposition and worsens cognitive impairment (Kang *et al.*, 2007; Lee *et al.*, 2009). The extent of the impact of stress on AD-related pathology depends on, among other factors, the duration of stress exposure. In Tg2576 mice, elevated Aβ is measurable after just 1 hour of restraint stress, and peaks 10 hours after cessation of the restraint (Kang *et al.*, 2007). Long-term social isolation stress (from weaning onward) anticipated age of onset for Aβ plaque deposition from 9 months to 6 months of age. It also reduced neurogenesis in hippocampus, which was associated with impaired contextual memory (Dong *et al.*, 2004).

In the 3xTg-AD mouse model, which carries 3 genes associated with familial AD in humans (to the APP, MAPT and PSEN1 genes), a single instance of 5 hour intense "modern life-like" stress (restraint stress on rotating platform accompanied by loud noise) increased Aß levels and reduced the number of synapse-bearing dendritic spines (Baglietto-Vargas *et al.*, 2015). 6 weeks of mild social stress (randomized cage composition for 6 hours, 2-3 times weekly) in the same mouse line increased both Aβ and decreases BDNF (Rothman *et al.*, 2012). 7 day treatment with the glucocorticoid receptor (GR) agonist dexamethasone (5mg/kg) in this model increased levels of APP, $A\beta_{40}$ and $A\beta_{42}$ and increased activity of BACE (Green *et al.*, 2006).

Similarly, 5 days of restraint stress increased levels of $A\beta_{42}$ and plaque deposition in the hippocampus of female but not male 5XFAD mice, which carry 5 familial AD mutations in APP and PSEN1 genes (Oakley *et al.*, 2006; Devi *et al.*, 2010). This is an interesting finding given that women are much more likely to develop AD than men

(Alzheimer's Association, 2014). However after 4 weeks of restraint stress, both male and female 5XFAD mice had increased levels of Aβ along with impaired spatial and fear memory, compared with unstressed littermates (Carroll *et al.*, 2011). Together these studies indicate that females harboring these genetic mutations may be more vulnerable to stress than males, but that long term chronic stress will ultimately exacerbate pathology in both sexes.

In most of the experiments discussed above, stress protocols were applied during the young adult period. Early-life stress can also result in worsened Aβ pathology later in life. Postnatal stress increases Aβ plaque burden and inflammatory markers and compromises survival later in life in APP/PS1 mice (Lesuis *et al.*, 2016; Hoeijmakers *et al.*, 2017). These results mirror the epidemiological findings in humans discussed earlier, which demonstrate that early life stress can particularly increase likelihood of developing AD.

3.8 Stress-induced changes to synapses and neuronal survival

Although NFTs and Aβ plaques are regarded as the primary markers of AD pathology, synapse and neuron loss are thought to be the net result of their presence and directly cause the cognitive and memory impairments associated with AD. Indeed, studies show that neuronal degeneration is a better predictor of dementia than tau or Aβ inclusions (Price *et al.*, 2001). Synaptic loss has the strongest correlation with the staging of dementia and with early stage AD (Scheff *et al.*, 2007; Nelson *et al.*, 2012). It has been proposed that synapse loss underlies the cognitive impairments in early stage AD and that this disruption of plasticity impairs neuronal viability, resulting in the neuron loss that characterizes later stages of the disease (Shankar & Walsh, 2009). Numerous lines of research indicate that chronic stress can directly lead to synapse loss and impaired neurogenesis. In this way, stress may promote the advent and accelerate the progression of AD.

The hippocampus, the origin point of AD pathology, is particularly stress-sensitive possibly because of its robust expression of GR and CRH receptor 1 (CRHR1) receptors (Braak & Braak, 1991; Braak *et al.*, 2006). It is a major target of stress-associated hormones (McEwen *et al.*, 1968), and stress-induced degeneration in the hippocampus is well documented (McEwen *et al.*, 1968; McEwen, 1998). In particular, chronic stress

dramatically shrinks apical dendrites in area CA3 of the hippocampus. Numerous studies have demonstrated that chronic restraint stress induces atrophy of apical dendrites (shorter length, fewer branch points) in hippocampal CA3 pyramidal neurons (Watanabe *et al.*, 1992; Magarin˜os & McEwen, 1995). While much of this work has been done in rats, it has been shown that this effect is preserved across species (Bartolomucci et al., 2002; Czeh et al., 2001; Magariños et al., 1996). Acute, as well as chronic stress can alter CA3 dendrites: a single exposure to a 5-hour stressor reduces CA3 dendritic spine density and long-term potentiation. Moreover, these effects correlate with stress-induced deficits in selected learning and memory processes (Bartolomucci, De Biurrun, Cz?h, *et al.*, 2002; Chen *et al.*, 2010).

The vast majority of dendritic spines have synapses, and thus their loss has profound functional consequences (Harris, 1999; Arellano *et al.*, 2007). Studies that examine specific synaptic markers find similar results to those that examine dendritic structure. Both chronic stress and GC exposure reduce the number of synapses between mossy fibers from dentate gyrus granule cells onto CA3 pyramidal cells (Sousa *et al.*, 2000). Additionally, multimodal stress – restraint combined with loud music, has a greater effect than either manipulation alone as measured by memory performance and reduction in synapse number in CA3 (Maras *et al.*, 2014).

Prolonged exposure to either chronic psychosocial stress or GCs does not impact cell number but does reduce CA3 and hippocampal volume, which may be accounted for through a loss of synapses (Czeh *et al.*, 2001; Tata *et al.*, 2006). In humans, hippocampal volume begins to decrease concomitantly with the onset of memory decline (Reiman *et al.*, 1998), suggesting that this is a highly relevant parameter.

While abundant evidence supports stress-induced deterioration in area CA3, there are fewer reports of changes in other areas of the hippocampus. Some studies have found that stress or GC induced dendritic decline in CA1 pyramidal neurons (Sousa *et al.*, 2000), but others have not (Woolley *et al.*, 1990; Alfarez *et al.*, 2008). Interestingly, one study did find that while 3 weeks of unpredictable stress did not affect CA1 dendritic length, if brain slices from these animals were subsequently exposed to elevated GC levels, there was a significant reduction in apical dendritic length, compared with slices from control animals

(Alfarez *et al.*, 2008). This suggests that some sensitization may occur in CA1 neurons in response to chronic stress that renders them more sensitive to future stress. Another study found that multimodal stress but not a single stressor (either restraint or loud noise) can reduce synapse number in CA1. It also induced a reduction in connectivity (as measured by c-fos) with the septum and thalamus and an increase in connectivity with the amygdala and the bed nucleus of the stria terminalis (Maras *et al.*, 2014). These results suggest that while CA1 may be less vulnerable to a single bout of chronic stress, repeated stressor exposure and/or facing multiple stressors simultaneously may lead to CA1 deterioration. This is particularly pertinent to the role of stress in neurodegeneration, as AD pathology particularly affects CA1 (Padurariu *et al.*, 2012; Masurkar, 2018).

Chronic stress has profound influence on other brain regions, in addition to the hippocampus. The prefrontal cortex (PFC) is involved in the processing of emotional stimuli as well as complex cognitive tasks (Cerqueira *et al.*, 2007). Prenatal stress impairs connectivity between the hippocampus and PFC and disrupts synaptic plasticity within the PFC (Mychasiuk *et al.*, 2012), which is similar to the reduced connectivity observed in humans after stressful experiences (Admon *et al.*, 2013). Furthermore, chronic subordination stress decreases serotonin turnover in the PFC in susceptible mice (Bartolomucci *et al.*, 2010). As in the hippocampus, chronic stress (both chronic social defeat stress or chronic variable stress) reduces dendritic spine density in the prefrontal cortex in a CRHR1-dependent manner (Chen *et al.*, 2008; Radley *et al.*, 2013; Shu & Xu, 2017). In wildtype rodents, chronic stress promotes Aβ accumulation and tau phosphorylation in the prefrontal cortex (PFC), as well as the hippocampus (Ray *et al.*, 2011; Sotiropoulos *et al.*, 2011; Yang *et al.*, 2014).

Stress also inhibits adult neurogenesis and impairs survival of newly born neurons in the dentate gyrus (Czeh *et al.*, 2001; Krugers *et al.*, 2010) A decline in neurogenesis occurs with aging and is thought to contribute to age-related cognitive impairment by reducing capacity for plasticity (Apple *et al.*, 2017). Thus, by impairing the formation and survival of new neurons, stress may further promote the decline in cognitive performance associated with AD. Acute stressor exposure reduces proliferation and increases the number of apoptotic granule cells in the dentate gyrus (Gould *et al.*, 1998; Heine *et al.*,

2005) while chronic stressor exposure additionally increases the expression of the cell cycle inhibitor p27Kip1 in the dentate gyrus (Heine *et al.*, 2004). GCs alone can impair neurogenesis by inhibiting cell proliferation and survival (Wong & Herbert, 2006). This is another mechanism by which chronic stress can aggravate age-related decline in brain having significant implication for neurodegenerative disorders.

3.9 Stress-induced promotion of neuroinflammation

Neuroinflammation is a common pathological feature in AD and other neurodegenerative diseases (Griffin *et al.*, 1989; Cribbs *et al.*, 2012; Sudduth *et al.*, 2013; Crotti & Glass, 2015; Herrero *et al.*, 2015). In response to insults, microglia and astrocytes secrete inflammatory factors which facilitate immune cell recruitment and clearance of infection and tissue damage. In AD, it is believed that neuroinflammation results as a reaction to accumulation of Aβ, and is one of the earliest features of the disease. Microglia respond to Aβ by phagocytosing the abnormal protein and secreting proinflammatory cytokines to recruit additional microglia to the plaques (Smith *et al.*, 2012; Bhaskar *et al.*, 2014). Astrocytes to a lesser degree can degrade Aβ and also secrete inflammatory mediators in response to Aβ (Carrero *et al.*, 2012).

This immune response appears to be initially beneficial, increasing clearance of Aβ (Shaftel *et al.*, 2007; Chakrabarty *et al.*, 2010). However, prolonged inflammation can be detrimental to neurons and synapses (Leszek *et al.*, 2016) and can ultimately impair microglial phagocytosis of Aβ (Hickman *et al.*, 2008), while simultaneously promoting Aβ production (Chong, 1997; Liaoi *et al.*, 2004) and tau hyperphosphorylation (Quintanilla *et al.*, 2004). Overall, neuroinflammation has a complex and multifaceted role in AD. While it can have beneficial effects by promoting Aβ clearance, it can also directly promote other aspects of AD neuropathology, increasing both Aβ burden and tau hyperphosphorylation and impairing synapse maintenance and neuronal survival.

Increased inflammation is a common phenotype of normal brain aging across species (Frank *et al.*, 2006), and may represent one mechanism by which age increases risk of AD. Additionally, it is well established that chronic or traumatic stressors increase neuroinflammation. Thus, by promoting inflammation, stress may facilitate the development of AD in a similar way to natural aging. A number of stressors promote

microglial activation, as measured by Iba1 activity (Calcia *et al.*, 2016). In particular, a very strong effect has been found in area CA1 of the hippocampus, which is particularly impaired in AD (Kojo *et al.*, 2010; Bian *et al.*, 2012). This increase in microglial activation has been demonstrated to lead to the secretion of cytokines and chemokines, which facilitate development of anxiety-like behavior (Tynan *et al.*, 2010; Wohleb *et al.*, 2011, 2012, 2013). Stress exposure also promotes production of proinflammatory monocytes in the bone marrow, which are released into general circulation and can migrate and localize in the brain (Wohleb *et al.*, 2011; Powell *et al.*, 2013; Heidt *et al.*, 2014).

Additionally, in recent studies it was demonstrated that activation of the C3aR1 receptor by TLQP-21 or C3a (Sahu *et al.*, 2019), which was previously linked with to both the stress response (Razzoli *et al.*, 2012) and microglial function (Doolen *et al.*, 2017), increases microglial phagocytosis of Aβ (Cho *et al.*, 2020; El Gaamouch *et al.*, 2020) and improves amyloid pathology in the 5XFAD mouse model of AD (El Gaamouch *et al.*, 2020). However, activation of C3aR1 has also been shown to promote early synapse loss (Hong *et al.*, 2016), cognitive decline (Shi *et al.*, 2017) and tau pathology (Litvinchuk *et al.*, 2018). This biphasic contribution is consistent with the dual role that microglial activation plays in AD pathology, and the C3aR1-mediated signaling pathway may represent an important mediator of stress-induced microglial activation and inflammation in AD.

Furthermore, prior stressor exposure can potentiate the CNS inflammatory response to subsequent immune challenges (Frank *et al.*, 2007; Yoo *et al.*, 2011; Wohleb *et al.*, 2012; Giovanoli *et al.*, 2013). This mechanism could be particularly relevant to the contribution of early life and middle life stress to AD risk in old age.

3.10 Potential Mechanisms of stress-induced exacerbation of neurodegeneration and AD

There are multiple potential mediators of stress-induced effects on neurodenegeration and AD. At this point, the best researched mediators are two of the primary HPA axis hormones: CRH and GCs.

Glucocorticoids. GCs are the main output of the HPA axis. Under normal circumstances, GCs exert negative feedback on the hypothalamus and pituitary, returning

GC levels to baseline, but in some instances of repeated stress exposure, GC hypersecretion can persist. The seminal Glucocorticoid Cascade Hypothesis suggested that age-related GR loss results in GC hypersecretion, and that subsequent stress-induced GCs both directly damage hippocampal neurons and impair their ability to withstand any additional damage or insult, resulting in accelerated neuron degeneration and death (Sapolsky *et al.*, 1986). It furthermore proposes that this is the major mechanism by which hippocampal degeneration occurs with age and promotes AD.

An extensive body of research indicates that aging increases basal HPA axis function and stress responsiveness (Sapolsky, 1992). Aged rats have fewer GR receptors in the hippocampus and to a smaller extent, in the amygdala (Sapolsky *et al.*, 1983). Given that much of the GC negative feedback on the paraventricular nucleus is mediated by neurons in the hippocampus, this may be responsible for the impaired termination of the stress response observed in aged individuals. In rats, 3 months of corticosterone injections that replicate the high physiological range resulted in depleted GR in the hippocampus, which did not change after 4 months of recovery. This also resulted in a reduced number of cells in area CA3 and the appearance of "dark microglia" (Sapolsky *et al.*, 1985). Exogenous glucocorticoids also potentiate the capacity for Aβ infusion to promote tau hyperphosphorylation and intracellular accumulation (Sotiropoulos *et al.*, 2011). In humans, several case studies indicate that high dose corticosteroids can induce long-lasting impairments in learning and memory, similar to those observed in patients with dementia (Arndt *et al.*, 2004; Sacks & Shulman, 2005). Similarly, patients with Cushing's Syndrome frequently manifest with psychiatric and cognitive dysfunction termed "steroid dementia" (Bernini & Tricò, 2016). However, while some aspects of the glucocorticoid cascade hypothesis, have been substantiated, it has become clear that GC action alone cannot account for aging and AD-related hippocampal degeneration.

Further experiments have demonstrated that the stress/GC-induced decrease in hippocampal volume is now primarily attributed to dendritic loss rather than neural death (Czeh *et al.*, 2001; Tata *et al.*, 2006) and several stress-induced effects on AD pathology have been shown to be glucocorticoid independent (Chen *et al.*, 2008, 2010; Radley *et al.*, 2013; Shu & Xu, 2017).

Corticotropin Releasing Hormone. CRH has also been shown to be a primary mediator of stress effects on several neurodegenerative phenomena. Direct injection of CRH into the brain results in increased Aβ in the interstitial fluid (Kang *et al.*, 2007). Repeated administration of a CRHR1 agonist into the basolateral amygdala is sufficient to increase APP and Aβ in prefrontal cortex (Ray *et al.*, 2011).

Additionally, pharmacological blockage of CRHR1 receptors prevents an increase in Aβ induced by acute restraint stress. 2 weeks of restraint stress in adrenalectomized wildtype mice increases levels of phosphorylated tau but can be prevented by administering a CRHR1 antagonist (Rissman *et al.*, 2007). Phosphorylated tau is also blocked in CRHR1 knock-out mice but not in CRHR2 knock-out mice, suggesting a specific role for CRHR1 mediated signaling (Rissman *et al.*, 2007). In this case, it is possible that GCs and CRH have redundant effects on tau phosphorylation. Exacerbations in pathology produced by restraint stress in a mouse model that expresses mutant human tau can similarly be prevented by a CRHR1 antagonist (Carroll *et al.*, 2011).

It is clear that both GCs and CRH are important mediators of both the stress response, and stress-effects on neurodegeneration. Less clear however is the precise roles they play. A single exposure to a 5-hour stressor reduces CA3 dendritic spine density and long-term potentiation and these effects correlate with stress-induced memory deficits (Chen *et al.*, 2010). Both GR and CRHR1 are implicated in this effect. Chronic exposure to GCs similarly reduces CA3 apical dendritic complexity (Woolley *et al.*, 1990). However, direct infusion of a CRHR1 antagonist into the brain prevented the spine loss and memory impairments caused by a 5-hour stress exposure (Chen *et al.*, 2010). Thus, both mechanisms may be at play but with different timescales, with CRHR1 mediating acute spine loss and GR mediating chronic stress induced dendritic shortening.

Catecholamines. Though it has been less well studied in the context of neurodegeneration, the actions of the SAM axis and sympathetic nervous system in AD pathogenesis must be considered. Epinephrine and norepinephrine, the major effectors of these systems respectively, do not cross the blood brain barrier, and thus circulating levels released from the adrenal glands and sympathetic nerves do not directly act on the CNS (Weil-Malherbe *et al.*, 1959). However, the catecholamines-mediated actions, such as

increasing blood pressure may indirectly contribute to the development of AD. Hypertension, particularly in midlife, is a risk factor for AD (Luchsinger *et al.*, 2005) and antihypertensive medications have been associated lower incidence of AD diagnosis and better cognitive function (Hajjar *et al.*, 2005; Khachaturian, 2006; Hoffman *et al.*, 2009). Additionally, norepinephrine released by sympathetic nerves promotes the production and release of myeloid cells, which are trafficked throughout the body and release pro-inflammatory cytokines (Dhabhar *et al.*, 2012; Hanke *et al.*, 2012; Heidt *et al.*, 2014). This can lead directly to increased neuroinflammation, which is associated with AD, and also to the promotion of other diseases such as atherosclerosis, which increases risk for AD (Kalback *et al.*, 2004).

Norepinephrine is also secreted by catecholaminergic neurons in the brain, whose activity is particularly increased in response to acute stress and facilitate a number of anxiety-like behavioral responses (for review, see Morilak et al., 2005). The locus coeruleus (LC) is the main source of norepinephrine in the brain, and has widespread projections to the cortex, hippocampus and amygdala, among many other brain regions. LC neurons degenerate early in AD, and evidence indicates that this promotes further disease progression (Zarow *et al.*, 2003; Grudzien *et al.*, 2007; Kelly *et al.*, 2017). However, the role of noradrenergic signaling in AD pathogenesis is complicated and seemingly contradictory. Selective ablation of noradrenergic neurons increases Aβ deposition in the APP23 model (Heneka *et al.*, 2006), the APP717 model (Kalinin *et al.*, 2007) and the APP/PS1 model (Jardanhazi-Kurutz *et al.*, 2010) and increases levels of phosphorylated tau in female APP/SL mice (Oikawa *et al.*, 2010).The β2 adrenergic receptor (AR) agonist terbutaline prevents LTP inhibition induced by exogenous application of Aβ to rat hippocampal sections (Wang *et al.*, 2009) and an antagonism of β2AR with ICI 118,551 in the 3xTg model was found to increase Aβ levels and further impaired cognitive function (Branca *et al.*, 2014). The above evidence suggests that noradrenergic signaling may play a protective role in AD, but is contradicted by several other studies, which indicate that it may exacerbate AD pathogenesis. Stimulating α_2 adrenergic receptor disrupts APP interaction with Golgi sorting receptors, altering the outcome of its proteolytic processing to promote Aβ generation and subsequent

neuropathology (Chen *et al.*, 2014). In APP/PS1 mice, administration of a selective α_2 receptor antagonist ameliorates AD-related cognitive deficits (Scullion *et al.*, 2011; Chen *et al.*, 2014). Activation of β_2AR enhances γ secretase activity, and thus Aβ production in both transgenic AD mouse models and wildtype mice (Ni *et al.*, 2006; Yu *et al.*, 2010). Antagonism of either or both β_1 and β_2ARs can reduce Aβ production in amyloidosis mouse models of AD (Ni *et al.*, 2006; Wang *et al.*, 2013). Blockade of β_2AR receptors also reduces stress-induced Aβ generation in nontransgenic mice (Yu *et al.*, 2010). Inhibition of both β_1 and β_2ARs with propanalol improves cognitive function both in the amyloidosis Tg2576 mouse model and in the accelerated aging SAMP8 model (Dobarro, Gerenu, *et al.*, 2013; Dobarro, Orejana, *et al.*, 2013). Thus, it is clear that norepinephrine and the neurons in the LC that produce it, have an intimate association with AD pathogenesis. While ablation of neurons in the LC clearly is detrimental to health and cognition, the outcome of noradrenergic signaling may be highly dependent on contextual factors including stage of disease progression, the receptors it interacts with and the outcome being measured. The specificity of noradrenergic signaling may be key, with LC neurons participating in circuits that cannot be recapitulated by CNS-wide α or β adrenergic receptor stimulation. **Glutamate.** Acute restraint stress elevates glutamate levels in the hippocampus in a glucocorticoid-dependent manner (Lowy *et al.*, 1993). GC induced glutamate secretion likely plays a role in stress-induced dendritic remodeling, as blocking NMDA receptors blocks this effect (Magarin˜os & McEwen, 1995). Excess glutamatergic activity is also associated with neuron loss following trauma and is implicated in neurodegeneration and aging. Aged rats treated with riluzole, which increases glutamate uptake through glial transporters, were protected against age-related cognitive decline and dendritic spine loss (Pereira *et al.*, 2014). Riluzole also prevented many age-related hippocampal gene expression changes. In particular, it prevented gene expression changes associated with AD in humans (Pereira *et al.*, 2017). This suggests that excess glutamate signaling is a key modulator of stress or GC induced dendritic retraction and cognitive decline.

Cellular senescence. A core tenant of the stress concept originally described by Hans Selye was that stress, like aging, was the "results of life's wear and tear" (Selye, 1959). The field's understanding of stress has been refined since then, but the link between

stress and aging has endured. In addition to AD, stress is observed to increase risk for a number of conditions and diseases associated with aging, including hypertension, atherosclerosis, diabetes and dementia (Dimsdale, 2008; Murdock *et al.*, 2016; Razzoli *et al.*, 2018; Yuede *et al.*, 2018; Zhang *et al.*, 2020). Given its contribution to a number of aging-related diseases as well as to biological aging itself, is it possible that stress promotes these diseases at least in part by impacting a fundamental aging mechanism?

One potential mediator of this interaction has gained momentum recently: the process known as cellular senescence. Cellular senescence, the phenomenon by which cells cease to divide and undergo other distinctive phenotypic changes, reflects a deterioration of function with age on a cellular level, and is believed to contribute to aging at an organismal level (Hayflick & Moorhead, 1961; McHugh & Gil, 2018). After entering senescence, cells do not necessarily die; on the contrary they become resistant to apoptosis (Campisi & d'Adda di Fagagna, 2007; Childs *et al.*, 2014; Kirkland *et al.*, 2017; Gorgoulis *et al.*, 2019). Though viable, senescent cells undergo major gene expression changes, secreting a number of pro-inflammatory factors collectively termed the senescence-associated secretory phenotype (SASP) (Coppé *et al.*, 2010). In this way, senescent cells can alter their tissue microenvironment and detrimentally affect the function of neighboring cells. Thus, just a few senescent cells could alter the activity of a far greater number of other cells either increasing the number of senescent cells or affecting the functions of neighboring cells. Increasing evidence suggests that senescent cells, which accumulate throughout the lifetime, may be major drivers of functional decline associated with aging. Thus far, senescent cells have been shown to actively drive a number of diseases, including atherosclerosis (Childs *et al.*, 2016), cancer (Campisi & d'Adda di Fagagna, 2007) and AD (Bussian *et al.*, 2018; Musi *et al.*, 2018; Zhang *et al.*, 2019). Specifically, NFT bearing neurons extracted from post-mortem human tissue and the rTg4510 tauopathy mouse model tissues have transcriptomic profiles consistent with that of senescent cells (Musi *et al.*, 2018). Oligodendrocyte precursor cells associated with Aβ plaques in brain tissue from AD patients or APP/PS1 mice also express senescence markers (Zhang *et al.*, 2019). Additionally, pharmacological or pharmacogenetic elimination of senescent cells in two different tauopathy mouse models (rTg4510 and PS19) reduced NFT burden, attenuated brain volume loss and improved cognition and memory (Bussian *et al.*, 2018; Musi *et al.*,

2018). Pharmacological removal of senescent cells in a mouse model characterized by Aβ deposits also lessened Aβ plaque load and improved cognition (Zhang *et al.*, 2019). These studies provide strong evidence that senescent cells play an important, but as yet understudied role in AD.

Evidence in humans suggests that chronic stress might accelerate aging by promoting cellular senescence. Women who report higher levels of stress have shorter telomeres in circulating immune cells and less telomerase activity than those with low reported levels of stress (Epel *et al.*, 2004). Shortened telomeres are the classical trigger for cellular senescence (Hayflick & Moorhead, 1961), and higher stress levels are also associated with greater oxidative stress – an independent senescence promoter (Aschbacher *et al.*, 2013). Low socioeconomic status and life stress have been associated with lower telomere length in some (Cherkas *et al.*, 2006) but not all studies (Adams *et al.*, 2007; Rentscher *et al.*, 2019), and increased $p16^{INK4}$ expression (Rentscher *et al.*, 2019). Finally, a recent study demonstrated that lifelong psychosocial stress in mice shortened lifespan and increased expression of senescence markers such as p16 and p53 in several organs in subordinate individuals (Razzoli *et al.*, 2018). These findings are particularly relevant in the context of human literature demonstrating that shorter telomeres increases risk for AD (Zhan *et al.*, 2015). Together, these findings indicate that senescent cells may be key mediators in stress-induced promotion of AD, possibly through their secretion of pro-inflammatory factors and dysregulation of local tissue homeostasis.

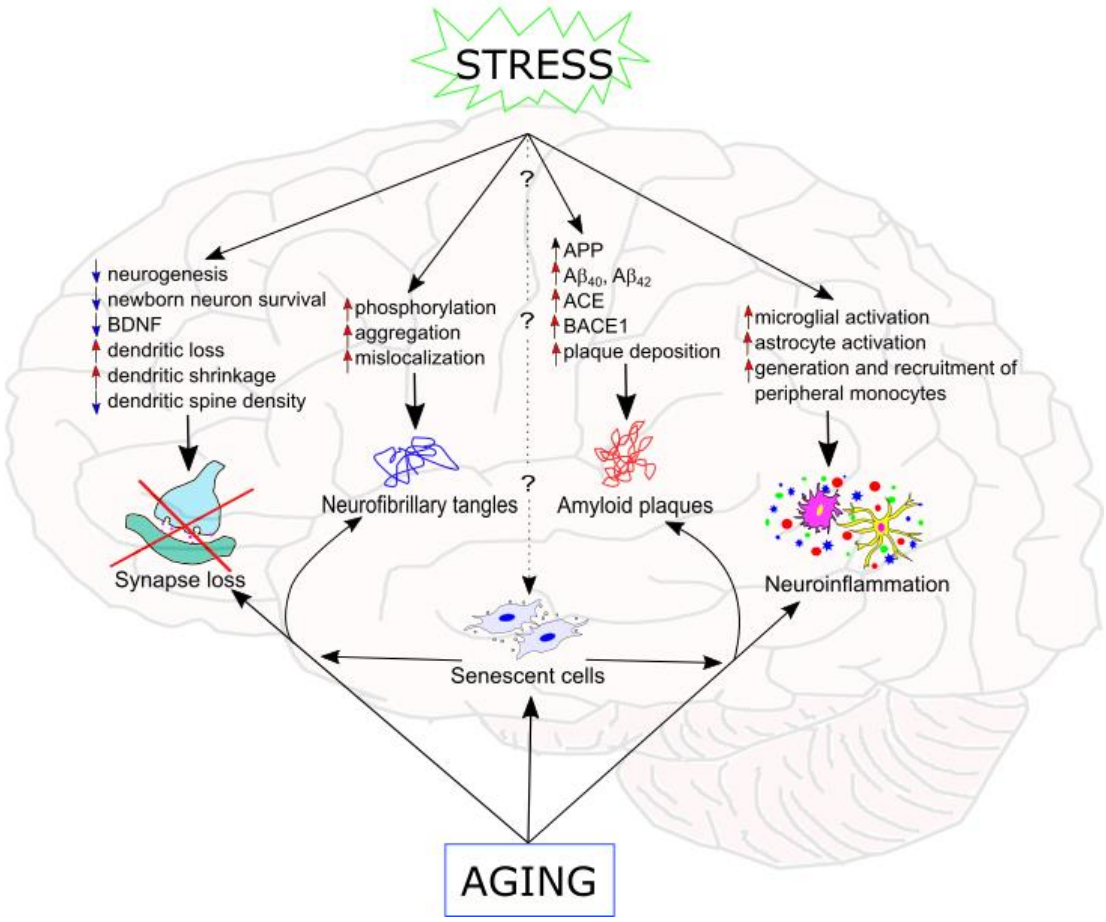

Figure 1 Diagram of stress-induced and aging-associated changes in Alzheimer`s disease (AD) neuropathological changes.

3.11 Conclusions

Strong evidence indicates that stress contributes to the onset and progression of AD, one of the most common and devastating diseases associated with aging. Human literature indicates that high levels of stress increase risk for developing AD, and that stress can accelerate the age of onset in individuals genetically predisposed to develop the disease. We have gained important insights into the mechanisms that might underlie this association through rodent research, in which stress also consistently increases AD-related measures. In wildtype rodents, stress promotes expression of molecular markers implicated in the disease, including hyperphosphorylated tau, and APP and A□. It also reduces synapse number in key areas related to early stage AD. Stress in rodent models of AD results in exacerbated molecular and behavioral pathologies and can advance the age at

which animals begin to show signs of decline. The molecular underpinnings of these effects have yet to be fully understood. Both glucocorticoids and CRH have been shown to play important, and connected roles in producing these AD-related changes.

An emerging mechanism to consider is the impact of stress on the aging and senescence process per se. Senescent cells can secrete pro-inflammatory factors, which have been shown to exacerbate pathological features of AD. They may be an important mediator of stress-induced neuroinflammation, which is appears to be an active driver of AD pathology. Age is the greatest risk factor for AD, and a long history of research supports the theory that stress impacts and accelerates the aging process. However, the aging aspect of AD is particularly challenging to study mechanistically, given the vast difference in lifespan between humans and rodent models as well as the resource burden of waiting for animals to age naturally before performing experiments. Most transgenic AD rodent models have shorter lifespans than their wildtype counterparts which is perhaps a double-edged sword for understanding the connection between aging and AD. On the one hand, the accelerated timeline towards frailty and death in these transgenic models of AD is an opportunity to study the relationship between AD pathophysiology and aging mechanisms. On the other, these interactions may not reflect mechanisms of normal aging and the dramatic phenotype of these models may obfuscate the roles of other physiological mechanisms. An important task for the future will be to identify if and how stress-induced cellular senescence in the brain and stress-induced AD neuropathology, and to develop interventions to ameliorate the current burden of AD on our society.

CHAPTER 4

PARSING THE EFFECTS OF SOCIAL AND PSYCHOLOGICAL STRESS ON THE PS19 MOUSE MODEL OF TAUOPATHY

Others' Contributions: Sara Graves performed neuropathological analyses. Maria Razzoli, Rachel Mansk, Nivedita Sabarinathan, and Jean-Pierre Pallais assisted with in vivo stress studies. Jan van Deursen and Darren Baker supplied the PS19 mice.

4.1 Summary

Chronic stress particularly that associated with low socioeconomic status increases risk for developing neurodegenerative disorders such as Alzheimer's disease (AD). Despite many advances in understanding the etiology of AD, it remains unclear which aspects of the disease are affected by environmental factors. The detrimental effects of stress in transgenic mouse lines modeling Amyloid β pathology have been extensively studied. Similarly, certain types of stress have repeatedly been demonstrated to increase tau phosphorylation in wildtype mice. However, the impact of stress on pathological tau isoforms has been surprisingly understudied, and no research to date has demonstrated an effect of social stress on tau phosphorylation. Here, we examined the effects of two stress paradigms — chronic subordination stress (CSS) and chronic restraint stress — on the PS19 mouse model of tauopathy. Both CSS and restraint stress induced the characteristic stress phenotypes, previously documented in wildtype mice, in the PS19 mice. We find

that CSS, but not restraint stress induces selective deficits in certain components of spatial learning but does not increase tau phosphorylation. In fact, CSS-exposed mice have a reduction in the phosphorylated tau epitope AT8, and at a transcript level express lower levels of both the pathological human tau gene and endogenous mouse tau gene. Overall, our results suggest that social stress may affect AD risk via a mechanism independent of tau phosphorylation and aggregation.

4.2 Introduction

Tauopathies are a class of neurodegenerative disorders that include Alzheimer's disease (AD), frontotemporal dementia, and chronic traumatic encephalopathy (Orr *et al.*, 2017). These diseases are characterized by abnormal aggregation of the microtubule associated protein tau, resulting in the formation of insoluble intracellular aggregates termed neurofibrillary tangles (NFTs) (Goedert *et al.*, 1988; Wischik *et al.*, 1988). There are currently no disease-modifying therapies to treat tauopathies, and such fundamental details as whether tau plays a causal or reactionary role in AD remain disputed (Hardy & Selkoe, 2002; Selkoe & Hardy, 2016; Bilgel *et al.*, 2021).

Life stress increases risk for developing AD, related dementias (Johnston, 2000; Bonanni *et al.*, 2018; Yuede *et al.*, 2018), and Parkinson's Disease (Hemmerle *et al.*, 2012). In particular, several measures of socioeconomic status (SES) predict risk for AD. Low SES can confer an immense burden of stress involving economic insecurity, uncertainty about future stability, and feelings of exclusion or marginalization due to occupational or economic status (Marmot *et al.*, 1991; Stringhini *et al.*, 2017; Marmot, 2020). As lack of access to resources cannot entirely explain the health risks associated with low SES, it is thought that the stress conferred by low social status is a primary driver of this association (Lachman & Weaver, 1998; Cohen *et al.*, 2006). Low education and occupational attainment increase risk of AD on their own, but low socioeconomic status combined with genetic factors such as the APOE4 allele synergistically increase AD risk to an even greater extent (Stern *et al.*, 1994; Räihä *et al.*, 1998).

The latter result in particular indicates an interaction between stress and genetics in the development of AD. Although the effect of stress on tau phosphorylation has been

extensively studied in wildtype mice (Lyons & Bartolomucci, 2020), little work has been published on the effects of stress in transgenic mice that model tau pathology.

Non-social stress in wildtype rodents has repeatedly been demonstrated to promote tau phosphorylation and synthesis of amyloid precursor protein and Amyloid-β (Aβ), but not to the point of inducing NFTs or plaques (Korneyev *et al.*, 1995; Rosa *et al.*, 2005; Rissman *et al.*, 2007; Sayer *et al.*, 2008; Yan *et al.*, 2010; Ray *et al.*, 2011; Filipcik *et al.*, 2012; Kvetnansky *et al.*, 2016). However, the studies cited above employed paradigms that were not social in nature, such as cold-water stress, restraint stress, immobilization stress, and chronic unpredictable mild stress. Additionally, they were conducted in wildtype mice, which express a form of tau that is much less prone to phosphorylation and does not aggregate into NFTs as the human form of tau can (Nelson *et al.*, 1996).

As wildtype mice do not naturally develop either of the two major neuropathologies associated with AD – Aβ plaques and NFTs – most AD research in rodents employs transgenic mouse models that have genetic mutations associated with familial AD in humans. Studies in these transgenic animal models have found that short-term stress exacerbates the characteristic neuropathology of many of these models (Green *et al.*, 2006; Kang *et al.*, 2007; Lee *et al.*, 2009; Carroll *et al.*, 2011; Rothman *et al.*, 2012; Vijgen *et al.*, 2012; Lesuis *et al.*, 2016; Hoeijmakers *et al.*, 2017). However, despite the long-known association between stress and tau phosphorylation, the consequences of stress have been explored far more in mouse models featuring Aβ pathology (i.e., mice that express versions of human genes associated with pathological Aβ) than in transgenic mouse models of tauopathy. Moreover, no studies to date have studied the effect of social stress in mouse models of tauopathy.

It is documented that different stress paradigms can produce different behavioral and physiological phenotypes (Marin *et al.*, 2006). One previous study found that chronic exposure to predictable restraint stress impaired recovery from a cortical lesion to a greater extent than unpredictable variable stress (Zucchi *et al.*, 2009). Given our divergent findings regarding the effects of chronic subordination stress (CSS) and restraint stress on senescence markers in the brain (see Chapter 1), and the recently established link between senescence and tauopathy (Bussian *et al.*, 2018; Musi *et al.*, 2018), here we tested the

hypothesis that the more severe CSS model would exacerbate the behavioral and/or neuropathological deficits in a tauopathy mouse model to a greater extent than restraint stress. For these experiments we used mice derived from the MAPTP301SPS19 (PS19) mouse model of tauopathy which expresses a variant of the human MAPT gene (MAPT P301S) that is prone to phosphorylation and subsequent aggregation (Yoshiyama *et al.*, 2007). Previously it was demonstrated that chronic restraint stress, but not chronic variable stress, worsened fear memory and increased levels of phosphorylated tau in the brains of PS19 mice (Carroll *et al.*, 2011). Thus, it seemed a particularly useful model to study the effects of CSS.

In these experiments, we subjected PS19 mice between the ages of 5 and 8 months to either CSS, restraint stress, or kept them singly housed as controls. We then assessed their performance in behavioral assays designed to measure different types of learning and memory. Finally, we compared several measures of neuropathology between control and CSS mice to determine whether they would present with the same exacerbation of pathology previously reported in restraint exposed PS19 mice.

4.3 Results

Validation of PS19 genotype and phenotype

The founding mice for the PS19 line were generated on a B6xC3 F1 strain but have since been bred onto the C57BL/6J strain (Yoshiyama *et al.*, 2007). To validate that the transgene encoding the pathological variant of the human tau gene was properly expressed in our mice, we used qPCR to measure mRNA levels of the human tau (*hTau*) transcript. As expected, we found expression for this gene to be robust in PS19 mice but undetectable in wildtype mice (**Figure 1A**).

PS19 mice also displayed a marked decrease in anxiety-like behavior compared with wildtype (*hTau* negative) littermates, as previously reported in the model (López-González *et al.*, 2015). PS19 mice spent significantly more time in open arms and less time in closed arms of the Elevated Plus Maze, compared with *hTau* transgene negative littermates (**Figure 1C, 1D**).

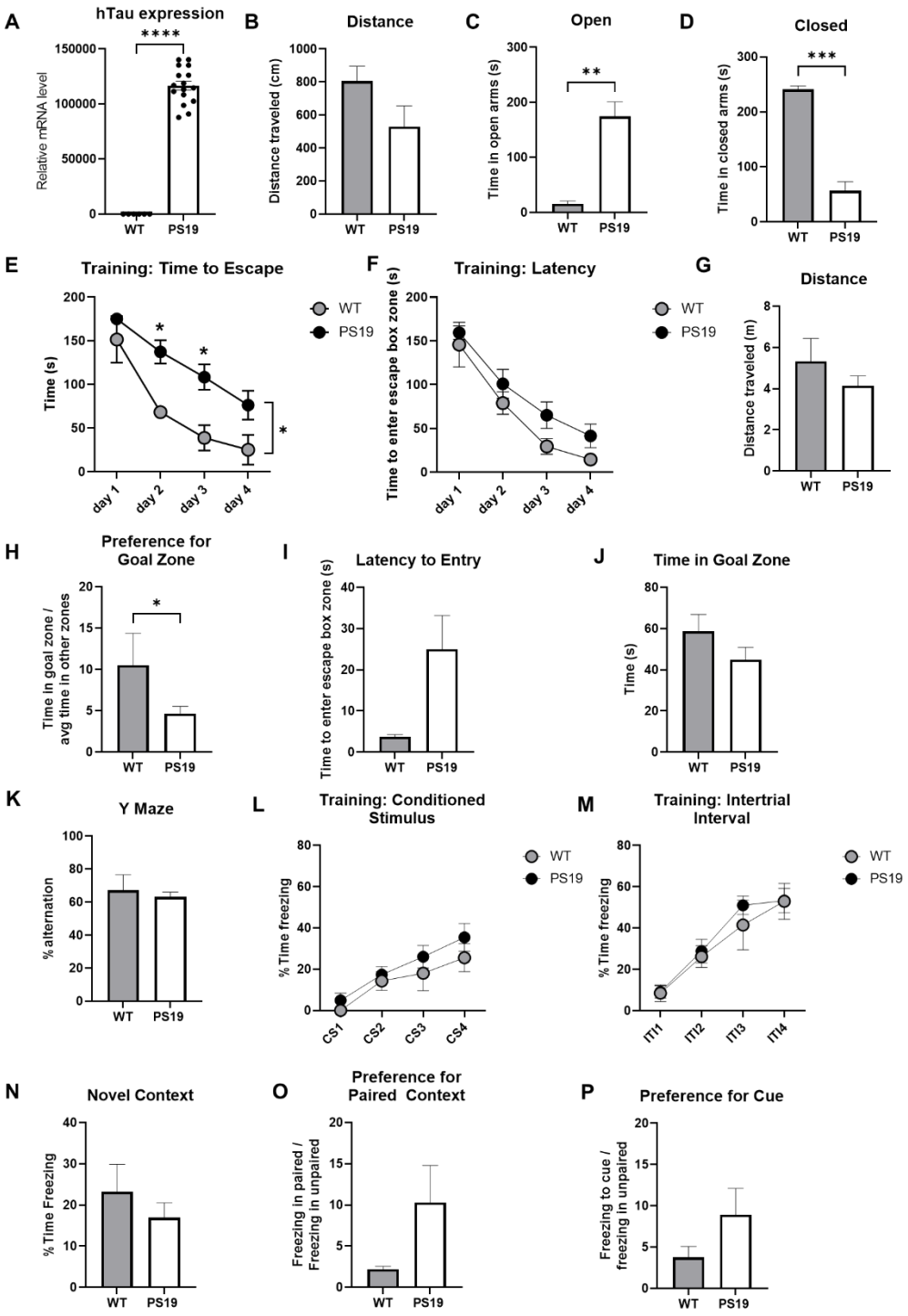

Figure 1 Validation of PS19 genotype and phenotype A) Relative abundance mRNA expression of human *MAPT* gene with the P301S mutation. Wildtype mice express negligible levels of the gene, while all PS19 mice transcriptionally express the gene. Unpaired t-test, p<.0001 **B)** There were no significant differences in distance traveled in the Elevated Plus Maze test between groups. Unpaired t-test. **C)** PS19 mice spent significantly more time in the open arms of the Elevated Plus

Maze than wildtype mice. Unpaired t test, p=0.0099. **D)** PS19 mice spent significantly less time in the closed arms of the Elevated Plus Maze than wildtype mice. Unpaired t test, p=0.0002. **E)** PS19 did not show as steep and learning curve in Barnes Maze training in terms of average time to enter escape hole on each day of training. 2-way repeated measures ANOVA with Tukey posthoc, significant main group effect of training day (p<.0001), significant main group effect of genotype (p = 0.0137), no significant interaction of day x genotype (p=0.2699). **F)** No significant differences between wildtype and PS19 mice in average daily latency to enter escape hole zone during Barnes Maze training. 2-way repeated measures ANOVA with Tukey posthoc, significant main group effect of training day (p < 0.0001), no significant effect of group (p = 0.2576) no significant interaction. **G)** No significant difference in distance traveled during Barnes Maze probe trial. Unpaired t test (p=.2667). H) PS19 mice display significantly less preference for the goal quadrant during Barnes Maze probe trial compared with wildtype mice. Unpaired t test p = 0.0412. **I)** No significant difference between wildtype and PS19 mice in latency to enter escape hole zone during Barnes Maze probe trial. Unpaired t test p= 0.1645. **J)** No significant differences between wildtype and PS19 mice in total time spent in goal quadrant during Barnes Maze probe trial. **K)** No significant difference in %alternation in Y maze. Unpaired t test p = 0.5903. **L)** No significant difference between wildtype and PS19 mice in %time freezing to the conditioned stimulus (cue) that immediately preceded foot shock during Fear Conditioning training phase. Both groups froze more with successive cue presentations. 2-way repeated measures ANOVA, significant main effect of trial number p<0.0001. **M)** No significant difference between wildtype and PS19 mice in %time freezing during intertrial intervals (between cue + shock presentation) in Fear Conditioning training phase. Both groups froze more with successive cue presentations. 2-way repeated measures ANOVA, significant main effect of trial number p<0.0001. **N)** Both wildtype and PS19 mice froze very little when placed in the novel (non-shock paired) context in Fear Conditioning. Unpaired t-test p = 0.4013. **O)** No significant difference between wildtype and PS19 mice in proportion of %time freezing in the shock-paired context vs the unpaired novel context. Both groups showed marked preference in freezing more in the paired context. Unpaired t-test, p = 0.3291. **P)** Both groups showed marked preference in freezing more when presented with shock-paired cue than when in the novel context. No significant difference between wildtype and PS19 mice in proportion of %time freezing in the shock-paired context vs the unpaired novel context. Unpaired t-test, p = 0.3591. * indicates p<0.05, ** indicates p<0.01 *** indicates p<0.001, **** indicates p<0.0001. Unless otherwise specified histogram bars represent group mean, and error bars represent standard error.

As expected from previous studies, mice positive for the *hTau* gene manifested cognitive deficits in spatial memory in the Barnes maze by 7-months of age. Specifically, PS19 mice did not shorten their time to enter the escape hole zone over four days of training to the same degree as their *hTau* negative littermates (Main group effect p<.05; **Figure 1E**). They also displayed significantly lower preference for the goal quadrant of the maze during the probe trial (p<.05; **Figure 1H**). Conversely, PS19 mice did not demonstrate any

reductions in spontaneous alternation in the Y maze, nor did they manifest any changes to freezing behavior in the Delay Fear Conditioning assay compared with wildtype littermates (**Figure 1O, 1P**).

PS19 mice subjected to CSS or restraint develop opposite metabolic phenotypes and increased anxiety-related behavior

At the start of the 6-week long experiment, mice in all groups were an average age of 6-months-old (range was 5-8 months). Consistent with previously reported characterizations in wildtype mice, PS19 mice exposed to CSS exhibited hyperphagia, consuming significantly more food per day than singly housed control mice ($p<.05$; **Figure 2A**), while restraint mice displayed no significant difference from controls in food intake (**Figure 2A**). Similarly, there was a significant effect of group on body weight change over the course of the experiment ($p<.05$; **Figure 2B**).

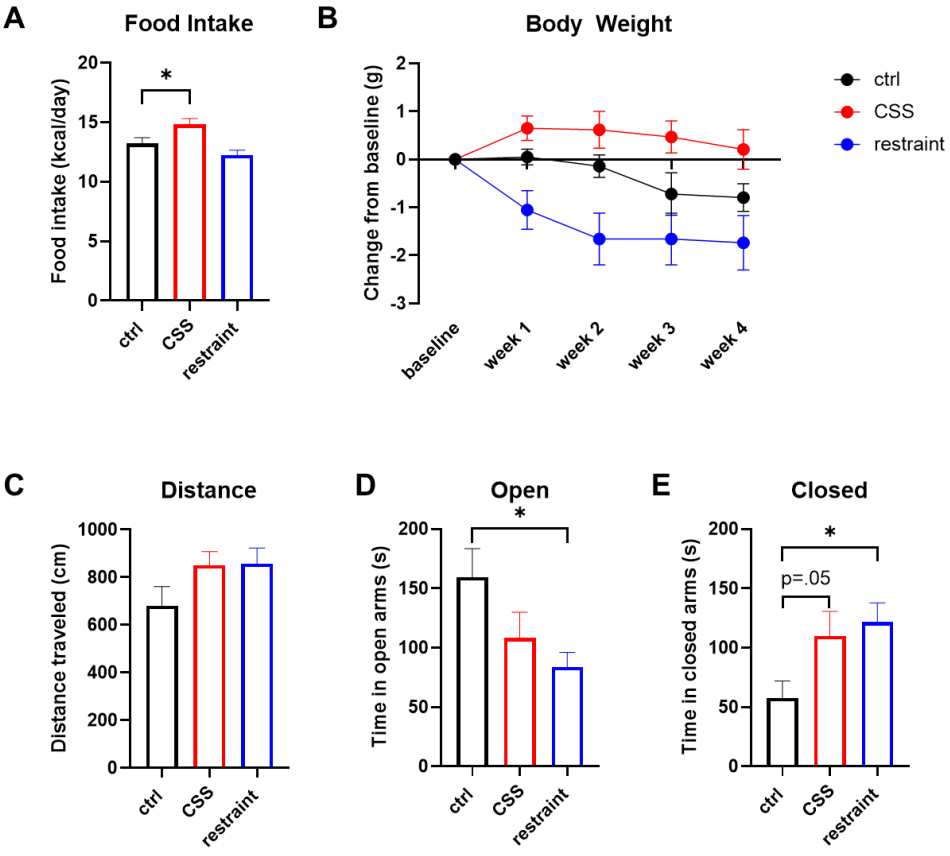

Figure 2. PS19 mice subjected to CSS or restraint develop opposite metabolic phenotypes and increased anxiety-like behavior A) CSS-exposed PS19 mice consumed significantly more calories per day than unstressed singly housed control mice $p = 0.0382$. Restraint mice exhibited no change in food intake compared with controls $p = 0.2415$. 1-way ANOVA with Dunnet's

multiple comparisons test. **B)** CSS-exposed mice were the only group to have a positive body weight change over the 4 weeks of stress. Mixed-effects model (REML) with Tukey posthoc. Group: $p<0.0001$. **C)** No significant difference between groups in distance traveled during Elevated Plus Maze. 1-way ANOVA. **D)** Restraint-exposed mice spent significantly less time in the open arms of the Elevated Plus Maze than controls ($p = 0.0377$) while CSS-exposed mice did not ($p=0.1566$). 1-way ANOVA with Dunnett's multiple comparisons test, significant effect of group, $p=0.0492$. **E)** Restraint exposed mice spent significantly more time in the closed arms of the EPM ($p=0.0258$) than control mice. CSS exposed mice trended strongly towards spending more time in the closed arms than control mice ($p=0.0545$). 1-way ANOVA with Dunnet's multiple comparisons test. Significant effect of group $p=0.0228$. * indicates $p<0.05$, ** indicates $p<0.01$ *** indicates $p<0.001$, **** indicates $p<0.0001$. Unless otherwise specified histogram bars represent group mean, and error bars represent standard error.

In the elevated plus maze, CSS and restraint-exposed mice displayed behavior consistent with an anxiety-like phenotype; they spent significantly more time in the closed arms of the maze compared with control mice ($p\leq.05$; **Figure 2D**). Restraint mice also spent significantly less time in the open arms and CSS exposed mice trended in this same direction but not to a degree that achieved statistical significance (**Figure 2E**). The total distance traveled during the course of the trial did not vary between groups, indicating that these results are not due to any differences in mobility or activity (**Figure 2C**).

CSS and chronic restraint stress minimally affect performance in learning/memory tasks

To ascertain the extent to which CSS and restraint would affect cognition in PS19 mice, we employed a series of behavioral tests assessing spatial learning/memory (Barnes Maze), working memory (Y maze) and fear-associated memory (Delay Fear Conditioning).

In the Barnes Maze, mice in all groups took less time to enter the escape hole with each successive day of training (Main effect of training day $p<.05$; **Figure 3A**). Though restraint-exposed mice entered the escape hole faster on days 2 and 3 than control mice (**Figure 3A**), they took the same amount of time to first locate the hole (**Figure 3B**). Interestingly, while both control and restraint-exposed mice significantly improved their latency to find the escape hole with each successive day of training, CSS mice displayed a flatter learning curve on latency to locate the hole (**Figure 2A**) and showed no significant shortening in latency to locate the hole on any day (**Figure 3B**).

However, during the final day probe trial in which the escape hole was covered, all groups displayed a similar latency to enter the escape hole zone, spent a similar amount of time in the quadrant where the escape hole was previously located, and displayed a similar degree of preference for the goal quadrant over other quadrants (**Figure 3C, 3D, 3E, 3F**).

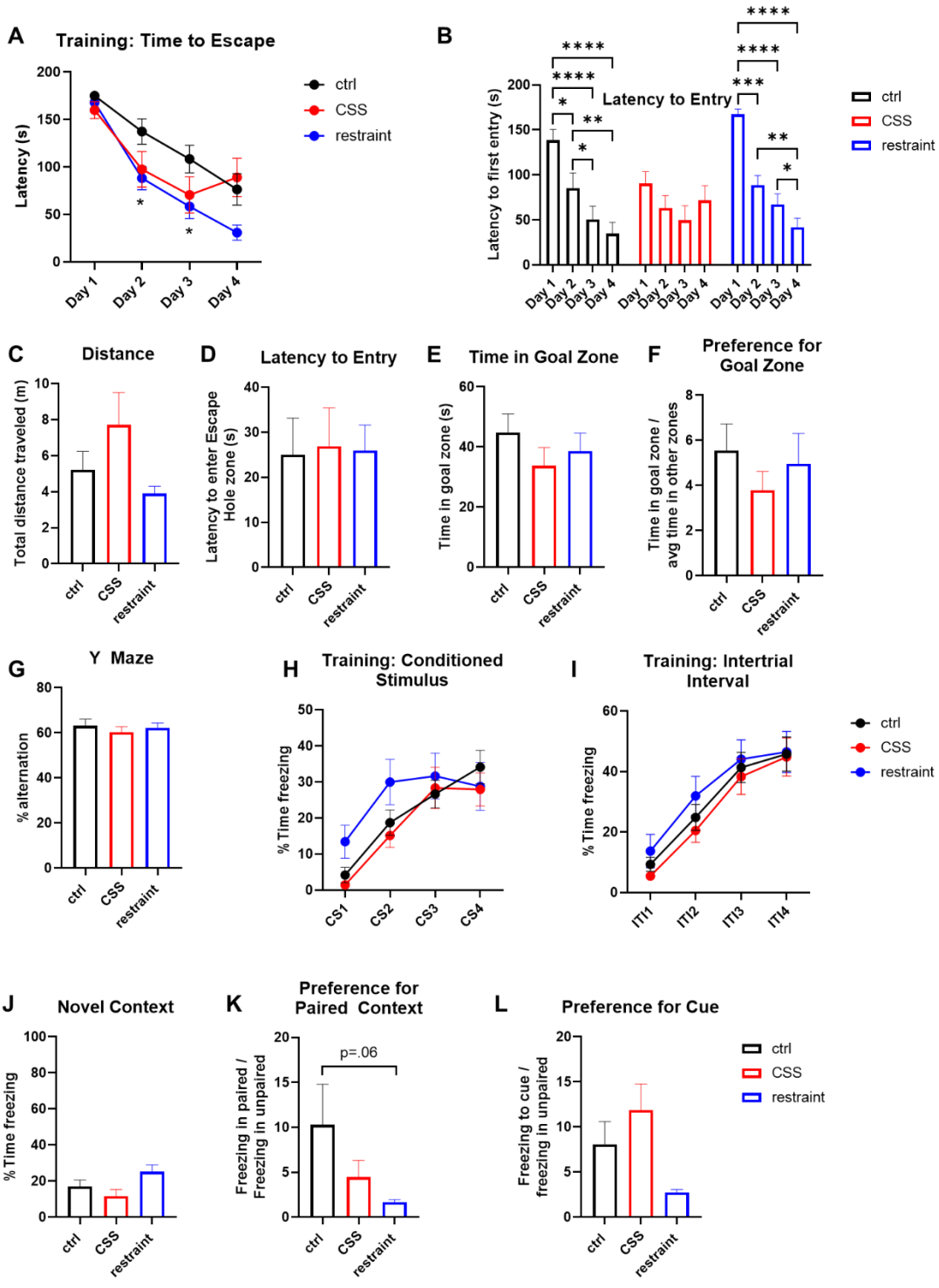

Figure 3 CSS and chronic restraint stress minimally affect performance in learning/memory tasks A) All groups took less time to enter the escape hole with successive training days (significant main effect of training day $p<0.0001$, no significant main effect of group $p=0.4065$). 2-way repeated measures ANOVA with Tukey posthoc. **B)** CSS-exposed mice were the only group to

show no significant decrease in latency to first enter escape hole zone other the course of training days. 2-way repeated measures ANOVA with Tukey posthoc, significant main effect of training day $p<0.0001$, significant interaction of training day and group $p<0.0001$). **C)** No significant difference in distance traveled during Barnes Maze probe trial 1-way ANOVA with Dunnett's multiple comparisons test. **D)** No significant difference between groups in latency to enter escape hole zone during probe trial of Barnes Maze. 1-way ANOVA with Dunnett's multiple comparisons test. **E)** No significant differences between groups in time spent in goal quadrant of Barnes Maze during probe trial. 1-way ANOVA with Dunnett's multiple comparisons test. **F)** No significant differences between groups in preference for goal zone vs other zones in Barnes Maze during probe trial. 1-way ANOVA with Dunnett's multiple comparisons test. **G)** No significant differences between groups in %alternation in Y-Maze. 1-way ANOVA with Dunnett's multiple comparisons test. **H)** All groups froze more with successive shock-paired cue presentations in Fear Conditioning training (significant main effect of cue presentation $p=0.0001$). No significant differences between groups (no significant main effect of group $p=0.2001$). 2-way repeated measures ANOVA with Tukey post hoc. **I)** All groups froze more between successive intertrial intervals between cue/shock presentations (main effect of interval $p<0.0001$). No significant differences between groups (no main group effect $p=0.4895$). 2-way repeated measures ANOVA with Tukey post hoc. **J)** All groups froze very little when placed in a novel (non-shock paired) context. No significant differences between groups. 1-way ANOVA with Dunnett's multiple comparisons test. **K)** Restraint exposed mice trend towards less freezing in shock-paired context relative to novel context ($p= 0.0762$). 1-way ANOVA with Dunnett's multiple comparisons test. **L)** Significant effect of group on amount of time freezing in the shock-paired context vs the unpaired novel context ($p=0.0361$) with restraint-exposed mice displaying less preference. 1-way ANOVA with Dunnett's multiple comparisons test. * indicates $p<0.05$, ** indicates $p<0.01$ *** indicates $p<0.001$, **** indicates $p<0.0001$. Unless otherwise specified histogram bars represent group mean, and error bars represent standard error.

No stress-induced changes to spatial working memory were evident from the results of the Y Maze. Spontaneous alternation behavior was consistent across groups (**Figure 3G**).

Previously it was reported that restraint stress reduced freezing time in response to presentation of shock-paired context and cue, indicative of impaired fear-associated memory (Carroll et al., 2011). Mice in all groups learn to associate the conditioned stimulus (buzzing sound and flashing lights) with foot shock (**Figure 3H, 3I**), displaying an increase in freezing with subsequent cue presentations. All groups also exhibited little freezing the next day when placed in a novel context (**Figure 3J**) but restraint-exposed mice displayed less discrimination in freezing behavior compared with other groups although this did not reach statistical significance ($p=0.07$). When placed in the shock-associated context, or

when presented with the conditioned stimulus, restraint-exposed mice do not freeze much more than when placed in a novel context (**Figure 3K, 3L**).

Effect of CSS on neuropathology *see footnote regarding restraint stress

CSS did not increase either astrogliosis or microgliosis in the dentate gyrus region of the hippocampus (**Figure 4A**). There was also no change to the dentate gyrus width or total area (**Figure 4D, 4E, 4F**).

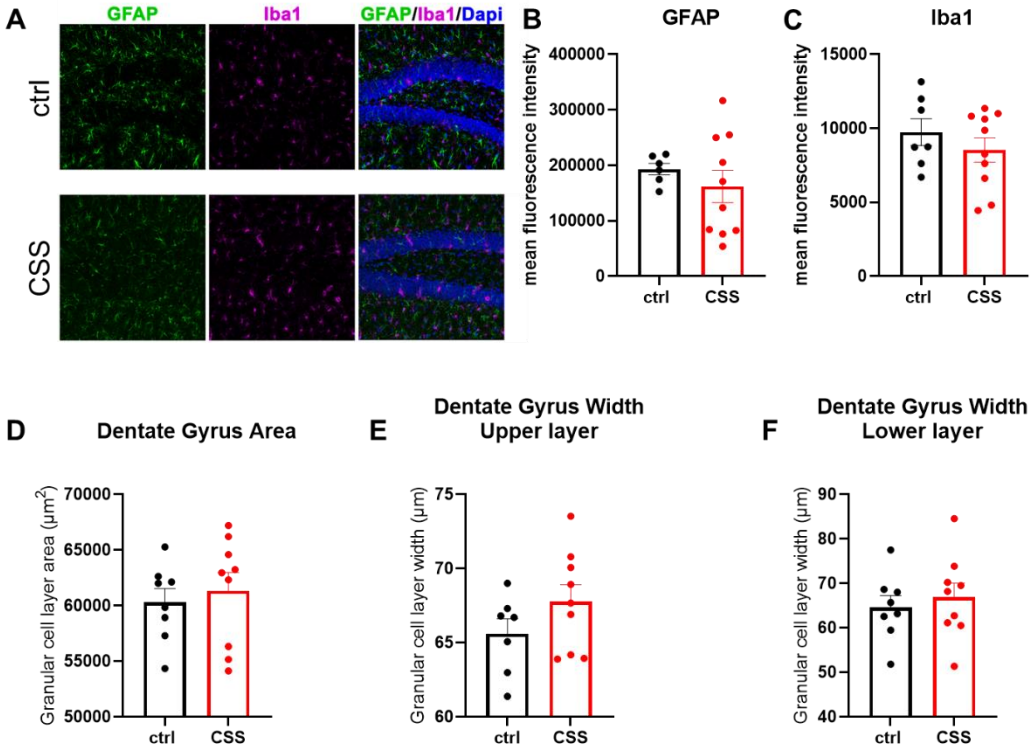

Figure 4 Effects of CSS on gliosis and dentate gyrus area A) Representative images of immunofluorescent staining for astrocytes (GFAP) and microglia (Iba1). **B)** No significant differences between groups in amount of GFAP staining. Unpaired t test. **C)** No significant differences between groups in amount of Iba1 staining. Unpaired t test. **D)** No significant differences between groups in dentate gyrus area. Unpaired t test. **E)** No significant difference in upper granular cell layer of dentate gyrus width between groups. Unpaired t test. **F)** No significant difference in lower granular cell layer of dentate gyrus width between groups. Unpaired t test. * indicates $p<0.05$, ** indicates $p<0.01$ *** indicates $p<0.001$, **** indicates $p<0.0001$. Unless otherwise specified histogram bars represent group mean, and error bars represent standard error.

CSS-exposed mice had significantly lower levels of the pTau epitope AT8 (**Figure 5D**), though not the epitope S404 (5E). This effect, can be attributed to a reduction in total tau expression as normalizing AT8 to levels of total tau abolishes this effect as previously reported (**Figure 5G, 5H**) (Lyons et al., 2021). At the transcript level, CSS mice also have lower expression of both the transgenic human tau gene and the endogenous mouse tau gene ($p<.05$; **Figure 5I**). Hippocampal mouse and human tau expression were stable across groups (**Figure 5J**).

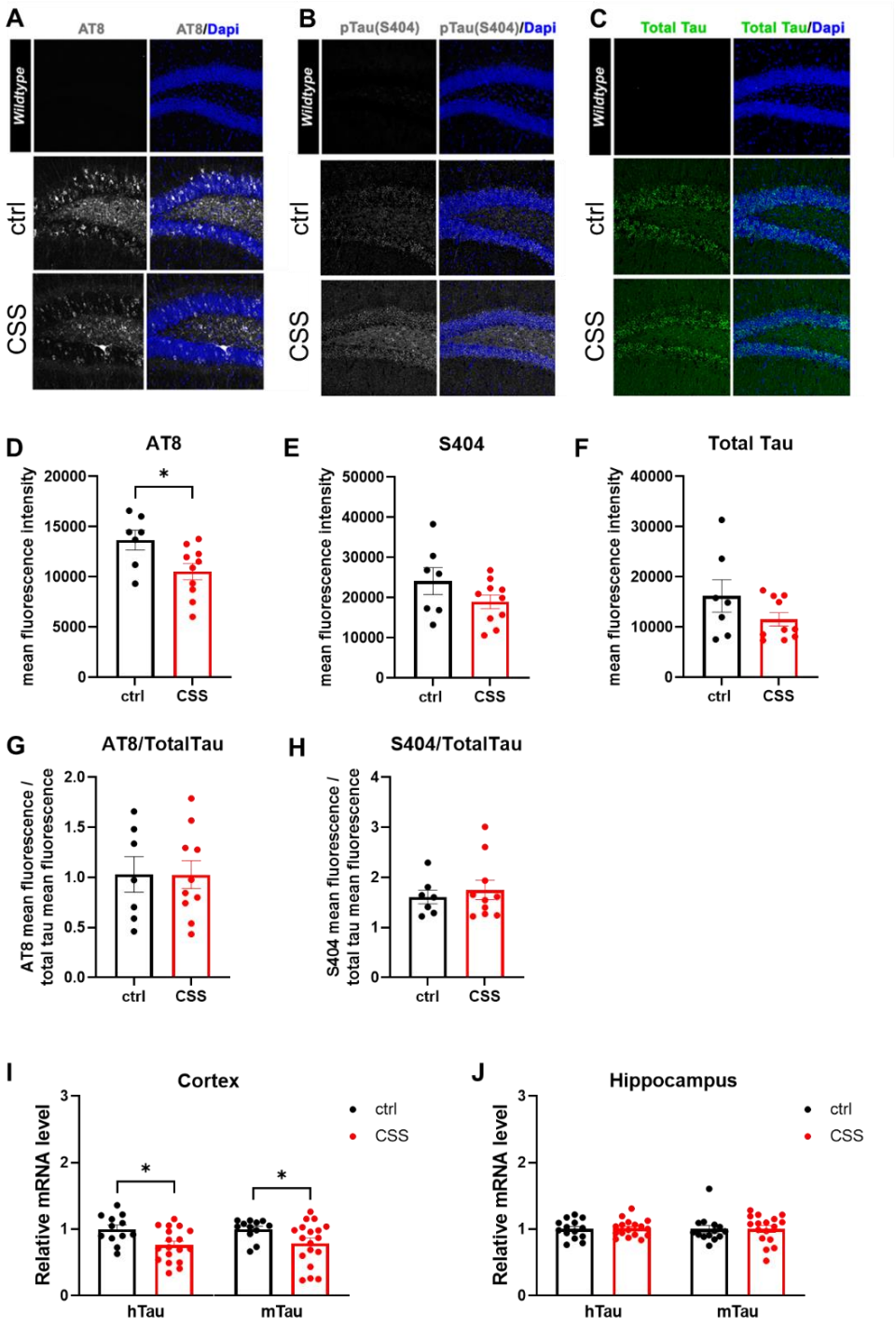

Figure 5 Effects of CSS on tau A) Representative images of immunofluorescent staining for phospho-tau epitope AT8. **B)** Representative images of immunofluorescent staining for phospho-tau epitope S404. **C)** Representative images of immunofluorescent staining for total human tau. **D)** CSS-exposed mice have significantly less AT8 immunofluorescence than control mice. Unpaired t test p = 0.0252. **E)** No significant differences between groups in amount of S404

immunofluorescence. Unpaired t test. **F)** No significant differences between groups in amount of total human tau immunofluorescence. Unpaired t test. G) AT8 immunofluorescence normalized to amount of total human tau immunofluorescence. No significant difference between groups. Unpaired t test. H) S404 immunofluorescence normalized to amount of total human tau immunofluorescence. No significant difference between groups. I) CSS-exposed PS19 mice have significantly lower expression of *hHau* ($p = 0.0104$) and *mTau* ($p = 0.0462$) mRNA in the cortex than singly-housed controls. Unpaired t test. J) There is no difference between control and CSS mice in *hTau* or *mTau* mRNA expression in the hippocampus. Unpaired t test. * indicates $p<0.05$, ** indicates $p<0.01$ *** indicates $p<0.001$, **** indicates $p<0.0001$. Unless otherwise specified histogram bars represent group mean, and error bars represent standard error.

4.4 Discussion

Chronic stress and several measures of low SES status increase risk for tauopathies such as (Marmot *et al.*, 1991; Stern *et al.*, 1994; Räihä *et al.*, 1998; Moceri *et al.*, 2001; Stringhini *et al.*, 2017; Marmot, 2020). However, very little research has been performed studying the effect of social stress, or low social status in genetic mouse models of tauopathy.

Non-social stress in wildtype rodents has repeatedly been demonstrated to promote tau phosphorylation and synthesis of amyloid precursor protein and Aβ, but not to the point of inducing NFTs or plaques (Korneyev *et al.*, 1995; Rosa *et al.*, 2005; Rissman *et al.*, 2007; Sayer *et al.*, 2008; Yan *et al.*, 2010; Ray *et al.*, 2011; Filipcik *et al.*, 2012; Kvetnansky *et al.*, 2016). The studies cited above were not performed in humanized transgenic mouse models, and employed paradigms that were not social in nature, such as cold-water stress, restraint stress, immobilization stress, and chronic unpredictable mild stress.

Stress phenotypes

Consistent with previous characterizations in wildtype mice, PS19 mice exposed to CSS became hyperphagic, and did not lose weight over the course of the 4-weeks of stress (Sanghez *et al.*, 2013). Restraint exposed mice on the other hand consumed a similar number of calories per day but lost more weight than control mice (**Figure 2A, 2B**). Notably, CSS mice were the only group that did not average a net loss in body weight over the course of the experiment. Overall, our data in PS19 mice confirm the general

observation that stress can elicit a dichotomous effect on energy balance (Razzoli & Bartolomucci, 2016).

The Elevated Plus Maze is a commonly used test to evaluate anxiety-like behavior in rodents based on their natural aversion to exposed and elevated areas (Komada *et al.*, 2008; Kraeuter *et al.*, 2019). CSS and restraint mice both exhibited behavior consistent with an anxiety-like phenotype, spending more time in the closed arms of the maze and less time in the open arms (**Figure 2D, 2E**). There were no group differences in the total distance traveled on the apparatus, indicating that the differences in arm preference are not the result of altered mobility or activity. This finding is particularly notable as a known feature of the PS19 model is reduced anxiety-like behavior (López-González *et al.*, 2015), which we also observed (**Figure 1C, 1D**). Together these data indicate successful application of both chronic stress paradigms in PS19 mice.

Effect of stress on measures of learning and memory

To ascertain the extent to which CSS and restraint would affect cognition in PS19 mice, we employed a series of behavioral tests assessing working memory (Y maze) spatial learning/memory (Barnes Maze), and fear-associated memory (delay fear conditioning). At the time of the behavioral tests following 4 weeks of stress, all groups of mice were an average age of 7 months. At this age, PS19 mice have previously been demonstrated to manifest cognitive impairment when compared to WT littermates (Takeuchi *et al.*, 2011; Lasagna-Reeves *et al.*, 2016).

The Y maze is an assay measuring spatial working memory that takes advantage of a mouse's innate drive to explore its surroundings (Prieur & Jadavji, 2019). Maximizing exploration in this apparatus takes the form of alternating entries between the 3 arms of the maze. Neither CSS nor restraint stress affected spontaneous alternation in the Y-maze, indicative of unaffected working memory under the present experimental conditions.

The Barnes Maze is frequently used to measure spatial learning and memory in rodents (Barnes, 1979; Pitts, 2018) and is preferred over the more stressful Morris Water Maze (requires water immersion) in the context of chronic stress experiments to avoid exposure to the heterotypical stress of water immersion. In the Barnes Maze, mice are placed on a brightly lit, elevated platform with 20 holes — 19 covered and one connected

to an escape hatch — around the perimeter. Visual cues are placed on the walls of the testing room to provide spatial navigation cues. Over the course of 4 days of training mice learn the fixed location of the escape hole. On the fifth day, a probe trial is conducted in which the escape hole is covered, and the mouse's memory is evaluated based on the time it takes to navigate to the escape hole's previous position, and how much time it spends in that target area of the maze. All groups took less time to enter the escape hole with each successive day of training (**Figure 3A**). Interestingly, restraint-exposed mice took less time to enter the escape hole on days 2 and 3 of training, though they had a similar latency to first enter the escape hole zone on these days (**Figure 2B**), suggesting that this behavior may be explained by higher motivation to escape rather than stronger learning compared with controls. Indeed, control mice found the escape hole in the same amount of time but did not necessarily immediately enter it. This motivation to escape the brightly lit open platform would be consistent with the anxiety-like behavior displayed by restraint-exposed mice in the elevated plus maze. Although CSS mice completed the training trials in a similar amount of time to other groups, they did not significantly improve their time to find the escape hole zone over days of training. Contrary to controls and restraint mice, CSS mice did not display a significant difference in latency to enter the hole on any day (**Figure 3B**). This may indicate some impairment in spatial learning processes induced by CSS.

However, in the probe trial, all groups displayed a similar latency to enter the escape hole zone, spent a similar amount of time in the quadrant where the escape hole was previously located, and displayed a similar degree of preference for the goal quadrant over other quadrants. CSS mice trended towards longer latency and reduced preference but not to a statistically significant extent. Future studies might use the reverse learning trial paradigm, in which the position of the escape hole is moved to a different spatial location. That could reveal additional features of spatial memory retention and cognitive flexibility (Gawel *et al.*, 2019).

In Delay Fear Conditioning, a conditioned stimulus (CS), — in this case a buzzing sound and flashing lights — is immediately followed by the unconditioned stimulus (US), a foot shock (Ewald *et al.*, 2014). Previously it was reported that restraint stress reduced freezing time in response to presentation of shock-paired context and CS, indicative of impaired fear-associated memory (Carroll *et al.*, 2011). PS19 mice independently have

been reported to manifest impairments in context-associated fear memory (Lasagna-Reeves *et al.*, 2016). Mice in all groups learn to associate the CS with foot shock, as evidenced by an increase in freezing with successive cue presentations. All groups exhibited little freezing the next day when placed in a novel context restraint-exposed mice displayed less discrimination in freezing behavior compared with other groups although at a non-statistically significant level; when placed in the shock-associated context, or when presented with the conditioned stimulus, restraint-exposed mice did not freeze more than when placed in a novel context.

Although the only measure that CSS appeared to affect was spatial learning (latency to find escape hole in Barnes Maze training), it is known that neuropathology frequently precedes the appearance of behavioral deficits; therefore, we next sought to characterize the degree of neurodegenerative pathology in the brains of mice exposed to CSS (Yoshiyama *et al.*, 2007). Astrogliosis and microgliosis are markers of neuroinflammation characteristic to AD and related tauopathies and are associated with age-related decline in PS19 mice (Leyns & Holtzman, 2017; Patel *et al.*, 2022). CSS did not increase either astrogliosis or microgliosis in the hippocampus of our PS19 mice. CSS also did not affect the dentate gyrus granular cell layer width or area, which is known to shrink preceding the appearance of Aβ plaque pathology in other AD mouse models (Redwine *et al.*, 2003).

Effects of CSS on neuropathology

Tau phosphorylation, and subsequent aggregation into NFTs is the primary pathological feature of the PS19 model. We performed immunofluorescent staining for phosphorylated tau epitopes AT8 and S404 and quantified the abundance of the staining. Interestingly CSS reduced the abundance of AT8 signal. As found previously, this change can be attributed though to a slight reduction in total human tau expression (Lyons *et al.*, 2021). There was no CSS effect on S404. Though not statistically significant at a protein level, CSS lowered gene expression of the transgenic *hTau* gene and the endogenous mouse tau gene in the cortex.

Our findings suggest that social stress may not impact tau phosphorylation. This illustrates the complexity of stress responses and the relevance of specific stress models in experimental contexts. Although stress-induced tau phosphorylation is a generally known

and accepted phenomenon, we could not find any other literature that evaluated the effect of CSS/CPS/social defeat stress on tau in either wildtype or transgenic rodents (see chapter 2), however there have been several studies that used different stress paradigms with social components. A model of chronic mild social stress (random cage composition 6h/day 2-3 days/week for 6 weeks) in the 3X-Tg-AD mouse model induced no changes in tau phosphorylation, though it did elevate Aβ levels (Rothman *et al.*, 2012). Studies that subjected Tg2576 mice to isolation for 3 months (Kang *et al.*, 2007), or 5-8 months (Dong *et al.*, 2004) also did not report changes in tau pathology, though the stressed mice in both studies had increases in Aβ and plaque deposition. A deeper understanding of the neural circuits and endocrine responses elicited by different forms of stress will be necessary to properly interpret research and extrapolate basic research to clinical relevance. Other biological mechanisms should be explored regarding the effects of social stress on tauopathy diseases.

4.5 Conclusions

Here, we tested the effects of a social and a non-social psychological stress paradigm on functional and neuropathological deficits in the PS19 mouse model of tauopathy. We find that while both CSS and restraint increase anxiety and affect energy balance in a model-specific way (positive energy balance with CSS and negative energy balance with restraint), neither model induces strong deficits in learning and memory. CSS does induce some impairment in spatial learning, as assessed in the Barnes Maze, but it does not exacerbate tau pathology, gliosis, or affect dentate gyrus volume. In fact, 4 weeks of CSS reduces hippocampal pTau burden, and downregulates expression of both the mutant human tau and the endogenous mouse tau genes in the cortex. Our results suggest that mouse models fail to recapitulate the strong effect of stress as a risk factor for tauopathies like AD, and that social stress in mice may mildly affect AD risk in a tau-independent manner.

Footnote:

Owing to ongoing supply-chain shortages associated with the COVID-19 pandemic, neuropathological assessments of the PS19 mice subjected to restraint stress were delayed and will be conducted as soon as possible at a later date

4.6 Methods

Subjects

MAPTP301SPS19 (PS19) mice were originally purchased from The Jackson Laboratory (stock no. 008169) and subsequently bred in the Mayo Clinic colony to C57BL/6J. At the start of the experiments, the mice ranged in age from 5-9 months (average age 6.3 months). Mice were randomized to receive CSS (N=19), restraint stress (N=15), or be singly housed as controls (N=22). The mice were fed ad libitum a standard (2018 Tecklad Diet). Mice were housed on a 12h:12h light:dark cycle for the duration of the experiments. All procedures were conducted with the approval of the University of Minnesota Institutional Animal Care and Use Committee.

Chronic subordination stress (CSS): Male PS19 mice were paired with mice from the aggressive CD1 strain (Charles River Labs). Daily, between the hours of 9:00am and 11:00am, the paired PS19 and CD1 mice were allowed to interact for a maximum of 10 minutes. Aggressive/submissive behaviors were scored by observers to determine the social rank of each of the paired mice. All PS19 mice included in the results achieved a subordinate status. Following this daily interaction, a perforated partition was used to separate the mice, maintain a threat to the subordinate mouse by allowing continuous sensory contact, but preventing any additional physical contact. N=19

Restraint stress: Mice were restrained for 3 hours daily from approximately 9:00am to 12:00pm 6 days/week in modified 50mL conical tubes (Carroll et al., 2011). N=15

Control mice were singly housed and handled daily. N=21

At sacrifice, mice were anesthetized with isoflurane and transcardially perfused with ice cold PBS until runoff ran clear. Brains were removed, halved sagitally, and one half was flash-frozen in liquid nitrogen, and the other placed in 4% PFA for fixation. Flash-frozen tissue samples were stored at −80°C.

Statistical analysis

Unless otherwise specified, all statistical analyses (described individually below) were performed using Graphpad Prism.

Behavioral assays

Following the final day of CSS or restraint, mice were tested in a series of behavioral assays to assess their anxiety-like phenotype, their spatial learning and memory, spatial working memory, and fear-associated memory. The tests were run in the order presented below, allowing 1 day off between the Barnes Maze and Y maze, and another day off following Delay Fear Conditioning prior to the day of sacrifice.

Behavioral testing was performed with the support and guidance of the Mouse Behavior Core at the University of Minnesota. ANY-maze software (Stoelting Co.; Wood Dale, IL, USA) was used in conjunction with paired video cameras to track and record animal movements during all behavioral testing unless otherwise stated. Statistical analysis was performed with 1-way ANOVA with Dunnett's multiple comparisons test to test change from control group.

Elevated plus maze.

Mice were placed into the center of a 0.5m tall plus shaped-maze (55cm x 55 cm) with two open arms and two arms. Mice were allowed to freely explore the maze undisturbed for 5 minutes, and time in the open arms, closed arms, and center were scored using Ethovision by an observer blinded to experimental group.

Y Maze

Short-term spatial memory was assessed via Y maze. Animals underwent 30 min acclimation periods in the testing room prior to testing. Cues were visible on walls of the testing room as well as within the maze, at the end of each arm (extra-maze and intra-maze, respectively). The Y maze was constructed out of opaque white plastic and located at the center of the testing room lit to 150 lm. For all trials, animals were placed at the end of the start arm, furthest point from center. The 8 min recognition trial was then performed, with all three arms were available for exploration. The order of arm entries was recorded and scored for percentage of alternating choices between the 3 arms. The Y maze was also cleaned between each trial/animal to avoid confounds due to scent. Statistical analysis was performed with 1-way ANOVA with Dunnett's multiple comparisons test to test change from control group.

Barnes Maze

Spatial learning and memory were assessed via Barnes maze (San Diego Instruments; San Diego, CA, USA), in accordance with established protocols (Barnes, 1979; Pitts, 2018). The maze itself consists of a white plastic circular top with 20, evenly sized and evenly spaced holes around the perimeter. Spatial cues were placed on all four walls of the behavioral testing room, lit to 300 lm during testing. Mice were acclimatized to the testing room for 30 min at the beginning of each training session. Training days consisted of 4 trials per day for 4 days. Training trials ended when the subject climbed into the escape box located under 1 of the holes or when the maximum trial duration of 180 seconds was reached. Upon entering the escape box during training, room lights turned off and animals remained in the escape box for 60 s before returning to their home cage in the testing room to await the next trial. While the platform was rotated between each trial on each day (to obscure the impact any animal scents or non-spatial cues on the maze), the location of the escape box and goal quadrant relative to the room remained constant during all training trials and days. Subjects were run in small groups of six mice or less, so that no more than 20 min passed between trials for a given animal during training. On the day following the last training trial, memory was assessed in single 90 second probe trial, in which the target escape box in the goal quadrant was replaced with a false box cover identical to the other 19 holes, and the exploration pattern of each subject was examined.

Training time to escape, and training latency were analyzed by 2-way repeated measures ANOVA with Tukey post hoc. Probe trial analyses were performed by 1-way ANOVA with Dunnett's multiple comparisons test to test change from control group.

Delay Fear Conditioning

Delay fear conditioning was conducted using the Near-Infrared (NIR) Video Fear Conditioning package for mice (Med Associates, Inc.; Fairfax, VT, USA). On day one, mice are acclimatized to a context conditioning environment (specific olfactory, tactile, and visual elements). They then receive 5 conditioned stimulus (CS) cue presentations — buzzing sound, flashing lights — followed immediately by a foot shock spaced 1 minute apart.

After 24 h, mice are returned to the context conditioning environment and scored for percentage time freezing during a 5 min test in that context. After at least 3 hours rest, the

mice are placed in a novel context (different olfactory cue, different flooring, curved walls) and the percentage time freezing is scored. After 3 minutes in the novel context, the auditory/visual cue previously paired with foot shock is played again, and percentage time freezing is scored.

%freezing during training phase was analyzed by 2-way repeated measures ANOVA with Tukey post hoc. Probe trial analyses were performed by 1-way ANOVA with Dunnett's multiple comparisons test to test change from control group.

qPCRs

RNA from was extracted using a PureLink RNA Mini Kit (for all other tissues; Thermo Fisher Scientific) according to the manufacturer's protocol. Transcription into cDNA was performed using the iScript cDNA synthesis kit (Bio-Rad) according to the manufacturer's directions. Each cDNA sample was run in duplicate using the iTaq Universal SYBR Green PCR Master Mix (Bio-Rad) to a final volume of 10µl in a CFX Connect thermal cycler and optic monitor (Bio-Rad). The expression of genes was normalized to the geometric mean of two housekeeping genes – actin and GAPDH. Fold change was calculated using the delta-delta Ct method. Statistical analysis was performed using unpaired t tests.

Immunofluorescence

Mice were transcardially perfused with ice-cold Dulbecco's phosphate-buffered saline (DPBS; pH 7.4) until fluid runoff was clear. Brains were extracted and stored for 20-24 hours in 4% PFA at 4 ºC and then cryoprotected by incubating in a 30% sucrose solution for at least 48 h at 4 ºC. Samples were sectioned into 30-µM-thick coronal sections and stored in antifreeze solution (300 g sucrose, 300 ml ethylene glycol, 500 ml PBS) at -20ºC. Briefly, free-floating coronal sections were permeabilized with 0.5% Triton in tris-buffered solution with 0.5% tween-20 (TBS-T) for 1 hour at room temperature, blocked with 5% BSA in TBS-T for 30 minutes at room temperature, incubated in primary antibodies diluted in blocking buffer [chicken anti-GFAP (Abcam ab4674, 1:1000), rabbit anti-iba1 (Novus NBP2-19019, 1:1000), mouse IgG1 anti-pTau (AT8) (Invitrogen MN1020, 1:500), rabbit anti-pTau (pS404, Invitrogen 44-758G, 1:500), and/or mouse IgG1 anti human Tau (Invitrogen MN1000, 1:500)] for 15-18 h at 4 ºC then in secondary antibodies at 1:500 diluted in PBS for 2 h at room temperature. Sections were mounted on glass slides, counter-

stained with Dapi for 20 min, cover slipped in aqueous-based mounting media, and imaged on a Zeiss LSM 880 confocal system using multi-track configuration. Mean fluorescence intensity (MFI) measurements were performed on sum-projected z-stacks (z=20) using ImageJ software. Dentate gyrus area and width were measured manually in ImageJ software. Statistical analysis was performed using unpaired t tests.

CHAPTER 5

LIFELONG CHRONIC PSYCHOSOCIAL STRESS INDUCES A PROTEOMIC SIGNATURE OF ALZHEIMER'S DISEASE IN WILDTYPE MICE

Chapter 3 contains work that was previously published in *The European Journal of Neuroscience*

Lyons, C.E., Zhou, X., Razzoli, M., Chen, M., Xia, W., Ashe, K., Zhang, B., & Bartolomucci, A. (2021) Lifelong chronic psychosocial stress induces a proteomic signature of Alzheimer's disease in wildtype mice. *Eur. J. Neurosci.*, **55**, 2971–2985.

5.1 Summary

Late onset, sporadic Alzheimer's disease (AD) accounts for the vast majority of cases. Unlike familial AD, the factors that drive the onset of sporadic AD are poorly understood, although aging and stress play a role. The early onset/severity of neuropathology observed in most genetic mouse models of AD hampers the study of the role of aging and environmental factors; thus, alternate strategies are necessary to understand the contributions of these factors to sporadic AD. We demonstrate that mice acquiring a low social status (subordinate) in a lifelong chronic psychosocial stress (CPS) model, accrue widespread proteomic changes in the frontal/temporal cortex during aging. To better understand the significance of these stress-induced changes, we compared the differentially expressed proteins (DEPs) of subordinate mice to those of patients at varying stages of dementia. Sixteen and fifteen DEPs upregulated in subordinate mice were also upregulated in patients with mild cognitive impairment (MCI) and AD, respectively. Seven of those upregulated proteins (CPE, ERC2, GRIN2B, SLC6A1, SYN1, WFS1) were shared

by subordinate mice and patients with MCI or AD. Finally, comparison with a spatially detailed transcriptomic database revealed that the superior frontal gyrus and hippocampus had the greatest overlap between mice subjected to lifelong CPS and AD patients. Overall, most of the overlapping proteins were functionally associated with enhanced NMDA receptor mediated glutamatergic signaling, an excitotoxicity mechanism known to affect neurodegeneration. These findings support the association between stress and AD progression and provide valuable insight into potential early biomarkers and protein mediators of this relationship.

5.2 Introduction

Alzheimer's disease (AD) is a multifaceted, debilitating disorder that is driven by a number of genetic and environmental factors, including stress (Yuede *et al.*, 2018). Only an estimated 5-10% of cases can be explained by known familial genetic mutations (Cacace *et al.*, 2016). The remaining majority of AD cases are termed "sporadic" AD and are likely driven by a complex set of interactions between genes, environment and aging. Though it has proven difficult to study, gaining a better understanding of the molecular underpinnings of sporadic AD is a critical mission for research and public health.

Chronic stress and low socioeconomic status are linked to an increased risk of AD in humans. Stress at multiple stages of the lifespan has been shown to increase risk of AD diagnosis. Low socioeconomic status both in childhood and adulthood increases risk for AD (Stern *et al.*, 1994; Räihä *et al.*, 1998; Moceri *et al.*, 2001). Higher reactivity to stress in adults predicted a dementia diagnosis 30 years later, even within twin pairs (Crowe *et al.*, 2007). Later in life, patients already diagnosed with mild cognitive impairment (MCI) are more likely to progress to full dementia over a 2-3 year period if they experience one or more highly stressful events (Peavy *et al.*, 2012). Research in animal models of AD recapitulates this association between stress and AD pathology (for review see (Lyons & Bartolomucci, 2020)).

Though age-related cognitive decline is common across species (Benice *et al.*, 2006; Nagahara *et al.*, 2010; Mota *et al.*, 2019) only humans are known to develop AD (Gallagher & Nicolle, 1993; Herndon *et al.*, 1997). Wildtype rodents do not develop AD, nor its two hallmarks, neurofibrillary tangles (NFTs) and amyloid β (Aβ) plaques. Stress

in wildtype rodents is known to promote tau phosphorylation and synthesis of amyloid precursor protein and Aβ, but not to the point of inducing NFTs or plaques (Korneyev *et al.*, 1995; Rosa *et al.*, 2005; Rissman *et al.*, 2007; Sayer *et al.*, 2008; Yan *et al.*, 2010; Ray *et al.*, 2011; Filipcik *et al.*, 2012; Kvetnansky *et al.*, 2016). Transgenic rodent models of AD that carry copies of human genes linked to familial AD have been used extensively to understand the underlying pathophysiology of these protein aggregates. Numerous studies in these transgenic animal models have found that short-term stress exacerbates the characteristic neuropathology of many of these models (Green *et al.*, 2006; Kang *et al.*, 2007; Lee *et al.*, 2009; Carroll *et al.*, 2011; Rothman *et al.*, 2012; Vijgen *et al.*, 2012; Lesuis *et al.*, 2016; Hoeijmakers *et al.*, 2017). Many transgenic mouse models develop severe cognitive deficits and neuropathologies at relatively young ages, which allows experiments to be carried out on a short timeline. Unfortunately, this attribute also removes the greatest risk factor for AD from the picture - aging (Lyons & Bartolomucci, 2020). Thus, these models cannot entirely recapitulate the biology of the disease as it occurs in humans, particularly for sporadic AD, which is per se not linked to genetic mutations. This limitation may be a factor in why, despite many advances in understanding the pathophysiology of Aβ plaques and tau aggregates, the treatment options developed using these animal models have not proved effective thus far (Mullane & Williams, 2013; Egan *et al.*, 2018).

Alternative approaches to understanding the etiology of sporadic AD can be informed by the commonalities between wildtype rodents exposed to known risk factors for AD, such as old age and stress, and human AD patients. By understanding the shared biology of patients affected by AD and laboratory animals exposed to environmental risk factors for the disease, we might gain a stronger understanding of how AD develops. Such an approach could illuminate the dysregulation of key molecular pathways involved in shaping vulnerability to sporadic AD.

Previous work from our lab found that lifelong chronic psychosocial stress (*Lifelong CPS*) anticipates the onset of organ-specific diseases and shortens lifespan in subordinate mice compared to dominant C57BL/6J mice (Razzoli *et al.*, 2018). Dominant C57BL/6J have comparable lifespan and age-associated disease onset to normal control

C57BL/6J mice (Razzoli *et al.*, 2018, Razzoli et al., under review). Two months into the aging phase, subordinate mice exhibited increased fecal corticosterone metabolites compared with dominant mice, consistent with a chronic stress phenotype. Of particular note, subordinate mice developed early-stage atherosclerosis, a striking finding in a wildtype mouse. This remarkable finding led us to ask whether the potent *Lifelong CPS* exposure could induce characteristics of AD, another aging-associated disease that do not normally manifest in wildtype mice. In this study, we conducted unbiased proteomic profiling on biobank tissue from our *Lifelong CPS* study. We then compared this molecular signature in mice to a proteomic analysis in patients diagnosed with Mild Cognitive Impairment (MCI) or AD as well as with a gene expression profile for AD (Wang *et al.*, 2016; Bai *et al.*, 2020). This led us to identify many differentially expressed proteins (DEPs) shared by subordinate mice in the lifelong CPS with patients with MCI or AD which can inform on underlying molecular mechanisms of AD transition.

5.3 Results

We performed whole proteome profiling of frontal/temporal cortex of five randomly selected subordinate and dominant C57BL/6J mice from the tissue biobank collected in our previous *Lifelong CPS* experiment **Appendix Table 3** summarizes the healthspan of the mice selected for this study). We then compared the relative protein abundance between the two groups. An unbiased proteomic analysis revealed a significant difference in protein expression between *Lifelong CPS* subordinate and dominant mice. The analysis identified a total of 75 upregulated proteins and 125 down-regulated proteins (**Figure 1B**, $p<0.05$ *Empirical Bayes-moderated t-test).* Gene Ontology enrichment analysis for these differentially expressed proteins (DEPs) revealed them to be involved in many neuron-related biological processes. Specifically, the most highly enriched biological processes are associated with synaptic transmission and nervous system development, including “chemical synaptic transmission” (Fold Enrichment (FE) = 7.51), adjusted p-value (adj. p) = 2.12E-07) (**Figure 1D**), “neuron projection development” (FE = 4.52, adj.p = 9.29E-04) (**Figure 1E**), “Long-term potentiation” (FE = 8.91, adj.p = 6.56E-05) (**Figure 1F** as well as “Alzheimer's disease” (FE = 3.41, 1.21E-03) (**Figure 1G**). We also performed a similar proteomic analysis in age matched mice subjected to CPS for just the 4 weeks prior to sacrifice (*Old age CPS*). Results showed minimal differences from

controls (**Appendix Supplementary Figure 3B**. *Empirical Bayes-moderated t-test, NS*) and no neuron associated biological processes enriched for these DEPs (the most enriched biological process was “translational initiation” (adj.p = 0.014)). Considering that the dominant experimental mice from the *Lifelong CPS* study have comparable lifespan and age-associated disease onset to normal control C57BL/6J mice (Razzoli *et al.*, 2018, Razzoli et al., under review), these results indicate that lifelong subordination stress is critical to elicit major differences in neuron processes-related protein expression in the cerebral cortex of mice. Experimental differences between the *lifelong CPS* and the old age CPS (see methods) preclude a direct statistical comparison of the two data sets.

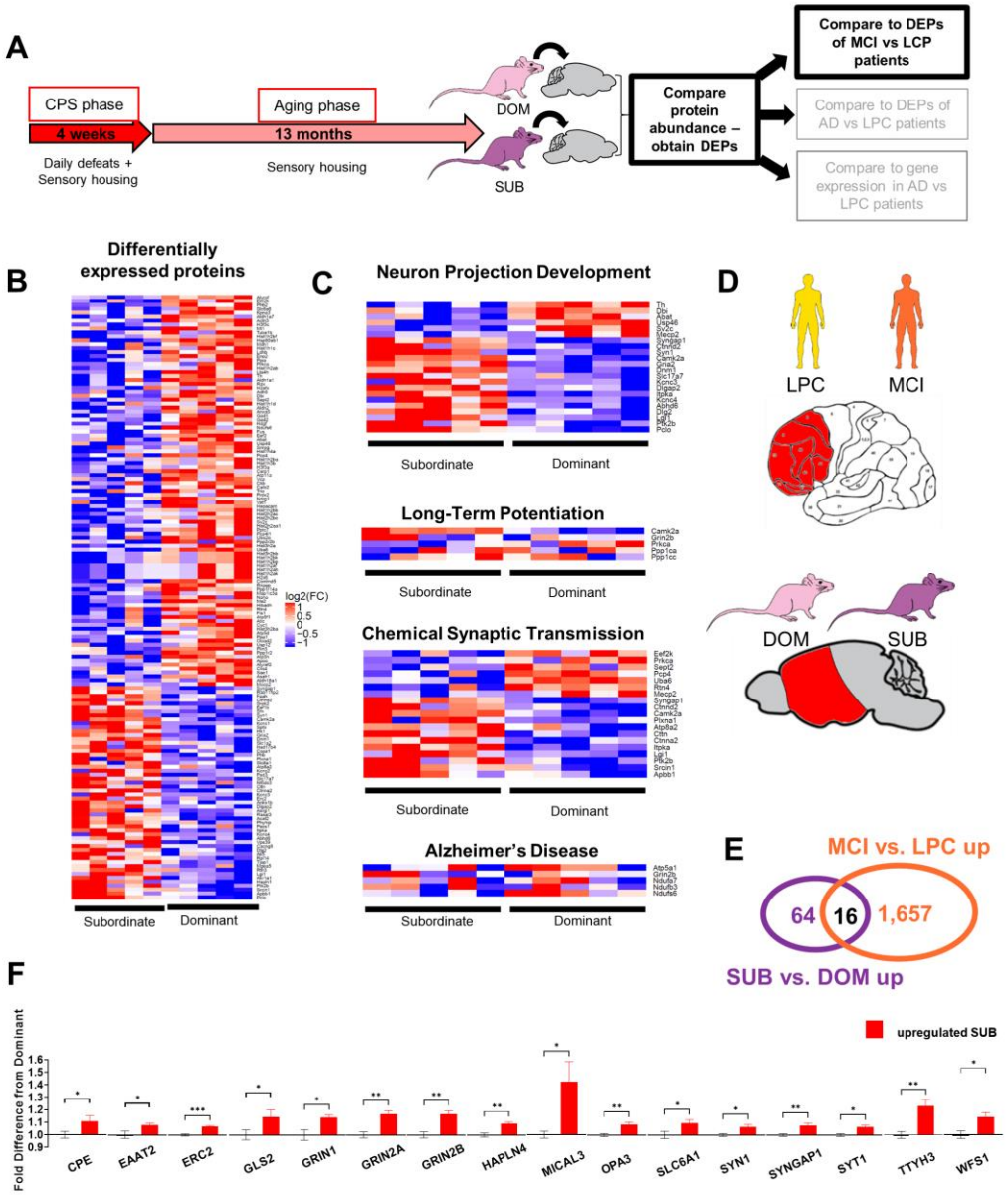

Figure 1 DEPS and the **proteomic overlap between lifelong CPS mice MCI patients A)** Experimental overview. **B)** Heat map of differentially expressed proteins between subordinate and dominant mice. A total of 64 proteins were significantly upregulated and 113 proteins were significantly downregulated in subordinate mice, versus dominant mice of the same strain ($p < .05$). **C)** Gene Ontology Analysis revealed top altered biological processes of the lifelong Chronic Psychosocial Stress (CPS) DEPs. "Chemical synaptic transmission" (Fold Enrichment (FE) = 7.51, adjusted p value (adj. p) = 2.12E-07), "neuron projection development" (FE = 4.52, adj. p = 9.29E-04), "Long-term potentiation" (FE = 8.91, adj. p = 6.56E-05) and "Alzheimer's Disease" (FE = 3.41, 1.21E-03). **D)** Highlights brain the regions from humans (low pathology controls LPCs, and

mild cognitive impairment MCI) and mice (subordinate SUB and dominant DOM). **E)** Venn Diagram showing total number of upregulated proteins in MCI (vs. LCP) and SUB (vs. DOM). A total of 16 proteins were shared, FE = 3.17 (adj p = 1.2E-4). **F)** Histogram shows the 16 DEPs upregulated in both the frontal cortex of patients with MCI, and in the frontal/temporal cortex of mice subjected to lifelong CPS. *p < .05 Fisher's exact test with BH correction

To further interrogate the biological roles of the DEPs in mice exposed to *lifelong CPS*, we tested the overlap between the stress signature in the mouse study with recently published molecular signatures of MCI and AD (Bai *et al.*, 2020). This database includes whole proteome profiling of frontal cortical samples from human patients categorized as 1) Low pathology controls (LPC), which contained low pathology of Aβ plaques and NFTs, 2) MCI which exhibited some Aβ pathology and small but measurable deficits in cognition 3) AD with high pathology scores of plaques and tangles (Bai *et al.*, 2020).

First, we compared DEPs to the MCI signature (Bai *et al.*, 2020). We found 16 proteins upregulated in subordinate mice that were also significantly upregulated in MCI patients compared to LPCs (**Figure 1E**, Venn Diagram), which was significantly more than random chance (FE = 3.17, adj. p=8.67E-04). These overlapping proteins were CPE (carboxypeptidase E), EAAT2 (Excitatory Amino Acid Transporter 2), ERC2, (ELKS/RAB6-Interacting/CAST Family Member 2), GRIN1 (Glutamate ionotropic receptor NMDA type subunit 1), GRIN2A, (NMDA receptor type subunit 2A), GRIN2B (NMDA receptor type subunit 2B), GLS2 (Glutaminase 2), HAPLN4 (Hyaluronan and Proteoglycan Link Protein 4), MICAL3, (Microtubule Associated Monooxygenase), OPA3 (Optic atrophy 3 protein), SLC6A1 (Solute Carrier Family 6 Member 1), SYN1 (Synapsin-1), SYNGAP1 (Synaptic Ras GTPase-activating protein 1), SYT1 (Synaptotagmin 1), TTYH3 (Tweety Family Member 3), and WFS1 (Wolframin ER Transmembrane Glycoprotein) (**Figure 1F**). A number of these proteins serve functions related to glutamatergic synaptic transmission, and in particular NMDA receptor signaling.

We next compared the DEPs from our mice to the proteomic changes observed in patients with diagnosed AD (Bai *et al.*, 2020) and we found significant overlap of DEPs in subordinate mice with the AD vs LPC signature (**Figure 2**; FE = 3.12; adj. p = 1.9E-3). A number of these proteins were the same as those overlapping with the MCI signature,

including CPE, ERC2, GRIN2B, SLC6A1, SYN1 and WFS1. Additional overlapping proteins were ACADL (Acyl-CoA Dehydrogenase Long Chain), CAMK2A (Calcium/calmodulin-dependent protein kinase type II subunit alpha), CTTN (Cortactin), GRIN2D (NMDA receptor type subunit 2B), INVS (Inversin), OXR1 (Oxidation Resistance Protein 1), PYGB (Glycogen phosphorylase B), WDR1 (WD Repeat Domain 1 and YWHAH (14-3-3 protein eta). There was no significant overlap between the samples in downregulated DEPs in the mouse study. Also, there was no significant overlap with the DEPs between MCI and AD samples, indicating that *Lifelong CPS* mainly induces changes shared by MCI and AD, rather than changes involved in the escalation from MCI to AD.

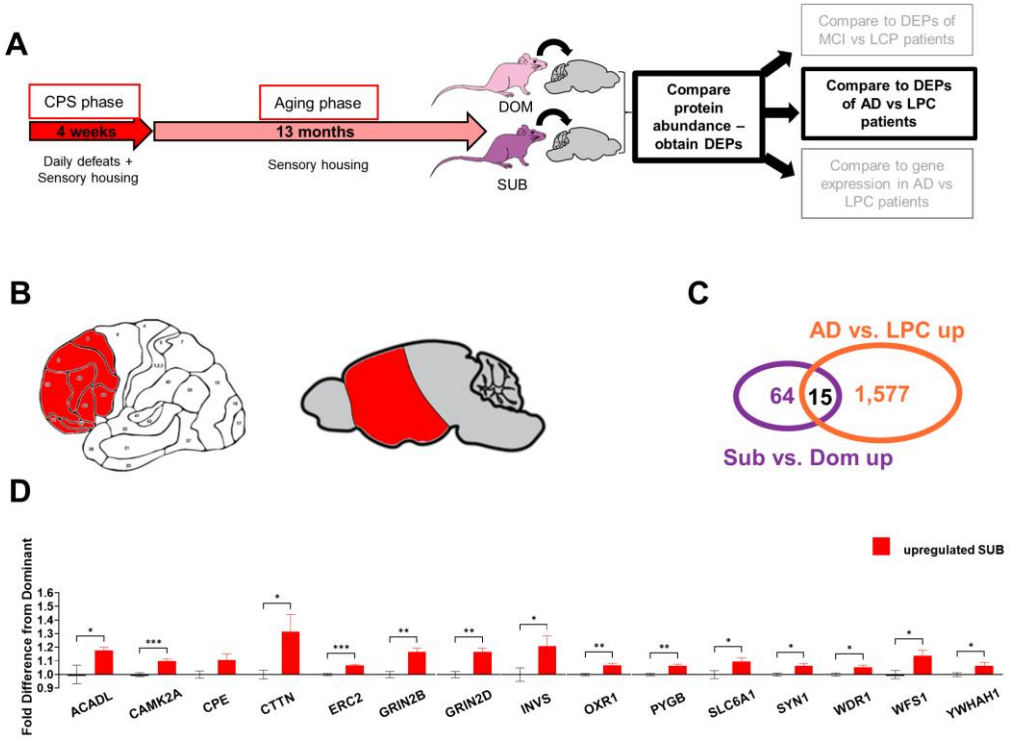

Figure 2 Proteomic overlap between lifelong CPS mice and AD patients A) Experimental overview, highlighting analyses portrayed in this figure. **B)** Illustration of brain areas from AD/LPC patients and SUB/DOM lifelong CPS mice compared in proteomic analysis. **C)** Venn Diagram showing the degree of overlap between the two samples. **D**) There were 15 DEPs upregulated in both the frontal cortex of patients with AD, and in the frontal/temporal cortex of mice subjected to lifelong CPS. *p < .05 Fisher's exact test with BH correction. SUB, subordinate; DOM, dominant

These proteomic comparisons informed us of the cellular processes induced by lifelong stress that are also altered in progressive AD. However, these data were derived from a fairly broad brain region in the human studies (frontal cortex). To gain greater insight into which brain regions included in the mouse frontal/temporal cortex might have the most similarity to changes in human AD, we compared our mouse data to spatially specific human gene expression data (Wang *et al.*, 2016). We used a hypergeometric distribution test to calculate the significance of enrichment between top DEPs and AD gene expression signature for 19 different brain regions. Unlike the previous analyses, this test compared proteomic data to transcriptomic data. While this limits the interpretation of this analysis on its own, the concordance in the overlapping proteins with those found in the proteome vs proteome analyses detailed above increases our confidence in the results. We found that proteins upregulated in cortex of subordinate mice were most significantly enriched with upregulated genes identified from AD patients in the superior frontal gyrus (BM8-SFG) (FE = 5.48, adjusted p = 0.011) (**Figure 3C**), while proteins downregulated in subordinate mice were enriched mostly with AD signatures from hippocampus (FE=12.02, adjusted p = 0.019) (**Figure 3C**). In particular, there were 9 proteins upregulated both in the cortex of mice subjected to *lifelong CPS* and in the SFG of human AD patients, and 5 key proteins downregulated in our mouse samples as well as the hippocampus of AD patients (**Figure 2B**).The shared upregulated genes were ATP6V1A (V-type proton ATPase catalytic subunit A), ARL6IP5 (PRA1 family protein 3), CAMK2A (Calcium/calmodulin-dependent protein kinase type II subunit alpha), CTTN (Cortactin), EAAT2 (Excitatory amino acid transporter 2), OGT (O-Linked N-Acetylglucosamine (GlcNAc) Transferase), OXR1 (Oxidation Resistance Protein 1), RTN3 (Reticulon-3) and SYT1 (Synaptotagmin-1). The downregulated genes were BCAT1 (Branched chain amino acid transaminase 1), GAD2 (Glutamate decarboxylase 2), GUK1 (Guanylate Kinase 1), PCP4 (Purkinje cell protein 4) and VGLUT2 (vesicular glutamate transporter 2) (**Figure 3E**). A number of these same genes were also enriched in the proteomic data of AD (CAMK2A, CTTN, OXR1) or MCI patients (EAAT2, SYT1). This consistency among the 3 comparisons lends credence to these stress-related changes as playing a possible role in AD progression. Overall, these results suggest that *lifelong CPS* induces changes at a molecular level that are consistent with those seen in AD.

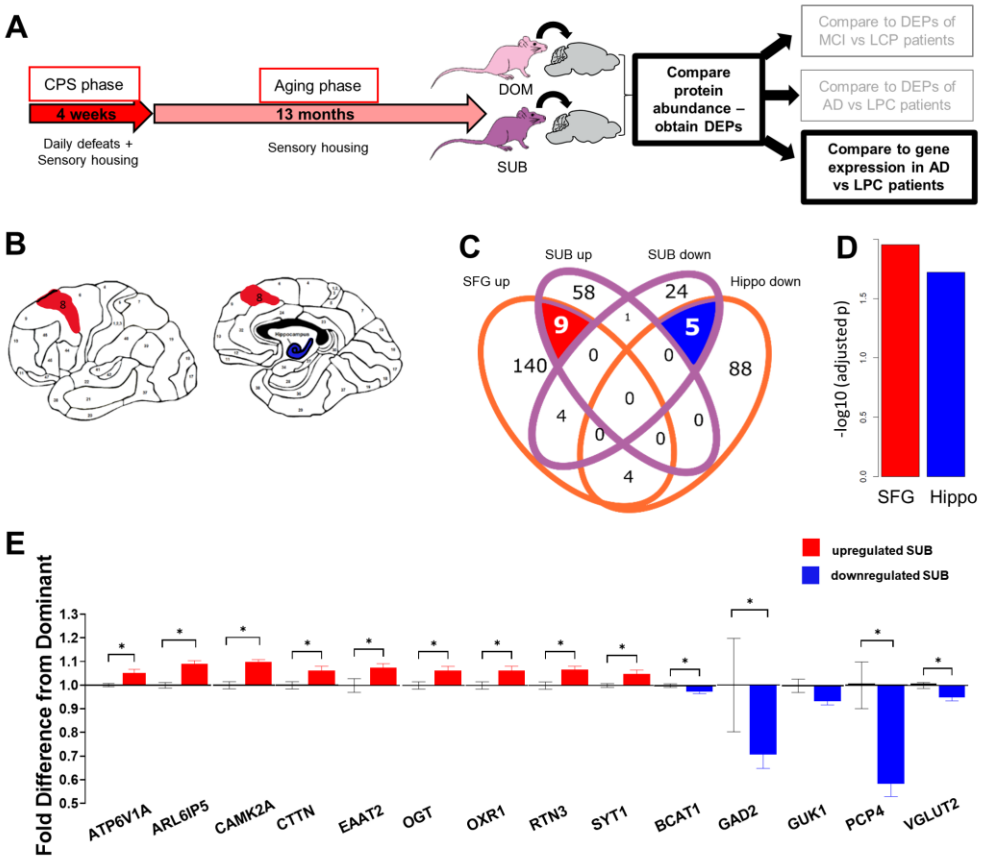

Figure 3 Overlap between proteomic changes in lifelong CPS mice and regionally-specific transcriptomic changes in AD patients A) Experimental overview, highlighting the analyses presented in this figure. **B)** Wang et al. described differential RNA expression profiles in post-mortem brains of AD patients in 19 different brain regions. Areas with the greatest overlap in gene expression with lifelong CPS mice are highlighted in red (upregulated, superior frontal gyrus) and blue (downregulated, hippocampus). **C)** Venn diagram of top DEPs in subordinate (SUB) versus dominant (DOM) and the Alzheimer's disease signatures identified from Mount Sinai Brain Bank. Upregulated proteins in the neural cortex of lifelong CPS mice were significantly enriched with upregulated genes identified from AD patients in Superior Frontal Gyrus (BM8-SFG) (Fold Enrichment (FE) = 5.48, adj. p =.011). Downregulated proteins in lifelong stress mice were enriched with AD signatures in the hippocampus (FE = 12.02, adj p =.019). DEPs between old age stress and control mice had no significant enrichment with AD signatures. **D)** Enrichment analysis of the top DEPs of SUB and the AD signatures (Red = upregulated and blue = downregulated in mice and patients). **E)** Relative expression of the 9 up and 5 downregulated proteins associated with AD in humans that were also altered in subordinate mice. $^{*}p < .05$ Fisher's test with BH correction

Finally, we measured the expression of classical molecular markers of AD in mice subjected to *lifelong CPS*. Somewhat surprisingly, and at variance with other data obtained with non-social stress models like restraint (Rissman *et al.*, 2007) or chronic unpredictable mild stress (Yang *et al.*, 2014), subordinate mice had slightly but significantly lower level of the phosphorylated tau epitope PHF1 than dominant mice (**Appendix Supplementary Figure 3A**). This difference cannot be entirely explained by changes in total tau levels, which trend lower in subordinate mice, but not to the same degree and not with statistical significance (**Appendix Supplementary Figure 4C**). There was not a significant difference in abundance of the epitope AT8 (**Appendix Supplementary Figure 4B**). As would be expected in non-transgenic wildtype mice, the experimental subjects showed undetectable levels of aggregated Aβ (**Appendix Supplementary Figure 4D**).

5.4 Discussion

Chronic stress is known to increase risk for AD in humans, as well as to exacerbate Aβ and tau pathology in transgenic mouse models (Lyons & Bartolomucci, 2020). We now show that *lifelong CPS* in a wildtype mouse can induce changes to the proteome that mimic a molecular signature of progressive AD. This novel finding lends further support to the hypothesis that life stress plays a role in AD predisposition, adding to the previous literature that shows stress-induced changes to AD markers in wildtype mice (Rissman *et al.*, 2007; Yan *et al.*, 2010; Lopes *et al.*, 2016). Critically, our findings also indicate several key proteins whose differential expression may drive or simply be a biomarker, of this phenomenon. Namely, CPE, ERC2, GRIN2B, SLC6A1, SYN1 and WFS1 proteins were upregulated in subordinate mice exposed to *Lifelong CPS* as well as in both MCI and AD samples. Similarly, CAMK2A, CTTN, EAAT2, OXR1 and SYT1 were differentially expressed in subordinate mice and were upregulated at the gene expression level in the SFG of AD patients and at the protein level in patients affected by MCI or AD.

Our *lifelong CPS* model includes experimental C57BL/6J mice becoming either subordinate or dominant. It was previously shown that subordinate mice in this paradigm have a shorter lifespan, higher circulating corticosterone levels, and earlier onset of age-related pathologies, than dominant mice, which maintained standard profiles similar to

unstressed mice (Razzoli *et al.*, 2018). The dominant mice thus served as a reference point to compare subordinate mice of the same strain.

The Gene Ontology enrichment analysis indicated that the DEPs in the brains of subordinate mice exposed to *lifelong CPS* were related to several neuronal processes, the most significant of which were "chemical synaptic transmission", "neuron projection development", "long-term potentiation" and "Alzheimer's Disease". This indication that some of the DEPs in subordinate mice subjected to *lifelong CPS* may be linked to AD prompted us to further interrogate this association, by comparing our proteomic data with human profiles of progressive AD. First, we compared our DEPs with a proteomic characterization of the frontal cortex of patients with MCI, a condition which frequently advances to AD (Morris *et al.*, 2001). Next, we compared our DEPs to those of patients diagnosed with AD. Finally, to learn which brain regions in AD shared the most similarity to the stressed mice, we performed a comparison with a gene expression database across 19 brain regions of humans diagnosed with AD.

A number of proteins were upregulated in subordinate mice as well as in both MCI and AD brains. These proteins including CPE, ERC2, GRIN2B, SLC6A1, SYN1 and WFS1. Moreover, many of the overlapping proteins from the individual comparisons are involved in the same cellular processes. Across all three analyses, the most striking trend to emerge from the lists of overlapping DEPs, was upregulation of proteins related to excitatory synaptic transmission.

There were 16 proteins upregulated in both the frontal cortex of patients with MCI, and of subordinate mice subjected to *lifelong CPS*. Notably, the overlapping proteins include many regulators of excitatory synaptic transmission, both on the presynaptic and postsynaptic side. These included multiple proteins involved in NMDA receptor signaling. NMDA receptors are generally composed of two GluN1 subunits and two GluN2 subfamily subunits. Both types of subunit were upregulated in MCI and *lifelong CPS*. GRIN1 is the GluN1 subunit while GRIN2A and GRIN2B are two of the four members of the GluN2 subunit family (Moriyoshi *et al.*, 1991). NMDA receptors are activated by simultaneous glutamate release and membrane depolarization. Their activation allows Ca^{2+} entry into the cell, which under normal conditions, regulates physiological processes like

synaptic plasticity; however excessive intracellular Ca2+ can damage cellular structure and activate cell death pathways (Li & Wang, 2016). This process, termed excitatory neurotoxicity leads to gradual loss of synaptic function and neuronal death, and is known to play a role in AD and other neurodegenerative diseases (Choi, 1988; Wang & Reddy, 2017; Kodis *et al.*, 2018). In particular, receptors containing the GRIN2B subunit are predominantly found at extrasynaptic locations and their stimulation results in increased cell death (Liu *et al.*, 2007). An increase in NMDA receptors, particularly extrasynaptic ones, would exaggerate the response to glutamatergic signaling, leading to greater influx of Ca^{2+} and thus a greater risk of excitotoxicity.

GRIN2B was also found to be one of the overlapping upregulated proteins with AD, along with another subtype GRIN2D. Further supporting vulnerability to excitotoxicity as a shared feature of lifelong stress and AD is the mutual upregulation of CAMK2A. CAMK2A, one of the subunits that makes up the Ca2+/calmodulin-dependent kinase II (CAMK2). Post mortem analyses of AD patients' brains have shown that neurons in the subiculum and area CA1 of the hippocampus have increased expression of CAMK2 (McKee *et al.*, 1990; Wang *et al.*, 2005). CAMK2 mediates many of the effects of NMDA receptor activation by glutamate and has been proposed to play a critical role in axonal degeneration induced by glutamate excitotoxicity (Hernández *et al.*, 2018). Additionally, a substrate for CAMK2 is SYNGAP1, which was also upregulated with lifelong stress and MCI. SYNGAP1 is a regulator of synaptic plasticity and can both insert and remove AMPA receptors from the post synaptic membrane (Araki *et al.*, 2020; Gamache *et al.*, 2020). Phosphorylation of SYNGAP1 by CAMK2 preferentially favors removal of AMPA receptors. This could exacerbate the weakening and loss of synapses that characterizes AD.

Other shared features of *lifelong CPS* mice and the brains of MCI and AD patients included the upregulation of proteins involved in presynaptic vesicle release. Presynaptic proteins SYN1 (upregulated in both MCI and AD) and SYT1 (upregulated in AD) regulate the organization and release of synaptic vesicles respectively. Similarly, though its function is not fully understood, ERC2 (upregulated in both MCI and AD) is one of the components of the cytomatrix at the nerve terminals active zone, which regulates vesicle fusion and neurotransmitter release (Siksou *et al.*, 2007). Thus, in addition to postsynaptic changes that increase glutamate-NMDA receptor signaling, there may also be enhanced release of

glutamate from the presynaptic side. Finally, DLGAP2 is a postsynaptic density scaffolding protein that stabilizes both AMPA and NMDA receptors at the membrane (Ranta *et al.*, 2000).

Following up on this, we extended our study to perform a hypergeometric comparison of DEPs in our subordinate *lifelong CPS* mice with RNA sequencing data from human patients with AD. While this analysis is limited in that it compares proteomic changes with transcriptomic changes, it is valuable as this human dataset includes characterization of specific brain regions. It revealed that the greatest proteomic overlap between the *lifelong CPS* mouse and AD patient brains was in the SFG and hippocampus. There were 14 key proteins that overlapped with the AD signature in humans. Consistent with the comparisons with MCI AD proteomic data, these changes highlighted proteins involved in synaptic transmission. SYT1 is the calcium sensor that gates fusion of the synaptic vesicle with the presynaptic membrane and exocytosis (Südhof, 2013). Recent evidence indicates that it also plays a role in postsynaptic long-term potentiation as a calcium sensor that recruits AMPA receptors to the membrane (Wu *et al.*, 2017). EAAT2 was also upregulated AD patients and in mice subjected to *lifelong CPS*. EAAT2 is the principal transporter that clears glutamate from extracellular space (Kim *et al.*, 2011). Upregulation of this protein could be a compensatory mechanism due to increased glutamatergic signaling. In contrast to these increases in proteins involved in excitatory signaling, GAD2 mRNA is downregulated. This glutamate decarboxylase enzyme is responsible for catalyzing the production of GABA, the major inhibitory neurotransmitter. At the same time, SLC6A1 was upregulated in mice subjected to lifelong stress and AD patients at the protein level. This transporter removes GABA from extracellular space, terminating its signaling. This along with the increases in proteins related to glutamate release further suggests that there may be a shared excitatory/inhibitory imbalance in subordinate mice and patients with AD.

Each of the comparative analyses we conducted suggests that subordinate mice subjected to *lifelong CPS* share a dysregulation in glutamatergic signaling with MCI and AD patients. The upregulation of CAMK2A, SYN1, and SYT1 in subordinate mice indicates that their synaptic function may facilitate excessive glutamatergic signaling. Furthermore, the increase on the postsynaptic side of NMDA receptor subunits GRIN1,

GRIN2A, GRIN2B and GRIN2D indicates enhanced sensitivity to glutamate. Thus, excitotoxicity may be a crucial mechanism by which high stress promotes AD in humans, and it warrants further investigation.

Glutamatergic signaling plays a dichotomous role in AD. While excessive glutamate/NMDAR signaling causes excitotoxicity, insufficient glutamate/NMDAR signaling compromises LTP and cell survival. Stress is associated with both of these phenomena. Previous reports have linked chronic stress to impaired glutamate reuptake and subsequent neurotoxic effects (Yang *et al.*, 2005). However, impaired LTP is a well-known component of AD pathology and reports have shown that selective enhancement of AMPAR signaling ameliorates stress-induced cognitive deficits in mice injected i.c.v. with Aβ (Monteiro-Fernandes *et al.*, 2020). These opposing roles of glutamate in AD have not been fully reconciled in the literature, although involvement of extra-synaptic NMDARs (the precise nature of which is debated) appears to be important (Zhou *et al.*, 2013). The analyses outlined here suggest that chronic stress, in addition to inducing marker of synapse loss, as previously reported, also may in the long-term promote proteomic changes associated with excitotoxicity.

In contrast to the shared molecular signature with MCI and AD discussed above, subordination in the *lifelong CPS* was not associated with an increase, but actually with a modest but significant decrease in phosphorylated tau (pTau; as expected Aβ plaques were not present in wildtype mice). To the best of our knowledge this is the first study testing the effect of a lifelong social stress model on pTau level. Nevertheless, previous studies have shown a generally robust link between stress exposure and tau phosphorylation (reviewed in (Lyons & Bartolomucci, 2020)). Even among stressors known to induce tau hyperphosphorylation, there appear to be differences in the underlying mechanisms. It has been suggested that temperature-sensitive kinases mediate tau phosphorylation in response to strong physical stressors, such as cold-water stress and starvation (Planel *et al.*, 2001, 2004), while CRH/CRHR1 signaling is required for restraint stress induced tau phosphorylation (Rissman *et al.*, 2007). Stressor types thus may affect tau phosphorylation differently. The divergence of current with previous results may be due to a differential effect of social vs. non-social stress models like restraint (Rissman *et al.*, 2007; Carroll *et*

al., 2011) or chronic unpredictable mild stress (Yang *et al.*, 2014). Additionally, the present is the first study conducted after lifelong social stress in mice.

5.5 Conclusion

In sum, this study provides valuable insight into the profound effect that lifelong psychosocial stress can have on individual brain proteomic changes. Additionally, we demonstrate that *lifelong CPS* in wildtype mice induces a proteomic signature with substantial overlap with the molecular changes found in human patients affected by MCI or AD. These findings and the associated identification of relevant biomarkers provide an insight into how an environmental risk factor like stress constitutes a considerable risk factor for the development of sporadic AD.

5.6 Materials and Methods

In the present study we performed a molecular characterization of mouse and human brains obtained from the following experiments (see below for further details): 1) Lifelong CPS: Brains are derived from a tissue bank of C57BL/6J mice exposed to *Lifelong CPS* for 17 months (Razzoli et al. 2018). In this study, mice were exposed to daily agonistic interaction and sensory contact for 4 weeks followed by 14 months of continuous sensory contact to maintain the psychological threat. Mice were stratified according to their social rank. 2) A brain bank of patients affected by MCI, AD or LPC (low pathology controls) in which a proteomic and/or a transcriptomic analysis was performed (Wang et al., 2016; Bai et al., 2020). The human samples are from the Banner Sun Health Research Institute and Mount Sinai/JJ Peters VA Medical Center NIH Brain and Tissue Repository. 3) Old Age CPS: a dedicated 4 week-long CPS experiment conducted in mice from the NIA aging colony.

Lifelong Chronic Psychosocial Stress (CPS): The lifelong CPS consisted of a randomized experimental design in which adult C57BL/6J mice (Jackson Labs) were paired with mice from the highly aggressive CD1 strain (Charles River) or the mildly aggressive Sv129Ev strain (Taconic) (Razzoli *et al.*, 2018). No individually housed mice were included in the experimental design. Subjects included in the present analyses are 1) C57BL/6J mice that acquired a subordinate status when paired with a CD1 male and 2) C57BL/6J that acquired a dominant status when paired with a Sv129Ev male. A tissue bank was collected in a subgroup of subjects at 17 months of age. For this proteomic study, 5

brains from C57BL/6J dominant or subordinate mice were randomly selected and processed as described below. General methods were described in (Razzoli *et al.*, 2018). Briefly, the model consisted of two phases: a 4-week CPS phase, which included daily social defeat and sensory contact housing followed by an aging phase, during which time the mice remained in sensory contact housing. During the CPS phase, resident and intruder mice were allowed to interact for a maximum of 10 minutes daily between 8:30 and 9:30am. Following this interaction, a perforated partition was used to separate the two mice, which allowed continuous sensory contact but precluded any physical contact. During the daily interaction, the aggressive behaviors were scored to determine each animal's social status as subordinate or dominant as previously described (Bartolomucci *et al.*, 2010; Dadomo *et al.*, 2011).The aging phase extended until the mice reached 17 months of age. Thus, dominant and subordinate mice were continuously exposed to an agonistic context while in sensory contact from the age of 3 months to 17 months. The mice were fed ad libitum a standard (D12405B, Research Diets Inc). Starting at 10 months of age, the mice were fed a maintenance diet (D10012M, Research Diets Inc.) because of its better balance of essential nutrients tailored for aged rodents. Mice were sacrificed at 17 months of age, while they were still in apparent good health; this age precedes the rapid decline of the lifespan curve typical of this strain. For hormone analysis, feces were collected 2 months after the end of the CPS phase and immunoreactive corticosterone metabolites using a 5α-pregnane-3β,11β,21-triol-20-one enzyme immunoassay as previously described (Heinzmann *et al.*, 2014; Razzoli *et al.*, 2018). At 17 months of age, mice were euthanized by CO_2 inhalation in the morning (between 8 and 10 a.m.). Brains were removed, halved sagitally, and one half was flash-frozen in liquid nitrogen, and the other placed in 4% PFA for fixation. Flash-frozen tissue samples were stored at −80°C. After PFA fixation at room temperature, the hemibrains were transferred to 70% ethanol and stored at room temperature.

Old Age CPS: 16-month-old C57BL/6 mice were received from the NIA aged rodent colony located at Charles River Laboratories where they were fed a proprietary diet. After 2 weeks acclimation they were randomized to either receive 4 weeks of CPS, as described in the CPS phase of the lifelong CPS experiment, or were singly housed as controls. Consistent with previous studies in young mice (Sanghez *et al.*, 2013), for the first week,

mice were fed a standard diet (10% kcal from fat, D12405B, Research Diets Inc.). They were then fed a high fat diet from the second to fourth week of CPS (45% kcal from fat, D12451, Research Diets Inc.). At the conclusion of the 4 weeks of CPS, the now 17-month-old mice were sacrificed. Brains were removed and processed as described above. Plasma corticosterone was analyzed as previously described (Razzoli *et al.*, 2014). All animal studies were approved by University of Minnesota IACUC.

Human studies.

Proteomic study: Human data were obtained from recently published molecular signatures of progressive AD and MCI (Wang *et al.*, 2016; Bai *et al.*, 2020). This database includes whole proteome profiling of frontal cortical postmortem brain tissue samples provided by the Brain and Body Donation Program at the Banner Sun Health Research Institute. Clinical and pathological diagnoses were made based on previously established criteria (Beach *et al.*, 2015). Samples were categorized as 1) Low Pathology Control (LPC), which contained low pathology of Aβ plaques and NFTs 2) MCI which exhibited some Aβ pathology and small but measurable deficits in cognition 3) late stage AD with high pathology scores of plaques and tangles (Bai *et al.*, 2020). The whole proteome was profiled for 18 samples in each group using multiplexed tandem-mass-tag (TMT) method and two-dimensional liquid chromatography-tandem mass spectrometry (LC/LC-MS/MS) as previously described in detail (Pagala *et al.*, 2015; Bai *et al.*, 2017, 2020).

Transcriptomic study: Gene expression data came from the Mount Sinai/JJ Peters VA Medical Center NIH Brain and Tissue Repository. This brain bank collected large-scale gene expression profiles from 1,053 postmortem brain samples across 19 different cortical regions from 125 different individuals (Wang *et al.*, 2016). For each brain region, the gene expression changes associated with AD were identified between samples from cognitive normal individuals and samples from high severity dementia individuals using R package *limma* (Smyth, 2004) with p-values corrected by the Benjamini-Hochberg (BH) procedure. In total, 6,037 AD-associated genes identified with a false discovery rate cut-off of 0.05 and a fold change of 1.5 were used in the current study.

Sample preparation for Mass Spectrometry: Frontal and temporal cortex was dissected from snap frozen hemibrains and added to lysis buffer (2% SDS, 0.5M tetraethyl-

ammonium bicarbonate (TEAB), protease inhibitor cocktail) and homogenized by TissueLyser LT (Qiagen, Valencia, CA). Tissue homogenates were centrifuged at 17,000 × *g*, for 20 min at 4°C. The supernatant was transferred into a new vial for protein concentration measurement by BCA assay (Sigma Aldrich). Preparation of tryptic peptides for TMT 10-plex labelling was carried out according to the manufacturer's instructions (Thermo Fisher). 100 μg protein of each sample was transferred into a new vial and adjusted to a final volume of 100μL with TEAB and reduced with tris (2-carboxyethyl) phosphine at 55 °C for 1 hour, and then alkylated with iodoacetamide for 30 minutes in the dark. Proteins were precipitated by pre-chilled (-20°C) acetone and proceeded overnight. Methanol-chloroform precipitation was performed prior to protease digestion. In brief, four parts methanol was added to each sample and vortexed, one-part chloroform was added to the sample and vortexed, and three parts water was added to the sample and vortexed. The sample was centrifuged at 14,000 *g* for 4 min at room temperature and the aqueous phase was removed. The organic phases with protein precipitate at the surface was subsequently washed twice with four parts methanol and centrifuged with supernatant being removed subsequently. After air-drying, precipitated protein pellets were re-suspend with 100μL of 50mM TEAB and digested with trypsin overnight at 37 °C.

TMT-labeling and sample clean up: Tryptic digested peptides from brain samples were labeled with tandem mass tag (TMT) 10-plex reagents (Thermo Fisher) and were analyzed at the same time. Labelling of tryptic peptides was carried out according to manufacturer's instructions. Briefly, the TMT reagents (0.8 mg) were dissolved in 41 μL of anhydrous acetonitrile. Aliquots of samples were incubated with TMT reagents for 1 hour at room temperature. The reactions were quenched by 8μL of 5% hydroxylamine solution and reacted for 15 min. In TMT 10-plex labeling, set 1 (old age CPS) and set 2 (lifelong CPS) were sequentially labeled by Reagent 126, 127N, 127C, 128N, 128C,129N, 129C, 130N, 130C and 131, respectively. The combined TMT labelled samples were dried under SpeedVac, and then reconstituted by dilute trifluoroacetic acid solution followed by desalting by Oasis HLB 96-well μElutionplate (Waters) prior to LC-MS/MS analysis.

LC-MS/MS analysis: LC MS/MS was performed on a Q Exactive Orbitrap Mass Spectrometer (Thermo Fisher Scientific) coupled with a Dionex ultimate 3000 HPLC system equipped with a nano-ES ion source. The TMT labelled peptides were separated on

a C18 reverse-phase capillary column (PepMap, 75µm x150mm, Thermo Fisher) with linear gradients of 2–35% acetonitrile in 0.1% formic acid, at a constant flow rate of 300 nL/min for 220 min. The instrument was operated in the positive-ion mode with the ESI spray voltage set at 1.8 kV. A full scan MS spectra (300–1800 m/z) was acquired in the Orbitrap at a mass resolution of 70,000 with an automatic gain control target (AGC) of 3e6. Fifteen peptide ions showing the most intense signal from each scan were selected for higher energy collision-induced dissociation (HCD)-MS/MS analysis (normalized collision energy 32) in the Orbitrap at a mass resolution of 35,000 and AGC value of 1e5. Maximal filling times were 100 ms in full scans and 120 ms (HCD) for the MS/MS scans. Ions with unassigned charge states and singly charged species were rejected. The dynamic exclusion was set to 50 s and a relative mass window of 10 ppm. The data were acquired using ThermoXcalibur 3.0.

Proteomic data analysis and comparison with molecular signature of mild cognitive impairment and Alzheimer`s disease: Raw data were processed using Proteome Discoverer (Version 2.1, Thermo Fisher Scientific) and protein identities were searched against the *Mus musculus* Universal Protein Resource sequence database (UniProt, August, 2013). By excluding proteins with missing rate smaller than 20%, protein abundance profiles for 2,970 proteins were obtained to perform the following analysis. The missing values were imputed by using the k- nearest neighbor (KNN) approach (Troyanskaya *et al.*, 2001). Protein expression abundance was then log2 transformed and normalized by the non-parametric quantile normalization method. Significance of the difference between subordinate samples and dominant samples was calculated using an empirical Bayes method from the R package (Ritchie *et al.*, 2015). To visualize the DEPs in heatmaps, *z*-scores were calculated for each protein. Specifically, mean expression level was subtracted from the protein expression levels of the same protein, and then the values were divided by the standard deviation. P-values of Gene Ontology enrichment analysis on the biological process ontology were calculated using the Fisher's Exact test, then were adjusted by the BH procedure for correcting the multiple testing problem. The MCI versus LPCs and AD versus LPCs signatures were obtained from a proteomic study of human frontal cortical samples (Bai *et al.*, 2020). Only the top 3,000 most changed proteins were used. Samples were characterized as LPC, MCI and AD as described above. The Venn diagram of

overlapping among gene sets was visualized using the R package VennDiagram (Chen & Boutros, 2011). To compare the DEPs to the AD progression-related gene signatures, the protein accession numbers were mapped to gene symbols. A hypergeometric distribution test was used to calculate the significance of enrichment between the DEPs and Alzheimer's disease signature (Wang *et al.*, 2016). P-values were corrected by the Benjamini-Hochberg (BH) procedure (Benjamini & Hochberg, 1995).

Western Blot: Protein was extracted from frontal and temporal cortex in RIPA buffer (50 mm Tris-HCl, 150 mm NaCl, 1 mm EDTA, 0.5% Triton X-100, 1% sodium deoxycholate, 0.3% SDS, 0.1 mm PMSF, 0.2 mm 1,10-phenoanthroline monohydrate, Phosphatase Inhibitor Cocktail A (Sigma-Aldrich), Protease Inhibitor Cocktail (Sigma-Aldrich), and Phosphatase Inhibitor Cocktail 2 (Sigma-Aldrich) by drawing up and expulsing tissue through 1 ml Monoject syringes (Covidien) first without and then with 20G BD PrecisionGlide needles. Homogenates were nutated for 1 h at 4°C, then centrifuged at 13,000 rpm for 90 min at 4°C, and the supernatant was collected.

Protein concentration for each sample was determined with the Pierce BCA Protein Assay Kit (Thermo Fisher Scientific). Equal amounts of protein for each sample were loaded and separated using SDS-PAGE on 10.5-14% Criterion pre-cast Tris-HCl gels (Bio-Rad). Protein was transferred to nitrocellulose membranes (Bio-Rad), which were blocked with 5% BSA (Sigma-Aldrich) in 1× TBST buffer (10 mm Tris-Base (Sigma-Aldrich), 0.2 m NaCl (Macron Chemicals), 0.1% Tween-20 (Sigma-Aldrich), pH 7.4. Proteins were probed overnight with GAPDH (14C10, Cell Signaling Technology, 1:1000), β-III tubulin (79-720, ProSci, 1:10,000), Tau5 (AHB0042, Thermo Fisher Scientific, 1:30,000) PHF1 (pSer396/404, Peter Davies, 1:1500), AT8 (MN2010, Thermo Fisher, 1:1000) antibodies. Membranes were then incubated with IRDye-linked goat anti-mouse 800CW and goat anti-rabbit 680LT secondary antibodies (LI-COR Biosciences, 1:100,000) and reactivity was imaged using a LiCor imaging system (LI-COR Biosciences). Immunoreactivity was quantified by densitometry using OptiQuant version 3.0 software.

Immunohistochemistry: Immunohistochemistry was conducted in collaboration with the University of Minnesota Histology & Research Laboratory. Hemi-brains were embedded in paraffin and 10um brain sections were cut. The slides were deparaffinized and antigen

retrieval was performed by heating slides to 100˚ C in 6.0pH sodium citrate for 15 minutes. Nonspecific labeling was blocked with Rodent Block M (RMB961, Biocare Medical) in 5% nonfat dry milk. Sections were then probed with antibodies for 4G8 (Biolegend 9220-10), or phosphorylated-tau AT8 (Invitrogen MN1020). They were then labeled with biotinylated secondary antibodies (PK-4002 Vector Labs) and finally the chromogen DAB (SK-4100 Vector Labs) before being counterstained with hematoxylin.

Data Availability

The mouse proteomics data used in this study are available at https://www.synapse.org/#!Synapse:syn25487114/files/ . Human proteomic data from the Banner-Sun study is available via the AD Knowledge Portal (https://adknowledgeportal.synapse.org). The gene expression data from the Mount Sinai cohort can be found at (https://www.synapse.org/#!Synapse:syn3157699).

CHAPTER 6

CONCLUSIONS AND FUTURE DIRECTIONS

6.1 Summary of Findings

The central hypothesis of this dissertation was that chronic stress promotes cellular senescence and that in turn, stress-induced senescent cells (SNCs) could impact healthspan. Chronic stress is associated with shorter lifespan, and is a risk factor for a diverse range of aging-related diseases. Colloquially it has long been believed that intense stress accelerates aging. However, this relationship has remained poorly characterized, hampered in part by variability of stressors and stress responses themselves. This dissertation presented several studies interrogating the biological processes by which chronic stress may affect aging and disease risk, and probing the relevance of stressor type to these effects.

Chapter 2 provides the most rigorous evidence to date linking chronic stress with an increase in senescent cells. We found that 4-week exposure to one of two stress paradigms — CSS or restraint stress — is sufficient to increase expression of senescence markers in select organs. However, the exact gene expression profiles and organs affected were highly dependent on the stress paradigm. CSS-exposed mice manifested increased *p16* expression in PBMCs, scWAT, cortex and hippocampus, along with elevated *p21*, and SASP factors in the hippocampus. In contrast, restraint exposed male mice showed only elevated *p21* and *IL-1β* in the cortex and hippocampus.

Both stress paradigms exerted their greatest effect on senescence/SASP-related gene expression in the brain. We determined that the majority of cells in the brain induced to senesce by CSS were neurons and astrocytes. Although neurons are postmitotic cells, evidence suggests that they can take on a senescence-like phenotype under conditions that induce DNA damage. This process is implicated in neurodegenerative disease and suggests an avenue by which chronic stress can increase risk for these conditions. Spatial transcriptomic profiling of the brains of CSS-exposed mice implicated the DNA Damage

Response and elevated Ras/Raf signaling as mediators of CSS-induced senescence. CSS-induced SNCs also alter their local microenvironment via pathways including interleukin signaling, growth factor signaling, and changes to the extracellular matrix. In particular, they independently confirm IL-1β as a key feature of CSS-induced SNCs in the brain. In the hippocampus, SNCs were also associated with elevated glutamatergic neurotransmission.

However, a pharmacogenetic strategy to eliminate senescent cells was either neutral (in the short term) or detrimental to healthspan and lifespan (in the long term). While SNC clearance appears the likely cause of this negative effect – although paradoxical based on the present literature on the beneficial effects of SNC clearance - the present experimental approach does not rule out off-target effects of the pharmacological tool employed, ganciclovir (GCV)

Chapter 4 demonstrated differential effects of CSS and restraint stress in a mouse model of tauopathy – the PS19. Although CSS induced selective mild impairments in spatial learning, it did not affect any measures of memory or neuropathology assessed. In fact, CSS reduced abundance of the phosphorylated tau epitope AT8, and transcript levels of both transgenic human tau, and endogenous mouse tau. As a whole, these results suggest that CSS may affect neurodegenerative diseases such as Alzheimer's disease independently from enhancing tau pathology per se, further adding to both clinical and preclinical evidence illustrating the complexity of this etiopathology.

Chapter 5 follows up on the findings from Chapter 4 and presents an unbiased analysis of the proteomic changes shared by mice exposed to lifelong CSS and AD patients. This work replicates the lack-of-effect of CSS on tau pathology, while demonstrating that most of the overlapping proteins were functionally associated with enhanced NMDA receptor mediated glutamatergic signaling, an excitotoxicity mechanism known to affect neurodegeneration. These data are of great interest in light of the results in Chapter 2 in which high abundance of *p16*+ cells were associated with increased local glutamatergic signaling. These findings support the association between stress and AD progression and provide valuable insight into potential early biomarkers and protein mediators of this

relationship. The results of these studies provide novel insight into the mechanisms by which stress may affect aging and risk for neurodegenerative disease.

In sum, the major findings of this thesis are that 1) chronic stress can promote accumulation of SNCs 2) CSS-induced SNCs in the brain is p16-dependent and is associated with elevated DNA damage, Ras/Raf signaling, interleukin signaling and glutamatergic neurotransmission 3) enhanced glutamatergic signaling is a shared feature between mice exposed to lifelong CSS and human patients with AD 4) the type of stressor (social vs nonsocial) has a significant influence on the senescence and neurodegenerative phenotypes provoked.

6.2 Future Directions

Future experiments should follow up on our finding that pharmacogenetic SNC elimination (via GCV) is detrimental to healthspan and lifespan using either alternative genetic models for SNC clearance or senolytics. GCV has known hemotoxicity, and reported hepatotoxicity and neurotoxicity, so the effects on frailty and lifespan may be independent of SNCs. Alternate SNC-removal strategies will be necessary to determine whether long-term SNC elimination is harmful in the context of chronic stress. This will be vital to understanding the functional relevance of stress-induced senescence.

The mechanisms implicated in CSS-induced senescence should be further interrogated. In particular, independent confirmation of DNA damage should be performed, as should measurements of factors known to induce DNA damage, such as reactive oxygen species. Moreover, the spatial transcriptomic profiling of CSS-induced SNCs and their microenvironment produced an extremely rich dataset that can and should be interrogated further leading to testable predictions.

Future efforts should also determine whether the elevated glutamatergic signaling suggested independently in chapters 1 and 5 are related. Do CSS-induced SNCs mediate the enhancement of glutamatergic signaling observed at the protein level? In humans are SNCs associated with increase glutamatergic neurotransmission? And is this true in Alzheimer's disease?

Finally, we have independently replicated the finding that CSS can reduce the AT8 phosphorylated tau epitope, both in transgenic (PS19; Chapter 4) and wildtype (Chapter 5)

mice. These findings are at odds with studies using nonsocial stress models in wildtype rodents that consistently find increases in tau phosphorylation. This divergence could prove an interesting lens through which to evaluate the differences in stressor types.

Each question answered in this dissertation has revealed exponentially more areas to investigate. Ultimately, the direction of future research should be guided by the principle of positively advancing human health.

REFERENCES

AbdAlla, S., el Hakim, A., Abdelbaset, A., Elfaramawy, Y., & Quitterer, U. (2015) Inhibition of ACE Retards Tau Hyperphosphorylation and Signs of Neuronal Degeneration in Aged Rats Subjected to Chronic Mild Stress. *Biomed Res. Int.*, **2015**, 1–10.

Adachi, S., Kawamura, K., & Takemoto, K. (1993) Oxidative Damage of Nuclear DNA in Liver of Rats Exposed to Psychological Stress. *Cancer Res.*, **53**, 4153–4155.

Adams, J., Martin-Ruiz, C., Pearce, M.S., White, M., Parker, L., & Von Zglinicki, T. (2007) No association between socio-economic status and white blood cell telomere length. *Aging Cell*, **6**, 125–128.

Adams, P.D. (2007) Remodeling of chromatin structure in senescent cells and its potential impact on tumor suppression and aging. *Gene*, **397**, 84–93.

Adler, N.E., Boyce, T., Chesney, M.A., Cohen, S., Folkman, S., Kahn, R.L., & Syme, S.L. (1994) Socioeconomic Status and Health: The Challenge of the Gradient. *Am. Psychol.*, **49**, 15–24.

Admon, R., Leykin, D., Lubin, G., Engert, V., Andrews, J., Pruessner, J., & Hendler, T. (2013) Stress-induced reduction in hippocampal volume and connectivity with the ventromedial prefrontal cortex are related to maladaptive responses to stressful military service. *Hum. Brain Mapp.*, **34**, 2808–2816.

Albanese, C., Johnson, J., Watanabe, G., Eklund, N., Vu, D., Arnold, A., & Pestell, R.G. (1995) Transforming p21(ras) mutants and c-Ets-2 activate the cyclin D1 promoter through distinguishable regions. *J. Biol. Chem.*, **270**, 23589–23597.

Alfarez, D.N., Karst, H., Velzing, E.H., Joëls, M., & Krugers, H.J. (2008) Opposite effects of glucocorticoid receptor activation on hippocampal CA1 dendritic complexity in chronically stressed and handled animals. *Hippocampus*, **18**, 20–28.

Alzheimer's, A. (2014) 2014 Alzheimer's disease facts and figures. *Alzheimer's Dement. J. Alzheimer's Assoc.*, **10**, e47–e92.

American Pyschological Association (2021) Stress and decision-making during the pandemic [WWW Document]. *Stress Am. TM 2021*,. URL https://www.apa.org/news/press/releases/stress/2021/october-decision-making

Apple, D.M., Solano-Fonseca, R., & Kokovay, E. (2017) Neurogenesis in the aging brain. *Biochem. Pharmacol.*, **141**, 77–85.

Araki, Y., Hong, I., Gamache, T.R., Ju, S., Collado-Torres, L., Shin, J.H., & Huganir, R.L. (2020) Syngap isoforms differentially regulate synaptic plasticity and dendritic development. *Elife*, **9**, 1–28.

Archie, E.A., Tung, J., Clark, M., Altmann, J., & Alberts, S.C. (2014) Social affiliation matters: both same-sex and opposite-sex relationships predict survival in wild female baboons. *Proceedings. Biol. Sci.*, **281**.

Arellano, J.I., Espinosa, A., Fairén, A., Yuste, R., & DeFelipe, J. (2007) Non-synaptic dendritic spines in neocortex. *Neuroscience*, **145**, 464–469.

Arndt, M., Kunert, H.J., Saß, H., & Norra, C. (2004) Kognitive störungen nach aksidenteller hoch dosierter kortisontherapie. *Nervenarzt*, **75**, 904–907.

Arriagada, P. V, Growdon, J.H., Hedley-Whyte, E.T., & Hyman, B.T. (1992) Neurofibrillary tangles but not senile plaques parallel duration and severity of Alzheimer's disease. *Neurology*, **42**, 631–639.

Aschbacher, K., O'Donovan, A., Wolkowitz, O.M., Dhabhar, F.S., Su, Y., & Epel, E. (2013) Good stress, bad stress and oxidative stress: insights from anticipatory cortisol reactivity. *Psychoneuroendocrinology*, **38**, 1698–1708.

Atanackovic, D., Schulze, J., Kröger, H., Brunner-Weinzierl, M.C., & Deter, H.C. (2003) Acute psychological stress induces a prolonged suppression of the production of reactive oxygen species by phagocytes. *J. Neuroimmunol.*, **142**, 159–165.

Bagchi, M., Milnes, M., Williams, C., Balmoori, J., Xumei, Y., Stohs, S., & Bagchi, D. (1999) Acute and chronic stress-induced oxidative gastrointestinal injury in rats, and the protective ability of a novel grape seed proanthocyanidin extract. *Nutr. Res.*, **19**, 1189–1199.

Baglietto-Vargas, D., Chen, Y., Suh, D., Ager, R.R., Rodriguez-Ortiz, C.J., Medeiros, R., Myczek, K., Green, K.N., Baram, T.Z., & LaFerla, F.M. (2015) Short-term modern life-like stress exacerbates Aβ-pathology and synapse loss in 3xTg-AD mice. *J. Neurochem.*, **134**, 915–926.

Bai, B., Tan, H., Pagala, V.R., High, A.A., Ichhaporia, V.P., Hendershot, L., & Peng, J. (2017) Deep Profiling of Proteome and Phosphoproteome by Isobaric Labeling, Extensive Liquid Chromatography, and Mass Spectrometry. In *Methods in Enzymology*. Academic Press Inc., pp. 377–395.

Bai, B., Wang, X., Li, Y., Chen, P.C., Yu, K., Dey, K.K., Yarbro, J.M., Han, X., Lutz, B.M., Rao, S., Jiao, Y., Sifford, J.M., Han, J., Wang, M., Tan, H., Shaw, T.I., Cho, J.H., Zhou, S., Wang, H., Niu, M., Mancieri, A., Messler, K.A., Sun, X., Wu, Z., Pagala, V., High, A.A., Bi, W., Zhang, H., Chi, H., Haroutunian, V., Zhang, B., Beach, T.G., Yu, G., & Peng, J. (2020) Deep Multilayer Brain Proteomics Identifies Molecular Networks in Alzheimer's Disease Progression. *Neuron*, **105**, 975-991.e7.

Baker, D.J., Childs, B.G., Durik, M., Wijers, M.E., Sieben, C.J., Zhong, J., A. Saltness, R., Jeganathan, K.B., Verzosa, G.C., Pezeshki, A., Khazaie, K., Miller, J.D., & Van Deursen, J.M. (2016) Naturally occurring p16 Ink4a-positive cells shorten healthy lifespan. *Nature*, **530**, 184–189.

Baker, D.J., Wijshake, T., Tchkonia, T., LeBrasseur, N.K., Childs, B.G., van de Sluis, B., Kirkland, J.L., & van Deursen, J.M. (2011) Clearance of p16Ink4a-positive senescent cells delays ageing-associated disorders. *Nature*, **479**, 232–236.

Barnes, C.A. (1979) Memory deficits associated with senescence: A neurophysiological and behavioral study in the rat. *J. Comp. Physiol. Psychol.*, **93**, 74–104.

Bartolomucci, A. (2007) Social stress, immune functions and disease in rodents. *Front. Neuroendocrinol.*, **28**, 28–49.

Bartolomucci, A., Cabassi, A., Govoni, P., Ceresini, G., Cero, C., Berra, D., Dadomo, H., Franceschini, P., Dell'Omo, G., Parmigiani, S., & Palanza, P. (2009a) Metabolic Consequences and Vulnerability to Diet-Induced Obesity in Male Mice under Chronic Social Stress. *PLoS One*, **4**, e4331.

Bartolomucci, A., Cabassi, A., Govoni, P., Ceresini, G., Cero, C., Berra, D., Dadomo, H., Franceschini, P., Dell'Omo, G., Parmigiani, S., & Palanza, P. (2009b) Metabolic Consequences and Vulnerability to Diet-Induced Obesity in Male Mice under Chronic Social Stress. *PLoS One*, **4**, e4331.

Bartolomucci, A., Carola, V., Pascucci, T., Puglisi-Allegra, S., Cabib, S., Lesch, K.P., Parmigiani, S., Palanza, P., & Gross, C. (2010) Increased vulnerability to psychosocial stress in heterozygous serotonin transporter knockout mice. *DMM Dis.*

Model. Mech., **3**, 459–470.
Bartolomucci, A., De Biurrun, G., Cz?h, B., Van Kampen, M., & Fuchs, E. (2002) Selective enhancement of spatial learning under chronic psychosocial stress. *Eur. J. Neurosci.*, **15**.
Bartolomucci, A., De Biurrun, G., Czéh, B., Van Kampen, M., & Fuchs, E. (2002) Selective enhancement of spatial learning under chronic psychosocial stress. *Eur. J. Neurosci.*, **15**, 1863–1866.
Beach, T.G., Adler, C.H., Sue, L.I., Serrano, G., Shill, H.A., Walker, D.G., Lue, L., Roher, A.E., Dugger, B.N., Maarouf, C., Birdsill, A.C., Intorcia, A., Saxon-Labelle, M., Pullen, J., Scroggins, A., Filon, J., Scott, S., Hoffman, B., Garcia, A., Caviness, J.N., Hentz, J.G., Driver-Dunckley, E., Jacobson, S.A., Davis, K.J., Belden, C.M., Long, K.E., Malek-Ahmadi, M., Powell, J.J., Gale, L.D., Nicholson, L.R., Caselli, R.J., Woodruff, B.K., Rapscak, S.Z., Ahern, G.L., Shi, J., Burke, A.D., Reiman, E.M., & Sabbagh, M.N. (2015) Arizona Study of Aging and Neurodegenerative Disorders and Brain and Body Donation Program. *Neuropathology*, **35**, 354–389.
Benice, T.S., Rizk, A., Kohama, S., Pfankuch, T., & Raber, J. (2006) Sex-differences in age-related cognitive decline in C57BL/6J mice associated with increased brain microtubule-associated protein 2 and synaptophysin immunoreactivity. *Neuroscience*, **137**, 413–423.
Benjamini, Y. & Hochberg, Y. (1995) Controlling the False Discovery Rate: A Practical and Powerful Approach to Multiple Testing. *J. R. Stat. Soc. Ser. B*, **57**, 289–300.
Berger, J.M., Singh, P., Khrimian, L., Morgan, D.A., Chowdhury, S., Arteaga-Solis, E., Horvath, T.L., Domingos, A.I., Marsland, A.L., Kumar Yadav, V., Rahmouni, K., Gao, X.-B., & Karsenty, G. (2019) Mediation of the Acute Stress Response by the Skeleton. *Cell Metab.*,.
Bernini, G. & Tricò, D. (2016) Cushing's Syndrome and Steroid Dementia. *Recent Pat. Endocr. Metab. Immune Drug Discov.*, **10**, 50–55.
Bertram, L. & Tanzi, R.E. (2004) Alzheimer's disease: one disorder, too many genes? *Hum. Mol. Genet.*, **13**, 135R – 141.
Bhaskar, K., Maphis, N., Xu, G., Varvel, N.H., Kokiko-Cochran, O.N., Weick, J.P., Staugaitis, S.M., Cardona, A., Ransohoff, R.M., Herrup, K., & Lamb, B.T. (2014) Microglial derived tumor necrosis factor-α drives Alzheimer's disease-related neuronal cell cycle events. *Neurobiol. Dis.*, **62**, 273–285.
Bian, Y., Pan, Z., Hou, Z., Huang, C., Li, W., & Zhao, B. (2012) Learning, memory, and glial cell changes following recovery from chronic unpredictable stress. *Brain Res. Bull.*, **88**, 471–476.
Bierhaus, A., Wolf, J., Andrassy, M., Rohleder, N., Humpert, P.M., Petrov, D., Ferstl, R., Von Eynatten, M., Wendt, T., Rudofsky, G., Joswig, M., Morcos, M., Schwaninger, M., McEwen, B., Kirschbaum, C., & Nawroth, P.P. (2003) A mechanism converting psychosocial stress into mononuclear cell activation. *Proc. Natl. Acad. Sci. U. S. A.*, **100**, 1920.
Bilgel, M., Wong, D.F., Moghekar, A.R., Ferrucci, L., Resnick, S.M., & Alzheimer's Disease Neuroimaging Initiative (2021) Tau pathology mediates the effects of amyloid on neocortical tau propagation and neurodegeneration among individuals without dementia. *medRxiv*, 2021.07.01.21259866.
Blasco, M.A. (2005) Telomeres and human disease: ageing, cancer and beyond. *Nat. Rev.*

Genet., **6**, 611–622.
Bonanni, L., Franciotti, R., Martinotti, G., Vellante, F., Flacco, M.E., Di Giannantonio, M., Thomas, A., & Onofrj, M. (2018) Post Traumatic Stress Disorder Heralding the Onset of Semantic Frontotemporal Dementia. *J. Alzheimers. Dis.*, **63**, 203–215.
Boonstra, J. & Post, J.A. (2004) Molecular events associated with reactive oxygen species and cell cycle progression in mammalian cells. *Gene*, **337**, 1–13.
Braak, H., Alafuzoff, I., Arzberger, T., Kretzschmar, H., & Del Tredici, K. (2006) Staging of Alzheimer disease-associated neurofibrillary pathology using paraffin sections and immunocytochemistry. *Acta Neuropathol.*, **112**, 389–404.
Braak, H. & Braak, E. (1991) Neuropathological stageing of Alzheimer-related changes. *Acta Neuropathol.*, **82**, 239–259.
Branca, C., Wisely, E. V., Hartman, L.K., Caccamo, A., & Oddo, S. (2014) Administration of a selective β2 adrenergic receptor antagonist exacerbates neuropathology and cognitive deficits in a mouse model of Alzheimer's disease. *Neurobiol. Aging*, **35**, 2726–2735.
Briones, A., Gagno, S., Martisova, E., Dobarro, M., Aisa, B., Solas, M., Tordera, R., & Ramírez, M. (2012) Stress-induced anhedonia is associated with an increase in Alzheimer's disease-related markers. *Br. J. Pharmacol.*, **165**, 897–907.
Burd, C.E., Sorrentino, J.A., Clark, K.S., Darr, D.B., Krishnamurthy, J., Deal, A.M., Bardeesy, N., Castrillon, D.H., Beach, D.H., & Sharpless, N.E. (2013) Monitoring tumorigenesis and senescence in vivo with a p16 INK4a-luciferase model. *Cell*, **152**, 340–351.
Bussian, T.J., Aziz, A., Meyer, C.F., Swenson, B.L., van Deursen, J.M., & Baker, D.J. (2018) Clearance of senescent glial cells prevents tau-dependent pathology and cognitive decline. *Nature*, **562**, 578–582.
Cacace, R., Sleegers, K., & Van Broeckhoven, C. (2016) Molecular genetics of early-onset Alzheimer's disease revisited. *Alzheimer's Dement.*, **12**, 733–748.
Calcia, M.A., Bonsall, D.R., Bloomfield, P.S., Selvaraj, S., Barichello, T., & Howes, O.D. (2016) Stress and neuroinflammation: A systematic review of the effects of stress on microglia and the implications for mental illness. *Psychopharmacology (Berl).*,.
Campisi, J. & d'Adda di Fagagna, F. (2007) Cellular senescence: when bad things happen to good cells. *Nat. Rev. Mol. Cell Biol.*, **8**, 729–740.
Cannon, W.B. (1915) *Bodily Changes in Pain, Hunger, Fear and Rage: An Account of Recent Researches into the Function of Emotional Excitement.* D Appleton & Company, New York.
Carrero, I., Gonzalo, M.R., Martin, B., Sanz-Anquela, J.M., Arévalo-Serrano, J., & Gonzalo-Ruiz, A. (2012) Oligomers of beta-amyloid protein (Aβ1-42) induce the activation of cyclooxygenase-2 in astrocytes via an interaction with interleukin-1beta, tumour necrosis factor-alpha, and a nuclear factor kappa-B mechanism in the rat brain. *Exp. Neurol.*, **236**, 215–227.
Carroll, J.C., Iba, M., Bangasser, D.A., Valentino, R.J., James, M.J., Brunden, K.R., Lee, V.M.-Y., & Trojanowski, J.Q. (2011) Chronic stress exacerbates tau pathology, neurodegeneration, and cognitive performance through a corticotropin-releasing factor receptor-dependent mechanism in a transgenic mouse model of tauopathy. *J. Neurosci.*, **31**, 14436–14449.
Cerqueira, J.J., Mailliet, F., Almeida, O.F.X., Jay, T.M., & Sousa, N. (2007) The prefrontal

cortex as a key target of the maladaptive response to stress. *J. Neurosci.*, **27**, 2781–2787.

Cha, H., Farina, M.P., & Hayward, M.D. (2021) Socioeconomic status across the life course and dementia-status life expectancy among older Americans. *SSM - Popul. Heal.*, **15**, 2352–8273.

Chakrabarty, P., Jansen-West, K., Beccard, A., Ceballos-Diaz, C., Levites, Y., Verbeeck, C., Zubair, A.C., Dickson, D., Golde, T.E., & Das, P. (2010) Massive gliosis induced by interleukin-6 suppresses Aβ deposition in vivo : evidence against inflammation as a driving force for amyloid deposition . *FASEB J.*, **24**, 548–559.

Chang, F., Steelman, L.S., Lee, J.T., Shelton, J.G., Navolanic, P.M., Blalock, W.L., Franklin, R.A., & McCubrey, J.A. (2003) Signal transduction mediated by the Ras/Raf/MEK/ERK pathway from cytokine receptors to transcription factors: Potential targeting for therapeutic intervention. *Leukemia*, **17**, 1263–1293.

Charmandari, E., Tsigos, C., & Chrousos, G. (2005) Endocrinology of the stress response. *Annu. Rev. Physiol.*, **67**, 259–284.

Chen, H. & Boutros, P.C. (2011) VennDiagram: A package for the generation of highly-customizable Venn and Euler diagrams in R. *BMC Bioinformatics*, **12**.

Chen, Q. & Ames, B.N. (1994) Senescence-like growth arrest induced by hydrogen peroxide in human diploid fibroblast F65 cells. *Proc. Natl. Acad. Sci. U. S. A.*, **91**, 4130–4134.

Chen, Q.M., Liu, J., & Merrett, J.B. (2000) Apoptosis or senescence-like growth arrest: influence of cell-cycle position, p53, p21 and bax in H2O2 response of normal human fibroblasts. *Biochem. J.*, **347**, 543–551.

Chen, Y., Dubé, C.M., Rice, C.J., & Baram, T.Z. (2008) Rapid Loss of Dendritic Spines after Stress Involves Derangement of Spine Dynamics by Corticotropin-Releasing Hormone. *J. Neurosci.*, **28**, 2903–2911.

Chen, Y., Peng, Y., Che, P., Gannon, M., Liu, Y., Li, L., Bu, G., van Groen, T., Jiao, K., & Wang, Q. (2014) alpha(2A) adrenergic receptor promotes amyloidogenesis through disrupting APP-SorLA interaction. *Proc. Natl. Acad. Sci. U. S. A.*, **111**, 17296–17301.

Chen, Y., Rex, C.S., Rice, C.J., Dubé, C.M., Gall, C.M., Lynch, G., & Baram, T.Z. (2010) Correlated memory defects and hippocampal dendritic spine loss after acute stress involve corticotropin-releasing hormone signaling. *Proc. Natl. Acad. Sci. U. S. A.*, **107**, 13123–13128.

Cherkas, L.F., Aviv, A., Valdes, A.M., Hunkin, J.L., Gardner, J.P., Surdulescu, G.L., Kimura, M., & Spector, T.D. (2006) The effects of social status on biological aging as measured by white-blood-cell telomere length. *Aging Cell*, **5**, 361–365.

Childs, B.G., Baker, D.J., Kirkland, J.L., Campisi, J., & van Deursen, J.M. (2014) Senescence and apoptosis: dueling or complementary cell fates? *EMBO Rep.*, **15**, 1139–1153.

Childs, B.G., Baker, D.J., Wijshake, T., Conover, C.A., Campisi, J., & van Deursen, J.M. (2016) Senescent intimal foam cells are deleterious at all stages of atherosclerosis. *Science*, **354**, 472–477.

Cho, K., Jang, Y.J., Lee, S.J., Jeon, Y.N., Shim, Y.L., Lee, J.Y., Lim, D.S., Kim, D.H., & Yoon, S.Y. (2020) TLQP-21 mediated activation of microglial BV2 cells promotes clearance of extracellular fibril amyloid-β. *Biochem. Biophys. Res. Commun.*, **524**, 764–771.

Cho, K.A., Sung, J.R., Yoon, S.O., Ji, H.P., Jung, W.L., Kim, H.P., Kyung, T.K., Ik, S.J., & Sang, C.P. (2004) Morphological Adjustment of Senescent Cells by Modulating Caveolin-1 Status *. *J. Biol. Chem.*, **279**, 42270–42278.

Choi, D.W. (1988) Glutamate neurotoxicity and diseases of the nervous system. *Neuron,*.

Chong, Y. (1997) Effect of a carboxy-terminal fragment of the Alzheimer's amyloid precursor protein on expression of proinflammatory cytokines in rat glial cells. *Life Sci.*, **61**, 2323–2333.

Cohen, S., Doyle, W.J., & Baum, A. (2006) Socioeconomic status is associated with stress hormones. *Psychosom. Med.*, **68**, 414–420.

Colaianna, M., Schiavone, S., Zotti, M., Tucci, P., Morgese, M.G., Bäckdahl, L., Holmdahl, R., Krause, K.H., Cuomo, V., & Trabace, L. (2013) Neuroendocrine Profile in a Rat Model of Psychosocial Stress: Relation to Oxidative Stress. *Antioxid. Redox Signal.*, **18**, 1385.

Coppé, J.-P., Desprez, P.-Y., Krtolica, A., & Campisi, J. (2010) The senescence-associated secretory phenotype: the dark side of tumor suppression. *Annu. Rev. Pathol.*, **5**, 99–118.

Coppé, J.P., Rodier, F., Patil, C.K., Freund, A., Desprez, P.Y., & Campisi, J. (2011) Tumor suppressor and aging biomarker p16 INK4a induces cellular senescence without the associated inflammatory secretory phenotype. *J. Biol. Chem.*, **286**, 36396–36403.

Cribbs, D.H., Berchtold, N.C., Perreau, V., Coleman, P.D., Rogers, J., Tenner, A.J., & Cotman, C.W. (2012) Extensive innate immune gene activation accompanies brain aging, increasing vulnerability to cognitive decline and neurodegeneration: A microarray study. *J. Neuroinflammation*, **9**, 179.

Crotti, A. & Glass, C.K. (2015) The choreography of neuroinflammation in Huntington's disease. *Trends Immunol.,*.

Crowe, M., Andel, R., Pedersen, N.L., & Gatz, M. (2007) Do Work-related Stress and Reactivity to Stress Predict Dementia More Than 30 Years Later? *Alzheimer Dis. Assoc. Disord.*, **21**, 205–209.

Csernansky, J.G., Dong, H., Fagan, A.M., Wang, L., Xiong, C., Holtzman, D.M., & Morris, J.C. (2006) Plasma Cortisol and Progression of Dementia in Subjects With Alzheimer-Type Dementia. *Am. J. Psychiatry*, **163**, 2164–2169.

Czeh, B., Michaelis, T., Watanabe, T., Frahm, J., de Biurrun, G., van Kampen, M., Bartolomucci, A., & Fuchs, E. (2001) Stress-induced changes in cerebral metabolites, hippocampal volume, and cell proliferation are prevented by antidepressant treatment with tianeptine. *Proc. Natl. Acad. Sci.*, **98**, 12796–12801.

D'Angelo, G., Loria, A.S., Pollock, D.M., & Pollock, J.S. (2010) Endothelin activation of reactive oxygen species mediates stress-induced pressor response in dahl salt-sensitive prehypertensive rats. *Hypertension*, **56**, 282–289.

Dadomo, H., Sanghez, V., Cristo, L. Di, Lori, A., Ceresini, G., Malinge, I., Parmigiani, S., Palanza, P., Sheardown, M., & Bartolomucci, A. (2011) Vulnerability to chronic subordination stress-induced depression-like disorders in adult 129SvEv male mice. *Prog. Neuropsychopharmacol. Biol. Psychiatry*, **35**, 1461–1471.

Damjanovic, A.K., Yang, Y., Glaser, R., Kiecolt-Glaser, J.K., Nguyen, H., Laskowski, B., Zou, Y., Beversdorf, D.Q., & Weng, N.-P. (2007) Accelerated Telomere Erosion Is Associated with a Declining Immune Function of Caregivers of Alzheimer's Disease Patients. *J. Immunol.*, **179**, 4249–4254.

Davies, C.A., Mann, D.M., Sumpter, P.Q., & Yates, P.O. (1987) A quantitative morphometric analysis of the neuronal and synaptic content of the frontal and temporal cortex in patients with Alzheimer's disease. *J. Neurol. Sci.*, **78**, 151–164.

Davis, K.L., Davis, B.M., Greenwald, B.S., Mohs, R.C., Mathé, A.A., Johns, C.A., & Horvath, T.B. (1986) Cortisol and Alzheimer's disease, I: Basal studies. *Am. J. Psychiatry*, **143**, 300–305.

De Lange, T. (2005) Shelterin: the protein complex that shapes and safeguards human telomeres. *Genes Dev.*, **19**, 2100–2110.

De Lange, T. (2009) How telomeres solve the end-protection problem. *Science*, **326**, 948–952.

Debacq-Chainiaux, F., Borlon, C., Pascal, T., Royer, V., Eliaers, F., Ninane, N., Carrard, G., Friguet, B., de Longueville, F., Boffe, S., Remacle, J., & Toussaint, O. (2005) Repeated exposure of human skin fibroblasts to UVB at subcytotoxic level triggers premature senescence through the TGF-beta1 signaling pathway. *J. Cell Sci.*, **118**, 743–758.

Del C. Alonso, A., Grundke-Iqbal, I., & Iqbal, K. (1996) Alzheimer's disease hyperphosphorylated tau sequesters normal tau into tangles of filaments and disassembles microtubules. *Nat. Med.*, **2**, 783–787.

Demaria, M., Ohtani, N., Youssef, S.A., Rodier, F., Toussaint, W., Mitchell, J.R., Laberge, R.-M., Vijg, J., Van Steeg, H., Dollé, M.E.T., Hoeijmakers, J.H.J., de Bruin, A., Hara, E., & Campisi, J. (2014) An essential role for senescent cells in optimal wound healing through secretion of PDGF-AA. *Dev. Cell*, **31**, 722–733.

Devi, L., Alldred, M.J., Ginsberg, S.D., & Ohno, M. (2010) Sex- and brain region-specific acceleration of β-amyloidogenesis following behavioral stress in a mouse model of Alzheimer's disease. *Mol. Brain*, **3**, 34.

Dhabhar, F.S., Malarkey, W.B., Neri, E., & McEwen, B.S. (2012) Stress-induced redistribution of immune cells-From barracks to boulevards to battlefields: A tale of three hormones - Curt Richter Award Winner. *Psychoneuroendocrinology*, **37**, 1345–1368.

Di Micco, R., Fumagalli, M., Cicalese, A., Piccinin, S., Gasparini, P., Luise, C., Schurra, C., Garré, M., Giovanni Nuciforo, P., Bensimon, A., Maestro, R., Giuseppe Pelicci, P., & D'Adda Di Fagagna, F. (2006) Oncogene-induced senescence is a DNA damage response triggered by DNA hyper-replication. *Nature*, **444**, 638–642.

Dimri, G.P., Lee, X., Basile, G., Acosta, M., Scott, G., Roskelley, C., Medrano, E.E., Linskens, M., Rubelj, I., Pereira-Smith, O., & al., et (1995) A biomarker that identifies senescent human cells in culture and in aging skin in vivo. *Proc. Natl. Acad. Sci. U. S. A.*, **92**, 9363–9367.

Dimsdale, J.E. (2008) Psychological stress and cardiovascular disease. *J. Am. Coll. Cardiol.*, **51**, 1237–1246.

Dobarro, M., Gerenu, G., & Ramírez, M.J. (2013) Propranolol reduces cognitive deficits, amyloid and tau pathology in Alzheimer's transgenic mice. *Int. J. Neuropsychopharmacol.*, **16**, 2245–2257.

Dobarro, M., Orejana, L., Aguirre, N., & Ramírez, M.J. (2013) Propranolol restores cognitive deficits and improves amyloid and Tau pathologies in a senescence-accelerated mouse model. *Neuropharmacology*, **64**, 137–144.

Dong, H., Goico, B., Martin, M., Csernansky, C.A., Bertchume, A., & Csernansky, J.G.

(2004) Modulation of hippocampal cell proliferation, memory, and amyloid plaque deposition in APPsw (Tg2576) mutant mice by isolation stress. *Neuroscience*, **127**, 601–609.

Doolen, S., Cook, J., Riedl, M., Kitto, K., Kohsaka, S., Honda, C.N., Fairbanks, C.A., Taylor, B.K., & Vulchanova, L. (2017) Complement 3a receptor in dorsal horn microglia mediates pronociceptive neuropeptide signaling. *Glia*, **65**, 1976–1989.

Dulić, V., Beney, G., Frebourg, G., LF, D., & Stein, G. (2000) Uncoupling between phenotypic senescence and cell cycle arrest in aging p21-deficient fibroblasts. *Mol. Cell. Biol.*, **20**, 6741–6754.

Egan, M.F., Kost, J., Tariot, P.N., Aisen, P.S., Cummings, J.L., Vellas, B., Sur, C., Mukai, Y., Voss, T., Furtek, C., Mahoney, E., Harper Mozley, L., Vandenberghe, R., Mo, Y., & Michelson, D. (2018) Randomized Trial of Verubecestat for Mild-to-Moderate Alzheimer's Disease. *N. Engl. J. Med.*, **378**, 1691–1703.

El Gaamouch, F., Audrain, M., Lin, W.J., Beckmann, N., Jiang, C., Hariharan, S., Heeger, P.S., Schadt, E.E., Gandy, S., Ehrlich, M.E., & Salton, S.R. (2020) VGF-derived peptide TLQP-21 modulates microglial function through C3aR1 signaling pathways and reduces neuropathology in 5xFAD mice. *Mol. Neurodegener.*, **15**, 1–19.

Elo, I.T. (2009) Social Class Differentials in Health and Mortality: Patterns and Explanations in Comparative Perspective. *https://doi-org.ezp3.lib.umn.edu/10.1146/annurev-soc-070308-115929*, **35**, 553–572.

Epel, E.S., Blackburn, E.H., Lin, J., Dhabhar, F.S., Adler, N.E., Morrow, J.D., & Cawthon, R.M. (2004) Accelerated telomere shortening in response to life stress. *Proc. Natl. Acad. Sci. U. S. A.*, **101**, 17312–17315.

Epel, E.S., Lin, J., Dhabhar, F.S., Wolkowitz, O.M., Puterman, E., Karan, L., & Blackburn, E.H. (2010) Dynamics of telomerase activity in response to acute psychological stress. *Brain. Behav. Immun.*, **24**, 531–539.

Erben, L., He, M.-X., Laeremans, A., Park, E., & Buonanno, A. (2017) A Novel Ultrasensitive In Situ Hybridization Approach to Detect Short Sequences and Splice Variants with Cellular Resolution. *Mol. Neurobiol. 2017 557*, **55**, 6169–6181.

Eskiocak, S., Gozen, A.S., Yapar, S.B., Tavas, F., Kilic, A.S., & Eskiocak, M. (2005) Glutathione and free sulphydryl content of seminal plasma in healthy medical students during and after exam stress. *Hum. Reprod.*, **20**, 2595–2600.

Ewald, H., Glotzbach-Schoon, E., Gerdes, A.B.M., Andreatta, M., Müller, M., Mühlberger, A., & Pauli, P. (2014) Delay and trace fear conditioning in a complex virtual learning environment-neural substrates of extinction. *Front. Hum. Neurosci.*, **8**, 323.

Felitti, V.J., Anda, R.F., Nordenberg, D., Williamson, D.F., Spitz, A.M., Edwards, V., Koss, M.P., & Marks, J.S. (1998) Relationship of childhood abuse and household dysfunction to many of the leading causes of death in adults. The Adverse Childhood Experiences (ACE) Study. *Am. J. Prev. Med.*, **14**, 245–258.

Feng, D., Wang, B., Ma, Y., Shi, W., Tao, K., Zeng, W., Cai, Q., Zhang, Z., & Qin, H. (2016) The Ras/Raf/Erk Pathway Mediates the Subarachnoid Hemorrhage-Induced Apoptosis of Hippocampal Neurons Through Phosphorylation of p53. *Mol. Neurobiol.*, **53**, 5737–5748.

Feng, Q., Cheng, B., Yang, R., Sun, F.-Y., & Zhu, C.-Q. (2005) Dynamic changes of phosphorylated tau in mouse hippocampus after cold water stress. *Neurosci. Lett.*, **388**, 13–16.

Ferrucci, L. & Fabbri, E. (2018) Inflammageing: chronic inflammation in ageing, cardiovascular disease, and frailty.

Ferrucci, L., Semba, R.D., Guralnik, J.M., Ershler, W.B., Bandinelli, S., Patel, K. V., Sun, K., Woodman, R.C., Andrews, N.C., Cotter, R.J., Ganz, T., Nemeth, E., & Longo, D.L. (2010) Proinflammatory state, hepcidin, and anemia in older persons. *Blood*, **115**, 3810–3816.

Fielder, E., Von Zglinicki, T., & Jurk, D. (2017) The DNA Damage Response in Neurons: Die by Apoptosis or Survive in a Senescence-Like State? *J. Alzheimer's Dis.*,.

Filipcik, P., Novak, P., Mravec, B., Ondicova, K., Krajciova, G., Novak, M., & Kvetnansky, R. (2012) Tau protein phosphorylation in diverse brain areas of normal and CRH deficient mice: Up-regulation by stress. *Cell. Mol. Neurobiol.*, **32**, 837–845.

Flaherty, R.L., Owen, M., Fagan-Murphy, A., Intabli, H., Healy, D., Patel, A., Allen, M.C., Patel, B.A., & Flint, M.S. (2017) Glucocorticoids induce production of reactive oxygen species/reactive nitrogen species and DNA damage through an iNOS mediated pathway in breast cancer. *Breast Cancer Res.*, **19**.

Flint, M.S., Baum, A., Chambers, W.H., & Jenkins, F.J. (2007) Induction of DNA damage, alteration of DNA repair and transcriptional activation by stress hormones. *Psychoneuroendocrinology*, **32**, 470–479.

Flint, M.S., Baum, A., Episcopo, B., Knickelbein, K.Z., Liegey Dougall, A.J., Chambers, W.H., & Jenkins, F.J. (2013) Chronic exposure to stress hormones promotes transformation and tumorigenicity of 3T3 mouse fibroblasts. *Stress*, **16**, 114–121.

Folch, J., Junyent, F., Verdaguer, E., Auladell, C., Pizarro, J.G., Beas-Zarate, C., Pallàs, M., & Camins, A. (2011) Role of Cell Cycle Re-Entry in Neurons: A Common Apoptotic Mechanism of Neuronal Cell Death. *Neurotox. Res. 2011 223*, **22**, 195–207.

Frank, M.G., Baratta, M. V., Sprunger, D.B., Watkins, L.R., & Maier, S.F. (2007) Microglia serve as a neuroimmune substrate for stress-induced potentiation of CNS pro-inflammatory cytokine responses. *Brain. Behav. Immun.*, **21**, 47–59.

Frank, M.G., Barrientos, R.M., Biedenkapp, J.C., Rudy, J.W., Watkins, L.R., & Maier, S.F. (2006) mRNA up-regulation of MHC II and pivotal pro-inflammatory genes in normal brain aging. *Neurobiol. Aging*, **27**, 717–722.

Fulop, T., Larbi, A., Dupuis, G., Page, A. Le, Frost, E.H., Cohen, A.A., Witkowski, J.M., & Franceschi, C. (2018) Immunosenescence and inflamm-aging as two sides of the same coin: Friends or Foes? *Front. Immunol.*, **8**, 1960.

Gallagher, M. & Nicolle, M.M. (1993) Animal models of normal aging: Relationship between cognitive decline and markers in hippocampal circuitry. *Behav. Brain Res.*, **57**, 155–162.

Gamache, T.R., Araki, Y., & Huganir, R.L. (2020) Twenty years of syngap research: From synapses to cognition. *J. Neurosci.*,.

Games, D., Adams, D., Alessandrini, R., Barbour, R., Borthelette, P., Blackwell, C., Carr, T., Clemens, J., Donaldson, T., Gillespie, F., Guido, T., Hagopian, S., Johnson-Wood, K., Khan, K., Lee, M., Leibowitz, P., Lieberburg, I., Little, S., Masliah, E., McConlogue, L., Montoya-Zavala, M., Mucke, L., Paganini, L., Penniman, E., Power, M., Schenk, D., Seubert, P., Snyder, B., Soriano, F., Tan, H., Vitale, J., Wadsworth, S., Wolozin, B., & Zhao, J. (1995) Alzheimer-type neuropathology in transgenic mice overexpressing V717F β-amyloid precursor protein. *Nature*, **373**, 523–527.

Gawel, K., Gibula, E., Marszalek-Grabska, M., Filarowska, J., & Kotlinska, J.H. (2019) Assessment of spatial learning and memory in the Barnes maze task in rodents—methodological consideration. *Naunyn. Schmiedebergs. Arch. Pharmacol.*, **392**, 1.

Gerritsen, L., Wang, H.X., Reynolds, C.A., Fratiglioni, L., Gatz, M., & Pedersen, N.L. (2017) Influence of Negative Life Events and Widowhood on Risk for Dementia. *Am. J. Geriatr. Psychiatry*, **25**, 766–778.

Giovanoli, S., Engler, H., Engler, A., Richetto, J., Voget, M., Willi, R., Winter, C., Riva, M.A., Mortensen, P.B., Schedlowski, M., & Meyer, U. (2013) Stress in puberty unmasks latent neuropathological consequences of prenatal immune activation in mice. *Science (80-.).*,.

Girotti, M., Pace, T.W.W., Gaylord, R.I., Rubin, B.A., Herman, J.P., & Spencer, R.L. (2006) Habituation to repeated restraint stress is associated with lack of stress-induced c-fos expression in primary sensory processing areas of the rat brain. *Neuroscience*, **138**, 1067–1081.

Goedert, M., Wischik, C.M., Crowther, R.A., Walker, J.E., & Klug, A. (1988) Cloning and sequencing of the cDNA encoding a core protein of the paired helical filament of Alzheimer disease: Identification as the microtubule-associated protein tau. *Proc. Natl. Acad. Sci. U. S. A.*, **85**, 4051–4055.

Goh, X.X., Tang, P.Y., & Tee, S.F. (2021) 8-Hydroxy-2'-Deoxyguanosine and Reactive Oxygen Species as Biomarkers of Oxidative Stress in Mental Illnesses: A Meta-Analysis. *Psychiatry Investig.*, **18**, 603–618.

Gorgoulis, V., Adams, P.D., Alimonti, A., Bennett, D.C., Bischof, O., Bishop, C., Campisi, J., Collado, M., Evangelou, K., Ferbeyre, G., Gil, J., Hara, E., Krizhanovsky, V., Jurk, D., Maier, A.B., Narita, M., Niedernhofer, L., Passos, J.F., Robbins, P.D., Schmitt, C.A., Sedivy, J., Vougas, K., von Zglinicki, T., Zhou, D., Serrano, M., & Demaria, M. (2019) Cellular Senescence: Defining a Path Forward. *Cell*,.

Gould, E., Tanapat, P., McEwen, B.S., Flugge, G., & Fuchs, E. (1998) Proliferation of granule cell precursors in the dentate gyrus of adult monkeys is diminished by stress. *Proc. Natl. Acad. Sci.*, **95**, 3168–3171.

Green, K.N., Billings, L.M., Roozendaal, B., McGaugh, J.L., & LaFerla, F.M. (2006) Glucocorticoids increase amyloid-β and tau pathology in a mouse model of Alzheimer's disease. *J. Neurosci.*, **26**, 9047–9056.

Greider, C.W. & Blackburn, E.H. (1985) Identification of a specific telomere terminal transferase activity in tetrahymena extracts. *Cell*, **43**, 405–413.

Griffin, W.S.T., Stanley, L.C., Ling, C., White, L., MacLeod, V., Perrot, L.J., White, C.L., & Araoz, C. (1989) Brain interleukin 1 and S-100 immunoreactivity are elevated in Down syndrome and Alzheimer disease. *Proc. Natl. Acad. Sci. U. S. A.*, **86**, 7611–7615.

Grosse, L., Wagner, N., Emelyanov, A., Molina, C., Lacas-Gervais, S., Wagner, K.-D., & Bulavin, D. V. (2020) Defined p16High Senescent Cell Types Are Indispensable for Mouse Healthspan. *Cell Metab.*, **32**, 87-99.e6.

Grudzien, A., Shaw, P., Weintraub, S., Bigio, E., Mash, D.C., & Mesulam, M.M. (2007) Locus coeruleus neurofibrillary degeneration in aging, mild cognitive impairment and early Alzheimer's disease. *Neurobiol. Aging*, **28**, 327–335.

Gu, H.F., Tang, C.K., & Yang, Y.Z. (2012) Psychological stress, immune response, and atherosclerosis. *Atherosclerosis*, **223**, 69–77.

Gustke, N., Steiner, B., Mandelkow, E.M., Biernat, J., Meyer, H.E., Goedert, M., & Mandelkow, E. (1992) The Alzheimer-like phosphorylation of tau protein reduces microtubule binding and involves Ser-Pro and Thr-Pro motifs. *FEBS Lett.*, **307**, 199–205.

Hajjar, I., Keown, M., & Frost, B. (2005) Antihypertensive Agents for Aging Patients Who Are at Risk for Cognitive Dysfunction.

Hanke, M.L., Powell, N.D., Stiner, L.M., Bailey, M.T., & Sheridan, J.F. (2012) Beta adrenergic blockade decreases the immunomodulatory effects of social disruption stress. *Brain. Behav. Immun.*, **26**, 1150–1159.

Hara, M.R., Kovacs, J.J., Whalen, E.J., Rajagopal, S., Strachan, R.T., Grant, W., Towers, A.J., Williams, B., Lam, C.M., Xiao, K., Shenoy, S.K., Gregory, S.G., Ahn, S., Duckett, D.R., & Lefkowitz, R.J. (2011) A stress response pathway regulates DNA damage through β2- adrenoreceptors and β-arrestin-1. *Nature*, **477**, 349–353.

Hardy, J. & Selkoe, D.J. (2002) The Amyloid Hypothesis of Alzheimer's Disease: Progress and Problems on the Road to Therapeutics. *Science (80-.).*, **297**, 353–356.

Harley, C.B., Futcher, A.B., & Greider, C.W. (1990) Telomeres shorten during ageing of human fibroblasts. *Nat. 1990 3456274*, **345**, 458–460.

Harman, D. (2009) Origin and evolution of the free radical theory of aging: a brief personal history, 1954–2009. *Biogerontology 2009 106*, **10**, 773–781.

Harris, K.M. (1999) Structure, development, and plasticity of dendritic spines. *Curr. Opin. Neurobiol.*, **9**, 343–348.

Harris, M.L., Oldmeadow, C., Hure, A., Luu, J., Loxton, D., & Attia, J. (2017) Stress increases the risk of type 2 diabetes onset in women: A 12-year longitudinal study using causal modelling. *PLoS One*, **12**.

Hayflick, L. & Moorhead, P.S. (1961) The serial cultivation of human diploid cell strains. *Exp. Cell Res.*, **25**, 585–621.

Heidt, T., Sager, H.B., Courties, G., Dutta, P., Iwamoto, Y., Zaltsman, A., Von Zur Muhlen, C., Bode, C., Fricchione, G.L., Denninger, J., Lin, C.P., Vinegoni, C., Libby, P., Swirski, F.K., Weissleder, R., & Nahrendorf, M. (2014) Chronic variable stress activates hematopoietic stem cells. *Nat. Med.*, **20**, 754–758.

Heine, V.M., Maslam, S., Joëls, M., & Lucassen, P.J. (2004) Increased P27KIP1 protein expression in the dentate gyrus of chronically stressed rats indicates G1 arrest involvement. *Neuroscience*, **129**, 593–601.

Heine, V.M., Zareno, J., Maslam, S., Joëls, M., & Lucassen, P.J. (2005) Chronic stress in the adult dentate gyrus reduces cell proliferation near the vasculature and VEGF and Flk-1 protein expression. *Eur. J. Neurosci.*, **21**, 1304–1314.

Heinzmann, J.M., Kloiber, S., Ebling-Mattos, G., Bielohuby, M., Schmidt, M. V., Palme, R., Holsboer, F., Uhr, M., Ising, M., & Touma, C. (2014) Mice selected for extremes in stress reactivity reveal key endophenotypes of major depression: A translational approach. *Psychoneuroendocrinology*, **49**, 229–243.

Hemann, M.T., Strong, M.A., Hao, L.Y., & Greider, C.W. (2001) The Shortest Telomere, Not Average Telomere Length, Is Critical for Cell Viability and Chromosome Stability. *Cell*, **107**, 67–77.

Hemmerle, A.M., Herman, J.P., & Seroogy, K.B. (2012) Stress, depression and Parkinson's disease. *Exp. Neurol.*, **233**, 79–86.

Henderson, E.R. & Blackburn, E.H. (1989) An overhanging 3' terminus is a conserved

feature of telomeres. *Mol. Cell. Biol.*, **9**, 345–348.
Heneka, M.T., Ramanathan, M., Jacobs, A.H., Dumitrescu-Ozimek, L., Bilkei-Gorzo, A., Debeir, T., Sastre, M., Galldiks, N., Zimmer, A., Hoehn, M., Heiss, W.D., Klockgether, T., & Staufenbiel, M. (2006) Locus ceruleus degeneration promotes Alzheimer pathogenesis in amyloid precursor protein 23 transgenic mice. *J. Neurosci.*, **26**, 1343–1354.
Herbet, M., Korga, A., Gawrońska-Grzywacz, M., Izdebska, M., Piątkowska-Chmiel, I., Poleszak, E., Wróbel, A., Matysiak, W., Jodłowska-Jędrych, B., & Dudka, J. (2017) Chronic Variable Stress Is Responsible for Lipid and DNA Oxidative Disorders and Activation of Oxidative Stress Response Genes in the Brain of Rats. *Oxid. Med. Cell. Longev.*, **2017**, 7313090.
Hernández, D.E., Salvadores, N.A., Moya-Alvarado, G., Cataláncatalán, R.J., Bronfman, F.C., & Court, F.A. (2018) Axonal degeneration induced by glutamate excitotoxicity is mediated by necroptosis.
Hernández, F., Cuadros, R., Ollá, I., García, C., Ferrer, I., Perry, G., & Avila, J. (2019) Differences in structure and function between human and murine tau. *Biochim. Biophys. Acta - Mol. Basis Dis.*, **1865**, 2024–2030.
Herndon, J.G., Moss, M.B., Rosene, D.L., & Killiany, R.J. (1997) Patterns of cognitive decline in aged rhesus monkeys. *Behav. Brain Res.*, **87**, 25–34.
Herrero, M.T., Estrada, C., Maatouk, L., & Vyas, S. (2015) Inflammation in Parkinson's disease: Role of glucocorticoids. *Front. Neuroanat.*,.
Hickman, S.E., Allison, E.K., & El Khoury, J. (2008) Microglial dysfunction and defective β-amyloid clearance pathways in aging alzheimer's disease mice. *J. Neurosci.*, **28**, 8354–8360.
Hoeijmakers, L., Ruigrok, S.R., Amelianchik, A., Ivan, D., van Dam, A.-M., Lucassen, P.J., & Korosi, A. (2017) Early-life stress lastingly alters the neuroinflammatory response to amyloid pathology in an Alzheimer's disease mouse model. *Brain. Behav. Immun.*, **63**, 160–175.
Hoffman, L.B., Schmeidler, J., Lesser, G.T., Beeri, M.S., Purohit, D.P., Grossman, H.T., & Haroutunian, V. (2009) Less Alzheimer disease neuropathology in medicated hypertensive than nonhypertensive persons. *Neurology*, **72**, 1720–1726.
Hong, S., Beja-Glasser, V.F., Nfonoyim, B.M., Frouin, A., Li, S., Ramakrishnan, S., Merry, K.M., Shi, Q., Rosenthal, A., Barres, B.A., Lemere, C.A., Selkoe, D.J., & Stevens, B. (2016) Complement and microglia mediate early synapse loss in Alzheimer mouse models. *Science (80-.).*, **352**, 712–716.
Honig, L.S., Kang, M.S., Schupf, N., Lee, J.H., & Mayeux, R. (2012) Association of Shorter Leukocyte Telomere Repeat Length With Dementia and Mortality. *Arch. Neurol.*, **69**, 1332.
Horn, S.R., Leve, L.D., Levitt, P., & Fisher, P.A. (2019) Childhood adversity, mental health, and oxidative stress: A pilot study. *PLoS One*, **14**.
Hovatta, I., Tennant, R.S., Helton, R., Marr, R.A., Singer, O., Redwine, J.M., Ellison, J.A., Schadt, E.E., Verma, I.M., Lockhart, D.J., & Barlow, C. (2005) Glyoxalase 1 and glutathione reductase 1 regulate anxiety in mice. *Nat. 2005 4387068*, **438**, 662–666.
Hsiao, K., Chapman, P., Nilsen, S., Eckman, C., Harigaya, Y., Younkin, S., Yang, F., & Cole, G. (1996) Correlative memory deficits, Abeta elevation, and amyloid plaques in transgenic mice. *Science*, **274**, 99–102.

Jardanhazi-Kurutz, D., Kummer, M.P., Terwel, D., Vogel, K., Dyrks, T., Thiele, A., & Heneka, M.T. (2010) Induced LC degeneration in APP/PS1 transgenic mice accelerates early cerebral amyloidosis and cognitive deficits. *Neurochem. Int.*, **57**, 375–382.

Jeon, O.H., David, N., Campisi, J., & Elisseeff, J.H. (2018) Senescent cells and osteoarthritis: a painful connection. *J. Clin. Invest.*, **128**, 1229.

Jeon, O.H., Kim, C., Laberge, R.-M., Demaria, M., Rathod, S., Vasserot, A.P., Chung, J.W., Kim, D.H., Poon, Y., David, N., Baker, D.J., van Deursen, J.M., Campisi, J., & Elisseeff, J.H. (2017) Local clearance of senescent cells attenuates the development of post-traumatic osteoarthritis and creates a pro-regenerative environment. *Nat. Med.*, **23**, 775–781.

Jeong, J.Y., Lee, D.H., & Kang, S.S. (2013) Effects of Chronic Restraint Stress on Body Weight, Food Intake, and Hypothalamic Gene Expressions in Mice. *Endocrinol. Metab.*, **28**, 288.

Jiang, S.Z. & Eiden, L.E. (2016) Activation of the HPA axis and depression of feeding behavior induced by restraint stress are separately regulated by PACAPergic neurotransmission in the mouse. *Stress*, **19**, 374–382.

Johnston, D. (2000) A Series of Cases of Dementia Presenting with PTSD Symptoms in World War II Combat Veterans. *J. Am. Geriatr. Soc.*, **48**, 70–72.

Jurk, D., Wang, C., Miwa, S., Maddick, M., Korolchuk, V., Tsolou, A., Gonos, E.S., Thrasivoulou, C., Jill Saffrey, M., Cameron, K., & von Zglinicki, T. (2012) Postmitotic neurons develop a p21-dependent senescence-like phenotype driven by a DNA damage response. *Aging Cell*, **11**, 996–1004.

Kagan, J. (2016) An Overly Permissive Extension. *Perspect. Psychol. Sci.*, **11**, 442–450.

Kalback, W., Esh, C., Castaño, E.M., Rahman, A., Kokjohn, T., Luehrs, D.C., Sue, L., Cisneros, R., Gerber, F., Richardson, C., Bohrmann, B., Walker, D.G., Beach, T.G., & Roher, A.E. (2004) Atherosclerosis, vascular amyloidosis and brain hypoperfusion in the pathogenesis of sporadic Alzheimer's disease. *Neurol. Res.*, **26**, 525–539.

Kalinin, S., Gavrilyuk, V., Polak, P.E., Vasser, R., Zhao, J., Heneka, M.T., & Feinstein, D.L. (2007) Noradrenaline deficiency in brain increases β-amyloid plaque burden in an animal model of Alzheimer's disease. *Neurobiol. Aging*, **28**, 1206–1214.

Kalinin, S., Willard, S.L., Shively, C.A., Kaplan, J.R., Register, T.C., Jorgensen, M.J., Polak, P.E., Rubinstein, I., & Feinstein, D.L. (2013) Development of amyloid burden in African Green monkeys. *Neurobiol. Aging*, **34**, 2361–2369.

Kang, C., Xu, Q., Martin, T.D., Li, M.Z., Demaria, M., Aron, L., Lu, T., Yankner, B.A., Campisi, J., & Elledge, S.J. (2015) The DNA damage response induces inflammation and senescence by inhibiting autophagy of GATA4. *Science*, **349**, aaa5612.

Kang, J.-E., Cirrito, J.R., Dong, H., Csernansky, J.G., & Holtzman, D.M. (2007) Acute stress increases interstitial fluid amyloid-beta via corticotropin-releasing factor and neuronal activity. *Proc. Natl. Acad. Sci. U. S. A.*, **104**, 10673–10678.

Kang, T.W., Yevsa, T., Woller, N., Hoenicke, L., Wuestefeld, T., Dauch, D., Hohmeyer, A., Gereke, M., Rudalska, R., Potapova, A., Iken, M., Vucur, M., Weiss, S., Heikenwalder, M., Khan, S., Gil, J., Bruder, D., Manns, M., Schirmacher, P., Tacke, F., Ott, M., Luedde, T., Longerich, T., Kubicka, S., & Zender, L. (2011) Senescence surveillance of pre-malignant hepatocytes limits liver cancer development. *Nature*, **479**, 547–551.

Karas Montez, J., Hayward, M.D., Montez, J.K., & Hayward, M.D. (2014) Cumulative Childhood Adversity, Educational Attainment, and Active Life Expectancy Among U.S. Adults. *Demography*, **51**, 413–435.

Kelly, S.C., He, B., Perez, S.E., Ginsberg, S.D., Mufson, E.J., & Counts, S.E. (2017) Locus coeruleus cellular and molecular pathology during the progression of Alzheimer's disease. *Acta Neuropathol. Commun.*, **5**, 8.

Khachaturian, A.S. (2006) Antihypertensive Medication Use and Incident Alzheimer Disease. *Arch. Neurol.*, **63**, 686.

Khanna, K.K. & Jackson, S.P. (2001) DNA double-strand breaks: signaling, repair and the cancer connection.

Kiecolt-Glaser, J.K., Stephens, R.E., Lipetz, P.D., Speicher, C.E., & Glaser, R. (1985) Distress and DNA repair in human lymphocytes. *J. Behav. Med.*, **8**, 311–320.

Killin, L.O.J., Starr, J.M., Shiue, I.J., & Russ, T.C. (2016) Environmental risk factors for dementia: a systematic review. *BMC Geriatr.*, **16**, 175.

Kim, E.C. & Kim, J.R. (2019) Senotherapeutics: emerging strategy for healthy aging and age-related disease. *BMB Rep.*, **52**, 47.

Kim, K., Lee, S.G., Kegelman, T.P., Su, Z.Z., Das, S.K., Dash, R., Dasgupta, S., Barral, P.M., Hedvat, M., Diaz, P., Reed, J.C., Stebbins, J.L., Pellecchia, M., Sarkar, D., & Fisher, P.B. (2011) Role of Excitatory Amino Acid Transporter-2 (EAAT2) and glutamate in neurodegeneration: Opportunities for developing novel therapeutics. *J. Cell. Physiol.*,.

Kirkland, J.L., Tchkonia, T., Zhu, Y., Niedernhofer, L.J., & Robbins, P.D. (2017) The Clinical Potential of Senolytic Drugs. *J. Am. Geriatr. Soc.*, **65**, 2297–2301.

Kirkwood, T.B.L. & Kowald, A. (2012) The free-radical theory of ageing--older, wiser and still alive: modelling positional effects of the primary targets of ROS reveals new support. *Bioessays*, **34**, 692–700.

Kirschbaum, C., Pirke, K.M., & Hellhammer, D.H. (1993) The 'Trier Social Stress Test'--a tool for investigating psychobiological stress responses in a laboratory setting. *Neuropsychobiology*, **28**, 76–81.

Kivimäki, M., Vahtera, J., Tabák, A.G., Halonen, J.I., Vineis, P., Pentti, J., Pahkala, K., Rovio, S., Viikari, J., Kähönen, M., Juonala, M., Ferrie, J.E., Stringhini, S., & Raitakari, O.T. (2018) Neighbourhood socioeconomic disadvantage, risk factors, and diabetes from childhood to middle age in the Young Finns Study: a cohort study. *Lancet. Public Heal.*, **3**, e365–e373.

Kodis, E.J., Choi, S., Swanson, E., Ferreira, G., & Bloom, G.S. (2018) N-methyl-D-aspartate receptor–mediated calcium influx connects amyloid-β oligomers to ectopic neuronal cell cycle reentry in Alzheimer's disease. *Alzheimer's Dement.*, **14**, 1302–1312.

Kojo, A., Yamada, K., Kubo, K. ya, Yamashita, A., & Yamamoto, T. (2010) Occlusal disharmony in mice transiently activates microglia in hippocampal CA1 region but not in dentate gyrus. *Tohoku J. Exp. Med.*, **221**, 237–243.

Komada, M., Takao, K., & Miyakawa, T. (2008) Elevated plus maze for mice. *J. Vis. Exp.*, e1088.

Koolhaas, J.M., Bartolomucci, A., Buwalda, B., de Boer, S.F., Flügge, G., Korte, S.M., Meerlo, P., Murison, R., Olivier, B., Palanza, P., Richter-Levin, G., Sgoifo, A., Steimer, T., Stiedl, O., van Dijk, G., Wöhr, M., & Fuchs, E. (2011) Stress revisited:

A critical evaluation of the stress concept. *Neurosci. Biobehav. Rev.*, **35**, 1291–1301.
Koolhaas, J.M., De Boer, S.F., De Ruitter, A.J.H., Meerlo, P., & Sgoifo, A. (1997) Social stress in rats and mice. *Acta Physiol. Scand. Suppl.*, **161**, 69–72.
Kopeikina, K.J., Hyman, B.T., & Spires-Jones, T.L. (2012) Soluble forms of tau are toxic in Alzheimer's disease. *Transl. Neurosci.*, **3**, 223–233.
Korneyev, A., Binder, L., & Bernardis, J. (1995) Rapid reversible phosphorylation of rat brain tau proteins in response to cold water stress. *Neurosci. Lett.*, **191**, 19–22.
Korneyev, A.Y. (1998) Stress-Induced Tau Phosphorylation in Mouse Strains with Different Brain Erk 1 + 2 Immunoreactivity. *Neurochem. Res.*, **23**, 1539–1543.
Kraeuter, A.K., Guest, P.C., & Sarnyai, Z. (2019) The Elevated Plus Maze Test for Measuring Anxiety-Like Behavior in Rodents. *Methods Mol. Biol.*, **1916**, 69–74.
Krishnamurthy, J., Torrice, C., Ramsey, M., Kovalev, G., Al-Regaiey, K., Su, L., & Sharpless, N. (2004) Ink4a/Arf expression is a biomarker of aging. *J. Clin. Invest.*, **114**, 1299–1307.
Krugers, H.J., Lucassen, P., Karst, H., & Joels, M. (2010) Chronic stress effects on hippocampal structure and synaptic function: relevance for depression and normalization by anti-glucocorticoid treatment. *Front. Synaptic Neurosci.*, **2**, 24.
Kvetnansky, R., Novak, P., Vargovic, P., Lejavova, K., Horvathova, L., Ondicova, K., Manz, G., Filipcik, P., Novak, M., & Mravec, B. (2016) Exaggerated phosphorylation of brain tau protein in CRH KO mice exposed to repeated immobilization stress. *Stress*, **19**, 395–405.
Lachman, M.E. & Weaver, S.L. (1998) The sense of control as a moderator of social class differences in health and well-being. *J. Pers. Soc. Psychol.*, **74**, 763–773.
Lasagna-Reeves, C.A., de Haro, M., Hao, S., Park, J., Rousseaux, M.W.C., Al-Ramahi, I., Jafar-Nejad, P., Vilanova-Velez, L., See, L., De Maio, A., Nitschke, L., Wu, Z., Troncoso, J.C., Westbrook, T.F., Tang, J., Botas, J., & Zoghbi, H.Y. (2016) Reduction of Nuak1 Decreases Tau and Reverses Phenotypes in a Tauopathy Mouse Model. *Neuron*, **92**, 407–418.
Latimer, C.S., Shively, C.A., Keene, C.D., Jorgensen, M.J., Andrews, R.N., Register, T.C., Montine, T.J., Wilson, A.M., Neth, B.J., Mintz, A., Maldjian, J.A., Whitlow, C.T., Kaplan, J.R., & Craft, S. (2019) A nonhuman primate model of early Alzheimer's disease pathologic change: Implications for disease pathogenesis. *Alzheimers. Dement.*, **15**, 93–105.
Lee, B.Y., Han, J.A., Im, J.S., Morrone, A., Johung, K., Goodwin, E.C., Kleijer, W.J., DiMaio, D., & Hwang, E.S. (2006) Senescence-associated β-galactosidase is lysosomal β-galactosidase. *Aging Cell*, **5**, 187–195.
Lee, K.-W., Kim, J.-B., Seo, J.-S., Kim, T.-K., Im, J.-Y., Baek, I.-S., Kim, K.-S., Lee, J.-K., & Han, P.-L. (2009) Behavioral stress accelerates plaque pathogenesis in the brain of Tg2576 mice via generation of metabolic oxidative stress. *J. Neurochem.*, **108**, 165–175.
Lee, S.W., Fang, L., Igarashi, M., Ouchi, T., Lu, K.P., & Aaronson, S.A. (2000) Sustained activation of Ras/Raf/mitogen-activated protein kinase cascade by the tumor suppressor p53. *Proc. Natl. Acad. Sci. U. S. A.*, **97**, 8302–8305.
Lesuis, S.L., Maurin, H., Borghgraef, P., Lucassen, P.J., Van Leuven, F., & Krugers, H.J. (2016) Positive and negative early life experiences differentially modulate long term survival and amyloid protein levels in a mouse model of Alzheimer's disease.

Oncotarget, **7**, 39118–39135.
Leszek, J., E. Barreto, G., G|siorowski, K., Koutsouraki, E., Ávila-Rodrigues, M., & Aliev, G. (2016) Inflammatory Mechanisms and Oxidative Stress as Key Factors Responsible for Progression of Neurodegeneration: Role of Brain Innate Immune System. *CNS Neurol. Disord. - Drug Targets*, **15**, 329–336.
Leyns, C.E.G. & Holtzman, D.M. (2017) Glial contributions to neurodegeneration in tauopathies. *Mol. Neurodegener.*, **12**.
Li, J., Poi, M.J., & Tsai, M.-D. (2011) Regulatory mechanisms of tumor suppressor P16(INK4A) and their relevance to cancer. *Biochemistry*, **50**, 5566–5582.
Li, Q., Zhang, M., Chen, Y.J., Wang, Y.J., Huang, F., & Liu, J. (2011) Oxidative damage and HSP70 expression in masseter muscle induced by psychological stress in rats. *Physiol. Behav.*, **104**, 365–372.
Li, V. & Wang, Y.T. (2016) Molecular mechanisms of NMDA receptor-mediated excitotoxicity: Implications for neuroprotective therapeutics for stroke. *Neural Regen. Res.*,.
Liaoi, Y.F., Wang, B.J., Cheng, H.T., Kuo, L.H., & Wolfe, M.S. (2004) Tumor necrosis factor-α, interleukin-1β, and interferon-γ stimulate γ-secretase-mediated cleavage of amyloid precursor protein through a JNK-dependent MAPK pathway. *J. Biol. Chem.*, **279**, 49523–49532.
Lin, A.W., Barradas, M., Stone, J.C., Van Aelst, L., Serrano, M., & Lowe, S.W. (1998a) Premature senescence involving p53 and p16 is activated in response to constitutive MEK/MAPK mitogenic signaling. *Genes Dev.*, **12**, 3008–3019.
Lin, A.W., Barradas, M., Stone, J.C., Van Aelst, L., Serrano, M., & Lowe, S.W. (1998b) Premature senescence involving p53 and p16 is activated in response to constitutive MEK/MAPK mitogenic signaling. *Genes Dev.*, **12**, 3008–3019.
Litvinchuk, A., Wan, Y.W., Swartzlander, D.B., Chen, F., Cole, A., Propson, N.E., Wang, Q., Zhang, B., Liu, Z., & Zheng, H. (2018) Complement C3aR Inactivation Attenuates Tau Pathology and Reverses an Immune Network Deregulated in Tauopathy Models and Alzheimer's Disease. *Neuron*, **100**, 1337-1353.e5.
Liu, Y., Sanoff, H.K., Cho, H., Burd, C.E., Torrice, C., Ibrahim, J.G., Thomas, N.E., & Sharpless, N.E. (2009) Expression of p16INK4a in peripheral blood T-cells is a biomarker of human aging. *Aging Cell*, **8**, 439–448.
Liu, Y., Tak, P.W., Aarts, M., Rooyakkers, A., Liu, L., Ted, W.L., Dong, C.W., Lu, J., Tymianski, M., Craig, A.M., & Yu, T.W. (2007) NMDA receptor subunits have differential roles in mediating excitotoxic neuronal death both in vitro and in vivo. *J. Neurosci.*, **27**, 2846–2857.
Loft, S., Olsen, A., Møller, P., Poulsen, H.E., & Tjønneland, A. (2013) Association between 8-oxo-7,8-dihydro-2'-deoxyguanosine excretion and risk of postmenopausal breast cancer: nested case-control study. *Cancer Epidemiol. Biomarkers Prev.*, **22**, 1289–1296.
Lopes, S., Vaz-Silva, J., Pinto, V., Dalla, C., Kokras, N., Bedenk, B., Mack, N., Czisch, M., Almeida, O.F.X., Sousa, N., & Sotiropoulos, I. (2016) Tau protein is essential for stress-induced brain pathology. *Proc. Natl. Acad. Sci. U. S. A.*, **113**, E3755–E3763.
López-González, I., Aso, E., Carmona, M., Armand-Ugon, M., Blanco, R., Naudí, A., Cabré, R., Portero-Otin, M., Pamplona, R., & Ferrer, I. (2015) Neuroinflammatory gene regulation, mitochondrial function, oxidative stress, and brain lipid

modifications with disease progression in tau P301S transgenic mice as a model of frontotemporal lobar degeneration-tau. *J. Neuropathol. Exp. Neurol.*, **74**, 975–999.

López-López, A.L., Bonilla, H.J., Escobar Villanueva, M. del C., Brianza, M.P., Vázquez, G.P., & Alarcón, F.J.A. (2016) Chronic unpredictable mild stress generates oxidative stress and systemic inflammation in rats. *Physiol. Behav.*, **161**, 15–23.

Lowy, M.T., Gault, L., & Yamamoto, B.K. (1993) Rapid Communication: Adrenalectomy Attenuates Stress-Induced Elevations in Extracellular Glutamate Concentrations in the Hippocampus. *J. Neurochem.*, **61**, 1957–1960.

Luchsinger, J.A., Reitz, C., Honig, L.S., Tang, M.X., Shea, S., & Mayeux, R. (2005) Aggregation of vascular risk factors and risk of incident Alzheimer disease. *Neurology*, **65**, 545–551.

Lyons, C.E. & Bartolomucci, A. (2020) Stress and Alzheimer's disease: A senescence link? *Neurosci. Biobehav. Rev.*, **115**, 285–298.

Lyons, C.E., Zhou, X., Razzoli, M., Chen, M., Xia, W., Ashe, K., Zhang, B., & Bartolomucci, A. (2021) Lifelong chronic psychosocial stress induces a proteomic signature of Alzheimer's disease in wildtype mice. *Eur. J. Neurosci.*, **55**, 2971–2985.

Magariños, A.M. & McEwen, B.S. (1995) Stress-induced atrophy of apical dendrites of hippocampal CA3c neurons: Involvement of glucocorticoid secretion and excitatory amino acid receptors. *Neuroscience*, **69**, 89–98.

Magariños, A.M., McEwen, B.S., Flügge, G., & Fuchs, E. (1996) Chronic psychosocial stress causes apical dendritic atrophy of hippocampal CA3 pyramidal neurons in subordinate tree shrews. *J. Neurosci.*, **16**, 3534–3540.

Mandelkow, E.-M. & Mandelkow, E. (2012) Biochemistry and cell biology of tau protein in neurofibrillary degeneration. *Cold Spring Harb. Perspect. Med.*, **2**, a006247.

Mansur, R.B., Cunha, G.R., Asevedo, E., Zugman, A., Zeni-Graiff, M., Rios, A.C., Sethi, S., Maurya, P.K., Levandowski, M.L., Gadelha, A., Pan, P.M., Stertz, L., Belangero, S.I., Kauer-Sant' Anna, M., Teixeira, A.L., Mari, J.J., Rohde, L.A., Miguel, E.C., Mcintyre, R.S., Grassi-Oliveira, R., Bressan, R.A., & Brietzke, E. (2016) Socioeconomic Disadvantage Moderates the Association between Peripheral Biomarkers and Childhood Psychopathology.

Maras, P.M., Molet, J., Chen, Y., Rice, C., Ji, S.G., Solodkin, A., & Baram, T.Z. (2014) Preferential loss of dorsal-hippocampus synapses underlies memory impairments provoked by short, multimodal stress. *Mol. Psychiatry*, **19**, 811–822.

Marin, M.T., Cruz, F.C., & Planeta, C.S. (2006) Chronic restraint or variable stresses differently affect the behavior, corticosterone secretion and body weight in rats.

Marmot, M. (2020) Health equity in England: The Marmot review 10 years on. *BMJ*, **368**.

Marmot, M.G., Stansfeld, S., Patel, C., North, F., Head, J., White, I., Brunner, E., Feeney, A., Marmot, M.G., & Smith, G.D. (1991) Health inequalities among British civil servants: the Whitehall II study. *Lancet*, **337**, 1387–1393.

Martisova, E., Aisa, B., Guereñu, G., & Ramírez, M.J. (2013) Effects of early maternal separation on biobehavioral and neuropathological markers of Alzheimer's disease in adult male rats. *Curr. Alzheimer Res.*, **10**, 420–432.

Masliah, E., Mallory, M., Alford, M., DeTeresa, R., Hansen, L.A., McKeel, D.W., & Morris, J.C. (2001) Altered expression of synaptic proteins occurs early during progression of Alzheimer's disease. *Neurology*, **56**, 127–129.

Masurkar, A. V (2018) Towards a circuit-level understanding of hippocampal CA1

dysfunction in Alzheimer's disease across anatomical axes. *J. Alzheimer's Dis. Park.*, **8**.

McClintock, B. (1942) The Fusion of Broken Ends of Chromosomes Following Nuclear Fusion. *Proc. Natl. Acad. Sci.*, **28**, 458–463.

McEwen, B.S. (1998) Protective and Damaging Effects of Stress Mediators. *N. Engl. J. Med.*, **338**, 171–179.

McEwen, B.S., Weiss, J.M., & Schwartz, L.S. (1968) Selective retention of corticosterone by limbic structures in rat brain [18]. *Nature*,.

McHugh, D. & Gil, J. (2018) Senescence and aging: Causes, consequences, and therapeutic avenues. *J. Cell Biol.*, **217**, 65–77.

McKee, A.C., Kosik, K.S., Kennedy, M.B., & Kowall, N.W. (1990) Hippocampal Neurons Predisposed to Neurofibrillary Tangle Formation Are Enriched in Type II Calcium/Calmodulin-Dependent Protein Kinase. *J. Neuropathol. Exp. Neurol.*, **49**, 49–63.

Mejfa, S., Giraldo, M., Pineda, D., Ardila, A., Lopera, F., Mejia, S., Giraldo, ; M, Pineda, ; D, & Lopera, F. (2003) Nongenetic Factors as Modifiers of the Age of Onset of Familial Alzheimer's Disease, International Psychogeriah-ics.

Mo, C., Renoir, T., & Hannan, A.J. (2014) Effects of chronic stress on the onset and progression of Huntington's disease in transgenic mice. *Neurobiol. Dis.*, **71**, 81–94.

Moceri, V.M., Kukull, W.A., Emanual, I., Van Belle, G., Starr, J.R., Schellenberg, G.D., McCormick, W.C., Bowen, J.D., Teri, L., & Larson, E.B. (2001) Using census data and birth certificates to reconstruct the early-life socioeconomic environment and the relation to the development of Alzheimer's disease. *Epidemiology*, **12**, 383–389.

Molofsky, A. V., Slutsky, S.G., Joseph, N.M., He, S., Pardal, R., Krishnamurthy, J., Sharpless, N.E., & Morrison, S.J. (2006) Increasing p16INK4a expression decreases forebrain progenitors and neurogenesis during ageing. *Nat. 2006 4437110*, **443**, 448–452.

Monteiro-Fernandes, D., Silva, J.M., Soares-Cunha, C., Dalla, C., Kokras, N., Arnaud, F., Billiras, R., Zhuravleva, V., Waites, C., Bretin, S., Sousa, N., & Sotiropoulos, I. (2020) Allosteric modulation of AMPA receptors counteracts Tau-related excitotoxic synaptic signaling and memory deficits in stress- and Aβ-evoked hippocampal pathology. *Mol. Psychiatry*, 1–13.

Morilak, D.A., Barrera, G., Echevarria, D.J., Garcia, A.S., Hernandez, A., Ma, S., & Petre, C.O. (2005) Role of brain norepinephrine in the behavioral response to stress. *Prog. Neuro-Psychopharmacology Biol. Psychiatry*,.

Moriyoshi, K., Masu, M., Ishii, T., Shigemoto, R., Mizuno, N., & Nakanishi, S. (1991) Molecular cloning and characterization of the rat NMDA receptor. *Nature*, **354**, 31–37.

Morris, J.C. (2005) Early-stage and preclinical Alzheimer disease. *Alzheimer Dis. Assoc. Disord.*, **19**, 163–165.

Morris, J.C., Storandt, M., Miller, J.P., McKeel, D.W., Price, J.L., Rubin, E.H., & Berg, L. (2001) Mild Cognitive Impairment Represents Early-Stage Alzheimer Disease. *Arch. Neurol.*, **58**.

Morris, M.C. (2009) The role of nutrition in Alzheimer's disease: epidemiological evidence. *Eur. J. Neurol.*, **16 Suppl 1**, 1–7.

Mota, C., Taipa, R., das Neves, S.P., Monteiro-Martins, S., Monteiro, S., Palha, J.A.,

Sousa, N., Sousa, J.C., & Cerqueira, J.J. (2019) Structural and molecular correlates of cognitive aging in the rat. *Sci. Rep.*, **9**, 1–14.

Mullane, K. & Williams, M. (2013) Alzheimer's therapeutics: Continued clinical failures question the validity of the amyloid hypothesis—but what lies beyond? *Biochem. Pharmacol.*, **85**, 289–305.

Murdock, K.W., LeRoy, A.S., Lacourt, T.E., Duke, D.C., Heijnen, C.J., & Fagundes, C.P. (2016) Executive functioning and diabetes: The role of anxious arousal and inflammation. *Psychoneuroendocrinology*, **71**, 102–109.

Musi, N., Valentine, J.M., Sickora, K.R., Baeuerle, E., Thompson, C.S., Shen, Q., & Orr, M.E. (2018) Tau protein aggregation is associated with cellular senescence in the brain. *Aging Cell*, e12840.

Mychasiuk, R., Gibb, R., & Kolb, B. (2012) Prenatal stress alters dendritic morphology and synaptic connectivity in the prefrontal cortex and hippocampus of developing offspring. *Synapse*, **66**, 308–314.

Nagahara, A.H., Bernot, T., & Tuszynski, M.H. (2010) Age-related cognitive deficits in rhesus monkeys mirror human deficits on an automated test battery. *Neurobiol. Aging*, **31**, 1020–1031.

Nakhaee, A., Shahabizadeh, F., & Erfani, M. (2013) Protein and lipid oxidative damage in healthy students during and after exam stress. *Physiol. Behav.*, **118**, 118–121.

Nederhof, E. & Schmidt, M. V. (2012) Mismatch or cumulative stress: Toward an integrated hypothesis of programming effects. *Physiol. Behav.*, **106**, 691–700.

Nelson, P.T., Alafuzoff, I., Bigio, E.H., Bouras, C., Braak, H., Cairns, N.J., Castellani, R.J., Crain, B.J., Davies, P., Tredici, K. Del, Duyckaerts, C., Frosch, M.P., Haroutunian, V., Hof, P.R., Hulette, C.M., Hyman, B.T., Iwatsubo, T., Jellinger, K.A., Jicha, G.A., Kövari, E., Kukull, W.A., Leverenz, J.B., Love, S., Mackenzie, I.R., Mann, D.M., Masliah, E., McKee, A.C., Montine, T.J., Morris, J.C., Schneider, J.A., Sonnen, J.A., Thal, D.R., Trojanowski, J.Q., Troncoso, J.C., Wisniewski, T., Woltjer, R.L., & Beach, T.G. (2012) Correlation of Alzheimer Disease Neuropathologic Changes With Cognitive Status: A Review of the Literature. *J. Neuropathol. Exp. Neurol.*, **71**, 362–381.

Nelson, P.T., Stefansson, K., Gulcher, J., & Saper, C.B. (1996) Molecular evolution of tau protein: implications for Alzheimer's disease. *J. Neurochem.*, **67**, 1622–1632.

Ni, Y., Zhao, X., Bao, G., Zou, L., Teng, L., Wang, Z., Song, M., Xiong, J., Bai, Y., & Pei, G. (2006) Activation of β2-adrenergic receptor stimulates γ-secretase activity and accelerates amyloid plaque formation. *Nat. Med.*, **12**, 1390–1396.

Niedernhofer, L.J. & Robbins, P.D. (2018) Senotherapeutics for healthy ageing. *Nat. Rev. Drug Discov.*, **17**, 377–377.

O'brien, R.J. & Wong, P.C. (2011) Amyloid Precursor Protein Processing and Alzheimer's Disease.

Oakley, H., Cole, S.L., Logan, S., Maus, E., Shao, P., Craft, J., Guillozet-Bongaarts, A., Ohno, M., Disterhoft, J., Van Eldik, L., Berry, R., & Vassar, R. (2006) Intraneuronal beta-Amyloid Aggregates, Neurodegeneration, and Neuron Loss in Transgenic Mice with Five Familial Alzheimer's Disease Mutations: Potential Factors in Amyloid Plaque Formation. *J. Neurosci.*, **26**, 10129–10140.

Oddo, S., Vasilevko, V., Caccamo, A., Kitazawa, M., Cribbs, D.H., & LaFerla, F.M. (2006) Reduction of soluble Abeta and tau, but not soluble Abeta alone, ameliorates cognitive

decline in transgenic mice with plaques and tangles. *J. Biol. Chem.*, **281**, 39413–39423.

Ogrodnik, M., Evans, S.A., Fielder, E., Victorelli, S., Kruger, P., Salmonowicz, H., Weigand, B.M., Patel, A.D., Pirtskhalava, T., Inman, C.L., Johnson, K.O., Dickinson, S.L., Rocha, A., Schafer, M.J., Zhu, Y., Allison, D.B., von Zglinicki, T., LeBrasseur, N.K., Tchkonia, T., Neretti, N., Passos, J.F., Kirkland, J.L., & Jurk, D. (2021) Whole-body senescent cell clearance alleviates age-related brain inflammation and cognitive impairment in mice. *Aging Cell*, **20**, e13296.

Ohtani, N., Yamakoshi, K., Takahashi, A., & Hara, E. (2004) The p16INK4a-RB pathway: molecular link between cellular senescence and tumor suppression. *J. Med. Invest.*, **51**, 146–153.

Oikawa, N., Ogino, K., Masumoto, T., Yamaguchi, H., & Yanagisawa, K. (2010) Gender effect on the accumulation of hyperphosphorylated tau in the brain of locus-ceruleus-injured APP-transgenic mouse. *Neurosci. Lett.*, **468**, 243–247.

Okawa, Y., Ishiguro, K., & Fujita, S.C. (2003) Stress-induced hyperphosphorylation of tau in the mouse brain. *FEBS Lett.*, **535**, 183–189.

Olivieri, F., Prattichizzo, F., Grillari, J., & Balistreri, C.R. (2018) Cellular senescence and inflammaging in age-Related diseases. *Mediators Inflamm.*, **76**.

Omori, S., Wang, T.W., Johmura, Y., Kanai, T., Nakano, Y., Kido, T., Susaki, E.A., Nakajima, T., Shichino, S., Ueha, S., Ozawa, M., Yokote, K., Kumamoto, S., Nishiyama, A., Sakamoto, T., Yamaguchi, K., Hatakeyama, S., Shimizu, E., Katayama, K., Yamada, Y., Yamazaki, S., Iwasaki, K., Miyoshi, C., Funato, H., Yanagisawa, M., Ueno, H., Imoto, S., Furukawa, Y., Yoshida, N., Matsushima, K., Ueda, H.R., Miyajima, A., & Nakanishi, M. (2020) Generation of a p16 Reporter Mouse and Its Use to Characterize and Target p16high Cells In Vivo. *Cell Metab.*, **32**, 814-828.e6.

Oppong, E. & Cato, A.C.B. (2015) Effects of Glucocorticoids in the Immune System. Springer, New York, NY, pp. 217–233.

Orr, M.E., Sullivan, A.C., & Frost, B. (2017) A Brief Overview of Tauopathy: Causes, Consequences, and Therapeutic Strategies. *Trends Pharmacol. Sci.*, **38**, 637–648.

Pacák, K. & Palkovits, M. (2001) Stressor Specificity of Central Neuroendocrine Responses: Implications for Stress-Related Disorders. *Endocr. Rev.*, **22**, 502–548.

Padurariu, M., Ciobica, A., Mavroudis, I., Fotiou, D., & Baloyannis, S. (2012) Hippocampal neuronal loss in the CA1 and CA3 areas of Alzheimer's disease patients. *Psychiatr. Danub.*, **24**, 152–158.

Pagala, V.R., High, A.A., Wang, X., Tan, H., Kodali, K., Mishra, A., Kavdia, K., Xu, Y., Wu, Z., & Peng, J. (2015) Quantitative protein analysis by mass spectrometry. In *Protein-Protein Interactions: Methods and Applications: Second Edition*. Springer New York, pp. 281–305.

Pariante, C.M. & Lightman, S.L. (2008) The HPA axis in major depression: classical theories and new developments. *Trends Neurosci.*, **31**, 464–468.

Parks, C.G., Miller, D.B., Mccanlies, E.C., Cawthon, R.M., Andrew, M.E., Deroo, L.A., & Sandler, D.P. (2009) Telomere Length, Current Perceived Stress, and Urinary Stress Hormones in Women. *Cancer Epidemiol Biomarkers Prev*, **18**, 551–560.

Patel, H., Martinez, P., Perkins, A., Taylor, X., Jury, N., McKinzie, D., & Lasagna-Reeves, C.A. (2022) Pathological tau and reactive astrogliosis are associated with distinct

functional deficits in a mouse model of tauopathy. *Neurobiol. Aging*, **109**, 52–63.
Peavy, G.M., Jacobson, M.W., Salmon, D.P., Gamst, A.C., Patterson, T.L., Goldman, S., Mills, P.J., Khandrika, S., & Galasko, D. (2012) The influence of chronic stress on dementia-related diagnostic change in older adults. *Alzheimer Dis. Assoc. Disord.*, **26**, 260–266.
Pereira, A.C., Gray, J.D., Kogan, J.F., Davidson, R.L., Rubin, T.G., Okamoto, M., Morrison, J.H., & McEwen, B.S. (2017) Age and Alzheimer's disease gene expression profiles reversed by the glutamate modulator riluzole. *Mol. Psychiatry*, **22**, 296–305.
Pereira, A.C., Lambert, H.K., Grossman, Y.S., Dumitriu, D., Waldman, R., Jannetty, S.K., Calakos, K., Janssen, W.G., McEwen, B.S., & Morrison, J.H. (2014) Glutamatergic regulation prevents hippocampal-dependent age-related cognitive decline through dendritic spine clustering. *Proc. Natl. Acad. Sci.*, **111**, 18733–18738.
Perrottet, N., Decosterd, L.A., Meylan, P., Pascual, M., Biollaz, J., & Buclin, T. (2009) Valganciclovir in adult solid organ transplant recipients: Pharmacokinetic and pharmacodynamic characteristics and clinical interpretation of plasma concentration measurements. *Clin. Pharmacokinet.*, **48**, 399–418.
Peskind, E.R., Wilkinson, C.W., Petrie, E.C., Schellenberg, G.D., & Raskind, M.A. (2001) Increased CSF cortisol in AD is a function of APOE genotype. *Neurology*, **56**, 1094–1098.
Piechota, M., Sunderland, P., Wysocka, A., Nalberczak, M., Sliwinska, M.A., Radwanska, K., & Sikora, E. (2016) Is senescence-associated β-galactosidase a marker of neuronal senescence? *Oncotarget*, **7**, 81099.
Pitts, M. (2018) Barnes Maze Procedure for Spatial Learning and Memory in Mice. *BIO-PROTOCOL*, **8**.
Planel, E., Miyasaka, T., Launey, T., Chui, D.H., Tanemura, K., Sato, S., Murayama, O., Ishiguro, K., Tatebayashi, Y., & Takashima, A. (2004) Alterations in Glucose Metabolism Induce Hypothermia Leading to Tau Hyperphosphorylation through Differential Inhibition of Kinase and Phosphatase Activities: Implications for Alzheimer's Disease. *J. Neurosci.*, **24**, 2401–2411.
Planel, E., Yasutake, K., Fujita, S.C., & Ishiguro, K. (2001) Inhibition of Protein Phosphatase 2A Overrides Tau Protein Kinase I/Glycogen Synthase Kinase 3β and Cyclin-dependent Kinase 5 Inhibition and Results in Tau Hyperphosphorylation in the Hippocampus of Starved Mouse. *J. Biol. Chem.*, **276**, 34298–34306.
Poulsen, H.E., Nadal, L.L., Broedbaek, K., Nielsen, P.E., & Weimann, A. (2014) Detection and interpretation of 8-oxodG and 8-oxoGua in urine, plasma and cerebrospinal fluid. *Biochim. Biophys. Acta*, **1840**, 801–808.
Powell, N.D., Sloan, E.K., Bailey, M.T., Arevalo, J.M.G., Miller, G.E., Chen, E., Kobor, M.S., Reader, B.F., Sheridan, J.F., & Cole, S.W. (2013) Social stress up-regulates inflammatory gene expression in the leukocyte transcriptome via β-adrenergic induction of myelopoiesis. *Proc. Natl. Acad. Sci. U. S. A.*, **110**, 16574–16579.
Prather, A.A., Gurfein, B., Moran, P., Daubenmier, J., Acree, M., Bacchetti, P., Sinclair, E., Lin, J., Blackburn, E., Hecht, F.M., & Epel, E.S. (2015) Tired telomeres: Poor global sleep quality, perceived stress, and telomere length in immune cell subsets in obese men and women. *Brain. Behav. Immun.*, **47**, 155–162.
Price, J.L., Ko, A.I., Wade, M.J., Tsou, S.K., McKeel, D.W., & Morris, J.C. (2001) Neuron

Number in the Entorhinal Cortex and CA1 in Preclinical Alzheimer Disease. *Arch. Neurol.*, **58**, 1395.

Prieur, E. & Jadavji, N. (2019) Assessing Spatial Working Memory Using the Spontaneous Alternation Y-maze Test in Aged Male Mice. *BIO-PROTOCOL*, **9**.

Probin, V., Wang, Y., Bai, A., & Zhou, D. (2006) Busulfan selectively induces cellular senescence but not apoptosis in WI38 fibroblasts via a p53-independent but extracellular signal-regulated kinase-p38 mitogen-activated protein kinase-dependent mechanism. *J. Pharmacol. Exp. Ther.*, **319**, 551–560.

Puterman, E., Lin, J., Blackburn, E., O'Donovan, A., Adler, N., & Epel, E. (2010) The Power of Exercise: Buffering the Effect of Chronic Stress on Telomere Length. *PLoS One*, **5**, e10837.

Quintanilla, R.A., Orellana, D.I., González-Billault, C., & Maccioni, R.B. (2004) Interleukin-6 induces Alzheimer-type phosphorylation of tau protein by deregulating the cdk5/p35 pathway. *Exp. Cell Res.*, **295**, 245–257.

Radley, J.J., Anderson, R.M., Hamilton, B.A., Alcock, J.A., & Romig-Martin, S.A. (2013) Chronic stress-induced alterations of dendritic spine subtypes predict functional decrements in an hypothalamo-pituitary-adrenal-inhibitory prefrontal circuit. *J. Neurosci.*, **33**, 14379–14391.

Räihä, I., Kaprio, J., Koskenvuo, M., Rajala, T., & Sourander, L. (1998) Environmental differences in twin pairs discordant for Alzheimer's disease. *J. Neurol. Neurosurg. Psychiatry*, **65**, 785–787.

Ranta, S., Zhang, Y., Ross, B., Takkunen, E., Hirvasniemi, A., De La Chapelle, A., Gilliam, T.C., & Lehesjoki, A.-E. (2000) Positional cloning and characterisation of the human DLGAP2 gene and its exclusion in progressive epilepsy with mental retardation.

Ray, B., Gaskins, D.L., Sajdyk, T.J., Spence, J.P., Fitz, S.D., Shekhar, A., & Lahiri, D.K. (2011) Restraint stress and repeated corticotrophin-releasing factor receptor activation in the amygdala both increase amyloid-β precursor protein and amyloid-β peptide but have divergent effects on brain-derived neurotrophic factor and pre-synaptic proteins in the prefrontal cortex of rats. *Neuroscience*, **184**, 139–150.

Razzoli, M. & Bartolomucci, A. (2016) The Dichotomous Effect of Chronic Stress on Obesity. *Trends Endocrinol. Metab.*,.

Razzoli, M., Bo, E., Pascucci, T., Pavone, F., D'Amato, F.R., Cero, C., Sanghez, V., Dadomo, H., Palanza, P., Parmigiani, S., Ceresini, G., Puglisi-Allegra, S., Porta, M., Panzica, G.C., Moles, A., Possenti, R., & Bartolomucci, A. (2012) Implication of the VGF-derived peptide TLQP-21 in mouse acute and chronic stress responses. *Behav. Brain Res.*, **229**, 333–339.

Razzoli, M., Karsten, C., Yoder, J.M., Bartolomucci, A., & Engeland, W.C. (2014) Chronic subordination stress phase advances adrenal and anterior pituitary clock gene rhythms. *Am. J. Physiol. Regul. Integr. Comp. Physiol.*, **307**, R198-205.

Razzoli, M., Lindsay, A., Law, M.L., Chamberlain, C.M., Southern, W.M., Berg, M., Osborn, J., Engeland, W.C., Metzger, J.M., Ervasti, J.M., & Bartolomucci, A. (2020) Social stress is lethal in the mdx model of Duchenne muscular dystrophy. *EBioMedicine*, **0**, 102700.

Razzoli, M., Nyuyki-Dufe, K., Gurney, A., Erickson, C., McCallum, J., Spielman, N., Marzullo, M., Patricelli, J., Kurata, M., Pope, E.A., Touma, C., Palme, R., Largaespada, D.A., Allison, D.B., & Bartolomucci, A. (2018) Social stress shortens

lifespan in mice. *Aging Cell*, **17**, e12778.
Razzoli, M., Sanghez, V., & Bartolomucci, A. (2015) Chronic Subordination Stress Induces Hyperphagia and Disrupts Eating Behavior in Mice Modeling Binge-Eating-Like Disorder. *Front. Nutr.*, **1**.
Redwine, J.M., Kosofsky, B., Jacobs, R.E., Games, D., Reilly, J.F., Morrison, J.H., Young, W.G., & Bloom, F.E. (2003) Dentate gyrus volume is reduced before onset of plaque formation in PDAPP mice: A magnetic resonance microscopy and stereologic analysis. *Proc. Natl. Acad. Sci. U. S. A.*, **100**, 1381–1386.
Reiman, E.M., Uecker, A., Caselli, R.J., Lewis, S., Bandy, D., De Leon, M.J., De Santi, S., Convit, A., Osborne, D., Weaver, A., & Thibodeau, S.N. (1998) Hippocampal volumes in cognitively normal persons at genetic risk for Alzheimer's disease. *Ann. Neurol.*, **44**, 288–291.
Rentscher, K.E., Carroll, J.E., Polsky, L.R., & Lamkin, D.M. (2022) Chronic stress increases transcriptomic indicators of biological aging in mouse bone marrow leukocytes. *Brain, Behav. Immun. - Heal.*, **22**, 100461.
Rentscher, K.E., Carroll, J.E., Repetti, R.L., Cole, S.W., Reynolds, B.M., & Robles, T.F. (2019) Chronic stress exposure and daily stress appraisals relate to biological aging marker p16 INK4a. *Psychoneuroendocrinology*, **102**, 139–148.
Ressler, S., Bartkova, J., Niederegger, H., Bartek, J., Scharffetter-Kochanek, K., Jansen-Dürr, P., & Wlaschek, M. (2006) p16INK4A is a robust in vivo biomarker of cellular aging in human skin. *Aging Cell*, **5**, 379–389.
Reuben, A., Sugden, K., Arseneault, L., Corcoran, D.L., Danese, A., Fisher, H.L., Moffitt, T.E., Newbury, J.B., Odgers, C., Prinz, J., Rasmussen, L.J.H., Williams, B., Mill, J., & Caspi, A. (2020) Association of Neighborhood Disadvantage in Childhood With DNA Methylation in Young Adulthood. *JAMA Netw. Open*, **3**, e206095–e206095.
Rezatabar, S., Karimian, A., Rameshknia, V., Parsian, H., Majidinia, M., Kopi, T.A., Bishayee, A., Sadeghinia, A., Yousefi, M., Monirialamdari, M., & Yousefi, B. (2019) RAS/MAPK signaling functions in oxidative stress, DNA damage response and cancer progression. *J. Cell. Physiol.*, **234**, 14951–14965.
Rissman, R.A., Lee, K.-F., Vale, W., & Sawchenko, P.E. (2007) Neurobiology of Disease Corticotropin-Releasing Factor Receptors Differentially Regulate Stress-Induced Tau Phosphorylation.
Ritchie, M.E., Phipson, B., Wu, D., Hu, Y., Law, C.W., Shi, W., & Smyth, G.K. (2015) Limma powers differential expression analyses for RNA-sequencing and microarray studies. *Nucleic Acids Res.*, **43**, e47.
Robbins, P.D., Jurk, D., Khosla, S., Kirkland, J.L., Lebrasseur, N.K., Miller, J.D., Passos, J.F., Pignolo, R.J., Tchkonia, T., & Niedernhofer, L.J. (2021) Senolytic Drugs: Reducing Senescent Cell Viability to Extend Health Span. *Annu. Rev. Pharmacol. Toxicol.*, **61**, 779.
Rodier, F., Coppé, J.-P., Patil, C.K., Hoeijmakers, W.A.M., Muñoz, D.P., Raza, S.R., Freund, A., Campeau, E., Davalos, A.R., & Campisi, J. (2009) Persistent DNA damage signalling triggers senescence-associated inflammatory cytokine secretion. *Nat. Cell Biol.*, **11**, 973–979.
Rohleder, N. (2014) Stimulation of systemic low-grade inflammation by psychosocial stress. *Psychosom. Med.*, **76**, 181–189.
Romero, L.M., Dickens, M.J., & Cyr, N.E. (2009) The reactive scope model — A new

model integrating homeostasis, allostasis, and stress. *Horm. Behav.*, **55**, 375–389.
Rosa, M.L.N.M., Guimarães, F.S., de Oliveira, R.M.W., Padovan, C.M., Pearson, R.C.A., & Del Bel, E.A. (2005) Restraint stress induces β-amyloid precursor protein mRNA expression in the rat basolateral amygdala. *Brain Res. Bull.*, **65**, 69–75.
Rothman, S.M., Herdener, N., Camandola, S., Texel, S.J., Mughal, M.R., Cong, W.-N., Martin, B., & Mattson, M.P. (2012) 3xTgAD mice exhibit altered behavior and elevated Aβ after chronic mild social stress. *Neurobiol. Aging*, **33**, 830.e1-12.
Sacks, O. & Shulman, M. (2005) Steroid dementia: An overlooked diagnosis? *Neurology*, **64**, 707–709.
Sahu, B.S., Rodriguez, P., Nguyen, M.E., Han, R., Cero, C., Razzoli, M., Piaggi, P., Laskowski, L.J., Pavlicev, M., Muglia, L., Mahata, S.K., O'Grady, S., McCorvy, J.D., Baier, L.J., Sham, Y.Y., & Bartolomucci, A. (2019) Peptide/Receptor Co-evolution Explains the Lipolytic Function of the Neuropeptide TLQP-21. *Cell Rep.*, **28**, 2567-2580.e6.
Sanghez, V., Cubuk, C., Sebastián-Leon, P., Carobbio, S., Dopazo, J., Vidal-Puig, A., & Bartolomucci, A. (2016) Chronic subordination stress selectively downregulates the insulin signaling pathway in liver and skeletal muscle but not in adipose tissue of male mice. *Stress*, **19**, 214–224.
Sanghez, V., Razzoli, M., Carobbio, S., Campbell, M., McCallum, J., Cero, C., Ceresini, G., Cabassi, A., Govoni, P., Franceschini, P., de Santis, V., Gurney, A., Ninkovic, I., Parmigiani, S., Palanza, P., Vidal-Puig, A., & Bartolomucci, A. (2013) Psychosocial stress induces hyperphagia and exacerbates diet-induced insulin resistance and the manifestations of the Metabolic Syndrome. *Psychoneuroendocrinology*, **38**, 2933–2942.
Sapolsky, R.M. (1992) Do glucocorticoid concentrations rise with age in the rat? *Neurobiol. Aging*, **13**, 171–174.
Sapolsky, R.M., Krey, L.C., & McEwen, B.S. (1983) Corticosterone receptors decline in a site-specific manner in the aged rat brain. *Brain Res.*, **289**, 235–240.
Sapolsky, R.M., Krey, L.C., & McEwen, B.S. (1985) Prolonged glucocorticoid exposure reduces hippocampal neuron number: implications for aging. *J. Neurosci.*, **5**, 1222–1227.
Sapolsky, R.M., Krey, L.C., & McEwen, B.S. (1986) The Neuroendocrinology of Stress and Aging: The Glucocorticoid Cascade Hypothesis*. *Endocr. Rev.*, **7**, 284–301.
Sapolsky, R.M., Romero, L.M., & Munck, A.U. (2000) How Do Glucocorticoids Influence Stress Responses? Integrating Permissive, Suppressive, Stimulatory, and Preparative Actions*. *Endocr. Rev.*, **21**, 55–89.
Saretzki, G., Sitte, N., Merkel, U., Wurm, R.E., & Von Zglinicki, T. (1999) Telomere shortening triggers a p53-dependent cell cycle arrest via accumulation of G-rich single stranded DNA fragments. *Oncogene*, **18**, 5148–5158.
Sayer, R., Robertson, D., Balfour, D.J.K., Breen, K.C., & Stewart, C.A. (2008) The effect of stress on the expression of the amyloid precursor protein in rat brain. *Neurosci. Lett.*, **431**, 197–200.
Schaakxs, R., Wielaard, I., Verhoeven, J.E., Beekman, A.T.F., Penninx, B.W.J.H., & Comijs, H.C. (2016) Early and recent psychosocial stress and telomere length in older adults. *Int. Psychogeriatrics*, **28**, 405–413.
Schafer, M.J., White, T.A., Evans, G., Tonne, J.M., Verzosa, G.C., Stout, M.B., Mazula,

D.L., Palmer, A.K., Baker, D.J., Jensen, M.D., Torbenson, M.S., Miller, J.D., Ikeda, Y., Tchkonia, T., van Deursen, J.M., Kirkland, J.L., & LeBrasseur, N.K. (2016) Exercise Prevents Diet-Induced Cellular Senescence in Adipose Tissue. *Diabetes*, **65**, 1606–1615.

Scheff, S.W., Price, D.A., Schmitt, F.A., Dekosky, S.T., & Mufson, E.J. (2007) Synaptic alterations in CA1 in mild Alzheimer disease and mild cognitive impairment. *Neurology*, **68**, 1501–1508.

Scheuner, D., Eckman, C., Jensen, M., Song, X., Citron, M., Suzuki, N., Bird, T.D., Hardy, J., Hutton, M., Kukull, W., Larson, E., Levy-Lahad, L., Viitanen, M., Peskind, E., Poorkaj, P., Schellenberg, G., Tanzi, R., Wasco, W., Lannfelt, L., Selkoe, D., & Younkin, S. (1996) Secreted amyloid β–protein similar to that in the senile plaques of Alzheimer's disease is increased in vivo by the presenilin 1 and 2 and APP mutations linked to familial Alzheimer's disease. *Nat. Med.*, **2**, 864–870.

Schiavone, S., Jaquet, V., Sorce, S., Dubois-Dauphin, M., Hultqvist, M., Bäckdahl, L., Holmdahl, R., Colaianna, M., Cuomo, V., Trabace, L., & Krause, K.H. (2012) NADPH oxidase elevations in pyramidal neurons drive psychosocial stress-induced neuropathology. *Transl. Psychiatry*, **2**, 111.

Scullion, G.A., Kendall, D.A., Marsden, C.A., Sunter, D., & Pardon, M.C. (2011) Chronic treatment with the α 2-adrenoceptor antagonist fluparoxan prevents age-related deficits in spatial working memory in APP × PS1 transgenic mice without altering β-amyloid plaque load or astrocytosis. *Neuropharmacology*, **60**, 223–234.

Selkoe, D.J. (2001) Alzheimer's Disease: Genes, Proteins, and Therapy. *Physiol. Rev.*, **81**, 741–766.

Selkoe, D.J. & Hardy, J. (2016) The amyloid hypothesis of Alzheimer's disease at 25 years. *EMBO Mol. Med.*, **8**, 595–608.

Seluanov, A., Gorbunova, V., Falcovitz, A., Sigal, A., Milyavsky, M., Zurer, I., Shohat, G., Goldfinger, N., & Rotter, V. (2001) Change of the death pathway in senescent human fibroblasts in response to DNA damage is caused by an inability to stabilize p53. *Mol. Cell. Biol.*, **21**, 1552–1564.

Selye, H. (1936) A Syndrome Produced by Diverse Nocuous Agents. *Nature*, **138**.

Selye, H. (1950) Stress and the general adaptation syndrome. *Br. Med. J.*, **1**, 1383–1392.

Selye, H. (1959) Perspectives in stress research. *Perspect. Biol. Med.*, **2**, 403–416.

Shaftel, S.S., Kyrkanides, S., Olschowka, J.A., Miller, J.N.H., Johnson, R.E., & O'Banion, M.K. (2007) Sustained hippocampal IL-1β overexpression mediates chronic neuroinflammation and ameliorates Alzheimer plaque pathology. *J. Clin. Invest.*, **117**, 1595–1604.

Shankar, G.M. & Walsh, D.M. (2009) Alzheimer's disease: synaptic dysfunction and Aβ. *Mol. Neurodegener.*, **4**, 48.

Shi, Q., Chowdhury, S., Ma, R., Le, K.X., Hong, S., Caldarone, B.J., Stevens, B., & Lemere, C.A. (2017) Complement C3 deficiency protects against neurodegeneration in aged plaque-rich APP/PS1 mice. *Sci. Transl. Med.*, **9**.

Shu, Y. & Xu, T. (2017) Chronic Social Defeat Stress Modulates Dendritic Spines Structural Plasticity in Adult Mouse Frontal Association Cortex. *Neural Plast.*, **2017**, 6207873.

Signorello, L.B., Cohen, S.S., Williams, D.R., Munro, H.M., Hargreaves, M.K., & Blot, W.J. (2014) Socioeconomic Status, Race, and Mortality: A Prospective Cohort Study.

Am. J. Public Health, **104**, e98.
Siksou, L., Rostaing, P., Lechaire, J.P., Boudier, T., Ohtsuka, T., Fejtová, A., Kao, H.T., Greengard, P., Gundelfinger, E.D., Triller, A., & Marty, S. (2007) Three-dimensional architecture of presynaptic terminal cytomatrix. *J. Neurosci.*, **27**, 6868–6877.
Silk, J.B., Beehner, J.C., Bergman, T.J., Crockford, C., Engh, A.L., Moscovice, L.R., Wittig, R.M., Seyfarth, R.M., & Cheney, D.L. (2010) Strong and consistent social bonds enhance the longevity of female baboons. *Curr. Biol.*, **20**, 1359–1361.
Sivoňová, M., Žitňanová, I., Hlinčíková, L., Škodáček, I., Trebatická, J., Ďuračková, Z., Sivoň, M., Ovaá, O., Itň, I.Z.ˇ, Anovaá, A., Hlinč I ´, L., Kovaá, K., Koda´č, I.S.ˇ, Koda´č Ek, K., Trebaticka´b, J., Trebaticka´b, T., Ka, Z., & Urač, D.ˇ (2004) Stress The International Journal on the Biology of Stress Oxidative Stress in University Students during Examinations Oxidative Stress in University Students during Examinations. *Oxidative Stress Univ. Students Dur. Exam.*, **7**, 183–188.
Smith, J.A., Das, A., Ray, S.K., & Banik, N.L. (2012) Role of pro-inflammatory cytokines released from microglia in neurodegenerative diseases. *Brain Res. Bull.*,.
Smyth, G.K. (2004) Linear models and empirical bayes methods for assessing differential expression in microarray experiments. *Stat. Appl. Genet. Mol. Biol.*, **3**.
Snyder-Mackler, N., Burger, J.R., Gaydosh, L., Belsky, D.W., Noppert, G.A., Campos, F.A., Bartolomucci, A., Yang, Y.C., Aiello, A.E., O'Rand, A., Harris, K.M., Shively, C.A., Alberts, S.C., & Tung, J. (2020) Social determinants of health and survival in humans and other animals. *Science (80-.).*, **368**.
Solas, M., Aisa, B., Mugueta, M.C., Del Río, J., Tordera, R.M., & Ramírez, M.J. (2010) Interactions between age, stress and insulin on cognition: implications for Alzheimer's disease. *Neuropsychopharmacology*, **35**, 1664–1673.
Sommadossi, J.P. & Carlisle, R. (1987) Toxicity of 3'-azido-3'-deoxythymidine and 9-(1,3-dihydroxy-2-propoxymethyl)guanine for normal human hematopoietic progenitor cells in vitro. *Antimicrob. Agents Chemother.*, **31**, 452–454.
Son, S.W., Lee, J.S., Kim, H.G., Kim, D.W., Ahn, Y.C., & Son, C.G. (2016) Testosterone depletion increases the susceptibility of brain tissue to oxidative damage in a restraint stress mouse model. *J. Neurochem.*, **136**, 106–117.
Sotiropoulos, I., Catania, C., Pinto, L.G., Silva, R., Pollerberg, G.E., Takashima, A., Sousa, N., & Almeida, O.F.X. (2011) Stress Acts Cumulatively To Precipitate Alzheimer's Disease-Like Tau Pathology and Cognitive Deficits. *J. Neurosci.*, **31**, 7840–7847.
Sousa, N., Lukoyanov, N. V, Madeira, M.D., Almeida, O.F., & Paula-Barbosa, M.M. (2000) Reorganization of the morphology of hippocampal neurites and synapses after stress-induced damage correlates with behavioral improvement. *Neuroscience*, **97**, 253–266.
Spiga, F., Walker, J.J., Terry, J.R., & Lightman, S.L. (2014) HPA Axis-Rhythms. In *Comprehensive Physiology*. John Wiley & Sons, Inc., Hoboken, NJ, USA, pp. 1273–1298.
Stadtman, E.R. (1992) Protein oxidation and aging. *Science*, **257**, 1220–1224.
Stadtman, E.R. & Levine, R.L. (2000) Protein oxidation. *Ann. N. Y. Acad. Sci.*, **899**, 191–208.
Steptoe, A. & Zaninotto, P. (2020) Lower socioeconomic status and the acceleration of aging: An outcome-wide analysis. *Proc. Natl. Acad. Sci. U. S. A.*, **117**, 14911–14917.
Stern, Y., Gurland, B., Tatemichi, T.K., Tang, M.X., Wilder, D., & Mayeux, R. (1994)

Influence of Education and Occupation on the Incidence of Alzheimer's Disease. *JAMA J. Am. Med. Assoc.*, **271**, 1004.

Stringhini, S., Carmeli, C., Jokela, M., Avendaño, M., Muennig, P., Guida, F., Ricceri, F., d'Errico, A., Barros, H., Bochud, M., Chadeau-Hyam, M., Clavel-Chapelon, F., Costa, G., Delpierre, C., Fraga, S., Goldberg, M., Giles, G.G., Krogh, V., Kelly-Irving, M., Layte, R., Lasserre, A.M., Marmot, M.G., Preisig, M., Shipley, M.J., Vollenweider, P., Zins, M., Kawachi, I., Steptoe, A., Mackenbach, J.P., Vineis, P., Kivimäki, M., Alenius, H., Avendano, M., Barros, H., Bochud, M., Carmeli, C., Carra, L., Castagné, R., Chadeau-Hyam, M., Clavel-Chapelon, F., Costa, G., Courtin, E., Delpierre, C., D'Errico, A., Dugué, P.-A., Elliott, P., Fraga, S., Gares, V., Giles, G., Goldberg, M., Greco, D., Hodge, A., Irving, M.K., Karisola, P., Kivimäki, M., Krogh, V., Lang, T., Layte, R., Lepage, B., Mackenbach, J., Marmot, M., McCrory, C., Milne, R., Muennig, P., Nusselder, W., Panico, S., Petrovic, D., Polidoro, S., Preisig, M., Raitakari, O., Ribeiro, A.I., Ribeiro, A.I., Ricceri, F., Robinson, O., Valverde, J.R., Sacerdote, C., Satolli, R., Severi, G., Shipley, M.J., Stringhini, S., Tumino, R., Vineis, P., Vollenweider, P., & Zins, M. (2017) Socioeconomic status and the 25 × 25 risk factors as determinants of premature mortality: a multicohort study and meta-analysis of 1·7 million men and women. *Lancet*, **389**, 1229–1237.

Sturmlechner, I., Zhang, C., Sine, C.C., van Deursen, E.J., Jeganathan, K.B., Hamada, N., Grasic, J., Friedman, D., Stutchman, J.T., Can, I., Hamada, M., Lim, D.Y., Lee, J.H., Ordog, T., Laberge, R.M., Shapiro, V., Baker, D.J., Li, H., & van Deursen, J.M. (2021) p21 produces a bioactive secretome that places stressed cells under immunosurveillance. *Science (80-.).*, **374**, eabb3420.

Sudduth, T.L., Schmitt, F.A., Nelson, P.T., & Wilcock, D.M. (2013) Neuroinflammatory phenotype in early Alzheimer's disease. *Neurobiol. Aging*, **34**, 1051–1059.

Südhof, T.C. (2013) Neurotransmitter release: The last millisecond in the life of a synaptic vesicle. *Neuron*,.

Takeuchi, H., Iba, M., Inoue, H., Higuchi, M., Takao, K., Tsukita, K., Karatsu, Y., Iwamoto, Y., Miyakawa, T., Suhara, T., Trojanowski, J.Q., Lee, V.M.Y., & Takahashi, R. (2011) P301S mutant human tau transgenic mice manifest early symptoms of human tauopathies with dementia and altered sensorimotor gating. *PLoS One*, **6**.

Tata, D.A., Marciano, V.A., & Anderson, B.J. (2006) Synapse loss from chronically elevated glucocorticoids: Relationship to neuropil volume and cell number in hippocampal area CA3. *J. Comp. Neurol.*, **498**, 363–374.

Tatomir, A., Micu, C., & Crivii, C. (2014) The impact of stress and glucocorticoids on memory. *Clujul Med.*, **87**, 3.

Troyanskaya, O., Cantor, M., Sherlock, G., Brown, P., Hastie, T., Tibshirani, R., Botstein, D., & Altman, R.B. (2001) Missing value estimation methods for DNA microarrays. *Bioinformatics*, **17**, 520–525.

Tsuber, V., Kadamov, Y., & Tarasenko, L. (2014) Activation of antioxidant defenses in whole saliva by psychosocial stress is more manifested in young women than in young men. *PLoS One*, **9**.

Tung, J., Archie, E.A., Altmann, J., & Alberts, S.C. (2016) Cumulative early life adversity predicts longevity in wild baboons. *Nat. Commun.*, **7**, 11181.

Tynan, R.J., Naicker, S., Hinwood, M., Nalivaiko, E., Buller, K.M., Pow, D. V., Day, T.A.,

& Walker, F.R. (2010) Chronic stress alters the density and morphology of microglia in a subset of stress-responsive brain regions. *Brain. Behav. Immun.*, **24**, 1058–1068.
Uchihara, T., Endo, K., Kondo, H., Okabayashi, S., Shimozawa, N., Yasutomi, Y., Adachi, E., & Kimura, N. (2016) Tau pathology in aged cynomolgus monkeys is progressive supranuclear palsy/corticobasal degeneration- but not Alzheimer disease-like - Ultrastructural mapping of tau by EDX-. *Acta Neuropathol. Commun.*, **4**, 118.
Ulrich-Lai, Y.M. & Engeland, W.C. (2000) Hyperinnervation during adrenal regeneration influences the rate of functional recovery. *Neuroendocrinology*, **71**, 107–123.
Ulrich-Lai, Y.M. & Herman, J.P. (2009) Neural regulation of endocrine and autonomic stress responses. *Nat. Rev. Neurosci.*, **10**, 397–409.
Unno, K., Fujitani, K., Takamori, N., Takabayashi, F., Maeda, K.I., Miyazaki, H., Tanida, N., Iguchi, K., Shimoi, K., & Hoshino, M. (2011) Theanine intake improves the shortened lifespan, cognitive dysfunction and behavioural depression that are induced by chronic psychosocial stress in mice. In *Free Radical Research*. pp. 966–974.
van Deursen, J.M. (2019) Senolytic therapies for healthy longevity. *Science*, **364**, 636.
Vijgen, G.H.E.J., Bouvy, N.D., Teule, G.J.J., Brans, B., Hoeks, J., Schrauwen, P., & van Marken Lichtenbelt, W.D. (2012) Increase in Brown Adipose Tissue Activity after Weight Loss in Morbidly Obese Subjects. *J. Clin. Endocrinol. Metab.*, **97**, E1229–E1233.
Voorhees, J.L., Tarr, A.J., Wohleb, E.S., Godbout, J.P., Mo, X., Sheridan, J.F., Eubank, T.D., & Marsh, C.B. (2013) Prolonged Restraint Stress Increases IL-6, Reduces IL-10, and Causes Persistent Depressive-Like Behavior That Is Reversed by Recombinant IL-10. *PLoS One*, **8**.
Vyas, S., Rodrigues, A.J., Silva, J.M., Tronche, F., Almeida, O.F.X., Sousa, N., & Sotiropoulos, I. (2016) Chronic Stress and Glucocorticoids: From Neuronal Plasticity to Neurodegeneration. *Neural Plast.*, **2016**, 6391686.
Wang, H.X., Wahlberg, M., Karp, A., Winblad, B., & Fratiglioni, L. (2012) Psychosocial stress at work is associated with increased dementia risk in late life. *Alzheimer's Dement.*, **8**, 114–120.
Wang, J., Wright, H.M., Vempati, P., Li, H., Wangsa, J., Dzhuan, A., Habbu, K., Knable, L.A., Ho, L., & Pasinetti, G.M. (2013) Investigation of nebivolol as a novel therapeutic agent for the treatment of Alzheimer's disease. *J. Alzheimer's Dis.*, **33**, 1147–1156.
Wang, M., Roussos, P., McKenzie, A., Zhou, X., Kajiwara, Y., Brennand, K.J., De Luca, G.C., Crary, J.F., Casaccia, P., Buxbaum, J.D., Ehrlich, M., Gandy, S., Goate, A., Katsel, P., Schadt, E., Haroutunian, V., & Zhang, B. (2016) Integrative network analysis of nineteen brain regions identifies molecular signatures and networks underlying selective regional vulnerability to Alzheimer's disease. *Genome Med.*, **8**, 104.
Wang, Q. wen, Rowan, M.J., & Anwyl, R. (2009) Inhibition of LTP by beta-amyloid is prevented by activation of β2 adrenoceptors and stimulation of the cAMP/PKA signalling pathway. *Neurobiol. Aging*, **30**, 1608–1613.
Wang, R. & Reddy, P.H. (2017) Role of Glutamate and NMDA Receptors in Alzheimer's Disease. *J. Alzheimer's Dis.*,.
Wang, Y.J., Chen, G.H., Hu, X.Y., Lu, Y.P., Zhou, J.N., & Liu, R.Y. (2005) The expression of calcium/calmodulin-dependent protein kinase II-α in the hippocampus of patients

with Alzheimer's disease and its links with AD-related pathology. *Brain Res.*, **1031**, 101–108.

Watanabe, Y., Gould, E., & McEwen, B.S. (1992) Stress induces atrophy of apical dendrites of hippocampal CA3 pyramidal neurons. *Brain Res.*, **588**, 341–345.

Weil-Malherbe, H., Axelrod, J., & Tomchick, R. (1959) Blood-brain barrier for adrenaline. *Science (80-.).*, **129**, 1226–1227.

Welch, G. & Tsai, L. (2022) Mechanisms of DNA damage-mediated neurotoxicity in neurodegenerative disease. *EMBO Rep.*,.

Whitehead, J.C., Hildebrand, B.A., Sun, M., Rockwood, M.R., Rose, R.A., Rockwood, K., & Howlett, S.E. (2014) A clinical frailty index in aging mice: Comparisons with frailty index data in humans. *Journals Gerontol. - Ser. A Biol. Sci. Med. Sci.*, **69**, 621–632.

Wiegand, C., Heusser, P., Klinger, C., Cysarz, D., Büssing, A., Ostermann, T., & Savelsbergh, A. (2018) Stress-associated changes in salivary microRNAs can be detected in response to the Trier Social Stress Test: An exploratory study. *Sci. Rep.*, **8**, 1–13.

Wilson, R.S., Evans, D.A., Bienias, J.L., Leon, C.F.M. de, Schneider, J.A., & Bennett, D.A. (2003) Proneness to psychological distress is associated with risk of Alzheimer's disease. *Neurology*, **61**, 1479–1485.

Wischik, C.M., Novak, M., Thogersen, H.C., Edwards, P.C., Runswick, M.J., Jakes, R., Walker, J.E., Milstein, C., Roth, M., & Klug, A. (1988) Isolation of a fragment of tau derived from the core of the paired helical filament of Alzheimer disease. *Proc. Natl. Acad. Sci. U. S. A.*, **85**, 4506–4510.

Wohleb, E.S., Fenn, A.M., Pacenta, A.M., Powell, N.D., Sheridan, J.F., & Godbout, J.P. (2012) Peripheral innate immune challenge exaggerated microglia activation, increased the number of inflammatory CNS macrophages, and prolonged social withdrawal in socially defeated mice. *Psychoneuroendocrinology*, **37**, 1491–1505.

Wohleb, E.S., Hanke, M.L., Corona, A.W., Powell, N.D., Stiner, L.M., Bailey, M.T., Nelson, R.J., Godbout, J.P., & Sheridan, J.F. (2011) β-Adrenergic receptor antagonism prevents anxiety-like behavior and microglial reactivity induced by repeated social defeat. *J. Neurosci.*, **31**, 6277–6288.

Wohleb, E.S., Powell, N.D., Godbout, J.P., & Sheridan, J.F. (2013) Stress-induced recruitment of bone marrow-derived monocytes to the brain promotes anxiety-like behavior. *J. Neurosci.*, **33**, 13820–13833.

Wong, E.Y.H. & Herbert, J. (2006) Raised circulating corticosterone inhibits neuronal differentiation of progenitor cells in the adult hippocampus. *Neuroscience*, **137**, 83–92.

Woolley, C.S., Gould, E., & McEwen, B.S. (1990) Exposure to excess glucocorticoids alters dendritic morphology of adult hippocampal pyramidal neurons. *Brain Res.*, **531**, 225–231.

Wu, D., Bacaj, T., Morishita, W., Goswami, D., Arendt, K.L., Xu, W., Chen, L., Malenka, R.C., & Südhof, T.C. (2017) Postsynaptic synaptotagmins mediate AMPA receptor exocytosis during LTP. *Nature*, **544**, 316–321.

Xu, M., Pirtskhalava, T., Farr, J.N., Weigand, B.M., Palmer, A.K., Weivoda, M.M., Inman, C.L., Ogrodnik, M.B., Hachfeld, C.M., Fraser, D.G., Onken, J.L., Johnson, K.O., Verzosa, G.C., Langhi, L.G.P., Weigl, M., Giorgadze, N., LeBrasseur, N.K., Miller,

J.D., Jurk, D., Singh, R.J., Allison, D.B., Ejima, K., Hubbard, G.B., Ikeno, Y., Cubro, H., Garovic, V.D., Hou, X., Weroha, S.J., Robbins, P.D., Niedernhofer, L.J., Khosla, S., Tchkonia, T., & Kirkland, J.L. (2018) Senolytics improve physical function and increase lifespan in old age. *Nat. Med.*, **24**, 1246–1256.

Yaffe, K., Vittinghoff, E., Lindquist, K., Barnes, D., Covinsky, K.E., Neylan, T., Kluse, M., & Marmar, C. (2010) Posttraumatic stress disorder and risk of dementia among US veterans. *Arch. Gen. Psychiatry*, **67**, 608–613.

Yan, J., Sun, X.-B., Wang, H.-Q., Zhao, H., Zhao, X.-Y., Xu, Y.-X., Guo, J.-C., & Zhu, C.-Q. (2010) Chronic restraint stress alters the expression and distribution of phosphorylated tau and MAP2 in cortex and hippocampus of rat brain. *Brain Res.*, **1347**, 132–141.

Yang, C., Guo, X., Wang, G.H., Wang, H.L., Liu, Z.C., Liu, H., Zhu, Z.X., & Li, Y. (2014) Changes in tau phosphorylation levels in the hippocampus and frontal cortex following chronic stress. *Brazilian J. Med. Biol. Res. = Rev. Bras. Pesqui. medicas e Biol.*, **47**, 237–244.

Yang, C.H., Huang, C.C., & Hsu, K. Sen (2005) Behavioral stress enhances hippocampal CA1 long-term depression through the blockade of the glutamate uptake. *J. Neurosci.*, **25**, 4288–4293.

Yao, B., Meng, L., Hao, M., Zhang, Y., Gong, T., & Guo, Z. (2019) Chronic stress: a critical risk factor for atherosclerosis. *J. Int. Med. Res.*, **47**, 1429.

Yasunari, K., Matsui, T., Maeda, K., Nakamura, M., Watanabe, T., & Kiriike, N. (2006) Anxiety-Induced Plasma Norepinephrine Augmentation Increases Reactive Oxygen Species Formation by Monocytes in Essential Hypertension.

Yoo, K.Y., Lee, C.H., Park, J.H., Hwang, I.K., Park, O.K., Kwon, S.H., Choi, J.H., Kim, D.J., Kwon, Y.G., Kim, Y.M., & Won, M.H. (2011) Antioxidant enzymes are differently changed in experimental ischemic hippocampal CA1 region following repeated restraint stress. *J. Neurol. Sci.*, **302**, 33–42.

Yoshiyama, Y., Higuchi, M., Zhang, B., Huang, S.-M., Iwata, N., Saido, T.C., Maeda, J., Suhara, T., Trojanowski, J.Q., & Lee, V.M.-Y. (2007) Synapse loss and microglial activation precede tangles in a P301S tauopathy mouse model. *Neuron*, **53**, 337–351.

Yousefzadeh, M.J., Zhu, Y., McGowan, S.J., Angelini, L., Fuhrmann-Stroissnigg, H., Xu, M., Ling, Y.Y., Melos, K.I., Pirtskhalava, T., Inman, C.L., McGuckian, C., Wade, E.A., Kato, J.I., Grassi, D., Wentworth, M., Burd, C.E., Arriaga, E.A., Ladiges, W.L., Tchkonia, T., Kirkland, J.L., Robbins, P.D., & Niedernhofer, L.J. (2018) Fisetin is a senotherapeutic that extends health and lifespan. *EBioMedicine*, **36**, 18–28.

Yu, N.N., Wang, X.X., Yu, J.T., Wang, N.D., Lu, R.C., Miao, D., Tian, Y., & Tan, L. (2010) Blocking β2-adrenergic receptor attenuates acute stress-induced amyloid β peptides production. *Brain Res.*, **1317**, 305–310.

Yudkin, J.S., Kumari, M., Humphries, S.E., & Mohamed-Ali, V. (2000) Inflammation, obesity, stress and coronary heart disease: Is interleukin-6 the link? *Atherosclerosis*,.

Yuede, C.M., Timson, B.F., Hettinger, J.C., Yuede, K.M., Edwards, H.M., Lawson, J.E., Zimmerman, S.D., & Cirrito, J.R. (2018) Interactions between stress and physical activity on Alzheimer's disease pathology. *Neurobiol. Stress*, **8**, 158–171.

Zarow, C., Lyness, S.A., Mortimer, J.A., & Chui, H.C. (2003) Neuronal loss is greater in the locus coeruleus than nucleus basalis and substantia nigra in Alzheimer and Parkinson diseases. *Arch. Neurol.*, **60**, 337–341.

Zhan, Y., Song, C., Karlsson, R., Tillander, A., Reynolds, C.A., Pedersen, N.L., & Hägg, S. (2015) Telomere Length Shortening and Alzheimer Disease—A Mendelian Randomization Study. *JAMA Neurol.*, **72**, 1202.

Zhang, B., Ma, S., Rachmin, I., He, M., Baral, P., Choi, S., Gonçalves, W.A., Shwartz, Y., Fast, E.M., Su, Y., Zon, L.I., Regev, A., Buenrostro, J.D., Cunha, T.M., Chiu, I.M., Fisher, D.E., & Hsu, Y.C. (2020) Hyperactivation of sympathetic nerves drives depletion of melanocyte stem cells. *Nature*, **577**, 676–681.

Zhang, P., Kishimoto, Y., Grammatikakis, I., Gottimukkala, K., Cutler, R.G., Zhang, S., Abdelmohsen, K., Bohr, V.A., Misra Sen, J., Gorospe, M., & Mattson, M.P. (2019) Senolytic therapy alleviates Aβ-associated oligodendrocyte progenitor cell senescence and cognitive deficits in an Alzheimer's disease model. *Nat. Neurosci.*, **22**, 719–728.

Zhang, Y., Fujita, N., & Tsuruo, T. (1999) Caspase-mediated cleavage of p21Waf1/Cip1 converts cancer cells from growth arrest to undergoing apoptosis. *Oncogene*, **18**, 1131–1138.

Zhou, X., Hollern, D., Liao, J., Andrechek, E., & Wang, H. (2013) NMDA receptor-mediated excitotoxicity depends on the coactivation of synaptic and extrasynaptic receptors. *Cell Death Dis.*, **4**, e560–e560.

Zipple, M.N., Archie, E.A., Tung, J., Altmann, J., & Alberts, S.C. (2019) Intergenerational effects of early adversity on survival in wild baboons. *Elife*, **8**.

Zou, J., Lei, T., Guo, P., Yu, J., Xu, Q., Luo, Y., Ke, R., & Huang, D. (2019) Mechanisms shaping the role of ERK1/2 in cellular senescence (Review). *Mol. Med. Rep.*, **19**, 759–770.

Zucchi, F.C.R., Kirkland, S.W., Jadavji, N.M., van Waes, L.T., Klein, A., Supina, R.D., & Metz, G.A. (2009) Predictable stress versus unpredictable stress: A comparison in a rodent model of stroke. *Behav. Brain Res.*, **205**, 67–75.

APPENDIX

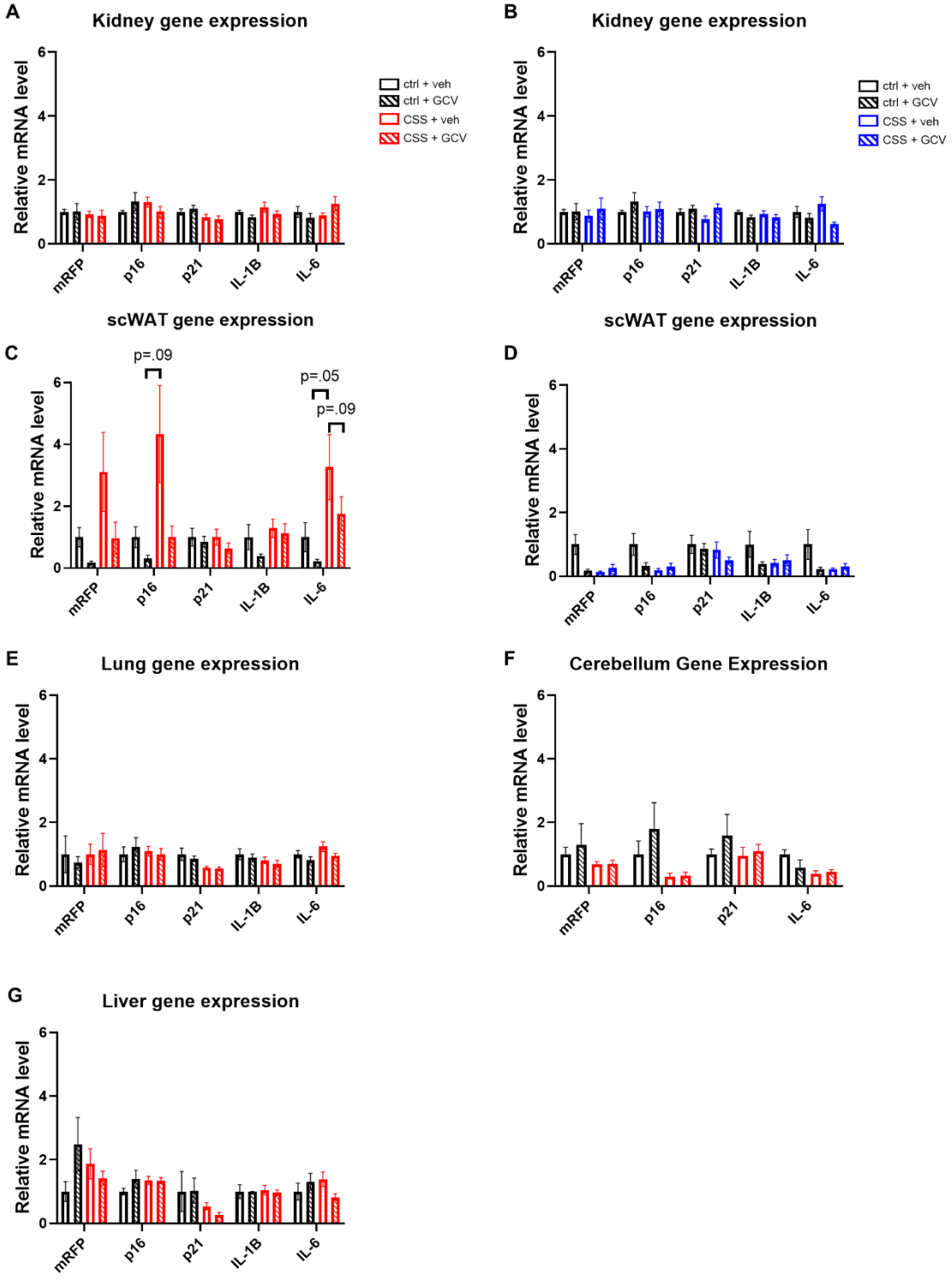
A
Kidney gene expression
Relative mRNA level
ctrl + veh
ctrl + GCV
CSS + veh
CSS + GCV
mRFP
p16
p21
IL-1B
IL-6
B
Kidney gene expression
C
scWAT gene expression
p=.09
p=.05
p=.09
D
scWAT gene expression
E
Lung gene expression
F
Cerebellum Gene Expression
G
Liver gene expression

Chapter 1, Supplementary Figure 1 Senescence and SASP gene expression in cerebellum, kidney, liver, lung A) Senescence/SASP-related gene expression in the kidney. Mixed-effects analysis (REML) with Tukey post hoc. No significant main effects or interaction. **B)** Senescence/SASP-related gene expression in the kidney. Mixed effects analysis (REML) with Tukey post hoc. No significant main effects or interaction. **C)** Senescence/SASP-related gene expression in the scWAT. CSS + veh mice trend strongly towards elevated *mRFP, p16* and *IL-6* but not to the point of statistical significance. Mixed effects analysis (REML) with Tukey post hoc. No significant main effects or interaction. **D)** Senescence/SASP-related gene expression in the scWAT. Mixed effects analysis (REML) with Tukey post hoc. No significant main effects or interaction. **E)** Senescence/SASP-related gene expression in the lung. Mixed-effects analysis (REML) with Tukey post hoc. No significant main effects or interaction. **F)** Senescence/SASP-related gene expression in the cerebellum. Mixed-effects analysis (REML) with Tukey post hoc. No significant main effects or interaction. **G)** Senescence/SASP-related gene expression in the liver. Mixed-effects analysis (REML) with Tukey post hoc. No significant main effects or interaction. * indicates $p<0.05$, ** indicates $p<0.01$ *** indicates $p<0.001$, **** indicates $p<0.0001$. Unless otherwise specified, Histogram bars represent group mean and error bars represent standard error.

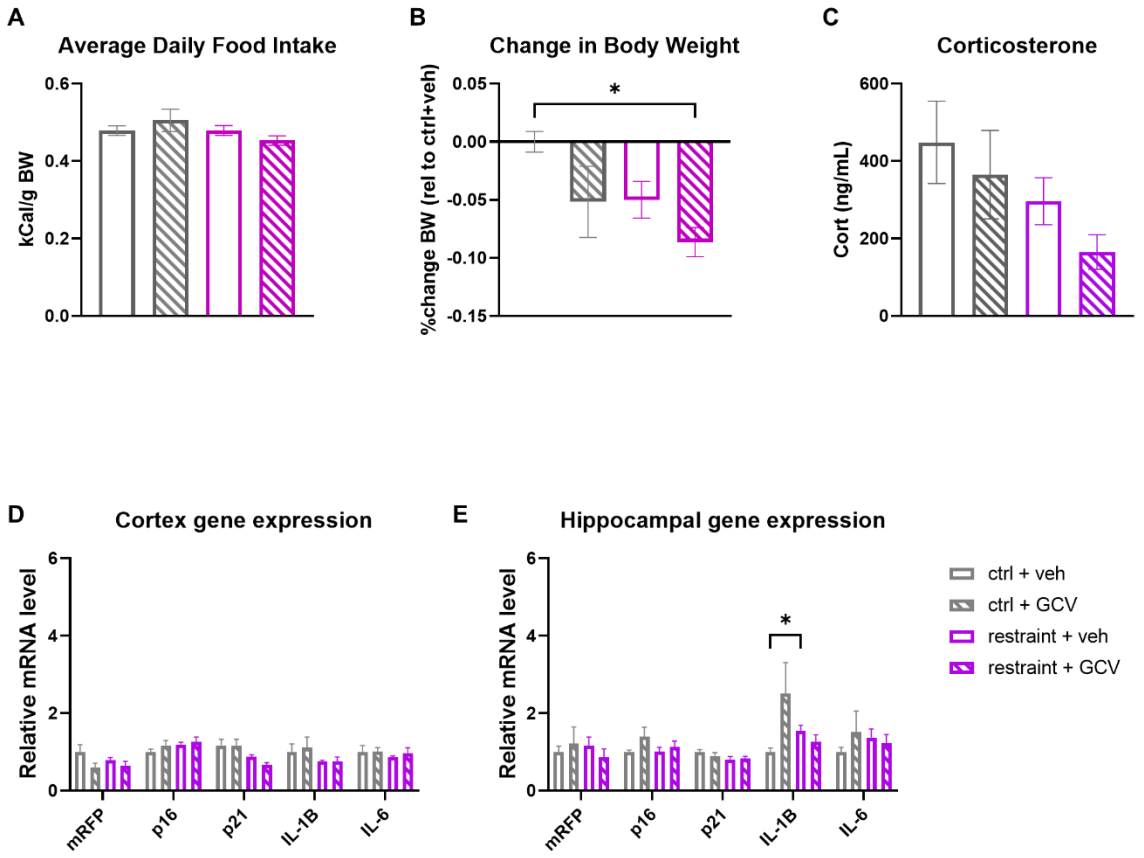

Chapter 2, Supplementary Figure 2 Female mice subjected to restraint stress develop expected metabolic phenotype but do not exhibit elevations in senescence-related gene expression A) There were no significant group differences in average daily calorie intake per gram body weight. 2-way ANOVA. **B)** Both restraint and GCV treatment reduce body weight over the course of 4-weeks. 2-way ANOVA. Restraint p=0.0372. GCV: p=0.0305. Restraint x GCV p=0.6895. Tukey post hoc. **C)** No significant effect of restraint or GCV on circulating corticosterone concentration. 2-way ANOVA. Restraint p=0.0533. GCV: p=0.2229. Restraint x GCV: p=0.7821. **D)** Senescence/SASP-related gene expression in the neural cortex. Mixed effects analysis (REML) with Tukey post hoc. No significant main effects or interaction. **E)** Senescence/SASP-related gene expression in the hippocampus. Mixed effects analysis (REML) Gene: p=0.0014. Group: p=0.2016. Gene x Group: p=0.0466. Tukey post hoc. * indicates p<0.05, ** indicates p<0.01 *** indicates p<0.001, **** indicates p<0.0001. Unless otherwise specified, Histogram bars represent group mean and error bars represent standard error.

Chapter 1. Supplementary Table 1: primer sequences used

Gene	Forward	Reverse
actin	GGCACCACACCTTCTACAATG	GGGGTGTTGAAGGTCTCAAAC
GAPDH	AGGTCGGTGTGAACGGATTTG	TGTAGACCATGTAGTTGAGGTCA
IL-1β	AAAAGCCTCGTGCTGTCG	AGGCCACAGGTATTTTGTCG
IL-6	GTTCTCTGGGAAATCGTGGA	GGTACTCCAGAAGACCAGAGGA
mRFP	GACCTCGGCGTCGTAGTG	AAGGGCGAGATCAAGATGAG
p16	GAGTCCGCTGCAGACAGACT	CCAGGCATCGCGCACATCCA
p21	GCCCGAGAACGGTGGAACTT	GACAAGGCCACGTGGTCCTC
TFII	TGGAGATTTGTCCACCATGA	GAATTGCCAAACTCATCAAAACT

Chapter 1 Supplementary Table 2: antibodies used

Antigen	Source	Dilution
Guinea Pig anti NeuN	ABN90 (Millipore)	1:000
Rabbit anti Iba1	019-19741 (Wako)	1:000
Chicken anti GFAP	AB5541 (Millipore)	1:500
Rabbit anti NG2	AB5320 (Millipore)	1:250
Mouse anti Pax7	DHSB	1:100
Rat anti murine F4/80	123102 (BioLegend)	1:100
Donkey anti rabbit AlexaFluor 647	Jackson Immuno	1:500
Donkey anti Guinea Pig AlexaFluor 488	Jackson Immuno	1:500
Donkey anti Chicken AlexaFluor 488	Jackson Immuno	1:500
Donkey anti Mouse AlexaFluor 647	Jackson Immuno	1:500
Donkey anti Rat Alexa Fluor 488	Jackson Immuno	1:500

Chapter 5, Supplementary Table 3: Behavioral, physiological and metabolic data for DOM and SUB mice used in Chapter 5 proteomic characterization.

Parameter	DOM avg	SUB avg	p value (t test)
Fecal corticosterone metabolites ng/.05g	14.20 ± 2.71	36.40 ± 4.08	0.0019
Aggression Exhibited (counts)	100.40 ± 2.46	1.00 ± 0.45	1.7722E-10
Aggression Received (counts)	2.00 ± 0.89	99.80 ± 7.00	7.0726E-07
Δ BW from baseline following CPS (g)	2.90 ± 0.76	3.24 ± 1.01	0.7949
Δ BW from baseline to 17mo (g)	18.80 ± 1.54	15.02 ± 0.95	0.0701
BW at 17mo (g)	45.82 ± 1.69	40.38 ± 0.99	0.0238
Δ FI from baseline following CPS (kCal)	2.38 ± 1.12	0.41 ± 1.58	0.3394
Δ FI from baseline to 17mo (kCal)	-0.54 ± 1.41	-0.92 ± 2.90	0.9078
FI at 17 mo (kCal)	13.17 ± 1.06	12.40 ± 2.53	0.7859
Δ fat free mass following CPS (g)	0.48 ± 0.37	2.76 ± 0.53	0.0080
Δ fat free mass at 17mo (g)	4.89 ± 0.76	6.81 ± 0.55	0.0756
fat free mass at 17mo	28.69 ± 0.78	28.05 ± 0.61	0.5354
Δ fat mass following CPS (g)	2.10 ± 0.74	0.26 ± 0.27	0.0475
Δ fat mass at 17mo (g)	13.49 ± 0.51	8.61 ± 0.84	0.0011
fat mass at 17mo (g)	15.02 ± 0.79	11.02 ± 0.97	0.0125
Δ fasting glucose from baseline following CPS (mg/dL)	7.00 ± 15.73	24.40 ± 14.98	0.4461

Δ fasting glucose from baseline at 17mo (mg/dL)	**11.40 ± 14.49**	**9.00 ± 15.90**	**0.9139**
Fasting glucose at 17mo (mg/dL)	**161.80 ± 8.46**	**147.40 ± 10.64**	**0.3204**

These data are consistent with that of the overall population of mice in the Lifelong CPS paradigm (Razzoli *et al.*, 2018)

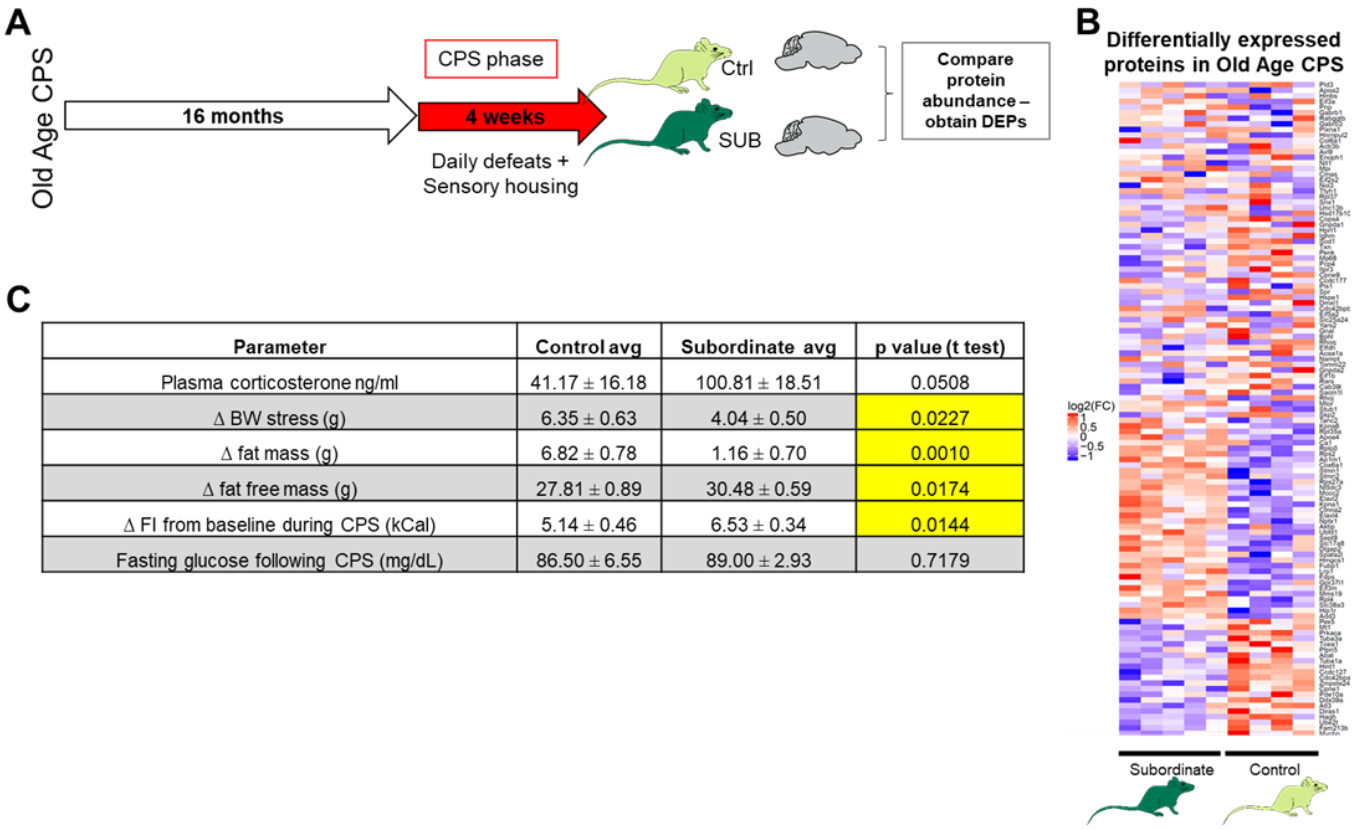

C

Parameter	Control avg	Subordinate avg	p value (t test)
Plasma corticosterone ng/ml	41.17 ± 16.18	100.81 ± 18.51	0.0508
Δ BW stress (g)	6.35 ± 0.63	4.04 ± 0.50	0.0227
Δ fat mass (g)	6.82 ± 0.78	1.16 ± 0.70	0.0010
Δ fat free mass (g)	27.81 ± 0.89	30.48 ± 0.59	0.0174
Δ FI from baseline during CPS (kCal)	5.14 ± 0.46	6.53 ± 0.34	0.0144
Fasting glucose following CPS (mg/dL)	86.50 ± 6.55	89.00 ± 2.93	0.7179

Chapter 5, Supplementary Figure 3: Wildtype mice subjected to CPS only in old age do not manifest develop proteomic changes associated with AD A. Experimental overview **B.** Heat map of differentially expressed proteins between 17 mo mice subjected to CPS and age-matched controls. There were 34 upregulated and 49 downregulated proteins in Old Age CPS mice, compared to controls ($p < 0.05$).

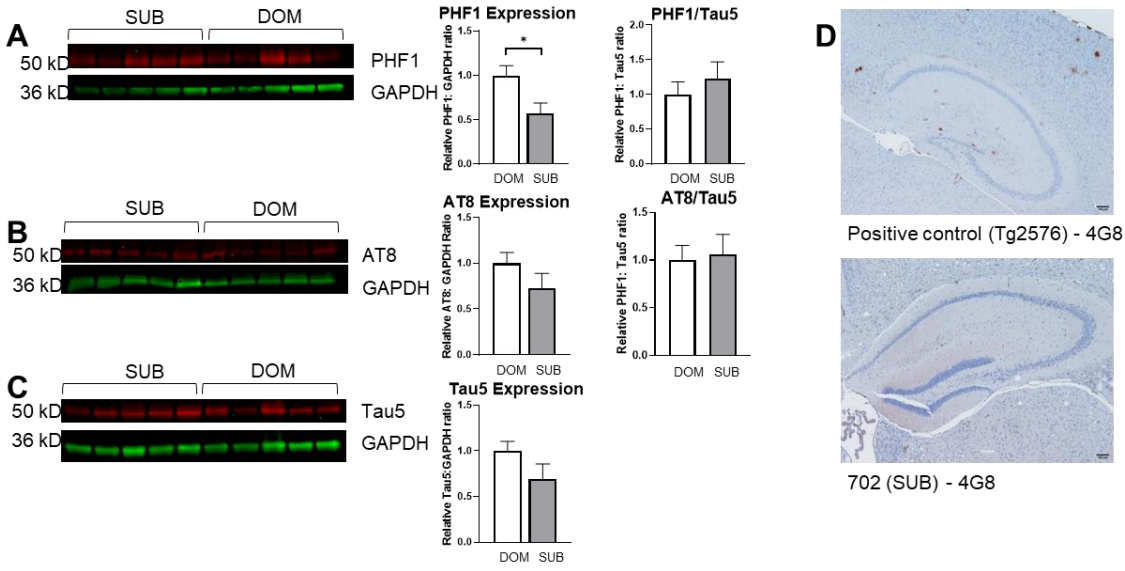

Chapter 5 Supplementary Figure 4: Wildtype mice subjected to lifelong CPS do not develop elevated tau or amyloid β A. Western blot analysis revealed that subordinate mice have significantly lower levels of the phospho-tau epitope PHF overall, but not when normalized to the amount of total tau (Tau5). **B.** Western blot for phospho-tau epitope AT8. There was not a significant difference between groups, even when normalized to the amount of total tau (Tau5). **C.** Western Blot for Tau5 indicated no significant difference between DOM and SUB. **D.** Immunohistochemistry for 4G8 indicates that neither groups expressed detectable levels of amyloid beta. * indicates $p<0.05$. t test. Values are expressed as ratios to DOM group average.